UNIVERSITÄT LEIPZIG

ANALYZING THE MICROBIOTA-MEDIATED EFFECTS OF ENVIRONMENTAL CHEMICALS ON MAIT CELLS

Der Fakultät für Lebenswissenschaften
der Universität Leipzig

genehmigte

DISSERTATION

zur Erlangung des akademischen Grades

Doctor rerum naturalium

(Dr. rer. nat.)

vorgelegt von

MSc Jannike Lea Krause

geboren am 14.03.1983 in Karlsruhe

Dekan: Prof. Dr. Marc Schönwiesner

Gutachter: Prof. Dr. Martin von Bergen

Prof. Dr. Emma Allen-Vercoe

Tag der Verteidigung: 09.04.2021

BIBLIOGRAPHISCHE DARSTELLUNG

Jannike Lea Krause

Analyzing the microbiota-mediated effects of environmental chemicals on MAIT cells

Fakultät für Lebenswissenschaften

Universität Leipzig

Dissertation

262 Seiten, 267 Literaturangaben, 19 Abbildungen, 0 Tabellen

Essentiell für die Gesundheit des Menschen sind sein Immunsystem und seine Mikrobiota. Die Mikrobiota umfasst sämtliche Mikroorganismen in und auf dem menschlichen Körper und steht in einer symbiotischen Beziehung mit diesem. Diese Symbiose ist das Resultat einer langen, gemeinsamen Entwicklung, welche anscheinend erst durch die Entstehung des adaptiven Immunsystems ermöglicht wurde. Das adaptive Immunsystem unterscheidet zwischen „Fremd“ und „Eigen“ und vermittelt Immuntoleranz, bspw. gegenüber der Mikrobiota oder ungefährlichen Antigenen. Chemikalien, wie Pestizide oder Inhaltsstoffe von Nahrungsmittelverpackungen, gelangen durch orale Aufnahme in unseren Körper. Dort können sie potentiell die Darmmikrobiota und direkt oder indirekt über Veränderungen der Mikrobiota das Immunsystem beeinflussen.

In den vergangenen Jahrzehnten wurden spezialisierte Immunzellen entdeckt, wie bspw. die Mukosa-assoziierten invarianten T-Zellen (MAIT-Zellen), welche häufig in Schleimhäuten, also an den Grenzschichten des Körpers, vorkommen. MAIT-Zellen erkennen mikrobielle Stoffwechselprodukte und zeigen nach Aktivierung zytotoxische Effekte. Ihnen wird eine wichtige, wenn auch noch unklare Rolle bei der Abwehr von Mikrobiota und in chronisch-entzündlichen Erkrankungen zugeschrieben.

In der vorliegenden Arbeit wurden Modellsysteme zur Kultivierung von mikrobiellen Gemeinschaften etabliert, um zunächst den direkten Effekt von Umweltchemikalien auf die Mikrobiota zu untersuchen. Die Kultivierung der verschiedenen Mikrobiota erfolgte sowohl kontinuierlich im Bioreaktor, als auch zeitlich begrenzt in anaeroben Anreicherungskulturen. Des Weiteren wurde überprüft, ob die Aktivierung von MAIT-Zellen durch mikrobiellen Stress beeinflusst werden kann, um schließlich Mikrobiota-vermittelte, indirekte Einflüsse von Umweltchemikalien auf MAIT-Zellen zu untersuchen.

Diese Arbeit leistet einen wichtigen Beitrag zur reproduzierbaren Kultivierung von mikrobiellen Gemeinschaften in Bioreaktoren um den Einfluss von Umweltchemikalien, sowohl direkt auf die Mikrobiota, als auch indirekt auf MAIT-Zellen, zu beurteilen.

List of Contents

LIST OF FIGURES

ZUSAMMENFASSUNG

In zahlreichen Studien wurden chemikalienbedingte unerwünschte Wirkungen sowohl auf das Immunsystem als auch auf die Darmmikrobiota festgestellt. Bisher berücksichtigen die Prüfrichtlinien der europäischen REACH-Verordnung zur Registrierung, Bewertung, Zulassung und Beschränkung chemischer Stoffe jedoch keine Auswirkungen von Chemikalien auf die Darmmikrobiota und auch nicht auf das Immunsystem.

Die Darmmikrobiota ist für die menschliche Gesundheit essentiell und steht in bidirektionalem Austausch mit dem Immunsystem des Wirts. Spezialisierte Immunzellen, wie z.B. Mucosal-assoziierte invariante T (MAIT)-Zellen, erkennen mikrobielle Metabolite, was diese Zellen potenziell sensitiv für mikrobiota-vermittelte Effekte chemischer Exposition macht. Daher wurde in der vorliegenden Arbeit untersucht, ob Umweltchemikalien, also Glyphosat, Chlorpyrifos und Bisphenole, die Reaktion der MAIT-Zellen indirekt modulieren können, indem sie zunächst die Mikrobiota verändern.

Um die Effekte einer Chemikalien-Exposition auf Mikrobiota zu analysieren und danach die MAIT-Zellmodulation zu untersuchen, wurden mit Erfolg geeignete Modellsysteme etabliert. Die etablierten Systeme umfassten sowohl die anaerobe Kultivierung einzelner Bakterienstämme und komplexer Gemeinschaften als auch die kontinuierliche Kultivierung definierter und komplexer Mikrobiota (Abbildung 1 A). Diese Kultivierungssystem wurden anschließend für die kurz- und langzeit chemische Exposition eingesetzt. Die Untersuchung der mikrobiota-vermittelten Wirkungen von Chemikalien auf Immunzellen, wie z.B. MAIT-Zellen, ist ein neuer Forschungsansatz. Daher wurden Modellsysteme zur Untersuchung der mikrobiota-vermittelten MAIT-Zellmodulation etabliert und angewandt (Abbildung 1 B).

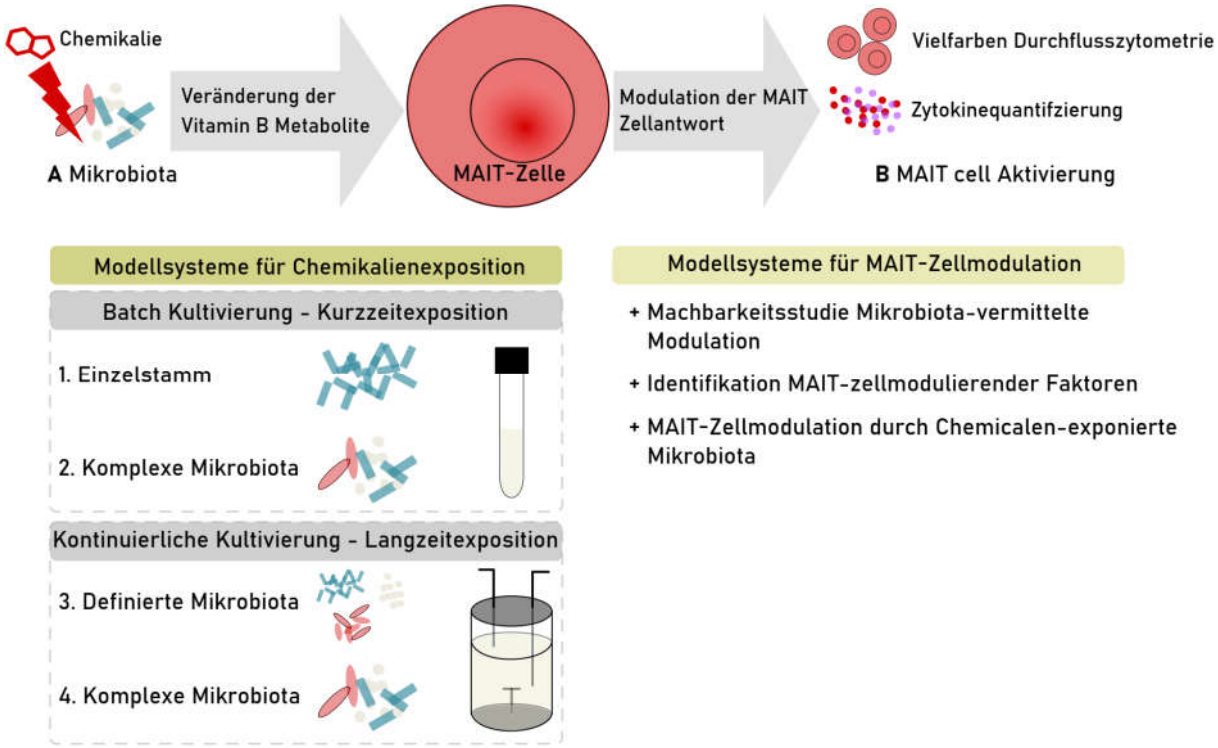

Abbildung 1. Grafische Darstellung der im vorliegenden PhD-Projekt behandelten Themen. A - Zur Untersuchung der mikrobiota-modulierenden Wirkungen von Chemikalien wurden geeignete Modellsysteme für die Kurz- und Langzeitexposition von Mikrobiota entwickelt. B - Das Konzept der MAIT-Zellmodulation über Mikrobiota wurde getestet und für weiteren Analysen verwendet.

Die *extended simplified human intestinal microbiota* (SIHUMIx) ist eine definierte Modellgemeinschaft der menschlichen Darmmikrobiota und wurde für die Kultivierung im Bioreaktor etabliert. Aufgrund ihrer geringen Komplexität sollte die Auflösung von Effekten durch Chemikalien-Exposition bis auf Artebene möglich sein. Mit Hilfe mehrerer Methoden , sowohl auf Zell-, Protein-, DNA- als auch Stoffwechselebene, wurde gezeigt, dass sich SIHUMIx reproduzierbar im Bioreaktor entwickelt (Publikation 1). Beginnend mit Tag 5 erreichte die Gemeinschaft einen konstanten Zustand und behielt diesen unter ungestörten Kulturbedingungen bei (Publikation 1 und Publikation 2). Im Anschluss an die erfolgreiche Etablierung von SIHUMIx für die Anwendung im Bioreaktor wurden der Effekt eines kurzzeitigen Säurestress untersucht. Diese Störung wurde genutzt um die Resistenz und Resilienz von SIHUMIx gegenüber einer starken aber unspezifischen Störung zu ermitteln. Metaproteomanalysen zeigten, dass die Taxonomie von SIHUMIx kaum beeinflusst wurde, wohingegen auf Einzelzellebene (Bakterien-Durchflusszytometrie) und auf funktionaler Ebene (Profil der kurzkettigen Fettsäuren) starke Effekte beobachtet wurden. Nach Ende der Störung entwickelte sich die Gemeinschaft wieder in den konstanten Zustand zurück und bewiese dabei

eine hohe Resilienz gegenüber eines Säurestresses (Publikation 1). Im Gegensatz dazu war SIHUMIx sehr resilient gegenüber Veränderungen der Medienverweilzeit (Publikation 2). Ebenfalls wurde SIHUMIx nur sehr wenig durch die Exposition von 45 µM Bisphenol S beeinflusst, sowohl hinsichtlich der Taxonomie als auch functional. Dennoch konnte anhand dieser Experimente gezeigt werden, dass sich SIHUMIx aufgrund der geringen Komplexität als Modellsystem eignet um den Einfluss von Chemikalien auf die Taxonomie und Funktion der Gemeinschaft im Detail zu untersuchen.

Sowohl Batch-Kultivierung als auch kontinuierliche Kultivierung wurde eingestzt um die Mikrobiota-modulierenden Eigenschaften von Glyphosat zu erforschen. Die Exposition von *Escherichia coli*, *Bifidobacterium adolescentis* und *Lactobacillus reuteri* mit 300 mg/L Glyphosat während der exponentiellen Wachstumsphase einer Batch-Kultivierung wirkte sich nur geringfügig auf Wachstum, Riboflavin- und Folat-Biosynthese aus (Publikation 4). Während der kontinuierlichen Kultivierung von Mikrobiota des Schweins wurden die Effekte einer hohen Glyphosatexposition (900 mg/L) auf die Taxonomie und Funktion anhand eines Multi-omics-Ansatz (Metaproteomanalyse, 16S rRNA-Genanalyse, ungerichtete und ungerichtete Metabolomanalyse) ermittelt. Es wurden nur schwache Effekte auf die Funktion der Gemeinschaft und keine Veränderungen hinsichtlich der Taxonomie beobachtet (Publikation 6). In diesem Kontext wurde eine sensitive Methode zur Quantifizierung von Glyphosat aus Bioreaktorflüssigkeiten etabliert (Publikation 5).

Darüber hinaus wurde die Wirkung der am häufigsten eingesetzten Bisphenole, Bisphenol A, Bisphenol F und Bisphenol S, in Batch-Kultur der Bakterienarten *Bacteroides thetaiotaomicron* und *Escherichia coli* und einer humanen Mikrobiota aus Fäzes untersucht. In der höchsten hemmten alle Bisphenole das Wachstum, reduzierten die Lebensfähigkeit und veränderten den Stoffwechsel der Mikroorganismen, wobei alle Mikroorganismen individuell reagierten. Hierbei waren die Mikrobiota-modulierenden Eigenschaften von Bisphenol A am stärksten und die von Bisphenol S am schwächsten (Publikation 7).

Das Konzept der Mikrobiota-vermittelten Auswirkung von Stress auf MAIT-Zellen wurde anhand eines Säurestress während der Kultivierung SIHUMIx untersucht. Der Säurestress hatte eine reduzierte die Fähigkeit von SIHUMIx MAIT-Zellen zu aktivieren und wurde von eine

verminderte Verfügbarkeit von Riboflavin begleitet. Im Gegenzug war das Potenzial MAIT-Zellen zu aktivieren mit ungestörten Kultivierungsbedingungen assoziiert. Im Rahmen dieser Arbeit wurden weitere Faktoren identifiziert, die die Stärke der MAIT-Zellaktivierung *in vitro* beeinflussen. Selbige waren die Diversität der Bakteriengemeinschaft und deren Zusammensetzung (Publikation 3). Nachdem das Konzept überprüft wurde, wurden die Mikrbiota-vermittelten Effekte von Glyphosat und Chlorpyrifos auf MAIT-Zellen untersucht. Chlorpyrifos, aber nicht Glyphosat, beeinflusste die Fähigkeit von *Escherichia coli*, *Bifidobacterium adolescentis* und *Lactobacillus plantarum* in den getesteten Konzentrationen (Publikation 4). Außerdem konnte gezeigt werden, dass Bisphenol A, Bisphenol F und Bisphenol S den Stoffwechsel von *Bacteroides thetaiotaomicron, Escherichia coli* und ebenfalls von komplexen Mikrobiota aus humanem Fäzes in der verwendeten Konzentrationen beeinflussen. Diese Veränderungen wirkten sich auf die Fähigkeit der Einzelstämme MAIT-Zelln zu aktivieren aus, wohingegen die komplexe Gemeinschaft bezüglich MAIT-Zellaktivierung nicht beeinträchtigt war (Publikation 7).

Mit der vorliegenden Arbeit wurde die methodische Grundlage für die Kultivierung von komplexe Mikrobiota gelegt, um die Mikrobiota-modulierenden Eigenschaften von Umweltchemikalien zu entschlüsseln. Darüber hinaus wurden in dieser Arbeit die etablierten Modellsysteme genutzt, um die Effekte von Glyphosat, Chlorpyrifos und Bisphenolen auf die Mikrobiota, und damit verbunden, potenzielle Effekte auf die Aktivierung von MAIT-Zellen zu untersuchen. Die etablierten Modellsystem erweisen sich als geeignet um die Nebeneffekte von Umweltchemikalien auf intestinale Mikrobiota und Immunzellen zu untersuchen. Die Verwendung dieser Modellsysteme könnte in Zukunft die Risikobewertung on Chemikalien in Bezug auf Nebenwirkungen auf intestinale Mikrobiota und Immunzellen erleichtern.

SUMMARY

Chemical-related adverse effects on both, the immune system and the intestinal microbiota, have been reported in several studies. However, the test guidelines of the European REACH regulation on the **R**egistration, **E**valuation, **A**uthorization and Restriction of **Ch**emicals do not consider chemical effects on the intestinal microbiota as well as on the immune system so far.

The intestinal microbiota is essential for human health and stands in bidirectional exchange with the host immune system. Specialized immune cells, such as mucosal-associated invariant T (MAIT) cells, recognize microbial metabolite, which renders these cells potentially susceptible to microbiota-mediated effects of chemical exposure. Thus, the present work investigated whether environmental chemicals, i.e. glyphosate, chlorpyrifos and bisphenols, can indirectly modulate the MAIT cell response by first affecting the microbiota.

To investigate effects of chemical exposure on microbiota and thereafter studying MAIT cell modulation, suitable model systems were successfully established. The established systems comprised anaerobe cultivation of individual strains of bacteria and complex communities in batch as well as the continuous cultivation of defined and complex microbiota (**Figure 1** A). These cultivation systems were then utilized for short-term and long-term chemical exposure. Assessing the microbiota-mediated effects of chemicals on immune cells, such as MAIT cells is a new research approach. Thus, model systems to study microbiota-mediated MAIT cell modulation have been established and applied (**Figure 1** B).

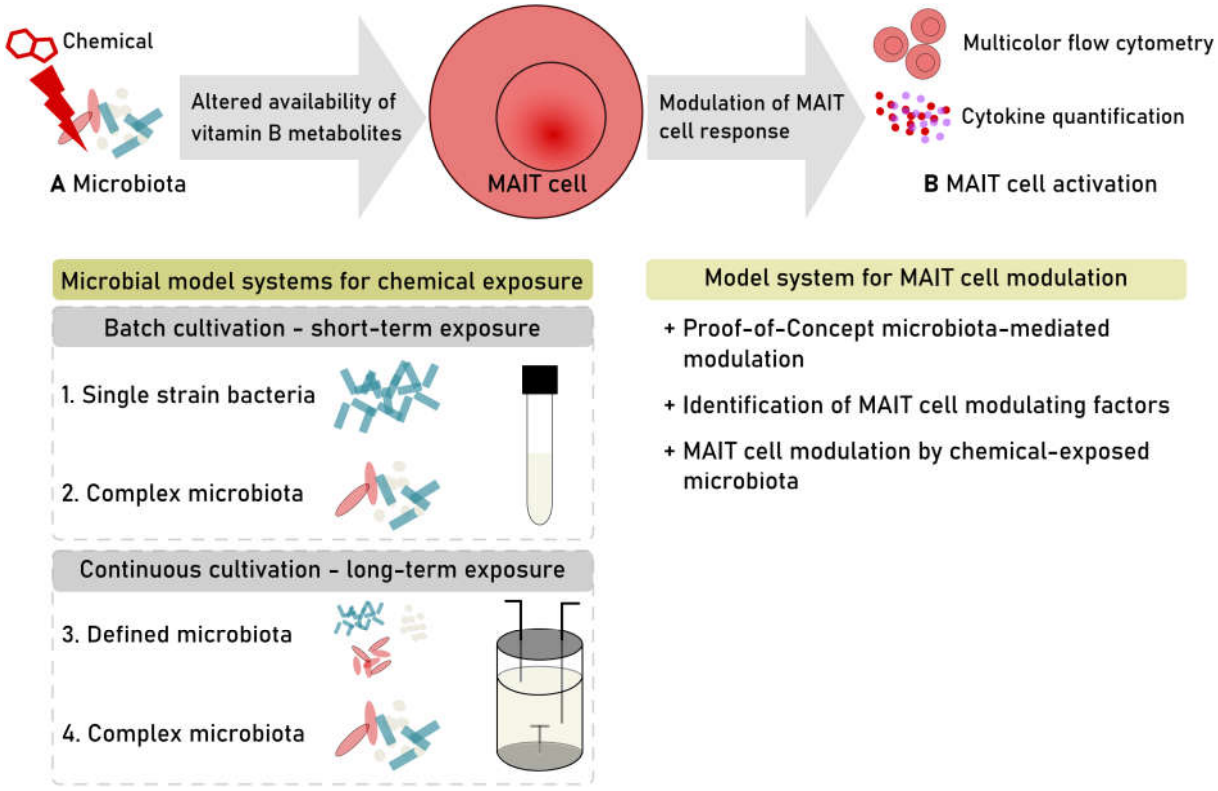

Figure 1. Graphical summary of topics addressed in the present PhD project. A – To investigate microbiota-modulating effects of chemicals suitable model systems for short- and long-term exposure of microbiota have been established. B – The concept of MAIT cell modulation *via* microbiota has been proven and then used in further analyses.

The extended simplified human intestinal microbiota (SIHUMIx), a defined human intestinal model community, was established for bioreactor use since the low community complexity may allow the resolution of effects down to strain-level. By applying a multi-method approach, which combined analyses on the cellular, the protein, the DNA and the metabolic level, it was shown that SIHUMIx establishes reproducibly within the bioreactor system (publication 1). Starting at day five the community reached and maintained a constant state under undisturbed cultivation conditions (publication 1 and publication 2). After the successful establishment of SIHUMIx for bioreactor use, the effect of a short term drop in pH on the community during cultivation was investigated. This disturbance was used to determine the resistance and resilience of SIHUMIx against an unspecific, but severe perturbation. Metaproteomics revealed that SIHUMIx was barely affected on the taxonomic level, whereby on the single cell level (microbial flow cytometry) and the functional level (short-chain fatty acid profile) SIHUMIx changed considerably. After the perturbation ended, the community recovered to the constant

state and thereby prove high resilience against the pH reduction (publication 1). In contrast, SIHUMIx showed high resistance against varying system retention times (publication 2). Similarly, SIHUMIx was only slightly affected by Bisphenol s exposure at 45 µM both on the taxonomic and functional level (publication 8). However, these experiments indicated, also due to the low complexity, that SIHUMIx is an appropriate model system to investigate the effects of chemicals on community taxonomy and function in detail.

Both batch and continuous cultivation procedures have been utilized to assess the microbiota-modulating properties of glyphosate. Exposure of *Escherichia coli*, *Bifidobacterium adolescentis* and *Lactobacillus reuteri* to 300 mg/L glyphosate during exponential growth in batch culture only showed minor effects on growth, riboflavin and folate biosynthesis (publication 4). During continuous cultivation, the effects of a high glyphosate concentration (900 mg/L) on the taxonomic and functional level of porcine microbiota were addressed by a multi-omics approach, including metaproteomics, 16S rRNA gene analysis, and untargeted as well as targeted metabolomics. Only slight effects on community function and no changes on the taxonomic level were observed (publication 6). In this context a sensitive method for glyphosate quantification from bioreactor liquids has been established (publication 5).

Furthermore, the effects of the most common bisphenols, bisphenol A, bisphenol F and bisphenol S, have been compared in batch culture using the bacterial single strains *Bacteroides thetaiotaomicron* and *Escherichia coli* as well as human fecal microbiota. Only at the highest bisphenol concentration microbial growth, viability and metabolism were affected, whereby all microbiota showed individual susceptibility toward bisphenol exposure. However, the microbiota-modulating properties of bisphenol A were strongest and those of bisphenol S weakest (publication 7).

In a proof-of-concept experiment microbial acid stress of SIHUMIx was linked to a decreased MAIT cell activating potential, which was mediated by a reduced availability of riboflavin. In contrast, the ability of SIHUMIx to activate MAIT cells was associated with undisturbed cultivation. More factors were identified that determine the strength of MAIT cell activation *in vitro*. I.e., microbial diversity and community compositions affected the MAIT cell activating potential of microbiota (publication 3). After the concept has been validated, the microbiota-

mediated MAIT cell modulating effects of glyphosate and chlorpyrifos were investigated in batch culture. Chlorpyrifos, but not glyphosate did alter the MAIT cell activating potential of *Escherichia coli*, *Bifidobacterium adolescentis* and *Lactobacillus reuteri* at the tested concentrations (publication 4). Furthermore, bisphenol A, bisphenol F and bisphenol S were shown to affect microbial metabolism of *Bacteroides thetaiotaomicron*, *Escherichia coli* as well as human fecal microbiota at the applied concentrations. Though an altered MAIT cell-activating potential was only observed for the bacterial single strains, the MAIT cell activating potential on the fecal microbiota was not affected (publication 7).

With this PhD project the methodological groundwork was laid for the cultivation of complex intestinal microbiota to assess the microbiota-modulating effects of environmental chemicals. Besides, this work has applied established model systems to determine the modulating effects of glyphosate, chlorpyrifos and bisphenols on microbiota and potentially associated effects on MAIT cell activation and thereby prove suitable to investigate the adverse effects of environmental chemicals on intestinal microbiota and immune cells. The utilization of these model systems may facilitate chemical risk assessment regarding adverse effects on intestinal microbiota and immune cells in the future.

1 INTRODUCTION

1.1 The human intestinal microbiota

Defining the healthy human microbiota

The intestinal microbiota, similar to the microbiota at other body sites, co-evolved with the human host (Ley et al., 2008). The human microbiota encompasses all microorganisms that live in mutualistic relationship in and on the human body, but also pathogenic, pathobiontic and opportunistic representatives can inhabit the microbiota. Already at the beginning of the 20th century, microbiologist recognized the importance of the intestinal microbiota for health and disease (Kendall, 1909). Primary intestinal pathogens, such as *Salmonella enterica subsp. enterica* or *Vibrio cholerae*, directly upon infection cause symptoms also in healthy individuals (Perez-Lopez et al., 2016). Pathobionts cover members of the intestinal microbiota like *Clostridium difficile* and *Helicobacter pylori*, whereby opportunistic pathogens are acquired from the environment and can endure for years within the host intestine without causing symptoms, e.g. *Listeria monocytogenes* (Chow et al., 2011; Manges et al., 2016; Perez-Lopez et al., 2016). Similarly, pathobionts and opportunists become symptomatic in immune-compromised individuals (Perez-Lopez et al., 2016).

Only since recently humans are considered as superorganisms living in mutualistic symbiosis with their microbial counterpart (Bäckhed et al., 2005; Ley et al., 2006). In mutualistic relationships, both the human host and the microbiota itself benefit from each other, a consequence of the continuing co-evolution (Ley et al., 2008). In the intestinal tract, the microbiota came upon a warm and nutrient-rich ecosystem. Simultaneously, the host acquired the microbial enzyme-repertoire that is helpful for digestion, whereby the microbes itself are important for immune system education (Maynard et al., 2012). The human intestinal microbiota encompasses the microbiota of the complete intestinal tract with a major focus on the densely populated regions, the small and the large intestine (**Figure 2**).

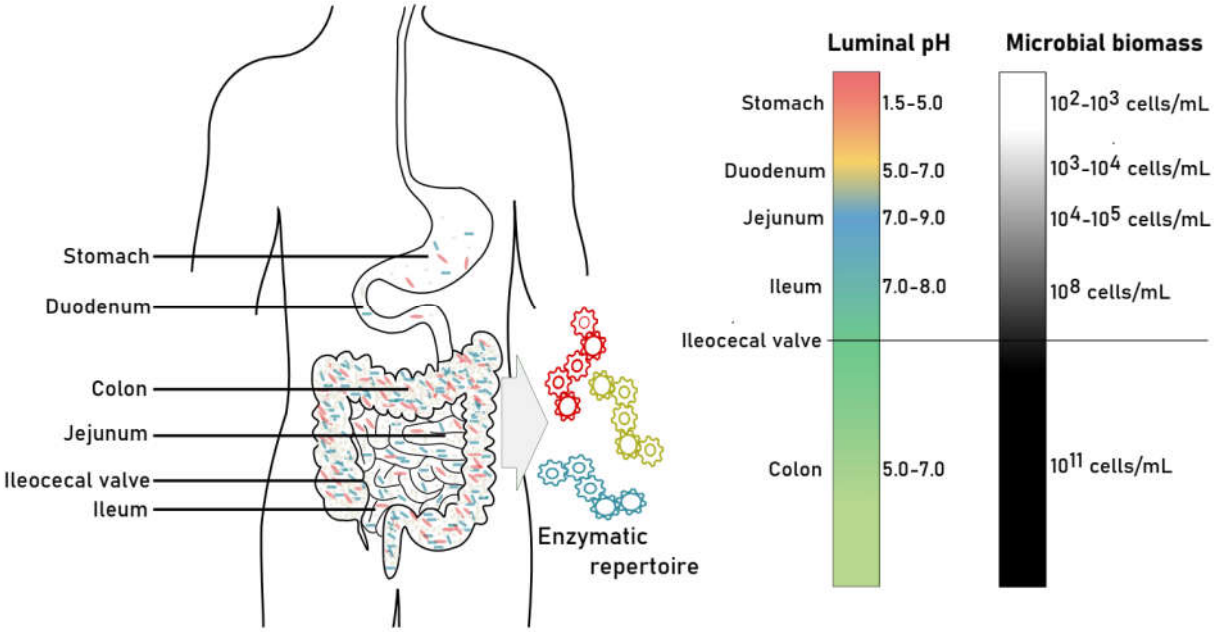

Figure 2. The human intestinal tract. The sections of the human intestinal tract differ with regard to luminal pH and microbial biomass. Starting from the stomach the pH increases down to the ileum and then slightly decreases in the colon. The microbial biomass increases and reaches a maximum in the colon. Figure adapted from (Walter and Ley, 2011).

Physiological parameters, such as pH and transit time, support digestion and thus nutrient availability for the host and thereby influence the microbial density within the intestinal tract. The microbial density increases from the stomach to the colon. The colon is among the most densely colonized ecosystems on earth harboring an equal number of microbial cells compared to the human body (Bäckhed et al., 2005; Sender et al., 2016).

Similar to other ecosystems, the intestinal microbiota can be described with ecological principles. These consider the intestinal community as a whole, whereby the communities at homeostasis maintain ecosystem function and service predominantly relevant for human health (Ley et al., 2006; Lloyd-Price et al., 2016; Relman, 2012). The intestinal microbiota relies on diversity and the stability properties resistance and resilience (Grimm et al., 1992; Levy et al., 2017a; Lloyd-Price et al., 2016; Relman, 2012). Diversity defines the species richness and evenness of the intestinal microbiota and is directly associated with the community stability properties. Resistance and resilience are community properties that describe the ability of a community to withstand a perturbation or to recover after a perturbation ends (Grimm et al., 1992; Levy et al., 2017a).

In combination with the longitudinal alterations within the intestinal microbiota taxonomy throughout life (Rajili▮-Stojanovi▮ et al., 2013), the existence of several healthy community states at equilibrium is anticipated (Levy et al., 2017a; Lozupone et al., 2012; Relman, 2012). These equilibrium states are dynamic as they undergo permanent changes (Sommer et al., 2017). The effect on the community upon perturbation depends on the intensity, the frequency and duration of the perturbation (Relman, 2012). When a perturbation exceeds the resistance and resilience of microbial community at equilibrium, the microbiota shifts to another equilibrium state.

Such a shift can have beneficial, detrimental or neutral implications for the host. A healthy intestinal microbiota maintains a healthy functional state despite the various external and internal factors, which can also be weighed as minor perturbations (Lloyd-Price et al., 2016; Lozupone et al., 2012). Insofar the effect is detrimental for the host the community state moved toward a dysbiotic state. Dysbiotic microbiota differ from healthy microbiota to that they functionally contribute to disease following the Koch's postulates (Levy et al., 2017a; Sommer et al., 2017; de Vos and de Vos, 2012). So far, the only consistency regarding dysbiotic microbiota is a loss of microbial diversity (Mosca et al., 2016). Most studies associate or correlate specific phenotypes to disease. Causal analysis, elucidating the effects of dysbiosis, are still shorthanded, though data is sparse albeit the number is increasing (de Vos and de Vos, 2012).

Within the human population, more than 1000 species were shown to potentially colonize the human intestinal tract (Almeida et al., 2019; Lagier et al., 2016). Out of these thousands of species, on average ~160 species were observed per healthy individual (MetaHIT Consortium et al., 2010; Turnbaugh et al., 2007), which extend the host genome by the bacteria-encoded genes – the intestinal genome (microbiome). The intestinal microbiome exhibits > 150 times more genes than its human host (Bäckhed et al., 2005; MetaHIT Consortium et al., 2010). On the one hand the healthy intestinal microbiota shows astonishing variation across healthy individuals (Eckburg, 2005), on the other hand surprisingly high functional similarity (Lozupone et al., 2012; MetaHIT Consortium et al., 2010; Turnbaugh et al., 2007). Over the last decade, thus scientist have moved from haunting the core gut microbiota, which aimed to identify individual species associated with health or disease, respectively, toward the identification of the healthy

gut microbiome, or being more specific, the functional core of healthy intestinal microbiota (Shafquat et al., 2014).

A healthy intestinal microbiota supports the enzymatic repertoire of the host and exhibits specific functions. I.e., the microbiota protects from the invasion of pathogenic microorganisms, which is called colonization resistance, and relies on the competition of the commensal and invading microorganisms for the same nutrients (Belkaid and Hand, 2014; Van der Waaij et al., 1971). To date it is estimated that up to 50% of the functions bestowed from the intestinal microbiota remain unknown (Costello et al., 2009; Lloyd-Price et al., 2016), suggesting future research to further elucidate these functions and the host-microbiota-interactions.

Factors that shape the intestinal microbiota

Which factors and to what extent these factors shape the intestinal microbiota is still part of an ongoing debate (Blaser, 2017; Rothschild et al., 2018). The human host and the intestinal microbiota rely on each other in a mutualistic symbiosis due to the co-evolution (Ley et al., 2006, 2008). By inhabiting the host and host behavior, the intestinal microbiota is shaped by a variety of internal and environmental factors (**Figure 3**).

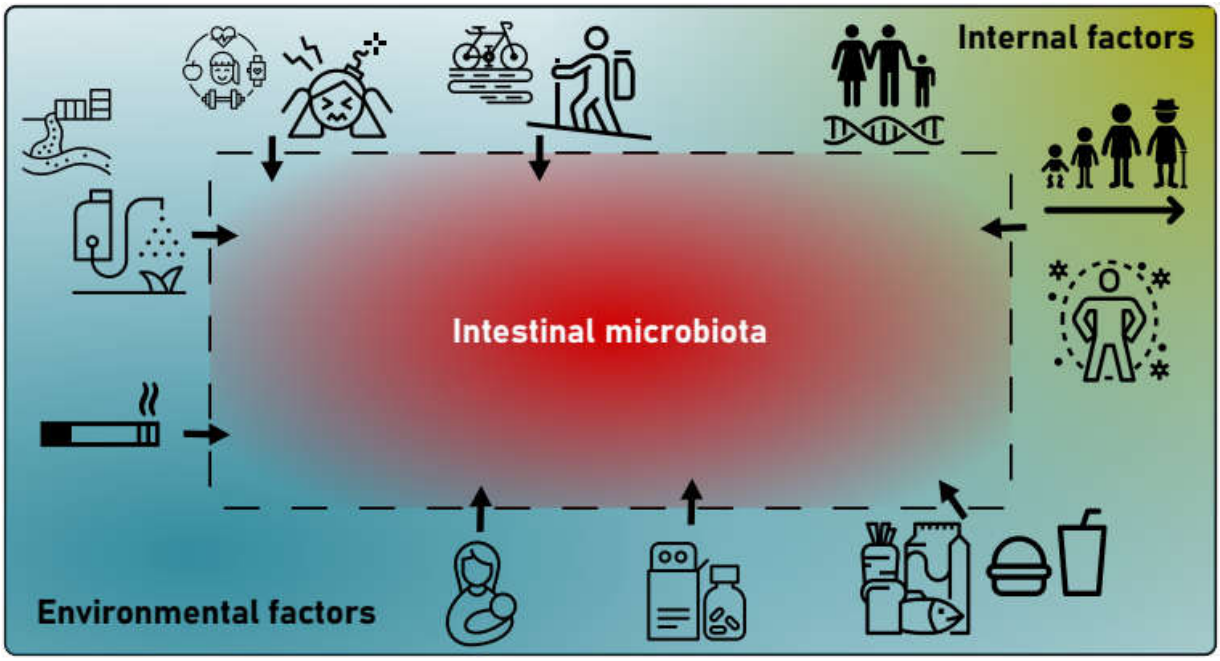

Figure 3. Factors that influence the intestinal microbiota. Internal factors such as host genetics, age and immune status affect the intestinal microbiota. Similarly, environmental factors like diet, mediaction, exposure to chemicals, stress and physical activity shape the intestinal microbiota.

E.g. host genetics, the aging process and the host immune system as a few examples constantly shape the intestinal microbiota (an vice versa, Goodrich et al., 2014; Org et al., 2015), whereby host genetics only play a minor role. Single nucleotide polymorphisms in mucin-encoding genes, e.g., can affect the intestinal microbiota composition in a bovine intestinal model, as the mucus composition favors growth of specialized mucus-degrading intestinal microbiota representatives (Fan et al., 2020). The host immune system controls intestinal colonization level by the secretion of secretory immunoglobulin A (sIgA), the most abundantly produced human antibody. SIgA then binds to the microbes, though the underlying mechanism are not fully understood (Pabst and Slack, 2020). Environmental factors associated with diet and lifestyle, such as medication, smoking, stress, physical activity etc., in a large part influence the composition of the intestinal microbiota (Rothschild et al., 2018).

At birth, newborns initially come in contact to microorganisms. Humans acquire their microbiota by mixed-mode transmission, which combines vertical transmission from the mother and horizontal transmission from the environment (Shapira, 2016). The mode of delivery is one of the first factors influencing microbiota composition. After vaginal birth newborns harbor predominantly vaginal microbiota and in contrast, babies born by caesarian section are colonized with the mothers' skin and oral microbiota (Bäckhed et al., 2015; Dominguez-Bello et al., 2010). The intestinal microbiota of vaginally born infants is initially high in *E. coli*, which then declines. *Bifidobacterium* sp. earlier colonize the infant gut at high abundances when born vaginally. In contrast, infants born by C-section showed a higher abundance of *Klebsiella* sp. and *Enterococcus fecalium.* Differences related to the mode of delivery perceived during the first months of life and declined within the first year of life (Chu et al., 2017; Reyman et al., 2019). The community functions adapt very early, presumably before extensive contact to other external factors start to shape community taxonomy (Chu et al., 2017; Kostic et al., 2015). Once infants start to take up more solid and more varied food, the microbiota successionally shifts towards an adult-like community state (Bäckhed et al., 2015; Conlon and Bird, 2014; Zhong et al., 2019) but does not reach adult-like configuration until the age of five (Cheng et al., 2016). Most importantly, the alpha-diversity, representing the number of observed species in the intestine, increases and the microbiota develops toward an individual-specific microbiota (Cheng et al., 2016; Kostic et al., 2015; Zhong et al., 2019). However

community structure and function of the maturing intestinal microbiota can persistently be affected by various factors, such as the gestational age, the mode of delivery, breast-feeding vs. formula-feeding, and the duration of breast-feeding, the afterwards fed pre-school diet (Bäckhed et al., 2015; Blaser, 2017; Bokulich et al., 2016; Dethlefsen and Relman, 2011; Zhong et al., 2019).

Urbanization also affect the intestinal microbiota by a higher level of sanitation, antibiotics use and simultaneously a lower level of outdoor activity. People grown up in city environments have less diverse microbiota and show a higher degree of inflammatory diseases (Tasnim et al., 2017). In contrast, early-life exposure to environments high in microbiota, e.g. on a farm in rural areas with contact to soil, animals etc., was shown to increase children health and diversify the intestinal microbiota (Mosca et al., 2016). Horizontal transmission of microbiota from the soil environment might also increase gut microbial diversity (Zhou et al., 2016). Recent studies reported that house-hold sharing leads to an approximation of the intestinal microbiota composition (Rothschild et al., 2018). To date, the patterns of microbiota transmission from the environment to the intestine to date remains elusive (Tasnim et al., 2017). Concluding, a large variety of factors determines the establishment of the individual intestinal microbiota leading to a marked variation between individual. The majority of variation can be explained by ethnicity, age and geography (Deschasaux et al., 2018; Huttenhower et al., 2012; Tasnim et al., 2017).

Once established, individual-specific microbiota remain in an equilibrium state in healthy adults (Faith et al., 2013), with a stable and an unstable, fluctuating proportion (Shapira, 2016). Nevertheless, the intestinal microbiota undergoes constant changes during a life-time (Rajili▮-Stojanovi▮ et al., 2013). The ingested diet is one of the most important environmental factors that permanently alters the intestinal microbiota composition and function (Gentile and Weir, 2018; Shapira, 2016). Diet can quickly, on a daily time scale, affect microbial composition in the intestine (David et al., 2014) and thus is thought to account for the normal, longitudinal variation in the intestinal microbiota, but also for the inter-individual variation (Rajili▮-Stojanovi▮ et al., 2013; Shapira, 2016). But also less obvious environmental factors like physical exercise (Mailing et al., 2019), physical and psychological stress (Karl et al., 2018) and life-style habits, such as smoking (Savin et al., 2018) act on the intestinal microbiota.

Since the industrial revolution, nutrition changed in the Western world including the United States, Canada and Western Europe. The intake of highly refined foodstuffs, such as grain flours, sugar and vegetable oils, as well as processed and animal-based food dramatically increased until today. Simultaneously, the consumption of coarse grains, fresh fruit and vegetables decreased. This lead to an elevated uptake of sugar, fat and animal products in the Western diet, parallel to a decreased fiber consumption, making the Western diet a high fat, high sugar, low fiber diet (Cordain et al., 2005; Popkin et al., 2012). However, since the 1990s, Western dietary patterns begun to spread in the developing and emerging countries, resulting in a Westernization in diet (Popkin et al., 2012).

All macronutrients, carbohydrate, fat and protein, were shown to affect the microbial composition and function in the intestine, as the composition of available nutrients favor microbial species that are capable of their utilization (Gentile and Weir, 2018). A high fat diet e.g. increased the amount of lipopolysaccharide in the circulation, suggesting an increase in intestinal permeability (Conlon and Bird, 2014; Moreira et al., 2012). Moreover, high fat diet was shown to favor inflammation in the intestine and in parallel induces the expression of microbial genes necessary for conversion of primary bile acids into secondary bile acids. Together these events elevate the risk for colon cancer (O'Keefe et al., 2015). Elevated protein levels from an animal-based diet are considered beneficial. These proteins deliver essential amino acids to the host and serve as nitrogen source for the intestinal microbiota (Conlon and Bird, 2014). In turn, the microbiota is capable of synthesizing beneficial metabolites from these amino acids, such as indoles and phenols, but also toxic metabolites like N-nitroso compounds, which can elevate cancer risk (Gentile and Weir, 2018). Dietary carbohydrates are the best studied macronutrients and can be divided in simple and complex carbohydrates. Simple carbohydrates include both mono- and oligo-saccharides, like glucose, fructose or sucrose. These simple carbohydrates are almost completely absorbed in the small intestine delivering energy to the host (Flint et al., 2012). Complex carbohydrates, or more specifically microbiota-accessible carbohydrates (MACs), such as resistant starch, xylan, pectin or arabinose cannot be digested by the human host (Kaoutari et al., 2013; Sonnenburg and Sonnenburg, 2014). The intestinal microbiota facilitates the digestion of these otherwise non-digestible MACs, for which humans lack the enzymatic repertoire (Ley et al., 2006; Sonnenburg and Sonnenburg, 2014). Thus, MACs pass

the small intestine and reach the colon for microbiota-facilitated degradation (Flint et al., 2012). For the specialized colonic microbiota, MACs resemble the most important energy source (Flint et al., 2012; Gentile and Weir, 2018). This reflects in an enrichment of genes from carbohydrate metabolism in commonly observed functions, encompassing 24% of the observed genes in adult colonic microbiota (Kurokawa et al., 2007). For energy supply, the colonic microbiota stepwise hydrolyze MACs into monosaccharides, which are afterwards fermented to essential, functional metabolites, the short-chain fatty acids (SCFAs, Cummings, et al., 1987). The most abundant SCFAs found in the colon are acetate, propionate and butyrate in decreasing concentration, representing 95% of the synthesized SCFAs (Ríos-Covián et al., 2016). Various bacteria can produce acetate, whereas propionate and butyrate synthesis is restricted to specific bacterial species (Louis et al., 2007; Reichardt et al., 2014). For SCFA synthesis, the microbiota rely on cross-feeding within the community and especially acetate is essential for butyrate production (den Besten et al., 2013a). Furthermore, caproate and branched short-chain fatty acids (BSCFAs) are produced. BSCFAs, such as isobutyrate, isovalerate, and 2-methylbutyrate, are synthesized from the branched amino acids valine, leucine and isoleucine (Rios-Covian et al., 2017). Estimated 95% of SCFAs and BSCFAs are instantly absorbed by the epithelium for utilization by the host (Roy et al., 2006). Indicating that SCFAs are important players in the mutualistic relationship between host and microbiota (Gentile and Weir, 2018).

Shifting the diet, e.g., toward lower MAC concentrations instantly resulted in a reduced production of SCFAs (David et al., 2014) and a loss of taxa from the intestinal microbiota. This loss of microbial diversity only partially recovered after return to a high MAC diet. Of far greater concern is that an altered microbiota could be inherited to future generations by vertical transmission during birth. This might at least partially explain the loss of microbial diversity in the Westernized world (Sonnenburg et al., 2016) and the increase of chronic inflammatory diseases (Hand et al., 2016). Especially inflammatory bowel disease is characterized by a loss of microbial diversity and, due to a starving microbiota that is caused by MAC restriction, extensive mucus-degradation (Gentile and Weir, 2018).

Accordingly, several factors have a profound impact on the intestinal microbiota composition and function. Perturbations, especially during crucial developmental stages, might pave the way for the initiation of chronic inflammatory diseases, which are an increasing health concern

(Blaser, 2017; Hand et al., 2016). A healthy intestinal microbiota is essential for host development, as the intestinal microbiota affects human health in various ways (Shapira, 2016).

The intestinal microbiota influences the human host

There is a bi-directional dialog between the host and the intestinal microbiota (Maynard et al., 2012). Most obvious, the intestinal microbiota protects the host from the invasion of pathogenic microorganisms, which is termed colonization resistance (Van der Waaij et al., 1971). Due to the enormous genetic potential of the microbiota (MetaHIT Consortium et al., 2010), metabolic processes of the microbiota affect the host, which is mediated by small molecules or metabolites (Li et al., 2018b; Oliphant and Allen-Vercoe, 2019). Approximately 50% of metabolites detected in feces and urine are modified by or derive from the intestinal microbiota (Zheng et al., 2011).

Metabolic processes encompass the *de novo* synthesis of metabolites and the modulation of host-metabolites and xenobiotics (Blacher et al., 2017; Collins and Patterson, 2020; Koppel et al., 2017; Spanogiannopoulos et al., 2016). Bioactive representatives thereof are involved in a variety of host processes as well as mucosal and systemic immune maturation (**Figure 4**, Blacher et al., 2017).

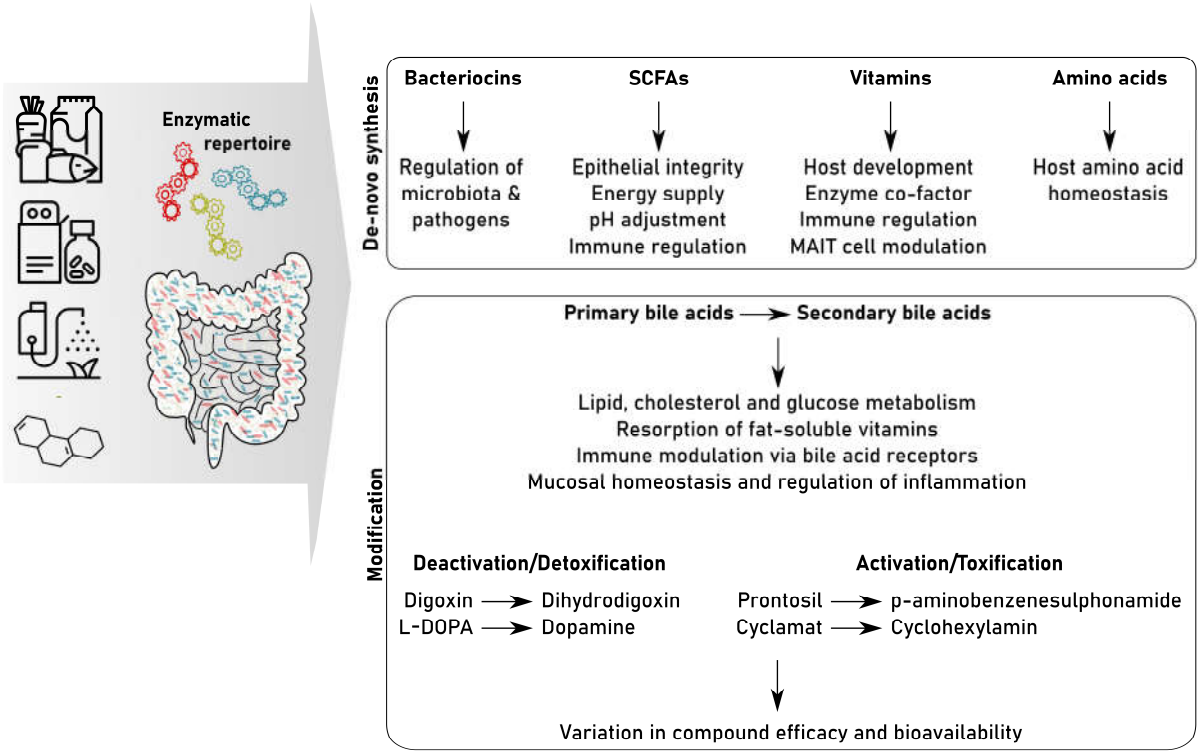

Figure 4. The intestinal microbiota is essential for metabolite synthesis and modification. The huge microbial enzymatic repertoire in the intestine facilitates the *de-novo* synthesis and the modification of metabolites, which can derive from the host, diet, medication or environmental chemicals.

The intestinal microbiota produces a variety of metabolites *de novo.* Short-chain fatty acids (SCFAs) are an important microbiota-derived metabolite group with various functions in the human host. By the *de novo* production of SCFAs, such as acetate, propionate and butyrate, the microbiota lowers the colonic pH preventing overgrowth of pH-sensitive microorganisms e.g. from the genera *Clostridia* or *Enterobacteria,* which also include pathogenic members (den Besten et al., 2013b). Furthermore, SCFA resemble an important energy source for the intestinal epithelial cells, with butyrate being the most important SCFA there (Hague et al., 1996). Moreover, SCFAs provide energy for the host in more distant organs, such as the liver, the heart and kidneys and affect host metabolism in the periphery and the immune system (den Besten et al., 2013b). Microbiota-derived bacteriocins regulate the microbiota composition and eliminate pathogens and some microbiota derived amino acids and vitamins constitute other bioactive metabolites (Li et al., 2018b). Vitamins are essential for the host and consequently have to be supplied exogenously (LeBlanc et al., 2013). They either derive from the diet or are synthesized *de novo* by prototrophic members of the intestinal microbiota. The microbiota, especially lactic-acid bacteria and *Bifidobacteria*, predominantly supplies the host with vitamin K and water-

soluble B-group vitamins (Hill, 1997). Furthermore, vitamins are cross-fed with auxotrophic species in the gut, which cannot produce these vitamins themselves (Magnusdottir et al., 2015; Rodionov et al., 2019). B-group vitamins are essential co-factors for enzymes involved in a variety of metabolic processes (LeBlanc et al., 2017). Riboflavin e.g. is essential for the conversion into flavin mononucleotide (FMN) and flavin adenine dinucleotide (FAD, Gutiérrez-Preciado et al., 2015; García-Angulo, 2017). FMN and FAD serve as co-factors in flavoenzymes and thus are essential for energy metabolism, oxidative stress response or the activation of other vitamins in the microbiota, but also in the host (García-Angulo, 2017). Moreover, riboflavin and folate are recognized by specialized immune cells, the mucosal-associated invariant T cells (Kjer-Nielsen et al., 2012). But also other vitamins, such as vitamin A and vitamin D, can modulate the immune system (Mora et al., 2008).

In addition to the *de novo* synthesis of metabolites, the intestinal microbiota modulates dietary metabolites, e.g. tryptophan, xenobiotics and host metabolites such as primary bile acids into bioactive compound. Bile acid (BA) metabolism follows a cyclic process of production, transport and recycling termed enterohepatic circulation. Primary bile acids (BAs), such as cholate or chenodeoxycholate, are synthesized in a multi-enzyme reaction in the liver (Singh et al., 2019; Wang et al., 2018). From there, primary BAs are secreted and collected in the gall bladder for bile formation. Bile comprises of 67% BAs, phospholipds and cholesterol in the soluble fraction as well as bile pigments (de Aguiar Vallim et al., 2013), which are then secreted into the duodenum in mixed micelles (Jia et al., 2018). There, BAs facilitate the resorption of lipids and fat-soluble vitamins due to their amphiphatic properties and are involved in various metabolic processes and BA- and bilirubin excretion (de Aguiar Vallim et al., 2013). Due to their antimicrobial properties BAs can alter the microbiota composition and, in turn, the microbiota affects the BAs pool (Jia et al., 2018; Wang et al., 2018) by the production of secondary BAs by structural conversion of primary BAs (Ridlon et al., 2006). The majority of BAs are absorbed in the distal ileum and transported back to the liver, where they are recycled (Jia et al., 2018). BAs bind to a variety of receptors for down-stream signaling, like the intestinal farnesoid X receptor (FXR), pregnane X receptor (PXR), constitutive androstane receptor (CAR), vitamin D receptor and the G-protein coupled receptor TGR5, whereby the intestinal microbiota was shown to potentiate BA-signaling through the two most important BA-receptors FXR and TGR5 (Jia et al., 2018).

Both these receptors are expressed by immune cells, such as monocytes, macrophages or NKT cells, and BAs also influence mucosal homeostasis and inflammation in the intestine (Chen et al., 2019; Schubert et al., 2017).

Xenobiotics denote foreign compounds, such as pharmaceuticals, food additives or environmental chemicals that potentially contaminate our food or drinking water (Collins and Patterson, 2020; Koppel et al., 2017; Spanogiannopoulos et al., 2016). Modulation of pharmaceuticals was observed already one century ago (Colebrook, 1936) and today it is approved that the microbiota interferes with pharmacokinetics in various ways. The microbiota inactivates pharmaceuticals, like Digoxin or L-DOPA, or activates xenobiotics into the bioactive compound as it has been proved for Prontosil and cyclamate (Koppel et al., 2017; Spanogiannopoulos et al., 2016). Similarly, the microbiota may toxify or detoxify environmental chemicals that enter the human body and thus be beneficial or harmful for the host (Collins and Patterson, 2020). However, the inter-individual variation of the intestinal microbiota can attribute for differences in enzyme activity and thus for the different susceptibility of individuals to pharmaceuticals or environmental chemicals (Spanogiannopoulos et al., 2016).

Some metabolites also influence more distal parts of the host, like the central nervous system, or the immune system in a bi-directional cross talk between the microbiota and immune system components (Blacher et al., 2017; Sharon et al., 2016).

The connection between intestinal microbiota, chronic inflammatory diseases and MAIT cells

Multifactorial immunologic chronic diseases (CIDs), such as IBD, T2D, obesity, or multiple sclerosis (MS), are of rising global concern (Hand et al., 2016). E.g. inflammatory bowel diseases (IBD) evolved in the US and in parts of Europe in the elderly population before 1940 simultaneous to industrialization (**Figure 5. Global incidence of inflammatory bowel disease (IBD) before 1940, in 1970 and in 2015.** The incidence of chronic inflammatory diseases, such as IBD increased especially in the Westernized World.2013a). Since then, the incidence of IBD among the total population started to increase in industrialized countries of North America, Europe and Oceania. Today IBD is a public health burden in the industrialized Western world as well as in newly industrialized countries around the globe, with still rising incidence (Kaplan, 2015; Kaplan and Ng, 2017; Ng et al., 2017). Similarly, the incidence and prevalence of other multifactorial, chronic inflammatory diseases (CIDs), such as Type II diabetes (T2D), obesity, and multiple sclerosis (MS) evolve in parallel to industrialization (Blüher, 2019; Filippi et al., 2018; Zheng et al., 2018). Especially for IBD and MS etiology is not fully understood, but scientist agree that genetic predisposition together with the impact of environmental and immunological factors initiate disease onset and promote disease progression (Kaplan, 2015; Milo and Kahana, 2010; Van Kaer et al., 2019).

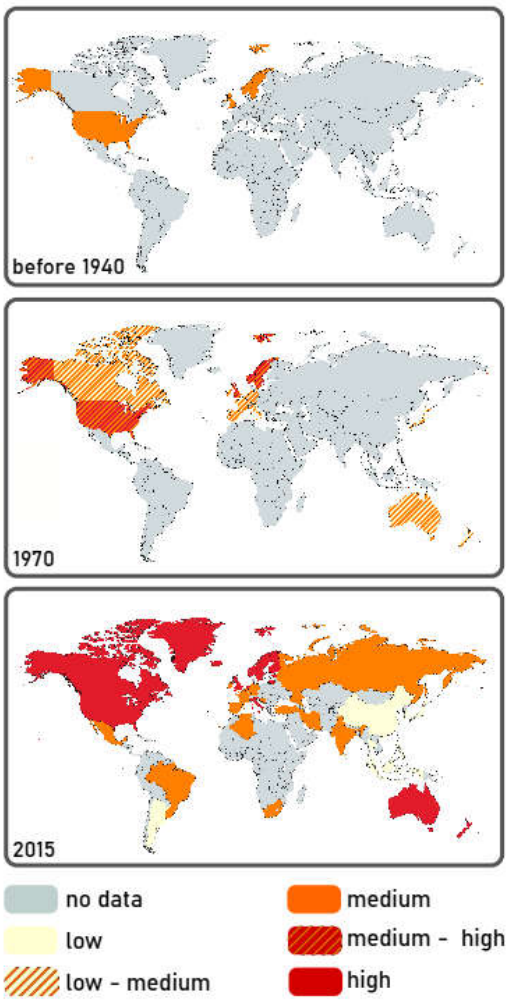

Figure 5. Global incidence of inflammatory bowel disease (IBD) before 1940, in 1970 and in 2015. The incidence of chronic inflammatory diseases, such as IBD increased especially in the Westernized World.

Patients suffering from CIDs possess less diverse intestinal microbiota (Blüher, 2019; Jangi et al., 2016; Manichanh et al., 2012; Turnbaugh et al., 2009; Zheng et al., 2018), but it is not clear

whether the reduced diversity is cause or consequence (Maynard et al., 2012). Furthermore, the epithelial barrier in CIDs frequently is impaired, resulting in increased intestinal permeability termed *leaky gut syndrome* (Mu et al., 2017). Interestingly, mucosal-associated invariant T (MAIT) cells are involved in the CIDs, though their actual role and function still have to be elucidated.

1.2 The human immune system

The distinction between adaptive and innate immunity is blurred

Since all living organisms have to fight pathogens, suitable defense systems evolved with innate immunity being evolutionary old compared to the adaptive immunity (**Figure 6**, Suckale et al., 2005).

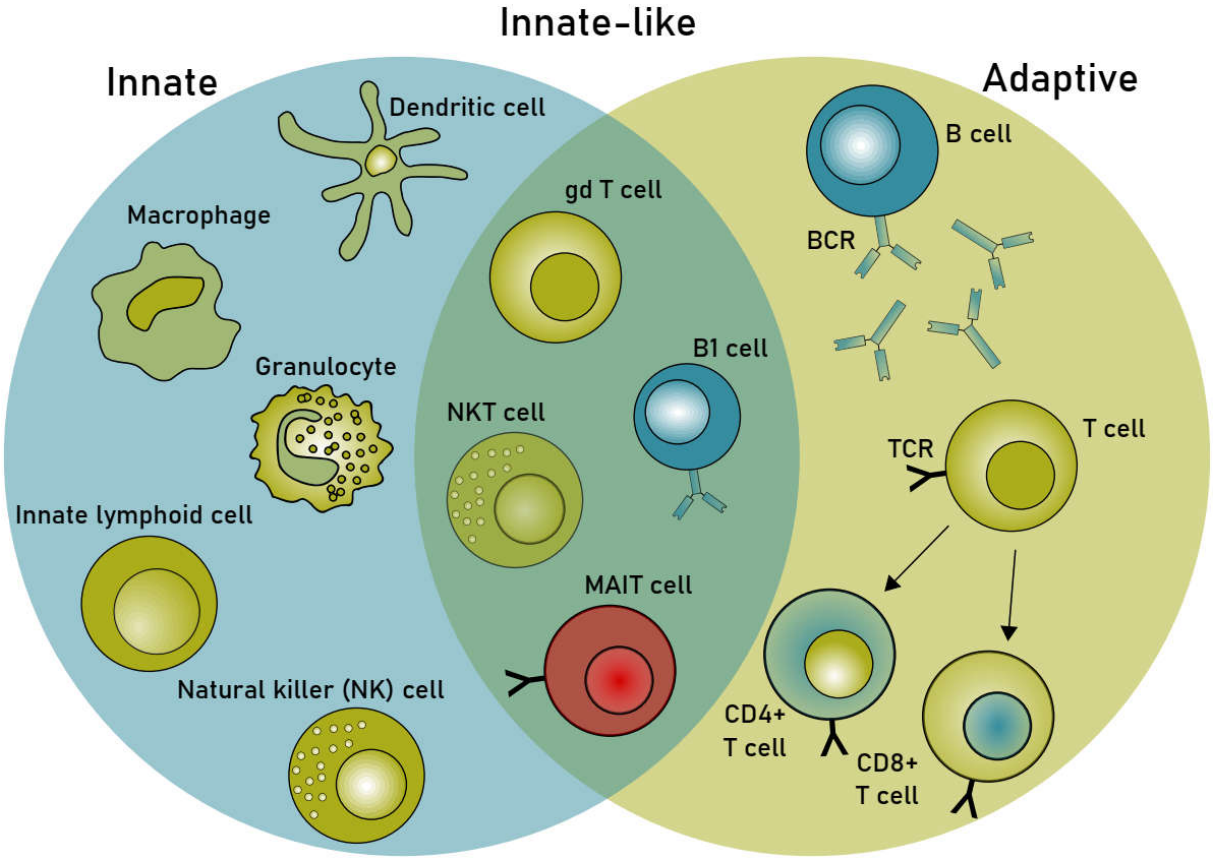

Figure 6. Overview of innate, innate-like and adaptive immune cells. The human immune system comprises of an innate and an adaptive arm of immunity and the functions are orchestrated by corresponding immune cells. Since recently, this classification has been extended by innate-like immune cells, which have both innate and adaptive properties.

Innate immune responses rely on the recognition of pathogen- or more correctly microbe-associated molecular patterns (PAMPs, MAMPs, Koropatnick, 2004) *via* pattern recognition receptors (PRRs, Janeway, 1989). In humans, these PRRs are primarily expressed by phagocytic cells, such as granulocytes, natural killer (NK) cells, monocytes, macrophages and dendritic cells (DCs), of which macrophages and DCs represent professional antigen-presenting cells (APCs, Lanier and Sun, 2009; Takeuchi and Akira, 2010). PRRs engagement elicits a pattern-specific response within hours to eliminate the invading pathogens (Medzhitov and Janeway, 1997). In contrast, adaptive immunity is an evolutionary new characteristic (Flajnik and Dupasquier, 2004; Pancer and Cooper, 2006). Adaptive immune responses are facilitated by circulating bone-marrow (B)- and thymus (T)-derived lymphocytes and mediate cellular and humoral immunity (Pancer and Cooper, 2006). These cells mediated processes take more time for pathogen elimination, but are more specific. T and B cells express antigen-specific receptors, the B-cell (BCR) and the T-cell receptor (TCR), respectively. Due to the rearrangement of VDJ gene segments in the TCR and immunoglobulin gene locus both receptors show increased diversity and in sum can recognize a much higher number of antigens than PRRs (Flajnik and Dupasquier, 2004; Pancer and Cooper, 2006). Upon specific antigen presentation and binding, B cells and T cells, insofar required co-stimuli are available, are activated and then expand clonally to eliminate the pathogen and to generate immunological memory. This immunological memory, in case of a repeated antigen recognition, is much faster and more efficient in the elimination of the pathogen (Dranoff, 2004, 2005).

However, the concept of a distinct innate and adaptive arm of immunity becomes blurred by the discovery of innate-like immune cells (Flajnik and Dupasquier, 2004; Lanier and Sun, 2009). Naïve innate-like lymphocytes exhibit properties of effector cells by two means. First, these cells express activation and memory markers and second they rapidly exert effector function after stimulation, such as cytokine release or cytotoxic activity (Lanier and Sun, 2009). To date, most innate or adaptive immune cells have an innate-like counterpart, like B1 cells, NKT cells, γδ T cells or mucosal-associated invariant T (MAIT) cells (Dranoff, 2004; Lanier and Sun, 2009; Van Kaer et al., 2019). Among these innate-like immune cells the antigen receptor is denoted *unconventional*, because antigen-binding is more restricted compared to conventional T cells due to non-peptide antigen binding (Lanier and Sun, 2009).

MAIT cells are a particular innate-like T cell subset

MAIT cells are an evolutionary conserved, innate-like T cell subset, of which the majority is CD8 positive (Treiner et al., 2003, 2005). Combining innate and adaptive properties, these cells exhibit an effector-memory phenotype (Dusseaux et al., 2011) and have the ability to directly kill infected cells (Gold et al., 2010). Furthermore, MAIT cells can immediately exert effector functions, such as secretion of cytokines and cytotoxic molecules, upon antigen or cytokine recognition (**Figure 7**, Kawachi et al., 2006; Kurioka et al., 2015; Le Bourhis et al., 2010).

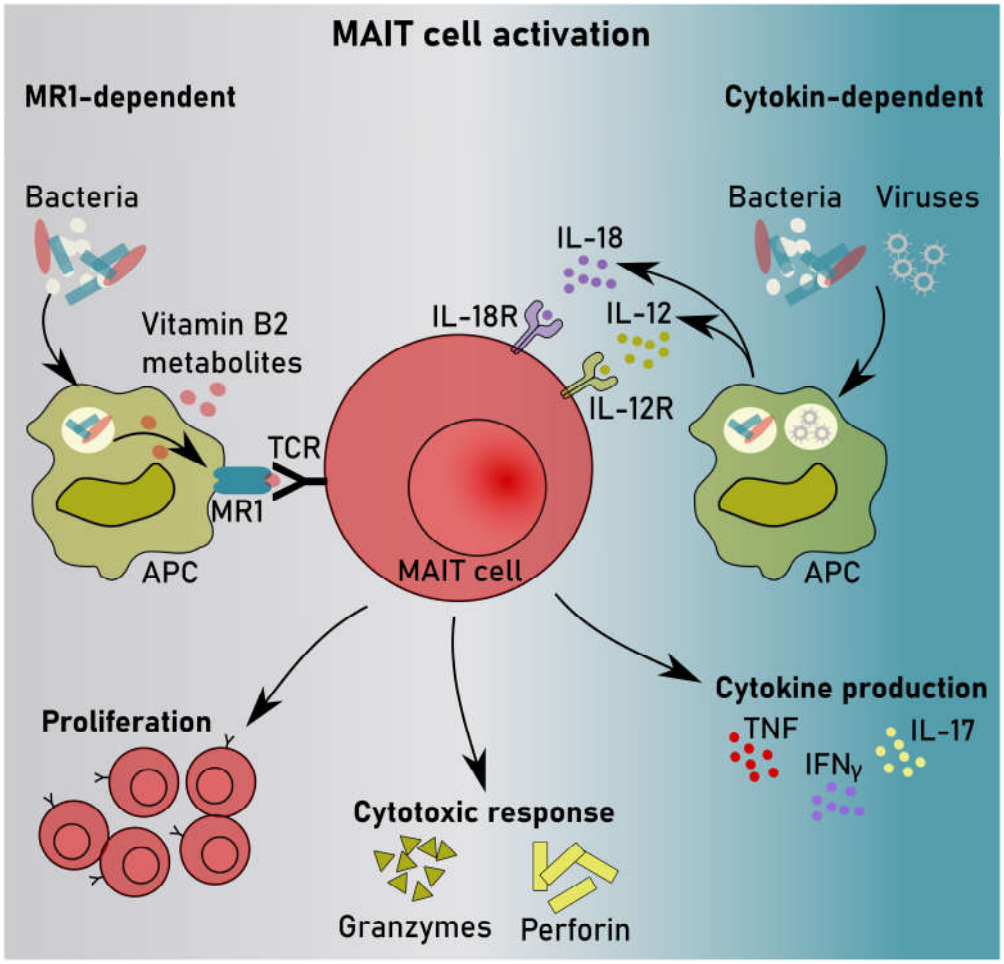

Figure 7. MAIT cell activation. MAIT cells can be activated MHC I-related protein 1 (MR1)-dependent, i.e. by the recognition of microbial riboflavin (vitamin B2) metabolites after presentation on MR1. In addition, MAIT cells can be activated in a cytokine dependent manner by the recognition of interleukine (IL)-12 and IL-18. Upon activation, MAIT cells proliferate and exert effector functions. I.e., the secret pro-inflammatory cytokines like TNF, IFNγ and IL-17 and cytotoxic molecules, such as granzymes or perforines.

Antigen presentation to MAIT cells is mediated via a non-classical major histocompatibility complex (MHC) class I molecule (denoted MHC class Ib), i.e. the MHC class 1-related protein 1

(MR1). The *Mr1* gene is expressed in all cell types (Huang et al., 2005) and this gene is highly conserved among mammals (Hashimoto et al., 1995; Riegert et al., 1998). Simultaneously, the MAIT cell T cell receptor (TCR) is restricted to MR1 and likewise shows high evolutionary conservation. The majority of MAIT cells express the semi-invariant alpha chain 7.2 (TCR vα7.2), which is encoded by the TRAV1-2 gene (TRAV1-2^{+} MAIT cells, (Gherardin et al., 2016; Kurioka et al., 2015; Tilloy et al., 1999). These MAIT cells recognize microbial metabolites from the riboflavin (vitamin B2) biosynthesis pathway in a MR1-dependent manner. However, a small fraction also recognizes folate (vitamin B9) metabolites after presentation on MR1 *in vitro* (Corbett et al., 2014; Eckle et al., 2015; Gherardin et al., 2016; Kjer-Nielsen et al., 2012). *In vitro* studies showed that the riboflavin precursors 5-(2-oxopropylideneamino)-6-D-ribitylaminouracil (5-OP-RU) and 5-(2-oxoethylideneamino)-6-D-ribitylaminouracil (5-OE-RU) activate MAIT cells, whereas the folate derivate 6-formylpterin (6-FP) and its synthetic analogue N-acetyl-6-formylpterin (Ac-6-FP) inhibit MAIT cell activation (Corbett et al., 2014; Kjer-Nielsen et al., 2012). In addition, MAIT cells can be activated MR1-independent in a cytokine-dependent manner via IL12 and IL18 (Ussher et al., 2014; Wilgenburg et al., 2016).

In the human body, MAIT cells reside at mucosal or barrier sites e.g. in the gut lamina propria (Treiner et al., 2003), the lung (Hinks et al., 2016), the female genital tract (Gibbs et al., 2017) and the skin (Teunissen et al., 2014). The localization of MAIT cell at barrier sites together with their ability to recognize and respond to microbial metabolites suggests a key role in host-microbiota-immune homeostasis (Napier et al., 2015). Furthermore, in humans MAIT cells account for to up to 10% of circulating T cells in peripheral blood (Tilloy et al., 1999) and with up to 50% of T cells they are common liver T cells (Dusseaux et al., 2011). Due to their high abundance in the liver, MAIT cells are suggested to contribute to the first line of defense against invading microorganisms especially from the intestine (Kurioka et al., 2016; Toubal et al., 2019), but their role in immunity still remains unclear (Godfrey et al., 2019). Recent research has focused on the MAIT cell activating potential of individual commensal and pathogenic microorganisms (Le Bourhis et al., 2013; Dias et al., 2017; Tastan et al., 2018). From these former studies it was assumed that microbial infections, and not commensal microbiota, trigger inflammation and thereby induce the entire repertoire of MAIT cell effector function (Tastan et al., 2018). Though, MAIT cells are not able to differentiate between commensal and pathogenic

bacteria due to antigen recognition and very little is known about the interaction of MAIT cells and commensal microbiota (Berkson and Prlic, 2017). However, fine-tuning of MAIT cell proliferation and effector functions, depending on location and stimuli, are suggested (Ghazarian et al., 2017).

Recent findings point out that MAIT cell frequency is reduced in the peripheral blood of patients suffering from autoimmune, allergic or inflammatory disorders. In parallel, MAIT cell activation and exhaustion is increased (Godfrey et al., 2019; Toubal et al., 2019). Furthermore, these patients show changes in gut homeostasis, including gut immunity, intestinal permeability and a loss host of microbial diversity (Toubal et al., 2019).

The reciprocal interaction between the intestinal microbiota and the immune system

Immunological research, in particular with regard to the intestinal microbiota, focused for a long time on infectious microorganisms (Gill and Finlay, 2011). However, most host-microbe-interactions at barrier sites of the body are mutualistic and do not relate to infectious disease (Koropatnick, 2004). It has been proposed that the vertebrate adaptive immune system co-evolved with its intestinal microbiota not to restrict microbial colonization, but to allow microbial colonization (McFall-Ngai, 2007). It was shown that the bi-directional host-microbiota-interactions peak in the interplay between the mutualistic microbiota and the immune system (Gill and Finlay, 2011; Hooper et al., 2012; Maynard et al., 2012). Intestinal mucosal immunity on the one hand has to limit the exposure of host tissue to intestinal microbiota, while on the other hand nutrient uptake has to be facilitated by reciprocal interactions to maintain intestinal homeostasis (Maynard et al., 2012).

The *mucosal firewall* is a layered defense system and comprises of the mucus layer, the highly responsive epithelium and the underlying tissues including various types of immune cells (**Figure 8**, Macpherson et al., 2009; Mowat and Agace, 2014).

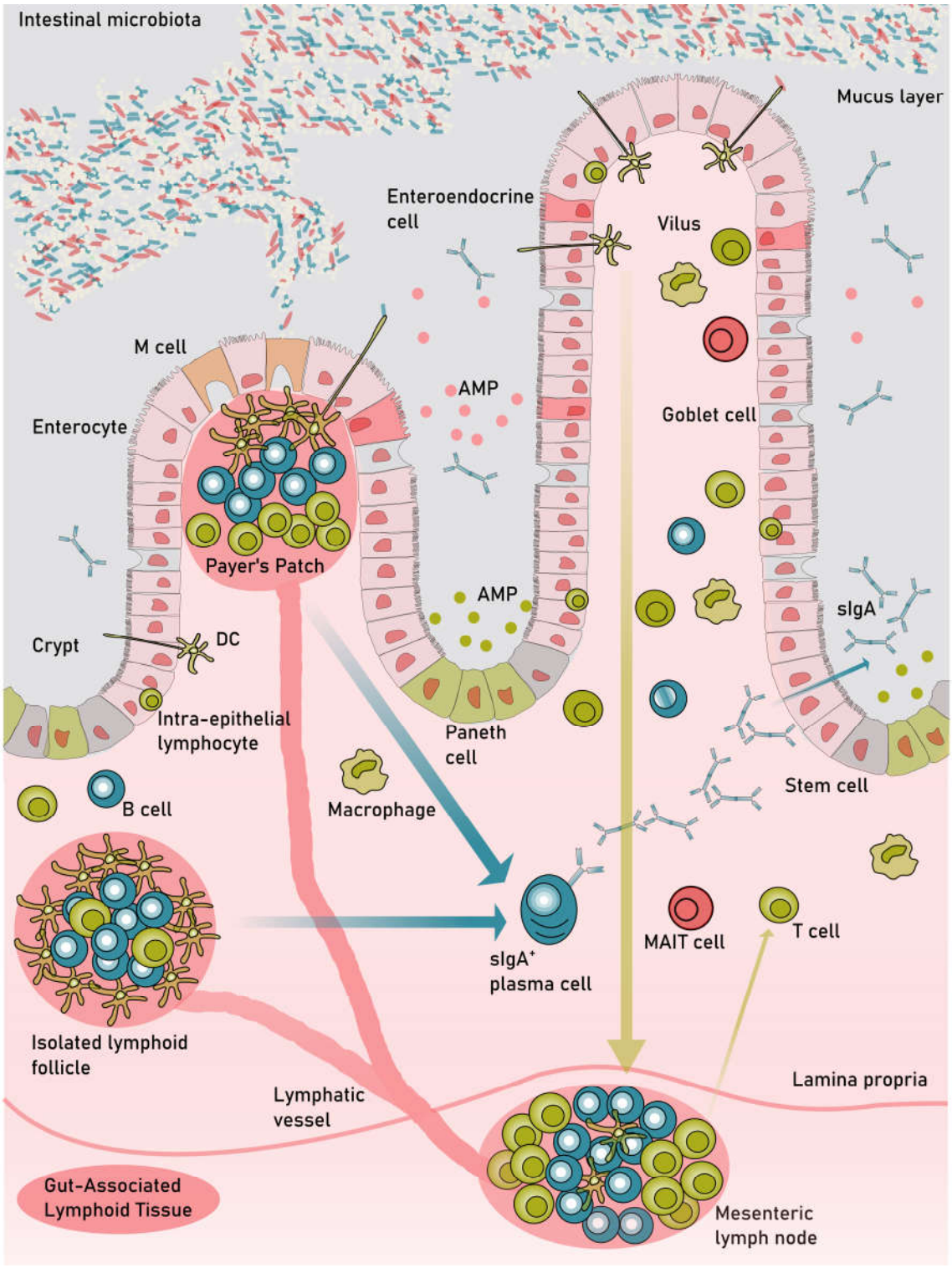

Figure 8. The intestinal mucosa in homeostasis. The intestinal microbiota and the mucosal tissue are physically separated by the epithelial and the mucus layer. The mucus layer is maintained by specialized mucus-secreting Goblet cells. Paneth cells are located in the epithelial crypts and secret antimicrobial peptides (AMP) to prevent microbial invasion. Epithelial M cells transcytose antigen to dendritic cells (DCs) that reside in the Payer's patches. Simultaneously, dendritic cells (DCs) sample antigen from the luminal content. After antigen recognition DCs interact with B and T cells in the gut-associated lymphoid tissues. B cells then differentiate into Ig A producing plasma cells and the secretory (s)IgA is trancytosed into the intestinal lumen affecting colonization levels. In addition, macrophages defend the mucosal tissue against invading microbes.

Following a standardized terminology (Brandtzaeg et al., 2008) inductive and effector sites of the mucosal immune system can be determined (Brandtzaeg and Pabst, 2004; Maynard et al., 2012; Mowat and Agace, 2014). The inductive sites, i.e. the sites of lymphocyte stimulation, include the mucosa-associated lymphoid tissues (MALTs), which are Payer's patches in the small intestine, isolated lymphoid follicles (ILF) and mesenteric lymph nodes (MLN). MALTs are subdivided regarding the anatomical region in the body, and thus are termed gut-associated lymphoid tissue (GALT) in the intestine (Brandtzaeg and Pabst, 2004; Brandtzaeg et al., 2008). Mucosal effector sites are formed by histological distinct compartments and comprise of the lamina propria (LP) and the epithelium with all the immanent effector immune cells (Brandtzaeg and Pabst, 2004; Mowat and Agace, 2014). The epithelium is formed by absorptive enterocytes and specialized enterocytes with distinct functions. Goblet cells, a type of specialized enterocytes, secret mucin glycoproteins that form the mucus layer (Knoop and Newberry, 2018). Mucin secretion is stimulated by butyrate, a stimulus from the healthy microbiota (Levy et al., 2017b; Maynard et al., 2012). The mucus layer physically separates the bacteria-dense lumen from the host epithelium and due to structural properties, on the one hand, toxic properties of some mucin glycoproteins in the other hand, the basal part of mucus layer remains sterile (Knoop and Newberry, 2018; Maynard et al., 2012; Mowat and Agace, 2014). Moreover, enterocytes, entero-endocrine cells and Paneth cells in the small intestine secrete antimicrobial peptides (AMPs) into the mucus layer to eliminate microbes and hence to keep the epithelium-close mucus layer sterile. Furthermore, epithelial cells transcytose secretory immunoglobulin A (sIgA) that eliminates invading microbes from the epithelium-close mucus layer. Both these mechanisms together shape the composition of the intestinal microbiota (Macpherson et al., 2009; Mukherjee and Hooper, 2015). When intestinal microbiota overcome the intestinal barrier, the abundant LP macrophages eliminate these microbes by phagocytosis (Macpherson et al., 2009). To this end, the immune system driven influences on intestinal homeostasis have been described. However, in this bi-directional cross talk, the microbiota modulates immune cells *via* a variety of microbial metabolites (**Figure 9**, Blacher et al., 2017; Levy et al., 2017b).

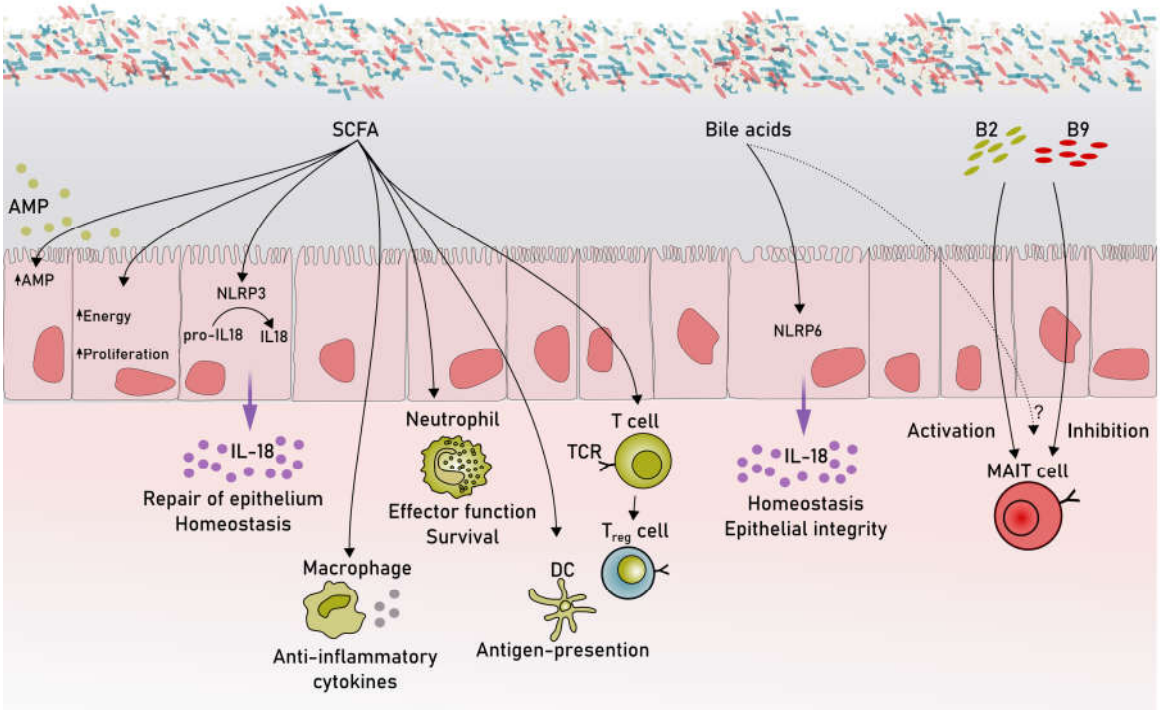

Figure 9. Microbial metabolites affect the immune system. Microbiota-derived metabolites, such as short-chain fatty acids (SFCAs), bile acids and vitamin B metabolites can modulate the intestinal immune response by interactions with immune cells or the epithelium. Adapted from Levy et al., 2017b.

SCFAs are the best-studied group of microbial metabolites with respect to their interactions in the intestine. They are an energy source for enterocytes, with butyrate being the most important SCFA for energy supply. Furthermore, butyrate induces proliferation and secretion of antimicrobial peptides (AMPs) by enterocytes (Corrêa-Oliveira et al., 2016) and modulates the effector functions and affects survival of neutrophils (Rodrigues et al., 2016). Butyrate also renders the effector functions of macrophages toward an anti-inflammatory cytokine response (Corrêa-Oliveira et al., 2016). SCFAs modify the antigen-presenting properties of both, macrophages and DCs (L. Millard et al., 2002). The effects of SCFA are not restricted to cells from the innate arm of immunity. E.g., it was shown that SCFAs promote the differentiation of naïve T cells to regulatory T cells (T_{reg}) and other types of effector cells (Corrêa-Oliveira et al., 2016). Other microbiota-derived metabolites also affect the epithelium or other immune cells. Bile acids, e.g., were shown to induce the production of IL-18 *via* NLRP6 and thus contribute to intestinal homeostasis (Blacher et al., 2017). In addition, microbial vitamin metabolites from the riboflavin and folate biosynthesis pathway can activate or inhibit MAIT cell activation *in vitro* and cytokine-mediated MAIT cell activation by IL-18 and IL-12 was reported (Kjer-Nielsen et

al., 2018; Wilgenburg et al., 2016). However, the influences of the intestinal microbiota via microbial metabolites is far from being understood. Nevertheless, it is obvious that an altered microbiota can have down-stream effects on immune system functions. Besides diet-induced alterations, the intestinal microbiota might be affected by the acute and chronic exposure to environmental chemicals (Licht and Bahl, 2019).

1.3 The risk of chemical exposure to human health

Chemical risk assessment in the European Union

8.3% of all deaths were estimated to be caused by exposure to environmental chemicals in 2004 (https://www.who.int/gho/phe/chemical_safety/en/ 22.06.2020, 22:05). With the aim to minimize adverse effects on human health and the environment, the European Union (EU) adopted the REACH regulation (Regulation (EC) No 1907/2006) in 2007 for chemical risk assessment. REACH governs the **R**egistration, **E**valuation, **A**uthorization and Restriction of **Ch**emicals (European Chemicals Agency, 2017) and applies to all chemicals that are used within the EU. Since 2009, more than 100 000 chemicals have been registered with REACH, which represents 97% of used and 99% of manufactured chemicals (Hartung and Rovida, 2009). However, the number of chemicals on the market as well as the amount of produced chemicals per year will continue to increase (Wilson and Schwarzman, 2009).

Chemicals with use at quantities >1 ton per year have to be registered at the European Chemicals Agency (ECHA). Therefore, physico-chemical, toxicological and eco-toxicological chemical properties, the chemicals' application, risk assessment as well as risk management plans have to be provided in registration dossiers (European Chemicals Agency, 2017). For risk assessment, *in vitro* and *in vivo* tests have to be conducted according to the production/import quantity (**Figure 10**, https://echa.europa.eu/regulations/reach/registration/information-requirements, 23.06.2020, 0:28).

	Physico-chemical properties data	Exo-toxicological data	Toxicological data
1-10 tons	Description of the state at 20°C / 101.3 kPa, Melting/freezing point, Boiling point, Relative density, Vapour pressure, Surface tension, Water solubility, Partition coefficient, Flash-point, Flammability, Explosive properties, Self-ignition temperature, Oxidising properties, Granulometry	Short-term toxicity on invertebrates & aquatic plants (short-term) Degradation	Skin irritation/corrosion/sensitation Eye irritation/severe damage Skin sensitisation Mutagenicity (in vitro, bacteria) Acute toxicity: oral
10-100 tons		Aquatic toxicity (short-term, fish) Aquatic toxicity (Activated sludge test) Degradation (abiotic) Fate in the environment (Adsorption/Desorption screening)	Skin irritation/corrosion (in vivo) Eye irritation/severe damage (in vivo) Skin sensitisation Mutagenicity (in vitro, mammlian cells) Acute toxicity: inhalation, dermal Reproductive toxicity (1 species) Repeated dose toxicity (28 days)
100-1000 tons	Stability in organic solvents Dissociation constant Viscosity	Aquatic toxicity (long-term, fish, invertebrate) Toxicity on terrestrial organisms (short-term) Degradation (biotic) Fate in the environment (Bioacculmulation/Adsorption/ Desorption screening)	Repeated dose toxicity (28 days, 90 days) Reproductive toxicity (pre-natal, generational, 1 species) Sub-chronic toxicity (90 days)
>1000 tons		Toxicity on terrestrial, sediment organisms (long-term) Degradation (biotic, further) Fate in the environment (further) Reproductive toxicity (long-term, birds)	Reproductive toxicity (pre-natal, generational, 1 species) Carcinogenicity

Figure 10. Overview on tests for risk assessment with REACH. Depending on the production volume the REACh regulation demands *in vitro* and *in vivo* tests for chemical risk assessment according to the OECD testing guidelines.

The evaluation process includes the evaluation of data completeness by ECHA. Another 5% of registration dossiers are evaluated regarding dossier quality, though the percentage of evaluated dossiers shall increase. Until 2023 20% of chemicals >100 tons/year and by 2027 20% of chemicals <100 tons/year are supposed to be evaluated (COMMISSION REGULATION (EU) 2020/507, 7 April 2020). For selected chemicals, i.e. high risk, high exposition and high volume chemicals, a detailed substance evaluation is performed in compliance with EU member states with higher priority (chemicals listed on Community Rolling Action Plan – CoRAP, https://echa.europa.eu/de/information-on-chemicals/evaluation/community-rolling-action-plan/corap-table, 23.06.20, 10:49). After evaluation, the ECHA identifies substances of very high concern (SVHCs), which are then listed on the candidate list of SVHC (REACH Annex XIV) for authorization (http://echa.europa.eu/candidate-list-table, 23.06.20, 11:17) or which are listed on the list of restricted substances (REACH Annex XVII, https://echa.europa.eu/de/substances-restricted-under-reach, 23.06.20, 11:23). The utilization and the import of SVHC chemicals from the candidate list have to be authorized by the ECHA upon an authorization request.

Following this procedure, the ECHA evaluated 274 chemicals in 2018 (https://echa.europa.eu/de/dossier-evaluation-progress-2018, 23.06.20, 10:23), which is 0.0027% of all registered chemicals. Regarding the high number of chemicals registered within the EU and the comparable low throughput of chemicals evaluated per year, the challenges deriving from REACH have been underestimated (Hartung and Rovida, 2009). Already before REACH, assessment of the OECD test guidelines (https://echa.europa.eu/de/support/oecd-eu-test-guidelines, 23.06.20, 12:43) applied with REACH revealed that these need to be updated to meet the current state of knowledge (Combes et al., 2004). Combes et al. (2004) claim that the whole process of toxicity analysis could be improved and made more efficient (Combes et al., 2004). Alike the US environmental protection agency (EPA), the ECHA should replace 40-year-old OECD test guidelines by suitable high-throughput methods (Hartung and Rovida, 2009).

Screening the OECD test guidelines shows that chemical effects on the intestinal microbiota and the immune system are not considered. Recently, the influence of non-caloric artificial sweeteners, which pass the intestine unmodified and thus come into contact with the intestinal microbiota, has been evaluated (Suez et al., 2014). The authors observed shifts in the composition and function of murine intestinal microbiota, resulting in glucose intolerance. Similarly, microbiota modifications associated with the consumption of non-caloric artificial sweeteners were observed in humans (Suez et al., 2014). Other studies showed that also pharmaceuticals influence the physiology, taxonomy and function of intestinal microbiota (Li et al., 2020; Maurice et al., 2013). Likewise the microbial transformation of pharmaceuticals has been reported (Spanogiannopoulos et al., 2016). Since the intestinal microbiota and the immune system are dependent on each other to maintain a healthy state (Maynard et al., 2012), modifications within the microbiota might impact on the immune system. Consequently, model systems have to be established also to investigation the effects of environmental chemicals, such as pesticides, food and water contaminants.

Analyzing the effects of chemical exposure on intestinal microbiota

Mainly together with the diet, pesticides and other contaminant chemicals coming from drinking water, food processing or packaging enter the human body (EFSA, 2008; Oates and Cohen, 2011). Thereby, these compounds potentially affect the intestinal microbiota. Since the

intestinal microbiota was shown to metabolize pharmaceuticals, which can have favorable and detrimental effects (Spanogiannopoulos et al., 2016) and the intestinal microbiota is now considered as potential player in the toxicity of environmental chemicals (Claus et al., 2016). Ethical restrictions prevent studying the potentially toxic effects of environmental chemicals directly on humans *in vivo* (Macfarlane and Macfarlane, 2007; Payne et al., 2012). Nevertheless, the major route of exposure to environmental chemicals such as pesticides, plasticizers, plastic components is oral uptake with the food (Licht and Bahl, 2019; Oates and Cohen, 2011). However, the effect of environmental chemicals on the consequently exposed intestinal microbiota are seldom considered or addressed in chemical risk assessment (Licht and Bahl, 2019).

To study the chemical-derived effects on the human intestinal microbiota, ethical and practical reasons play a role, e.g. they limit the access to microbial material from the intestine of healthy humans (Macfarlane and Macfarlane, 2007). Thus, most *in vivo* and *in vitro* studies are conducted using human fecal material (Macfarlane and Macfarlane, 2007; Payne et al., 2012). Both, *in vivo* and *in vitro* models are useful to assess microbiota-modulating or microbiota-disrupting properties of environmental chemicals (Wissenbach et al., 2016). However, both have their advantages and disadvantages and thus should be combined for a conclusive evaluation of treatment effects (Vrancken et al., 2019).

In vivo studies are the only model system that includes the host, but are rather costly and laborious (Macfarlane and Macfarlane, 2007). Depending on the animal, its metabolism and physiology the results might be incomparable to the human situation (Payne et al., 2012). Furthermore, *in vivo* studies pose some major challenges when evaluating microbiome-modulating effects. I.e., host effects can distort the conclusions drawn from analyzing the taxonomy or functional parameters of the microbiota (Payne et al., 2012). The microbiota at different facilities or animals with different genetic background can respond differently to the treatment (Gill and Finlay, 2011; Macpherson and McCoy, 2015). Depending on the housing conditions, cage-effects can derive from animal housing and exposure in separate treatment groups, which can facilitate misinterpretation of results. Moreover, in *in vivo* studies the characterization of the microbiota before and after treatment, similarly in the control and treatment group, is often neglected. This analysis, however, is essential to discriminate

treatment-related community shifts from usual microbiota variation (Macpherson and McCoy, 2015). Yet, this is also true for *in vitro* culture models.

Testing the impact of environmental chemicals on the intestinal microbiota cannot be accomplished with the required throughput in animal models. The use of *in vitro* culture models circumvents some challenges and drawbacks of *in vivo* models. In contrast to *in vivo* experiments, *in vitro* cultivation circumvents some challenges and drawbacks with being comparably inexpensive and posing the ability for automation and/or high-throughput studies (Macfarlane and Macfarlane, 2007; Vrancken et al., 2019). *In vitro* culture models allow to discriminate microbiota-modulating or -disrupting effects coming from the treatment, by excluding confounding host-effects, such as diet, age and host genetics (McDonald, 2017; Payne et al., 2012). Depending on the experimental setup different (anaerobic) cultivation procedures can be distinguished, i.e. batch cultivation, fed batch cultivation and continuous cultivation with increasing complexity (Payne et al., 2012; Vrancken et al., 2019).

Batch cultivation is simple with regard to the applied experimental equipment and thus little susceptible to technical faults. The cultivation is conducted in a closed system (e.g. bioreactor, Hungate tube) without the addition of nutrients (Vrancken et al., 2019). Optimally, microbial growth follows an S-shaped growth curve, indicating an initially high nutrient availability that allows cell division. Due to limitations of a key nutrient and/or the accumulation of toxic metabolites microbial growth comes to a halt, the culture reaches the stationary growth phase (McNeil and Harvey, 2008). Batch cultivation is suitable for short-term experiments simulating acute exposure or it is appropriate for chemical screening assays (McDonald, 2017).

To more realistically simulate growth conditions in the intestine and to extend the cultivation time (e.g. for chronic exposure), more complex continuous cultivation procedures have to be utilized (Payne et al., 2012). Continuous cultivation, either as single-stage or multi-stage bioreactor setups, are permanently supplied with fresh medium. In parallel, excess culture medium, including cells and toxic metabolites, is constantly removed (McNeil and Harvey, 2008). Cultivation parameters such as pH, temperature, stirring velocity, medium retention time and anaerobiosis of the bioreactor system can be neatly controlled (Licht and Bahl, 2019). Depending on the experimental setup, any physiologic situation can be mimicked as close as

possible, though these *in vitro* models do not aim to resemble the *in vivo* situation (Payne et al., 2012). The cultivation of intestinal bacteria under gut-like conditions in *in vitro* bioreactor systems is one opportunity to gain insights into the bacterial response to a treatment and have already been used to unravel the effect of dietary compounds or environmental chemicals (Joly et al., 2013; Reygner et al., 2016). Most often fecal bacteria are used for the inoculation of such bioreactor systems (Reygner et al., 2016; Joly et al., 2013; Auchtung et al., 2015; Tanner et al., 2014). However, true experimental replication of complex microbiota is hard to achieve due to the intra-individual and longitudinal heterogeneity of fecal samples (Payne et al., 2012). Furthermore, complex microbiota follow a stochastic development during continuous cultivation, which complicates the *in vitro* replication of bioreactors and the definition of a constant community state to start the treatment (Liu et al., 2018b). A constant community state, optimally replicated in several bioreactors, is a pivotal element of an experiment that aims to resolve treatment effects (Possemiers et al., 2004; Van den Abbeele et al., 2010).

Both, constancy and reproducibility, are hard to achieve with complex microbiota *in vitro* (Liu et al., 2018b; Payne et al., 2012). Moreover, analyses on the taxonomic and functional level ,e.g. by metaproteomics, exhibit a reduced depth of analysis with increasing community complexity and should be considered regarding the choice of model system (Lohmann et al., 2020). Hence, a reduced community complexity is essential to resolve treatment effects down to strain-level or to investigate microbe-microbe-interactions and cross-feeding as part of microbial ecology (Elzinga et al., 2019; Vrancken et al., 2019). In addition, the use of a synthetic intestinal microbiota can circumvent the challenges regarding the community reproducibility and the identification of suitable states to investigate the microbiota-modulating or microbiota-disrupting properties of environmental chemicals.

Simplified intestinal microbiota combine biologically important bacterial strains (Vrancken et al., 2019) and still represent the intestinal microbiota (Elzinga et al., 2019). The first synthetic intestinal microbiota, the Altered Schaedler Flora (ASF), was developed in the 1960s for the *in vivo* application in germ-free mice and comprises of eight murine bacterial strains (Schaedler et al., 1965). The ASF has been used extensively even though the representability of the intestinal microbiota in mice has been criticized. Based on the ASF, the 12-strain murine microbiota, oligoMM, has been developed thereby increasing the representability of the intestinal

microbiota (Elzinga et al., 2019). Since the former two microbiota represent murine microbiota, the extended simplified human intestinal microbiota SIHUMIx was developed with the aim to establish a human intestinal model community to investigate host-microbe-interactions *in vivo* (Becker et al., 2011). SIHUMIx comprises of eight bacterial strains commonly found in the human intestine. In mice, SIHUMIx formed a stable community, which was transferred to the offspring and produced a SCFA pattern, which was similar to the human physiologic situation (Becker et al., 2011). To date, these synthetic intestinal microbiota are used for both, *in vivo* and *in vitro* applications (Elzinga et al., 2019).

Analyzing chemical-derived effects on the microbiota and immune cells

The intestinal microbiota is exposed to environmental chemicals after oral uptake (Oates and Cohen, 2011). Alterations on the taxonomic or functional level of the microbiota might affects the immune system as, e.g. microbial metabolites such as SCFA or riboflavin metabolites were shown to influence regulatory T cells (Sakaguchi, 2000) or MAIT cells (Kjer-Nielsen et al., 2012), respectively. Furthermore, MAIT cells reside in the intestinal mucosa (Treiner et al., 2005) and due to the before-mentioned properties are potentially susceptible to microbiota-mediated effects of chemical exposure. Consequently, in the present work, the microbiota- and MAIT cell-modulating properties of environmental chemicals were evaluated. Compounds with proven oral exposure as main entrance route into the human body were selected, which are pesticides and compounds that leach from plastic products with food contact. Moreover, substances with high annual production volumes were selected for detailed investigations within the present PhD project, which were the herbicide glyphosate, the insecticide chlorpyrifos and bisphenols.

Glyphosate is one of the worldwide most frequently applied active ingredients with herbicidal action (Benbrook, 2016), which lead to its ubiquitous distribution in the environment (Silva et al., 2017, 2019) and proven human exposure (Gillezeau et al., 2019). Glyphosate-based herbicides are primarily applied in the agricultural sector, but also comprise non-agricultural applications (Hanke et al., 2010). Residual glyphosate was among the three most frequently detected pesticides on wheat in 2015. Simultaneously, glyphosate has also been measured on other food crops (European Food Safety Authority, 2017). This compound inhibits the 5-enolpyruvylshikimate-3-phosphate synthase (EPSPS), an enzyme that catalyzes the synthesis

of aromatic amino acids via the shikimate pathway (Amrhein et al., 1980). Two classes of the EPSPS exist in bacteria: the glyphosate sensitive class I EPSPS and the glyphosate insensitive class II EPSPS (Funke et al., 2009). Plants and most microorganisms synthesize aromatic amino acids via the shikimate pathway. In contrast, animals lack the shikimate pathway and thus the EPSPS. Therefore, glyphosate is considered safe for humans and animals (Myers et al., 2016). Nevertheless, glyphosate has antimicrobial properties (US patent 7771736 B2) and thus could potentially affect growth of sensitive species e.g. in the human intestine.

Chlorpyrifos is a organophosphate insecticide but exerts also nematicide and acaricide effects (John and Shaike, 2015). This compound is among the most frequently applied organophosphate insecticides (Harishankar et al., 2013) and operates by the irreversible inhibition of acetylcholinesterase in the synapses of the nervous system (Chanda, 1996). Chlorpyrifos was most often detected above the maximum residue level of plant products (European Food Safety Authority, 2017) and consequently enters the human body by the oral route. However, little is known about the impact of chlorpyrifos on the intestinal microbiota and its potential direct and indirect effects on human health.

Another ubiquitously occurring chemical is Bisphenol A (BpA, Vandenberg et al., 2007). Moreover, BpA is a high production chemicals with still increasing production volume (Lehmler et al., 2018) that was included on the candidate list of SVHC chemicals in 2018 due to its endocrine disrupting properties (https://echa.europa.eu/de/candidate-list-table, 23.06.20, 13:58). BpA is primarily used for the production of polycarbonate plastics and epoxy resins. Polycarbonate plastics and epoxy resins are, besides others, utilized for food-contact-applications and thus potentially contaminate food (European Food Safety Authority, 2015). Shortly after its introduction to the market in 1930 the endocrine disrupting properties of BpA have been noticed (Vandenberg et al., 2013). After recognizing the endocrine-disrupting properties of BpA, now regulation of BpA was tightened within the last decade. The tolerable daily intake (TDI) concentrations were reduced (Almeida et al., 2018) and BpA was classified as a substance of very high concern (SVHC) in 2018 in the European Union. These factors contributed to the increasing use of BpA-analogues, such as bisphenol F (BpF) and bisphenol S (BpS, Huang, 2018), which is reflected by the detection of BpA-like levels of BpF and BpS in human urine (Zhou et al., 2014). However, these analogues have a high structural similarity and

hence BpA-analogues might pose a similar risk (Rochester and Bolden, 2015). To date, BpS-derived riks is under assessment with REACH as chemical with higher priority listed on the CoRAP (https://echa.europa.eu/de/substance-information/-/substanceinfo/100.001.13). However, the risk of BpF is not evaluated within the EU, yet, although similar properties of BpF compared to BpA and BpS can be assumed (Rochester and Bolden, 2015). At least for endocrine-disruption BpA-analogues were shown to pose the same risk (Karrer et al., 2018). Since BpA was shown to influence the human intestinal microbiota on the taxonomic level (Lai et al., 2016), the microbiota-modulating/-disrupting effects of BpA- analogues, BpF and BpS have to be compared.

To elucidate the microbiota-modulating or -disrupting properties of environmental chemicals completely, taxonomic and functional analysis have to be combined. Multi-omics approaches provide insights on the level of community taxonomy and function (Fritz et al., 2013; Gao et al., 2017). Omics-techniques include metagenomics, metatranscriptomics, metaproteomics, meta-metabolomics and cytomics. Flow cytometry based single-cell analysis, cytomics, allow the online analysis of structural community dynamics, but do not resolve functional processes nor provide taxonomic information (Koch et al., 2013). Metagenomics allow the reconstruction of the microbial taxonomy within a community but does not discriminate live and dead cells (Shakya et al., 2019). Functional prediction based on metagenomics data has improved, but these functional predictions can only be verified by metatranscriptomics or metaproteomics (Hugenholtz and Tyson, 2008). Metatranscriptome analysis of RNA-sequencing data allows functional insights by analyzing the actively expressed genes within the microbiota at a given time point (Shakya et al., 2019). However, metaproteomics provides taxonomic and real functional information by analyzing the abundance of microbial proteins (Kleiner, 2019). With metabolomics, the microbial metabolome is analyzed. The metabolome complements metaproteomics since it is directly based upon the communities enzymatic activity (Tang, 2011).

In the present work the microbiota-modulating properties of glyphosate and BpX have been determined both on the taxonomic and functional level with cytomics, 16S rRNA amplicon sequencing, metaproteomics and untargeted as well as targeted metabolomics. To assess the indirect effects of environmental chemical exposure on MAIT cells, the exposed microbiota were used for MAIT cell stimulation. Direct effects of chemical exposure were investigated by

exposure of MAIT cells during stimulation. With multi-color flow cytometry, the modulation of MAIT cell activation was determined.

1.4 Aims of the present PhD project

The key role of the intestinal microbiota for human health has recently been acknowledged. Moreover, the close interactions between the intestinal microbiota and the immune system are the subject of intense research. Analyzing the microbiota- and immune-modulating properties of environmental chemicals is essential and can help to understand the rise of chronic inflammatory diseases, already among children, in the westernized world. To assess the microbiota-and immune-modulating properties of environmental chemicals suitable model systems were established and applied in the present PhD project (**Figure 11**):

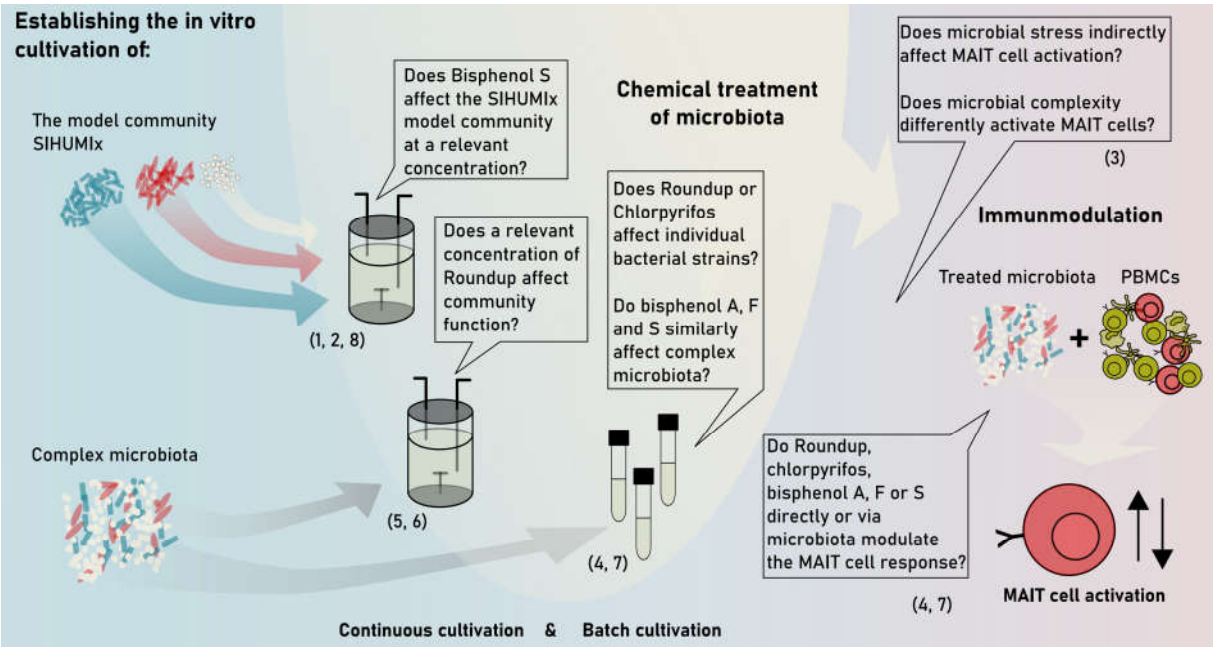

Figure 11. Aims of the present PhD project. Suitable model systems for the microbiota cultivation and chemical exposure *in vitro* were established ranging from continuous cultivation in bioreactors to batch cultivation. The present PhD project thereby focused on chemical-related microbiota-mediated modulation of MAIT cells. Boxes summarize corresponding research questions and numbers indicate the related publication.

1. Establishing the SIHUMIx model community for bioreactor use

To resolve effects down to strain-level, less complex, defined model communities, such as the extended simplified human intestinal microbiota (SIHUMIx), are most appropriate. Five fingerprinting techniques were compared regarding their suitability to follow the community

dynamics of SIHUMIx. The minimal time of cultivation for reaching a constant community state was identified and to determine which methods are appropriate to analyze perturbations in microbial cultures (publication 1). Moreover, the ability of SIHUMIx to resistance a perturbation was investigated, also giving insights on the behavior under extended cultivation (publication 2).

2. **Proof-of-concept – Can MAIT cells sense microbial exposure to acid pH?**

To study microbiota-mediated effects on the mucosal-associated invariant T (MAIT) cells, two *in vitro* model systems, the cultivation of intestinal microbiota and their subsequent use for MAIT cell stimulation, were combined. This raised the question whether the combination of both model system is suitable to identify microbial stress (publication 3).

3. **Does glyphosate alter intestinal microbiota on the functional or taxonomic level?**

Glyphosate-related effects on the intestinal microbiota were a central issue in the present PhD project, as this work has been funded by the German Federal Environmental Foundation (DBU) to study the effects of glyphosate on MAIT cells *via* the intestinal microbiota. Potential effects were assessed on the single strain and the community level. Effects of glyphosate/Roundup at a reasonable high concentration were investigated on the community level using pig colonic microbiota. The central question was, whether glyphosate-exposure affects intestinal microbiota with a focus on the functional level ((publication 4, publication 5 and publication 6).

4. **Do bisphenols directly or indirectly via the microbiota modulate MAIT cell activation?**

Bisphenols (BpX) represent a substance group with several analogues related to Bisphenol A and are among the most produced chemicals worldwide (Lehmler et al., 2018). Investigations focused on BpX-mediated functional or taxonomic level effects on complex intestinal microbiota and SIHUMIx (publication 7 and publication 8) and also encompassed immune-modulatory effects by BpX with a focus on MAIT cells (publication 7).

2 PUBLICATIONS

2.1 Overview of publications

Publication 1: Following the community development of SIHUMIx – a new intestinal *in vitro* model for bioreactor use

Jannike Lea Krause[#], Stephanie Serena Schaepe[#], Katarina Fritz-Wallace, Beatrice Engelmann, Ulrike Elisabeth Rolle-Kampczyk, Sabine Kleinsteuber, Florian Schattenberg, Zishu Liu, Susann Mueller, Nico Jehmlich, Martin von Bergen[#], Gunda Herberth[#]. [#] *these authors contributed equally*

Gut Microbes (2020), DOI: 10.1080/19490976.2019.1702431

Significance: Most studies investigate the microbiota-modulating effects of chemical contaminants using complex human microbiota. However, the reproducible cultivation of complex microbiota in bioreactors is challenging and the communities behave highly dynamic. In this study, the extended simplified intestinal human microbiota (SIHUMIx), a defined model community, was established as a valuable model for *in vitro* use by analyzing the community dynamics with five fingerprinting techniques (page 41).

Summary: The model community SIHUMIx has been grown reproducibly in the bioreactor system. All communities reached a constant community state within 5 days of cultivation, simultaneously on the cellular and the functional level. Acid stress affected SIHUMIx on the cellular and functional level, whereby the cellular and the functional level recovered with different velocity.

Publication 2: The simplified human intestinal microbiota (SIHUMIx) shows high structural and functional resistance against changing transit times in in vitro bioreactors

Stephanie Serena Schäpe[#], **Jannike Lea Krause**[#], Beatrice Engelmann, Katarina Fritz-Wallace, Florian Schattenberg, Zishu Liu, Susann Müller, Nico Jehmlich, Ulrike Rolle-Kampczyk, Gunda Herberth[#], Martin von Bergen[#]. [#]*these authors contributed equally*

Microorganisms (2019), DOI: 10.3390/microorganisms7120641

Significance: Various community functions that shape host-microbiota-interactions are potentially influenced by intestinal transit times. However, little is known about the effects on the composition and functionality of the gut microbiota that derive from changes in the intestinal transit time. Therefore, the in publication 1 established model community, SIHUMIx, was used (i) to investigate the influence of changing transit times on its community composition and function and simultaneously (ii) to monitor the community dynamics over a 15- day cultivation period (page 56).

Summary: The model community SIHUMIx was highly resistant against varying transit times on the taxonomic as well as the functional level. Five out of six communities reached a constant community state within 5 days of cultivation. The sixth community reached the constant state with delay on day 6 of cultivation. The untreated communities remained stable until day 15.

Publication 3: The activation of mucosal-associated invariant T (MAIT) cells is affected by microbial diversity and riboflavin utilization *in vitro*

Jannike Lea Krause, Stephanie Serena Schäpe, Florian Schattenberg, Susann Mueller, Grit Ackermann, Ulrike Elisabeth Rolle-Kampczyk, Nico Jehmlich, Arkadiusz Pierzchalski, Martin von Bergen, Gunda Herberth.

Frontiers in Microbiology (2020), DOI: 10.3389/fmicb.2020.00755

Significance: In the human body, MAIT cells encounter complex microbiota at mucosal sites and recognize microbial metabolites from the riboflavin and folate pathway *in vitro*. To date the MAIT cell interaction with microbial communities has not been studied, even though the interaction of both rather reflects the physiologic situation.

In this study, the response of MAIT cells to microbiota from single strains to complex communities was investigated. Using the model community SIHUMIx (publication 1) the contribution of the community members on MAIT cell activation was analyzed. This model community was also used to determine whether microbial stress indirectly affects the MAIT cell activation. Furthermore, the MAIT cell activating potential of microbiota with different diversity was compared, since microbial diversity is a major differences between healthy and diseased microbiota (page 7777).

Summary: The MAIT cell activating potential of SIHUMIx was directly related to the relative species abundances in the community, suggesting an additive relationship between species abundances and MAIT cell activation. Diverse microbial communities induced a low MAIT cell activation and showed a high riboflavin uptake. With decreasing diversity the riboflavin consumption decreased and in parallel the MAIT cell activating potential increased, suggesting a role of microbial diversity for MAIT cell activation. Microbial acid stress nullified the MAIT cell activating potential and proves that MAIT cells can perceive microbial stress.

Publication 4: Mucosal-associated invariant T-Cell (MAIT) activation is altered by chlorpyrifos- and glyphosate-treated commensal gut bacteria

Anne Mendler, Florian Geier, Sven-Bastiaan Haange, Arkadiusz Pierzchalski, **Jannike Lea Krause**, Ivonne Nijenhuis, Jean Froment, Nico Jehmlich, Urs Berger, Grit Ackermann, Ulrike Rolle-Kampczyk, Martin von Bergen, Gunda Herberth.

Journal of Immuntoxicology (2020) DOI: 10.1080/1547691X.2019.1706672

Significance: Environmental chemicals are suspected of affecting the intestinal microbiota. Thus, they potentially influence immune system components, which can result in a modulated immune response. Mucosal-associated invariant T (MAIT) cells recognize microbial metabolites and are therefore particularly sensitive to microbiota-mediated immune modulation.

Here, the influence of the insecticide chlorpyrifos and herbicide glyphosate on the MAIT cell activating or –inhibiting potential of common members of the human intestinal microbiota was investigated. Furthermore, the ability to produce MAIT cell modulating metabolites was approximated by metabolomics and metaproteomics (page 91).

Summary: *E. coli* activates MAIT cells, whereas *Bifidobacterium adolescentis* and *Lactobacillus reuteri* inhibit MAIT cell activation. During stimulation, chlorpyrifos increased the *E. coli*-mediated MAIT cell activation and in parallel lowered the inhibiting potential of *B. adolescentis* and *L. reuteri*. This reflected in an altered riboflavin and folate biosynthesis. Glyphosate showed only minor effects.

Publication 5: Quantification of glyphosate and AMPA from microbiome reactor fluids

Katarina Fritz▮Wallace[#], Beatrice Engelmann[#], **Jannike Lea Krause**, Stephanie Serena Schäpe, Judith Pöppe, Gunda Herberth, Uwe Rösler, Nico Jehmlich, Martin von Bergen, Ulrike Rolle▮ Kampczyk. [#] *these authors contributed equally*

Rapid Communications in Mass Spectrometry (2019) DOI: 10.1002/rcm.8668

Significance: Glyphosate-based herbicides are the most frequently applied plant protection products worldwide. In addition to enzyme-linked immunosorbent assays, several methods using a combination of liquid chromatography (LC) and mass spectrometry (MS) have been established for glyphosate quantification in water, soil, urine, blood or breast milk. However, the quantification of glyphosate from microbial culture medium has not been reported, and literature on the simultaneous quantification of glyphosate and its degradation product, aminomethylphosphonic acid (AMPA), are sparse (page 102).

Summary: In the present study, a time- and cost-effective, reliable method for the extraction of glyphosate and AMPA from a complex bioreactor medium was established and applied to quantify exposure-relevant concentrations of both compounds in complex bioreactor medium.

Publication 6: The glyphosate formulation Roundup influences the global metabolome of pig gut microbiota in vitro

Jannike Lea Krause[#], Sven-Bastiaan Haange[#], Stephanie Serena Schäpe, Beatrice Engelmann, Ulrike Rolle-Kampczyk, Katarina Fritz-Wallace, Zhipeng Wang, Nico Jehmlich, Dominique Türkowsky, Kristin Schubert, Judith Pöppe, Katrin Bote, Uwe Rösler, Gunda Herberth, Martin von Bergen.
[#]*these authors contributed equally*

Science of the total environment (2020) DOI: https://doi.org/10.1016/j.scitotenv.2020.140932

Significance: Glyphosate is the most widely used herbicide worldwide and potentially exhibits microbiota-modulating properties due to its antibiotic properties. Recent studies addressed microbiota-modulating effects primarily on the taxonomic level but lacked functional information.

Therefore, in this study, complex intestinal microbiota were cultivated in the presence of a high concentration of glyphosate from Roundup. The experimental setup allows the resolution of functional effects, by a combined approach of metaproteomis, metabolomics and 16S analysis (page 113).

Summary: Despite homogenization of the inoculum four different microbial communities developed. Upon glyphosate exposure only slight effects on microbial metabolism were observed. Community taxonomy was not affected.

Publication 7: Bisphenol A, bisphenol F and bisphenol S directly modulate MAIT cell activation

Jannike Lea Krause, Beatrice Engelmann, Ulrike Rolle-Kampczyk, Arkadiusz Pierzchalski, Martin von Bergen, Gunda Herberth

Environmental pollution to be submitted

Significance: Bisphenols (BpX) have been detected ubiquitously in the environment, but also in human specimen. The longest-known BpX compound, bisphenol A (BpA), is used for the production of polycarbonate plastics and epoxy resins, which are used, among others, for food-contact-applications and thus potentially contaminate food. The tightened regulation of BpA contributed to the increasing use of BpA-analogues, such as bisphenol F (BpF) and bisphenol S, which might not be safer alternatives.

In this study, the microbiota-modulating effects of BpA, BpF and BpS were investigated using three concentrations related to the acceptable daily intake concentration of BpA. Growth parameters and global community function of human intestinal microbiota were analyzed *in vitro*. Furthermore, the microbiota-mediated immune-modulatory properties of BpX on MAIT cells were determined (page 125**Fehler! Textmarke nicht definiert.**).

Publication 8: Environmentally relevant concentration of Bisphenol S shows slight effects on SIHUMIx

Stephanie S. Schäpe, **Jannike L. Krause**, Rebecca K. Masanetz, Sarah Riesbeck, Robert Starke, Ulrike Rolle-Kampczyk, Christian Eberlein, Hermann J. Heipieper, Gunda Herberth, Martin von Bergen , Nico Jehmlich

Microorganisms to be submitted

Significance: The intestinal microbiota is potentially exposed to BpX and microbial modulating properties of these compounds have been suggested. However, little is known on the mechanisms how BpX affect microbial activity and function.

In this study, BpS-mediated effects were investigated using the extended simplified human intestinal microbiota (SIHUMIx) in bioreactors to allow a detailed mechanistic analysis. Community taxonomy and community function were simultaneously analyzed by metaproteomics. Moreover, fatty acid methyl esters profiles were recorded to resolve changes in the membrane fatty acid composition of the microbiota (page 150).

Summary: At the concentration applied to SIHUMIx, no significant changes were observed on community taxonomy. One day after the start of the community showed an altered function, which vanished until the end of the experiment.

2.2 Full-text of publications

Publication 1: Following the community development of SIHUMIx – a new intestinal *in vitro* model for bioreactor use

GUT MICROBES
https://doi.org/10.1080/19490976.2019.1702431

Taylor & Francis
Taylor & Francis Group

METHOD

OPEN ACCESS Check for updates

Following the community development of SIHUMIx – a new intestinal *in vitro* model for bioreactor use

Jannike Lea Krause[a*], Stephanie Serena Schaepe[b*], Katarina Fritz-Wallace[b], Beatrice Engelmann[b], Ulrike Rolle-Kampczyk[b], Sabine Kleinsteuber[c], Florian Schattenberg[c], Zishu Liu[c], Susann Mueller[c], Nico Jehmlich[b], Martin Von Bergen[b,d*], and Gunda Herberth[a*]

[a]Department of Environmental Immunology, Helmholtz Centre for Environmental Research - UFZ, Leipzig, German; [b]Department of Molecular Systems Biology, Helmholtz Centre for Environmental Research - UFZ, Leipzig, Germany; [c]Department of Environmental Microbiology, Helmholtz Centre for Environmental Research - UFZ, Leipzig, Germany; [d]Institute of Biochemistry, Faculty of Biosciences, Pharmacy and Psychology, University of Leipzig, Leipzig, Germany

ABSTRACT

Diverse intestinal microbiota is frequently used in *in vitro* bioreactor models to study the effects of diet, chemical contaminations, or medication. However, the reproducible cultivation of fecal microbiota is challenging and the resultant communities behave highly dynamic. To approach the issue of reproducibility in *in vitro* models, we established an intestinal microbiota model community of reduced complexity, SIHUMIx, as a valuable model for *in vitro* use.

The development of the SIHUMIx community was monitored over time with methods covering the cellular and the molecular level. We used microbial flow cytometry, intact protein profiling and terminal restriction fragment length polymorphism analysis to assess community structure. In parallel, we analyzed the functional level by targeted analysis of short-chain fatty acids and untargeted metabolomics. The stability properties constancy, resistance, and resilience were approached both on the structural and functional level of the community. We show that the SIHUMIx community is highly reproducible and constant since day 5 of cultivation. Furthermore, SIHUMIx has the ability to resist and recover from a pulsed perturbation, with changes in community structure recovered earlier than functional changes.

Since community structure and function changed divergently, both levels need to be monitored at the same time to gain a full overview of the community development. All five methods are highly suitable to follow the community dynamics of SIHUMIx and indicated stability on day five. This makes SIHUMIx a suitable *in vitro* model to investigate the effects of e.g. medical, chemical, or dietary interventions.

ARTICLE HISTORY
Received 1 July 2019
Revised 21 October 2019
Accepted 3 December 2019

KEYWORDS
Bioreactor; flow cytometry; protein profiling; metabolomics; t-RFLP; short chain fatty acids; intestinal microbiota; in vitro model; simplified human intestinal microbiota (SIHUMI)

Introduction

The human intestinal microbiota is essential to human health and is even considered as an extra organ, as it provides enzymes for nutrient breakdown and produces essential nutrients, such as short-chain fatty acids (SCFA) and vitamins.[1–3] It was also shown that the intestinal microbiota modulates the immune system.[4,5] Due to the importance of the intestinal microbiota to human health and well-being, the effects of environmental stress on the intestinal microbiota can have serious consequences. For example, pesticides, but also other chemicals, like perfluoroalkyl acids or plasticizers, mainly enter the human body via the oral route thus potentially affecting the intestinal microbiota.[6,7]

Testing the impact of environmental influences (e.g., pesticides, nutrients) on the intestinal microbiota cannot be accomplished with the required throughput in animal models due to ethical and practical reasons. Thus, the development of suitable models is essential. The cultivation of intestinal bacteria under gut-like conditions is a relevant approach to gain insight into the bacterial response to environmental influences. The effect upon various treatments, e.g. of dietary compounds, the impact of pathogenic microorganisms on the intestinal microbiota or the response to chemicals has already been investigated in

CONTACT Gunda Herberth gunda.herberth@ufz.de Permoser Straße 15, Leipzig 04318, Germany
*These authors contributed equally
Supplemental data for this article can be accessed on the publisher's website.

in vitro bioreactor systems.[8,9] Most often fecal bacteria are cultivated in these bioreactor systems.[8–11] However, true experimental replication is hard to achieve due to the intra-individual and longitudinal heterogeneity of fecal samples.[12] Additionally, a variety of methods, like denaturing gradient gel electrophoresis (DGGE),[13] short chain fatty acid[14] and next-generation 16S rRNA sequencing analysis,[10] have been used to define constant *in vitro* community states, when the community remains unchanged (often referred to as stable state). This state is essential to start the treatment, since a starting point is a pivotal element for the experimental set up.[15,16] Depending on the method different results regarding the time of cultivation to reach such a state have been obtained.[16,17] Proceeding from this and from an ecological point of view the term *stability* is ambiguous.[18] Grimm and Wissel (1997) point out that *stability* itself is not a stability property and therefore extracted main stability properties.[19] Some of these are *constancy, resilience* and *resistance*. E.g., (1) *constancy* means that a system remains essentially unchanged, (2) *resistance* resembles the ability of a system to remain unchanged despite a perturbation and (3) *resilience* describes the ability of a system to recover to a reference state after a perturbation.[19]

To circumvent challenges regarding the community reproducibility and the identification of suitable states to introduce a treatment, we established the extended simplified human microbiota (SIHUMIx) as a model community for *in vitro* use. SIHUMIx comprises of eight bacterial species, *Anaerostipes caccae, Bifidobacterium longum, Bacteroides thetaiotaomicron, Blautia producta, Clostridium butyricum, Clostridium ramosum, Escherichia coli* and *Lactobacillus plantarum*, and covers the genera *Firmicutes, Bacteroidetes* and *Proteobacteria* that are dominant in human feces.[20] We tracked the dynamics during community adaptation with a multi-method approach, which combined standard fingerprinting and OMICs techniques. Methods like terminal restriction fragment length polymorphism[21] analysis, flow cytometric fingerprinting[22] and short chain fatty acid analysis[23] are widely applied in microbial community characterization. Moreover, we evaluated untargeted metabolomics and intact protein profiling,[24] as these methods have the potential to depict community development on the metabolic and structural level, respectively, even though these methods have not been used to follow community development yet.

Acidification of the colon lumen by a decreased luminal pH resembles a severe disturbance and has been reported from patients with active ulcerative colitis.[25] For those reasons, we on the one hand cultivated the SIHUMIx community unimpededly, and on the other hand perturbed the community with a decrease of pH during cultivation. The aims of our study were to clarify if the SIHUMIx community (i) behaves in a reproducible way, (ii) establishes a constant state, (iii) is sensitive and responsive to perturbations, and (iv) if such a perturbation can be traced both on the structural (FC) and metabolic level (SCFA).

Results

Development of SIHUMIx under defined chemostat conditions

In order to follow the community dynamics of SIHUMIx, pre-cultivated bacteria were inoculated into three parallel bioreactors A, B and C (day 0) and grown on complex intestinal medium (CIM, supplemental file 1: Table S1) at a dilution rate of $D = 0.04\ d^{-1}$. After an initial establishing phase of 24 h (day 1) the continuous cultivation was started and community structure and function were monitored daily in a 24 h interval until day 7 (Figure 1a). Samples were taken for flow cytometric fingerprinting analysis (FC), intact protein profiling (IPP) and t-RFLP profiling, to study possible variations on the cell, protein, and DNA level from biomass, respectively. In addition, community function was assessed with untargeted metabolomics and short chain fatty acid (SCFA) analysis from the culture supernatant.

By non-metric multidimensional scaling (NMDS), we visualized upcoming community variations in the three parallel bioreactors (Figure 1b, Supplemental file 2: input data for NMDS analysis). All methods, FC (1), IPP (2), t-RFLP profiling (3), untargeted metabolome analysis (4), and SCFA analysis (5) revealed the same development pattern of the SIHUMIx community for all reactors. The community structure and function during the first two days of cultivation were similar

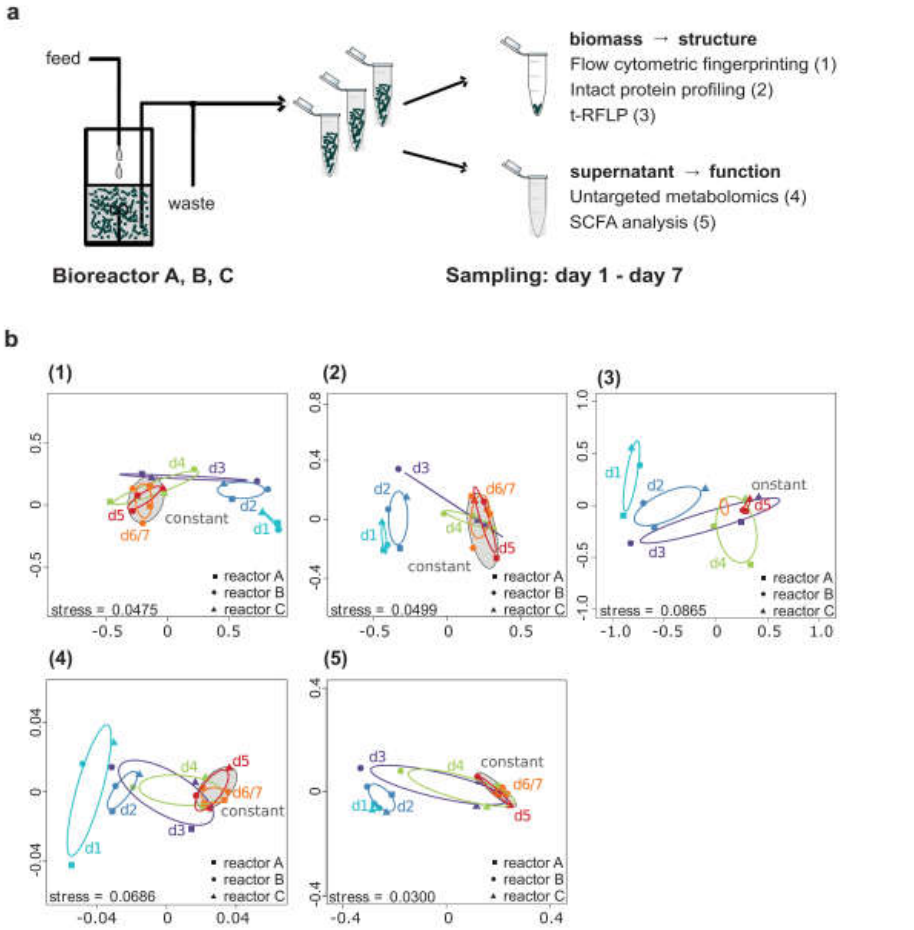

Figure 1. Experimental-set-up and development of the SIHUMIx community. (a) The SIHUMIx community was cultivated *in vitro*. After a sterile run the bioreactors A, B and C were inoculated (day 0) and after 24 h establishing time continuous cultivation started. Daily samples were taken from day 1 to day 7. Bacteria pellets were analyzed by flow cytometric fingerprinting (FC), t-RFLP and intact protein profiling (IPP) to investigate community structure. Culture supernatants were used for functional analysis namely SCFA analysis and untargeted metabolomics. (b) Community development was visualized by NMDS: (1) FC, (2) IPP, (3) t-RFLP, (4) SCFA, (5) untargeted metabolomics. Grouping was based on the day of cultivation.

and significantly different from the states of the communities at the end of the cultivation (p-value 0.03, pairwise Permanova, Supplemental file 1: Table S2, Table S3). The states of the communities on day 3 and day 4 lay between the states of the early communities and the late communities, thus mapping transitional states. Finally, the community on day 5 of all bioreactor replicates A, B and C was indistinguishable from the communities on day 6/7 (pairwise Permanova, Supplemental file 1: Table S2, Table S3).

For SCFA analysis, the concentrations of non-branched SCFA acetate, propionate, butyrate, valerate and caproate and the branched SCFA isobutyrate, isovalerate, isocaproate and 2-methyl

butyrate were measured. As implied from the NMDS plot (Figure 1b (4)), the absolute SCFA production changed notably during the time of cultivation (Figure 2b, supplemental file 1: Table S4). The dominating SCFA detected in the culture supernatant of SIHUMIx were acetate, propionate and butyrate. The acetate and butyrate concentrations increased, whereas the concentration of butyrate decreased during the time of cultivation. The concentration of 2-methylbutyate, isobutyrate and isovalerate also rose during the cultivation of SIHUMIx until day 7. Moreover, we observed an increasing total SCFA concentration during the time of cultivation. Clustering analysis based on the development of SCFA production revealed that data points related to the bioreactor samples clearly arranged in two major clusters with one cluster comprising all replicates A, B and C of day 1 and day 2 and the other cluster containing all replicates of day 5 and day 6/7 (Figure 2b). In the first days of cultivation, the communities produced above-average levels of acetate and butyrate and below-average levels of valerate, isobutyrate, propionate, 2-methyl-butyrate, and isovalerate. During the days 5, 6 and 7 of cultivation this SCFA pattern inversed. Caproate and isocaproate were not detected or below the detection limit. The SCFA production patterns of SIHUMIx was similar in all three bioreactors.

SIHUMIx shows a high reproducibility

To assess the reproducibility of the SIHUMIx community, two batches of single strain pre-cultures were used. Bioreactors A and B were inoculated with one and bioreactor C with the other batch of pre-cultures (day 0). During NMDS analysis Bray-Curtis (BC) distances were calculated for each method (Supplemental file 3: BC distance matrices). Based on the BC

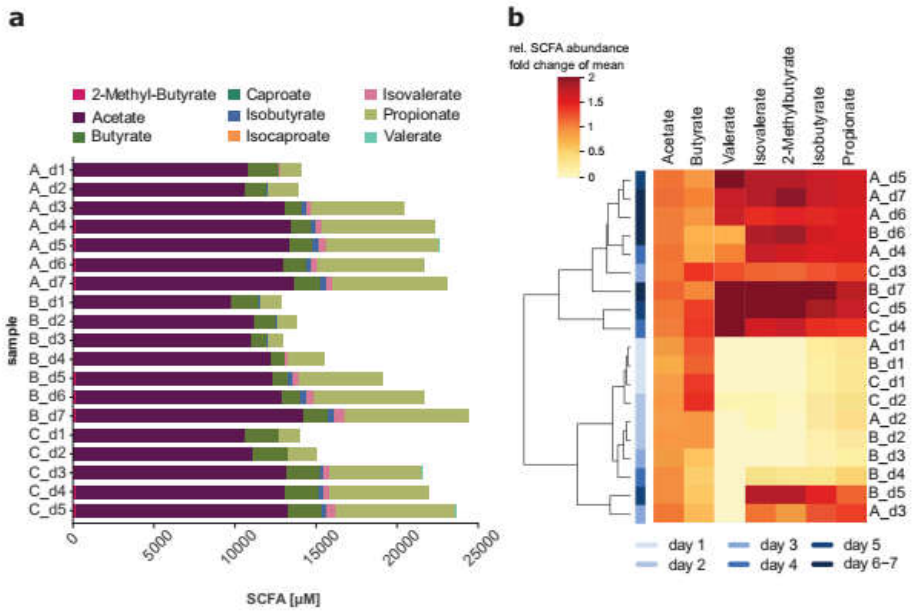

Figure 2. Short chain fatty acid (SCFA) production of SIHUMIx in three independent, parallel bioreactors A, B and C from day 1 to day 7. (a) The absolute SCFA concentrations were determined with targeted SCFA mass spectrometry metabolomics in the culture supernatant of SIHUMIx during cultivation. (b) Heatmap and hierarchical clustering of bioreactor samples based on the absolute SCFA production of SIHUMIx. Mean normalized absolute SCFA concentrations were used for hierarchical clustering. Above mean values are colored in red, mean values in orange and below mean values in yellow. The color code in hierarchical clustering analysis shows light blue color for early days with increasing saturation for later days of cultivation.

distances, the average BC similarity among replicates was determined after the initial establishing phase directly after inoculation (day 1) and at a later time point (day 5) (Figure 3a, Supplemental file 1: Table S5). For all the individual methods but t-RFLP (p-value <0.0001), the replicate BC similarity on day 1 and day 5 was very similar (two-way ANOVA, Supplemental file 1: Table S5). Structural analyses showed a lower BC similarity (FC: 0.89 and 0.93, IPP: 0.83 and 0.75, t-RFLP: 0.67 and 0.88) than metabolic analyses (SCFA: 0.98 and 0.89, untargeted metabolomics: 0.94 and 0.96) on day 1 and day 5, respectively.

The reproducibility of SIHUMIx was proved by metaproteomics and SCFA analysis. Microbial composition of SIHUMIx was analyzed based on the abundance of species-specific proteins.[26,27] The relative species abundances of SIHUMIx from bioreactor A and B on day 1 and day 5, respectively, were very similar (Figure 3b, Supplemental file 1: Table S6). The communities on day 1 mainly comprised of *E. coli, B. producta, A. caccae* and *B. thetaiotaomicron*. The remaining strains, *C. butyricum, C. ramosum, B. longum* and *L. plantarum*, contributed to less than 1% relative species abundance. On day 5 to day 7, the communities had changed considerably and comprised of more than ~60% *B. thetaiotaomicron*, ~10% *B. producta* and *E. coli* and ~2% *A. caccae*. Proteins of all other strains (*C. ramosum, C. butyricum, L. plantarum*, and *B. longum)* were detected, but they contributed to less than 2% species abundance (Supplemental file 1: Table S6). Furthermore, SCFA analysis revealed highly similar relative SCFA concentrations within the replicate bioreactors but the concentrations changed over time (Figure 3c). On day 1, the most abundant SCFAs in the supernatant were acetate,

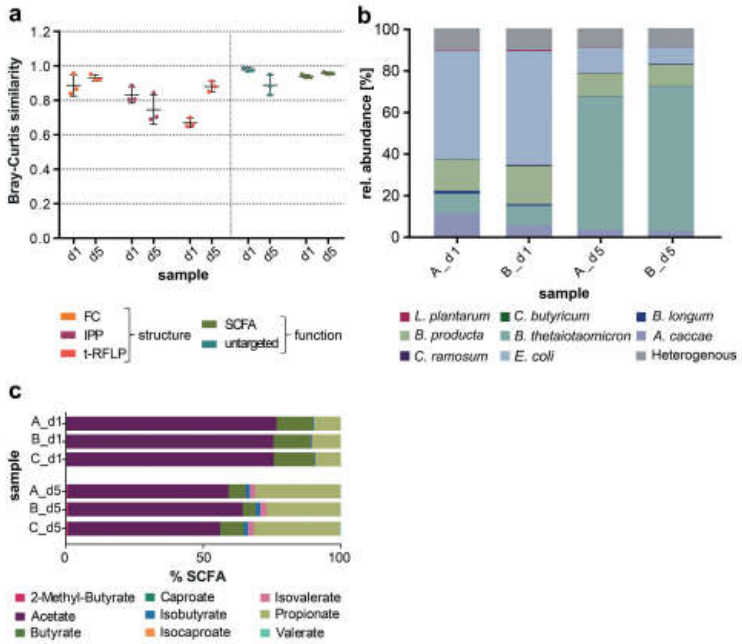

Figure 3. Reproducibility of SIHUMIx. (a) To analyze the reproducibility of SIHUMIx the Bray-Curtis (BC) similarity of bioreactor replicates A, B and C on day 1 and on day 5 (constant state) were determined. Calculations were based on different methods: flow cytometric fingerprinting analysis (FC), intact protein profiling (IPP), t-RFLP, SCFA analysis, and untargeted metabolomics. Data are shown as the mean ± standard deviation of triplicates. (b) Community structure was in detail analyzed by metaproteomics revealing the relative species abundances of the communities on day 1 and day 5 in bioreactors A and B. (c) SCFA production of the SIHUMIx communities was analyzed for the replicate bioreactors A, B and C on day 1 and day 5, respectively.

butyrate, and propionate in decreasing order. On day 5, the realtive SCFA composition was clearly different from that on day 1. The concentrations of acetate and butyrate decreased, but the concentration of propionate, isobutyrate, and isovalerate increased clearly on day 5 (Supplemental file 1: Table S7). Our results prove that SIHUMIx is a highly reproducible community in our bioreactor system, since community adaptation on taxonomy and SCFA levels were similar for all inocula.

SIHUMIx shows constant growth state starting on day 5

To evaluate the ability of SIHUMIx to reach a constant state, the Bray-Curtis (BC) distance values were used as described previously.[10] Therefore, the BC distances were calculated based on the analysis of cell abundances per cell population (technically termed as gate in FC method, Supplemental file 1: Figure S1), relative abundances of proteins, metabolites or SCFAs (IPP, untargeted and SCFA analysis, respectively) and relative abundance of terminal restriction fragments (t-RFLP, Supplemental file 3: BC distance matrices). The average BC similarity of all replicate samples (A, B, and C) compared to the replicates on days 6 and 7 (A and B) from day 1 until day 6 and 7 were visualized (Figure 4a). For all methods, the BC similarities followed the same trend: On day 1 and day 2, BC similarities were significantly lower compared to day 6/7 (pairwise PERMANOVA, p-values < 0.0001, Supplemental file 1: Table S8 and S9) but BC similarity increased steadily over time until day 5 (Supplemental file 1: Table S8 and S9). The average BC similarity on day 5 and day 6/7 compared to day 6/7 was

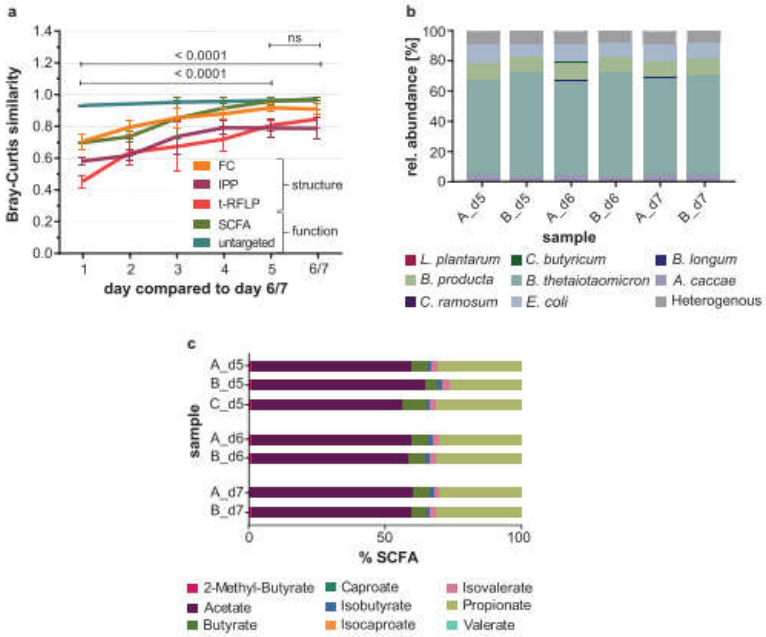

Figure 4. Development of SIHUMIx toward the constant state. (a) The average Bray-Curtis similarity (bioreactors A, B, C) on a given day of cultivation compared to the other bioreactors on day 6 and day 7 is shown for flow cytometric fingerprinting (FC), intact protein profiling (IPP), t-RFLP, SCFA analysis, and untargeted metabolomics. Data are shown as mean ± standard deviation. Comparison of community Bray-Curtis similarity by one-way ANOVA. (b) Species abundances in the SIHUMIx communities on day 5, day 6, and day 7 of bioreactors A and B based on metaproteomics. (c) Relative SCFA composition produced by the SIHUMIx communities in replicate bioreactors A, B and C on day 5, day 6, and day 7.

nearly identical and revealed community similarity on day 5. The BC similarity on day 5 compared to day 6/7 was as high as the replicate BC similarity on day 5, respectively (Supplemental file 1: Table S5). Constancy, respectively the structural and metabolic stability, of SIHUMIx was further analyzed by metaproteomics and SCFA profiles. On day 5, day 6, and day 7 the relative species abundances were very similar (Figure 4b) and SIHUMIx comprised mainly of *B. thetaiotaomicron, B. producta, E. coli* and *A. caccae*. The other four strains, *C. butyricum, C. ramosum, B. longum* and *L. plantarum*, contributed to less than 1% (Supplemental file 1: Table S6). SCFA analysis likewise revealed similar SCFA concentrations on day 5, day 6, and day 7 (Figure 4c). The major SCFAs in the supernatant were acetate, propionate, butyrate, isovalerate, and isobutyrate in decreasing order, whereas 2-methyl butyrate and isovalerate were produced only in very low concentrations (Supplemental file 1: Table S4 and Table S7).

SIHUMIx shows resistance and resilience after pulsed perturbation

Two bioreactors, D and E, were used to examine the dynamics of SIHUMIx when exposed to a pH-caused pulsed perturbation. Therefore, on day 4 the pH was set to 5.5 and reset to 6.5 after 24 h on day 5 (Figure 5a). Community dynamics were visualized in NMDS plots (Figure 5b) on the basis of (1) flow cytometric fingerprinting (FC) and (2) SCFA analysis that represent changes on the structural and functional level, respectively (Figure 5b). For comparison the constant state of SIHUMIx samples from bioreactors A, B, and C were included (gray ellipse, Figure 5b). The reference space defines the normal fluctuation of the constant SIHUMIx community and the threshold (tr, gray dashed line, Figure 5c) indicates the maximum fluctuation of SIHUMIx. The reference state resembles the center of the reference space and represents the mean of all samples used to build the reference space. Structural and functional deviations from the reference state in the disturbed bioreactors were followed. In addition, pH recording is shown to indicate the pH drop (red line). Maximal deviations were used to compute community resistance (RS) values. RS is the ability of a community to remain essentially unchanged in spite of a perturbation. Furthermore, resilience (RE) and elasticity (EL) were calculated. RE is the capability of a community to return to the reference state after a perturbation, and EL is the time it takes for a community to recover to the constant state.

After inoculation, the communities in bioreactors D and E were different compared to those from bioreactors A, B and C with regard to (1) community structure and (2) community function (Supplemental file: Figure S2). Nevertheless, these communities developed toward the constant state with respect to both community structure and function until day 3 (Figure 5b). This development was disturbed and immediately mirrored in structural and functional changes (Figure 5b,c). Generally, deviation values for the functional analysis were smaller than those for structural analysis. This became apparent in a smaller threshold value for the reference space (Figure 5c). Nevertheless, since the pH drop on day 5 community structure and function have been influenced

The community structure showed the strongest deviation from the reference state on day 5. The RS of bioreactor D was slightly higher than the RS of bioreactor E, with $RS_D = 0.64$ and $RS_E = 0.54$, respectively. After the pH drop, the community structure developed toward the constant state of the unimpeded community (ref. state) and the deviation values decreased. Samples from both bioreactors were fully recovered to the constant state on day 9, when the deviation values declined below the threshold. During the recovery process, the community in bioreactor E showed a similar resilience ($RL_E = 0.66$) compared to bioreactor D ($RL_D = 0.62$). The constant community state was kept until the end of the experiment on day 14. For bioreactor D the EL value was 0.018 d^{-1} and for bioreactor E 0.019 d^{-1}, respectively.

For community function, changes were also visible directly on day 5, but deviation values peaked on day 7. Here, the RS values were $RS_D = 0.78$ and $RS_E = 0.82$, respectively. After day 7 community functions developed toward the constant state. The community in bioreactor E recovered on day 14 and thus showed functional resilience ($RL_E = 0.60$) to a higher degree compared to the community in

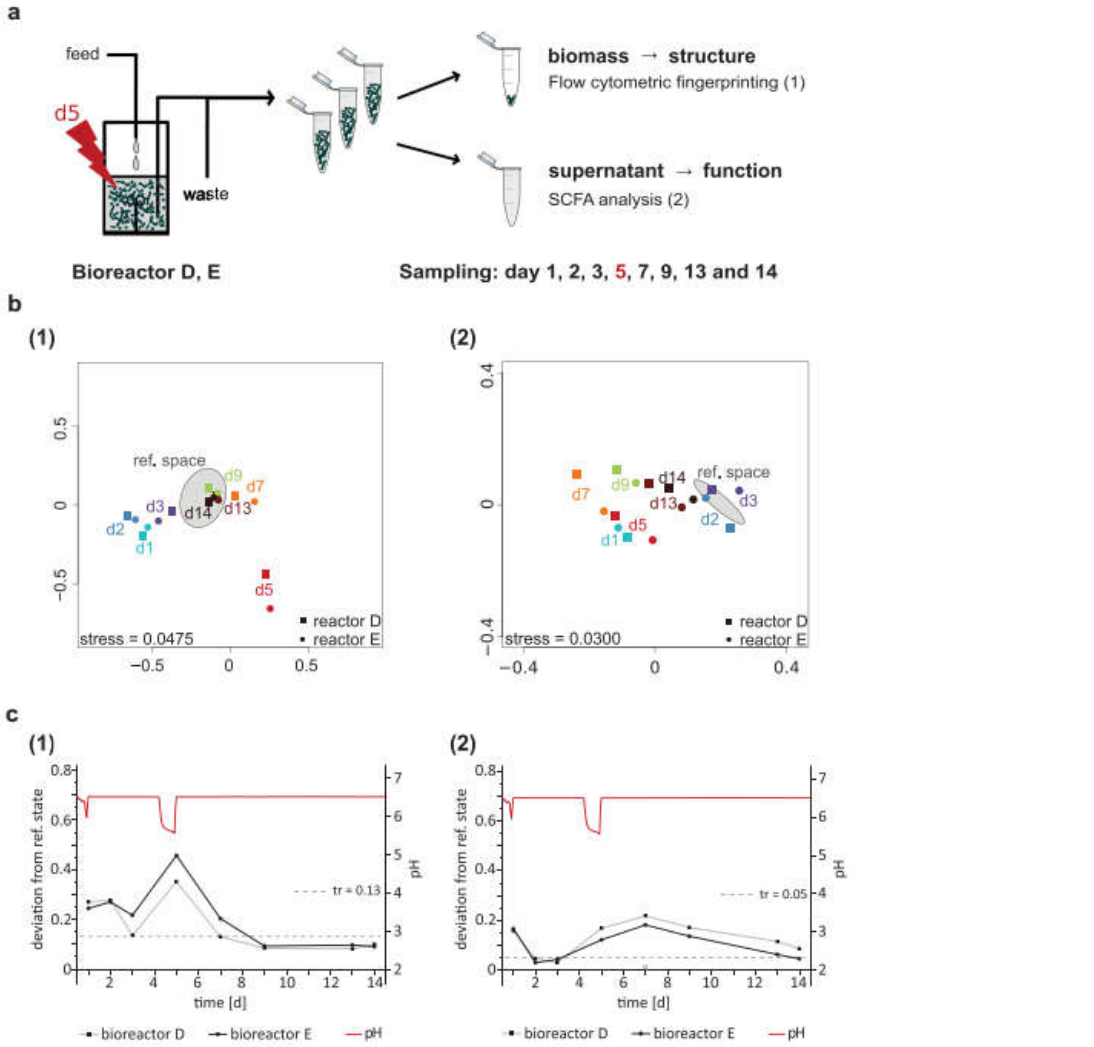

Figure 5. Experimental set-up and development of SIHUMIx before and after a pH drop. (a) The SIHUMIx community was cultivated *in vitro* and two replicate bioreactors D and E were inoculated (day 0). After 24 h the medium feed was turned on. On day 4, the pH was reduced from 6.5 to 5.5. After sampling on day 5, pH was reset to 6.5. Samples were taken on day 1, 2, 3, 5, 7, 9, 13 and 14. (b) Community structure was analyzed by (1) flow cytometric fingerprinting and community function by (2) SCFA analysis. The reference space of the SIHUMIx community resembles the unimpeded community of bioreactors A, B, C on days 5–7. (c) The deviation from the reference state (the center of the reference space) is shown for the communities in bioreactor D and E. The threshold of the reference space indicates the maximal deviation from the reference state in the constant community state. Communities with a deviation below the threshold are similar to the constant community, communities with above-threshold deviation are different from the constant community. The calculations are based on (1) flow cytometric fingerprinting analysis and (2) SCFA analysis.

bioreactor D (RL_D = 0.43). Bioreactor D did not recover until the end of the experiment on day 14. Compared to the recovery of the community structure, community function recovered at a slower velocity.

Discussion

Bioreactor systems are useful tools to investigate effects on the intestinal microbiota *in vitro*.[12,28] Most often complex fecal samples are used to inoculate bioreactors simulating the human intestine, but these complex inocula lack true biological replication.[12,16] It has recently been shown that despite the use of the same homogenous inoculum complex bacterial communities can develop toward completely different communities.[29] Besides, community structure can keep fluctuating over time in complex bacterial communities.[29,30] A variety of methods has been developed to analyze the community dynamics. In principle, the community structure and/or the community function are used to define an unchanged, constant state in complex communities. As *stability* is no stability property itself, we described the community development on the basis of the stability properties *constancy, resistance* and *resilience*.[19]

The major aim of this study was to establish an *in vitro* model community for bioreactor use that reproducibly develops toward a constant community state with regard to both community structure and function. Furthermore, we wanted to determine, if different methods similarly depict the community development. Therefore, we cultivated the SIHUMIx community under defined chemostat conditions and analyzed the community development on the structural and functional level with five different analytical methods.[20] Even though the SIHUMIx community comprised of only eight bacterial species SIHUMIx shares the major SCFA with complex fecal communities.[31] SIHUMIx produces high levels of acetate, propionate and butyrate and low levels of branched SCFA. Additionally, SIHUMIx covers the major phyla *Firmicutes, Bacteroidetes, Proteobacteria*, and *Actinobacteria*. Nevertheless contrasting fecal communities, the model community SIHUMIx is far less diverse. Under balanced state conditions, SIHUMIx was dominated by *B. thetaiotaomicron* (phylum *Bacteroides*). Besides, *E. coli* (phylum *Proteobacteria), B. producta* and *A. caccae* (phylum *Firmicutes*) were found in decreasing order with a relative species abundance >3%. The remaining bacterial strains were present with relative species abundances below 1%. Since we aimed to simulate the colonic environment as close as possible *in vitro*, we used a complex culture medium similar to other culture media used to cultivate fecal microbiota.[13,29,32] The culture medium contains mucin and since *B. thetaiotaomicron* is a known mucin degrader this species gains a growth advantage.[33] Microbial growth of the model community SIHUMI (SIHUMIx without *C. butyricum*) has been modeled in the absence and presence of mucin.[34] Bauer et al. show that in the presence of mucin *B. thetaiotaomicron* will be the dominant species in the community. Nevertheless, it has recently been shown that all SIHUMIx bacterial strains remain in the community during continuous cultivation of SIHUMIx for up to 14 days, even though four strains from the SIHUMIx community are low abundant with less than 1% relative species abundance [Schäpe et al. 2019 in *microorganisms*, accepted for publication].

With respect to community structure analyses, the range of methods used in bioreactor research is considerably large. Analyses like microbial flow cytometry (FC),[35] metaproteomics,[36] and DNA-based methods, such as 16S rRNA gene analysis, terminal restriction fragment length polymorphism (t-RFLP) analysis,[21] next-generation sequencing[10] or denaturing gradient gel electrophoresis (DGGE),[13] have been published. We wanted to analyze the community structure on different cellular levels and therefore applied FC, intact protein profiling (IPP) and t-RFLP to analyze the cell-, protein- and DNA-related structural development. T-RFLP profiling is frequently used to track community dynamics in bacterial communities and the choice of the target gene allows the analysis of distinct microbial domains or phyla.[37] FC has the ability to resolve changes down to the single cell level and is therefore highly sensitive. Furthermore, FC provides the option of next-generation 16S rRNA analysis after sorting of interesting cell populations.[38] In contrast to metaproteomics, the workflow of IPP is much faster and, even though no biological information is

generated, it provides a protein-based fingerprint.[39]

Community function of gut microbiota is routinely assessed using SCFA analysis and provides insights into the metabolic activity and thereby delivers specific information on the fermentation process.[16,17,40] In some studies, besides SCFA, other metabolites have been measured.[14,41] For that reason, we decided to include a more general approach in our analyses, specifically untargeted metabolomics.

To demonstrate the constant growth state of SIHUMIx, we compared the Bray-Curtis (BC) similarity of the communities on each day of cultivation to the communities on day 6/7. With proceeding adaptation, the BC similarity increased and reached a maximum on day 5. Then, the BC similarity on day 5 compare to day 6/7 was identical to the BC similarity of all samples on day 6/7. Thus, our results demonstrate that the SIHUMIx community starts to adapt directly after inoculation and then reaches a constant state with regard to both community structure (bacteria (FC), protein (IPP), and DNA (t-RFLP) composition) and community metabolism (SCFA analysis, untargeted metabolomics). Furthermore, compared to the *in vitro* cultivation of fecal communities the adaptation of SIHUMIx is very fast. This might result from the low diversity and the high abundance of *B. thetaiotaomicron*. McDonald et al. (2013) observed a structure-related constant state after 30 to 36 days of cultivation of fecal communities in their structural analysis with DGGE.[13] Liu et al. (2018) followed the development of their fecal community in the TWIN-SHIME by 16S rRNA and SCFA analyses.[17] In their study, the community structure became constant on day 10, whereas the communities' SCFA metabolism became constant not before day 17. Furthermore, in contrast to the complex fecal community, SIHUMIx develops simultaneously on the structural and metabolic level during adaptation.[17]

During the adaptation of SIHUMIx, all five methods similarly depicted the community development and indicated that the SIHUMIx community reached a constant state on day 5 with regard to community structure, as well as with regard to function. Since FC, t-RFLP and SCFA analyses have already been applied to follow complex community dynamics, we expected them to record the development of SIHUMIx reliably. However, to our knowledge, IPP and untargeted metabolomics have not been used to follow community dynamics, yet. Our results prove that both methods are suitable. For complex fecal communities, their suitability has to be validated.

It was observed that during cultivation microbial communities from the same homogenous inoculum can develop into different communities with regard to community structure.[29] This was not the case for SIHUMIx, which adapted to the system to a similar state in each bioreactor. To prove that for SIHUMIx, we used different batches of bacteria to inoculate replicate bioreactors. SIHUMIx unravels a highly reproducible development toward the same constant state. Surprisingly, directly after inoculation the communities from the disturbed bioreactors (D and E) were different compared to the unimpeded bioreactors. The only difference was that the pre-cultures for bioreactor A, B and C were grown for 72 h, whereas those for bioreactor D and E were cultivated for 48 h. However, the communities reached the same constant community state. This shows that the constant state of SIHUMIx is highly reproducible, but to achieve maximal reproducibility during the adaptation there is a need for standardized inocula. Generally, the BC similarity among replicates was slightly lower for structural analyses compared to functional analyses. Even though it is well known that community function is more stable than community structure,[42] the difference in the range of the BC similarity for structural and functional analyses is likely to result from the sample preparation. The medium background might have elevated the level of replicate BC similarity for metabolome analyses to ~0.95 in comparison to structural analyses that have ~0.80 BC similarity (BC similarity of 1 represents equality), since for structural analyses, bacteria pellets were used to prepare the cell suspensions, protein and DNA extracts. For targeted metabolomics, culture supernatants were used since SCFA are secreted into the medium.[43] Nevertheless, compared to the literature a BC similarity of 0.8 is already high.[10,17] The highly similar and reproducible community development is also visible in the relative species abundances and SCFA concentrations.

It has been found that acidification of the colon occurs in patients with active ulcerative colitis and resembles a severe disturbance.[25] Thus, we validated the responsiveness of the SIHUMIx community to a pH drop for 24 h. Since community structure and function can develop differently,[16,17] we tracked the community dynamics both on a structural and functional level. Since all methods are appropriate, we applied the most informative methods for structural and functional analysis, which are FC and SCFA analysis, respectively. Both methods clearly revealed the consequences of the pH drop and showed the similar behavior of the replicate bioreactors. Community structure responded and recovered faster than community function. This is in accordance with published studies that also found that community structure stabilizes earlier than community function.[16,17] Our data disclose that the SIHUMIx community, in comparison to the complex community of Liu et al., shows a higher resistance against the perturbation.[29] They introduced a long-term temperature perturbation, whereas we exposed the SIHUMIx community only for 24 h to a decreased pH. Nevertheless, the SIHUMIx community possesses the ability to recover to the constant state and therefore is highly resilient. However, to compare the *resistance* and *resilience* of both communities indisputably, the communities have to be exposed to the same perturbation.

SCFA analysis, untargeted metabolomics, FC, IPP, and t-RFLP were evaluated and proven appropriate to trace the development of the SIHUMIx community. Our results suggest that various methods are suitable to follow community dynamics, but it is important to analyze community development both on the structural and functional level at the same time.

Reproducibility with regard to structural and functional development and the ability to reach a reproducible constant state within five days are the major advantages of SIHUMIx. The constant community state of SIHUMIx shares features of a complex community with regard to both community structure and function. The community shows high resistance, even though it responds to perturbations, and has the ability to recover (resilience). These properties allow the investigation of effects on the community that result from environmental factors, like pesticides or plasticizers, but also dietary or medical interventions. Moreover, the usage of microbial model communities, like SIHUMIx, might help to replace animal models in order to evaluate treatment effects. At the same time, the cultivation of small model communities opens the opportunity to study microbial interactions on the species level. Furthermore, the contribution of individual species to resultant changes in the communities' performance is possible as well as the expansion of SIHUMIx to a more complex, but still defined model community. Thus, our results show that SIHUMIx is a suitable model for *in vitro* testing.

Materials and methods

A detailed description of materials and methods is given in the online repository of this journal (Supplemental file 4 – Methods).

Single stage bioreactor – experimental set-up

The cultivation was carried through in a Multifors 2 bioreactor (Infors). The reactors were inoculated with 1×10^9 bacterial cells per strain.

For the establishment of the SIHUMIx community as *in vitro* model, three parallel and independent 250 mL culture vessels (A, B, and C) were modified as chemostat. To investigate the effect of a pH drop on the SIHUMIx community, two parallel and independent bioreactors (D and E) were run for 14 days. The pH was reduced to 5.5 on day 4 and the community was exposed to the low pH for 24 h. After sampling on day 5, the pH was reset to the original pH of 6.5 until the end of the cultivation.

Sampling and sample analyses

Samples were taken in a 24 h interval starting the day after inoculation (d1). For t-RFLP analysis, IPP, SCFA analysis and untargeted metabolomics, samples were centrifuged (5,000 x g, 5 min, and 4° C). Cell pellets without supernatant were stored directly at −20°C for t-RFLP and IPP, whereas the supernatants for metabolome analysis were stored at −80°C. The cells for flow cytometric fingerprinting were harvested by centrifugation (3,200 x g, 10 min, and 4°C) and prepared directly.

It has been found that acidification of the colon occurs in patients with active ulcerative colitis and resembles a severe disturbance.[25] Thus, we validated the responsiveness of the SIHUMIx community to a pH drop for 24 h. Since community structure and function can develop differently,[16,17] we tracked the community dynamics both on a structural and functional level. Since all methods are appropriate, we applied the most informative methods for structural and functional analysis, which are FC and SCFA analysis, respectively. Both methods clearly revealed the consequences of the pH drop and showed the similar behavior of the replicate bioreactors. Community structure responded and recovered faster than community function. This is in accordance with published studies that also found that community structure stabilizes earlier than community function.[16,17] Our data disclose that the SIHUMIx community, in comparison to the complex community of Liu et al., shows a higher resistance against the perturbation.[29] They introduced a long-term temperature perturbation, whereas we exposed the SIHUMIx community only for 24 h to a decreased pH. Nevertheless, the SIHUMIx community possesses the ability to recover to the constant state and therefore is highly resilient. However, to compare the *resistance* and *resilience* of both communities indisputably, the communities have to be exposed to the same perturbation.

SCFA analysis, untargeted metabolomics, FC, IPP, and t-RFLP were evaluated and proven appropriate to trace the development of the SIHUMIx community. Our results suggest that various methods are suitable to follow community dynamics, but it is important to analyze community development both on the structural and functional level at the same time.

Reproducibility with regard to structural and functional development and the ability to reach a reproducible constant state within five days are the major advantages of SIHUMIx. The constant community state of SIHUMIx shares features of a complex community with regard to both community structure and function. The community shows high resistance, even though it responds to perturbations, and has the ability to recover (resilience). These properties allow the investigation of effects on the community that result from environmental factors, like pesticides or plasticizers, but also dietary or medical interventions. Moreover, the usage of microbial model communities, like SIHUMIx, might help to replace animal models in order to evaluate treatment effects. At the same time, the cultivation of small model communities opens the opportunity to study microbial interactions on the species level. Furthermore, the contribution of individual species to resultant changes in the communities' performance is possible as well as the expansion of SIHUMIx to a more complex, but still defined model community. Thus, our results show that SIHUMIx is a suitable model for *in vitro* testing.

Materials and methods

A detailed description of materials and methods is given in the online repository of this journal (Supplemental file 4 – Methods).

Single stage bioreactor – experimental set-up

The cultivation was carried through in a Multifors 2 bioreactor (Infors). The reactors were inoculated with 1×10^9 bacterial cells per strain.

For the establishment of the SIHUMIx community as *in vitro* model, three parallel and independent 250 mL culture vessels (A, B, and C) were modified as chemostat. To investigate the effect of a pH drop on the SIHUMIx community, two parallel and independent bioreactors (D and E) were run for 14 days. The pH was reduced to 5.5 on day 4 and the community was exposed to the low pH for 24 h. After sampling on day 5, the pH was reset to the original pH of 6.5 until the end of the cultivation.

Sampling and sample analyses

Samples were taken in a 24 h interval starting the day after inoculation (d1). For t-RFLP analysis, IPP, SCFA analysis and untargeted metabolomics, samples were centrifuged (5,000 x g, 5 min, and 4° C). Cell pellets without supernatant were stored directly at −20°C for t-RFLP and IPP, whereas the supernatants for metabolome analysis were stored at −80°C. The cells for flow cytometric fingerprinting were harvested by centrifugation (3,200 x g, 10 min, and 4°C) and prepared directly.

Details for flow cytometric fingerprinting, intact protein profiling, metaproteome analysis, targeted short chain fatty acid analysis, untargeted metabolome analysis and terminal restriction fragment length polymorphism are given in the supplementary online repository of this journal.

Acknowledgments

We thank the German Federal Environmental Foundation (DBU) for financial support of Jannike Lea Krause. We thank Prof. Dr. Michael Blaut (German Institute of Human Nutrition, Potsdam-Rehbruecke) for providing the SIHUMIx bacteria. We are thankful for technical assistance from Jeremy Knespel, Eva-Annamaria Stier, Kathleen Eismann and Nicole Gröger and for culture medium supply from Martina Kolbe.

Authors' contributions

JLK (Jannike Lea Krause) and SSS (Stephanie Serena Schaepe) performed the bioreactor experiments and evaluated the data. KFW (Katarina Fritz-Wallace), BE (Beatrice Engelmann) performed the metabolome analyses and were supported by URK (Ulrike Rolle-Kampczyk). JLK, FS (Florian Schattenberg) and ZL (Zishu Liu) performed the flow cytometric analyses with support from SM (Susann Mueller). JLK, did the t-RFLP analyses supported by SK (Sabine Kleinsteuber). SSS did metproteomics with support from NJ (Nico Jehmlich). MvB (Martin von Bergen) and GH (Gunda Herberth) conceptualized the study. All authors contributed to and approved the manuscript.

Availability of data and materials

Raw cytometric data can be found at flow repository ID: **FR-FCM-ZYVG** under: **https://flowrepository.org**.

Disclosure of potential conflicts of interest

The authors report no conflict of interest.

Funding

Stephanie Schäpe is grateful for support from a DFG-grant within the Priority Program [1656], and Martin von Bergen acknowledges partial funding by DFG Priority Program [1382].

ORCID

Ulrike Rolle-Kampczyk http://orcid.org/0000-0002-7728-6284
Sabine Kleinsteuber http://orcid.org/0000-0002-8643-340X
Zishu Liu http://orcid.org/0000-0001-6820-4593
Nico Jehmlich http://orcid.org/0000-0002-5638-6868
Martin Von Bergen http://orcid.org/0000-0003-2732-2977
Gunda Herberth http://orcid.org/0000-0003-0212-3509

References

1. Bäckhed F, Ley RE, Sonnenburg JL, Peterson DA, Gordon JI. Host-bacterial mutualism in the human intestine. Science. 2005;307:1915–1920. doi:10.1126/science.1104816.
2. Blumberg R, Powrie F. Microbiota, disease, and back to health: a metastable journey. Sci Transl Med. 2012;4:137rv7–137rv7. doi:10.1126/scitranslmed.3004184.
3. O'Hara AM, Shanahan F. The gut flora as a forgotten organ. EMBO Rep. 2006;7:688–693. doi:10.1038/sj.embor.7400731.
4. Levy M, Blacher E, Elinav E. Microbiome, metabolites and host immunity. Curr Opin Microbiol. 2017;35:8–15. doi:10.1016/j.mib.2016.10.003.
5. Thaiss CA, Zmora N, Levy M, Elinav E. The microbiome and innate immunity. Nature. 2016;535:65–74. doi:10.1038/nature18847.
6. Oates L, Cohen M. Assessing diet as a modifiable risk factor for pesticide exposure. Int J Environ Res Public Health. 2011;8:1792–1804. doi:10.3390/ijerph8061792.
7.. EFSA. Opinion of the scientific panel on contaminants in the food chain on Perfluorooctane Sulfonate (PFOS), Perfluorooctanoic Acid (PFOA) and their salts. EFSA J. 2008; 1–131.
8. Joly C, Gay-Quéheillard J, Léké A, Chardon K, Delanaud S, Bach V, Khorsi-Cauet H. Impact of chronic exposure to low doses of chlorpyrifos on the intestinal microbiota in the Simulator of the Human Intestinal Microbial Ecosystem (SHIME®) and in the rat. Environ Sci Pollut Res. 2013;20:2726–2734. doi:10.1007/s11356-012-1283-4.
9. Reygner J, Joly Condette C, Bruneau A, Delanaud S, Rhazi L, Depeint F, Abdennebi-Najar L, Bach V, Mayeur C, Khorsi-Cauet H. Changes in composition and function of human intestinal microbiota exposed to chlorpyrifos in oil as assessed by the SHIME® model. Int J Environ Res Public Health. 2016;13:1088. doi:10.3390/ijerph13111088.
10. Auchtung JM, Robinson CD, Britton RA Cultivation of stable, reproducible microbial communities from different fecal donors using minibioreactor arrays (MBRAs). Microbiome [Internet]. 2015;3:42. [cited 2018 Mar 3]. http://www.microbiomejournal.com/content/3/1/42.
11. Tanner SA, Zihler Berner A, Rigozzi E, Grattepanche F, Chassard C, Lacroix C. In vitro continuous fermentation model (PolyFermS) of the swine proximal colon for simultaneous testing on the same gut microbiota.

PLoS One. 2014;9:e94123. doi:10.1371/journal.pone.0094123.
12. Payne AN, Zihler A, Chassard C, Lacroix C. Advances and perspectives in in vitro human gut fermentation modeling. Trends Biotechnol. 2012;30:17–25. doi:10.1016/j.tibtech.2011.06.011.
13. McDonald JAK, Schroeter K, Fuentes S, Heikamp-deJong I, Khursigara CM, de Vos WM, Allen-Vercoe E. Evaluation of microbial community reproducibility, stability and composition in a human distal gut chemostat model. J Microbiol Methods. 2013;95:167–174. doi:10.1016/j.mimet.2013.08.008.
14. Carman RJ, Woodburn MA. Effects of low levels of ciprofloxacin on a chemostat model of the human colonic microflora. Regul Toxicol Pharmacol. 2001;33:276–284. doi:10.1006/rtph.2001.1473.
15. Possemiers S, VerthÃ© K, Uyttendaele S, Verstraete W. PCR-DGGE-based quantification of stability of the microbial community in a simulator of the human intestinal microbial ecosystem. FEMS Microbiol Ecol. 2004;49:495–507. doi:10.1016/j.femsec.2004.05.002.
16. Van den Abbeele P, Grootaert C, Marzorati M, Possemiers S, Verstraete W, Gerard P, Rabot S, Bruneau A, El Aidy S, Derrien M, et al. Microbial community development in a dynamic gut model is reproducible, colon region specific, and selective for bacteroidetes and clostridium cluster IX. Appl Environ Microbiol. 2010;76:5237–5246. doi:10.1128/AEM.00759-10.
17. Liu L, Firrman J, Tanes C, Bittinger K, Thomas-Gahring A, Wu GD, Van den Abbeele P, Tomasula PM. Establishing a mucosal gut microbial community in vitro using an artificial simulator. PLoS One. 2018;13:e0197692. doi:10.1371/journal.pone.0197692.
18. Grimm V, Schmidt E, Wissel C. On the application of stability concepts in ecology. Ecol Model. 1992;63:143–161. doi:10.1016/0304-3800(92)90067-O.
19. Grimm V, Wissel C. Babel, or the ecological stability discussions: an inventory and analysis of terminology and a guide for avoiding confusion. Oecologica. 1997;109:323–334. doi:10.1007/s004420050090.
20. Becker N, Kunath J, Loh G, Blaut M. Human intestinal microbiota: Characterization of a simplified and stable gnotobiotic rat model. Gut Microbes. 2011;2:25–33. doi:10.4161/gmic.2.1.14651.
21. Sträuber H, Schröder M, Kleinsteuber S. Metabolic and microbial community dynamics during the hydrolytic and acidogenic fermentation in a leach-bed process. Energy Sustain Soc. 2012;2:13. doi:10.1186/2192-0567-2-13.
22. Koch C, Müller S. Personalized microbiome dynamics – Cytometric fingerprints for routine diagnostics. Mol Aspects Med. 2018;59:123–134. doi:10.1016/j.mam.2017.06.005.
23. Wissenbach DK, Oliphant K, Rolle-Kampczyk U, Yen S, Höke H, Baumann S, Haange SB, Verdu EF, Allen-Vercoe E, von Bergen M. Optimization of metabolomics of defined in vitro gut microbial ecosystems. Int J Med Microbiol. 2016;306:280–289. doi:10.1016/j.ijmm.2016.03.007.
24. Jehmlich N, Schmidt F, Taubert M, Seifert J, von Bergen M, Richnow H-H VC. Comparison of methods for simultaneous identification of bacterial species and determination of metabolic activity by protein-based stable isotope probing (Protein-SIP) experiments. Rapid Commun Mass Spectrom. 2009;23:1871–1878. doi:10.1002/rcm.4084.
25. Nugent SG, Kumar D, Rampton DS, Evans DF. Intestinal luminal pH in inflammatory bowel disease: possible determinants and implications for therapy with aminosalicylates and other drugs. Gut. 2001;48:571–577. doi:10.1136/gut.48.4.571.
26. Ke X, Walker A, Haange S-B, Lagkouvardos I, Liu Y, Schmitt-Kopplin P, von Bergen M, Jehmlich N, He X, Clavel T, et al. Synbiotic-driven improvement of metabolic disturbances is associated with changes in the gut microbiome in diet-induced obese mice. Mol Metab. 2019;22:96–109. doi:10.1016/j.molmet.2019.01.012.
27. Kleiner M, Thorson E, Sharp CE, Dong X, Liu D, Li C, Strous M. Assessing species biomass contributions in microbial communities via metaproteomics. Nat Commun. 2017;8:1558. doi:10.1038/s41467-017-01544-x.
28. Macfarlane GT, Macfarlane S. Models for intestinal fermentation: association between food components, delivery systems, bioavailability and functional interactions in the gut. Curr Opin Biotechnol. 2007;18:156–162. doi:10.1016/j.copbio.2007.01.011.
29. Liu Z, Cichocki N, Hübschmann T, Süring C, Ofiţeru ID, Sloan WT, Grimm V, Müller S. Neutral mechanisms and niche differentiation in steady-state insular microbial communities revealed by single cell analysis: Non-equilibria systems. Environ Microbiol. 2019;21:164–181. doi:10.1111/emi.2019.21.issue-1.
30. Fernández A, Huang S, Seston S, Xing J, Hickey R, Criddle C, Tiedje J. How stable is stable? Function versus community composition. Appl Environ Microbiol. 1999;65:3697–3704.
31. Ríos-Covián D, Ruas-Madiedo P, Margolles A, Gueimonde M, de Los Reyes-gavilán CG, Salazar N. Intestinal short chain fatty acids and their link with diet and human health. Front Microbiol [Internet]. 2016;7:185. [cited 2019 Feb 13]. http://journal.frontiersin.org/Article/10.3389/fmicb.2016.00185/abstract.
32. Child MW, Kennedy A, Walker AW, Bahrami B, Macfarlane S, Macfarlane GT. Studies on the effect of system retention time on bacterial populations colonizing a three-stage continuous culture model of the human large gut using FISH techniques: the effect of system retention time on bacterial populations. FEMS Microbiol Ecol. 2006;55:299–310. doi:10.1111/fem.2006.55.issue-2.
33. Koropatkin NM, Cameron EA, Martens EC. How glycan metabolism shapes the human gut microbiota. Nat Rev Microbiol. 2012;10:323–335. doi:10.1038/nrmicro2746.

34. Bauer E, Zimmermann J, Baldini F, Thiele I, BacArena KC. Individual-based metabolic modeling of heterogeneous microbes in complex communities. PLoS Comput Biol. 2017;13:e1005544. doi:10.1371/journal.pcbi.1005544.
35. Brognaux A, Han S, Sørensen SJ, Lebeau F, Thonart P, Delvigne F. A low-cost, multiplexable, automated flow cytometry procedure for the characterization of microbial stress dynamics in bioreactors. Microb Cell Factories. 2013;12:100. doi:10.1186/1475-2859-12-100.
36. Kuhn R, Benndorf D, Rapp E, Reichl U, Palese LL, Pollice A. Metaproteome analysis of sewage sludge from membrane bioreactors. Proteomics. 2011;11:2738–2744. doi:10.1002/pmic.v11.13.
37. Schütte UME, Abdo Z, Bent SJ, Shyu C, Williams CJ, Pierson JD, Forney LJ. Advances in the use of terminal restriction fragment length polymorphism (T-RFLP) analysis of 16S rRNA genes to characterize microbial communities. Appl Microbiol Biotechnol. 2008;80:365–380. doi:10.1007/s00253-008-1565-4.
38. Koch C, Günther S, Desta AF, Hübschmann T, Müller S. Cytometric fingerprinting for analyzing microbial intracommunity structure variation and identifying subcommunity function. Nat Protoc. 2013;8:190–202. doi:10.1038/nprot.2012.149.
39. Usbeck JC, Wilde C, Bertrand D, Behr J, Vogel RF. Wine yeast typing by MALDI-TOF MS. Appl Microbiol Biotechnol. 2014;98:3737–3752. doi:10.1007/s00253-014-5586-x.
40. Baxter NT, Schmidt AW, Venkataraman A, Kim KS, Waldron C, Schmidt TM. Dynamics of human gut microbiota and short-chain fatty acids in response to dietary interventions with three fermentable fibers. mBio. 2019;10:e02566–18. doi:10.1128/mBio.02566-18.
41. Macfarlane GT, Macfarlane S, Gibson GR. Validation of a three-stage compound continuous culture system for investigating the effect of retention time on the ecology and metabolism of bacteria in the human colon. Microb Ecol. 1998;35:180–187. doi:10.1007/s002489900072.
42. Huttenhower C, Gevers D, Knight R, Abubucker S, Badger JH, Chinwalla AT, Creasy HH, Earl AM, FitzGerald MG, Fulton RS, et al. Structure, function and diversity of the healthy human microbiome. Nature. 2012;486:207–214.
43. LeBlanc JG, Chain F, Martín R, Bermúdez-Humarán LG, Courau S, Langella P. Beneficial effects on host energy metabolism of short-chain fatty acids and vitamins produced by commensal and probiotic bacteria. Microb Cell Factories [Internet]. 2017;16:79. [cited 2018 Dec 18]. http://microbialcellfactories.biomedcentral.com/articles/10.1186/s12934-017-0691-z.

Publication 2: The simplified human intestinal microbiota (SIHUMIx) shows high structural and functional resistance against changing transit times in in vitro bioreactors

microorganisms

MDPI

Article

The Simplified Human Intestinal Microbiota (SIHUMIx) Shows High Structural and Functional Resistance against Changing Transit Times in *In Vitro* Bioreactors

Stephanie Serena Schäpe [1,†], Jannike Lea Krause [2,†], Beatrice Engelmann [1], Katarina Fritz-Wallace [1], Florian Schattenberg [3], Zishu Liu [3], Susann Müller [3], Nico Jehmlich [1], Ulrike Rolle-Kampczyk [1], Gunda Herberth [2,†] and Martin von Bergen [1,4,*,†]

1 Department of Molecular Systems Biology, Helmholtz-Centre for Environmental Research—UFZ GmbH, 04316 Leipzig, Germany; stephanie.schaepe@ufz.de (S.S.S.); beatrice.engelmann@ufz.de (B.E.); katarina.fritz@ufz.de (K.F.-W.); nico.jehmlich@ufz.de (N.J.); ulrike.rolle-kampczyk@ufz.de (U.R.-K.)
2 Department of Environmental Immunology, Helmholtz-Centre for Environmental Research—UFZ GmbH, 04316 Leipzig, Germany; jannike-lea.krause@ufz.de (J.L.K.); gunda.herberth@ufz.de (G.H.)
3 Department of Environmental Microbiology, Helmholtz-Centre for Environmental Research—UFZ GmbH, 04316 Leipzig, Germany; florian.schattenberg@ufz.de (F.S.); zishu.liu@ufz.de (Z.L.); susann.mueller@ufz.de (S.M.)
4 Institute of Biochemistry, Faculty of Biosciences, Pharmacy and Psychology, University of Leipzig, 04103 Leipzig, Germany
* Correspondence: martin.vonbergen@ufz.de; Tel.: +49-341-235-1211
† These authors contributed equally to this work.

Received: 14 June 2019; Accepted: 20 September 2019; Published: 3 December 2019

check for updates

Abstract: Many functions in host–microbiota interactions are potentially influenced by intestinal transit times, but little is known about the effects of altered transition times on the composition and functionality of gut microbiota. To analyze these effects, we cultivated the model community SIHUMIx in bioreactors in order to determine the effects of varying transit times (TT) on the community structure and function. After five days of continuous cultivation, we investigated the influence of different medium TT of 12 h, 24 h, and 48 h. For profiling the microbial community, we applied flow cytometric fingerprinting and revealed changes in the community structure of SIHUMIx during the change of TT, which were not associated with changes in species abundances. For pinpointing metabolic alterations, we applied metaproteomics and metabolomics and found, along with shortening the TT, a slight decrease in glycan biosynthesis, carbohydrate, and amino acid metabolism and, furthermore, a reduction in butyrate, methyl butyrate, isobutyrate, valerate, and isovalerate concentrations. Specifically, *B. thetaiotaomicron* was identified to be affected in terms of butyrate metabolism. However, communities could recover to the original state afterward. This study shows that SIHUMIx showed high structural stability when TT changed—even four-fold. Resistance values remained high, which suggests that TTs did not interfere with the structure of the community to a certain degree.

Keywords: *In vitro* model; microbial community; flow cytometry; metaproteomics; metabolomics; short-chain fatty acids; intestinal microbiota; SIHUMIx; bioreactor

1. Introduction

The human intestine harbors hundreds of bacterial species that are associated with human health and disease [1,2]. This association is mainly due to changes in metabolic interactions with the host

caused by changes in the bacterial community structure and function. One of the primary roles of intestinal microbiota is the conversion of nutrients into bioactive compounds, which are taken up by the host [3,4]. Due to the enzymatic break-down of carbohydrates, proteins, and fatty acids, the intestinal microbiota produces essential nutrients, such as short-chain fatty acids (SCFA) and vitamins [5]. SCFA provide energy for intestinal epithelial cells and modulate the host immune system and, therefore, play a beneficial role in the host's health [6]. While carbohydrate fermentation results in SCFA production, the fermentation of proteins and amino acids results in the production of branched short-chain fatty acids (BCFA). BCFA such as isovalerate, isobutyrate, and 2-methyl butyrate are produced due to the fermentation of valine, leucine, and isoleucine and serve as precursors for fatty acid synthesis or as nitrogen donors for the production of other amino acids [7,8]. The concentration of these bioactive compounds depends on daily food intake and the type of food. Hence, nutrient concentrations in the gut change and can, thereby, affect metabolic interactions. Changes in nutrient concentrations can not only vary due to different amounts of food intake but also due to variations in intestinal transit times, dietary amount, and health state (e.g., infections) [9].

In the human population, differences in intestinal transit times (TTs) are often observed. They have been associated with differences in stool frequency and, therefore, have been linked to changes in the gut microbiota composition [10,11]. In healthy human individuals, the whole gut TT varies but takes approximately 27 h from which 18 h refer to the colonic TT [12–14]. Child et al. compared 20 h and 60 hTTs and found that 20 hTT resulted in a decrease or loss of bacterial populations, e.g., *Rumminococcus* and *Roseburia* compared to 60 hTT [15]. In addition to the community composition, the metabolism was also affected. Tottey et al. observed, at an increased TT from 48 h to 96 h, a decrease in biomass and an increase in protein fermentation, while SCFA production remained mainly unaffected [16]. Furthermore, changes in TT also affected the fermentation production of a single species. For example, *C. tyrobutyricum* showed a higher butyrate production within a shorter TT of 8 h compared to 16.7 h [17]. Nevertheless, all of these intestinal *in vitro* models used complex fecal communities, which evolve differently in *in vitro* systems [18,19].

The effect of intestinal TTs was investigated in the past in various bioreactor models by the use of different TTs, but effects on structure and function have not been fully understood [15,16,20]. *In vitro* bioreactor systems are useful tools to investigate environmental stressors on microbial communities, since they overcome the limitations of conventional culture techniques [5]. Most *in vitro* bioreactor models use fecal inocula and, therefore, face the problem of missing the establishment of a reproducible complex microbial community [21]. Moreover, for metaproteome analysis of complex microbial communities, the major challenge is to achieve sufficient proteome coverage in order to generate a comprehensive picture of the community structure and function [22,23]. To overcome these challenges, we recently established an extended simplified human intestinal microbiota (SIHUMIx) for *in vitro* use (Krause et al., in revision at *Gut Microbes journal*). This model community consists of eight bacterial species resembling, to a large extent, the metabolic activities found in the human intestine [24]. Rothe et al. [25] also selected the strains because the genome sequences were available. Functions that are known to be fulfilled by each species are given in Supplementary Material Table S1. Several previous studies with SIHUMIx have been published in which gnotobiotic mice were seeded with SIHUMIx or part of the SIHUMIx strains to investigate an interaction between host and gut microbiota [26–29]. Data from Becker et al. were also used for modelling approaches [30]. We found that SIHUMIx maintained its structure to a high degree when cultivated continuously and reached the ability to stay essentially unchanged after five days, which serves as the starting point for experimental treatments (Krause et al., in revision at *Gut Microbes journal*). In contrast to complex microbial communities, it is easier to unravel the impact of environmental stressors on a structural and functional level in simplified microbiota [5]. However, low complex bacterial communities are expected to be less stable against perturbations compared to complex communities [11].

Since different intestinal TTs have been shown to affect complex bacterial communities, the effects on structure and function are not fully understood. Therefore, we cultivated SIHUMIx with a 24-hTT

until the communities adapted to the system. The adaptation was followed by changes in TT to a faster (12 h) and a slower value (48 h), which results in a high, medium, and low availability of nutrients. The community structure and activity of SIHUMIx were investigated using microbial flow cytometry, metaproteomics, and short-chain fatty acids (SCFA) metabolomics analysis. We aimed to investigate, if (1) SIHUMIx shows structural or functional changes in response to a shift in TT, if (2) these parameters recover from lower and higher TTs to the original state, and if (3) visualized changes are restricted to specific species.

2. Materials and Methods

2.1. Simplified Human Intestinal Microbiota—SIHUMIx

The extended simplified human intestinal microbiota (SIHUMIx) consist of the following eight bacterial strains: *Anaerostipes caccae* (DSMZ 14662), *Bacteroides thetaiotaomicron* (DSMZ 2079), *Bifidobacterium longum* (NCC 2705), *Blautia producta* (DSMZ 2950), *Clostridium butyricum* (DSMZ 10702), *Clostridium ramosum* (DSMZ 1402), *Escherichia coli* K-12 *(MG1655)*, and *Lactobacillus plantarum* (DSMZ 20174) [24]. Further information on functions fulfilled by SIHUMIx is provided (Table S1). The cultivation protocol, growth conditions, and medium ingredients are provided in Supplementary Material S2.

2.2. Experimental Set-Up

For inoculation of the bioreactor system, the single strain bacteria were thawed from a fresh glycerol stock two weeks before the experiment started and grown in Brain-Heart-Infusion (BHI), as described (Supplementary Material Table S2). Bacteria from three-day-old cultures were counted at the Multi-Sizer 3 (Beckman Coulter, Brea, United States) and used for inoculation. On the day of inoculation (d0) 1×10^9 bacteria per strain (a total of 8×10^9 bacteria per 250 mL) were inoculated into the bioreactor. The continuous cultivation started after 24 h.

The bioreactor run can be divided into three phases: (i) the adaptation phase where the bacterial community was established (d1–d5), (ii) the intermediary phase where the effect of different nutrient flowrates on the community was investigated (d6–d10), and (iii) the last phase in which the varying TTs were set back and the communities were rebalanced (d11–d15). The control bioreactors (labeled as 24 hTTI and II) were run with a dilution rate of 0.04 h^{-1} (24 h transit time, hTT) during the whole experiment (d1–d15). The dilution rate was calculated as reported in Macfarlane et al. [20], which is equal to the physiological TT of the human colon [13]. In four other bioreactors, dilution rates of 0.04 h^{-1} were maintained for the adaptation phase and the set-back phase and were set to a dilution rate of 0.08 h^{-1} (labeled as 12 hTTI and II) and 0.02 h^{-1} (labeled as 48 hTTI and II), respectively, within the intermediary phase (d6–d10) (Figure 1).

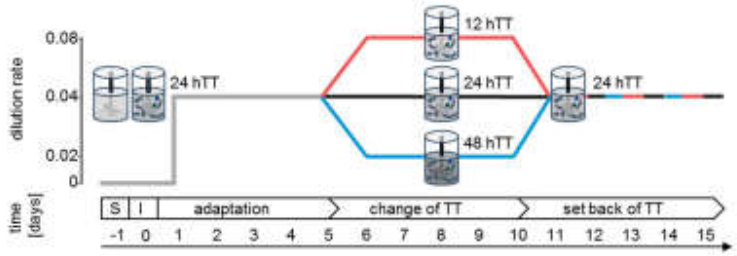

Figure 1. Set up of the bioreactor experiment: six bioreactors were run sterile for 24 h and inoculated with SIHUMIx (1×10^9 cells per species per 250 mL) on day zero. On day one, medium pumps were set to a dilution rate of 0.04 h^{-1} until day five (adaptation). On day five, the dilution rate was changed to 0.02 h^{-1} (48 hTTI and II) or 0.08 h^{-1} (12 hTTI and II) in two bioreactors, respectively (change of TT), and set back to 0.04 h^{-1} on day 10 to day 15 (set back of TT). By setting the dilution rate to 0.08 h^{-1}/0.04 h^{-1}/0.02 h^{-1}, the medium in the bioreactor was fully exchanged, which resulted in TTs of 12 h, 24 h, and 48 h, respectively. S = sterile run. I = inoculation.

2.3. *Sampling and Analysis*

During the whole experiment, samples were taken every 24 h starting the day after inoculation (d1). The stability properties of the community structure were analyzed using microbial flow cytometry [31,32]. Cell numbers were determined with electrical sensing using a Multisizer 3 Coulter Counter (Beckman Coulter, Brea, United States). The community structure and the functionality of SIHUMIx were analyzed using meta-proteomics. After sampling, the bacterial suspensions were centrifuged at 3200× *g* for 10 min at 4 °C and immediately frozen at −80 °C for subsequent sample analysis or used for the fixation of microbial flow cytometry or dry weight assessment. Supernatants of bacterial pellets were used for functional analysis with targeted metabolomics to perform SCFA profiling [33].

2.4. *Microbial Flow Cytometry*

2.4.1. Sample Preparation

The bacterial suspension was centrifuged (3200× *g*, 10 min, 4 °C) in conic glass tubes. Bacteria were treated with 2% formaldehyde [stock: 8% formaldehyde pH 7, diluted with PBS (6 mM Na_2HPO_4, 1.8 mM NaH_2PO_4, and 145 mM NaCl with bi-distilled water, pH 7)] for 30 min. The bacteria were centrifuged and resuspended in 70% ethanol for further fixation and long-term storage at −20 °C.

After a minimum of one day at −20 °C, the samples were stained with 0.24 µM 4′,6-di-amidino-2-phenyl-indole (DAPI, Sigma-Aldrich, St-Louis, USA) overnight, according to Koch et al. [31]. The measurement was performed according to Gelder et al. [34], but with a different neutral density filter (ND 2.6) for the side scatter (SSC) and measuring 250,000 cells in the cell gate (Supplementary Material, Figure S1). Raw cytometric data can be found at www.flowrespository.org with the flow repository ID: FR-FCM-Z24C.

For flow cytometric analysis and statistical data analysis, FlowJo V10 (FlowJo, LLC, Ashland, USA) was used to visualize each sample in 2D plots using forward scatter (FSC) vs. DAPI fluorescence. The relative cell abundance per gate was exported as .txt and jointly evaluated in R (vegan package) [35].

2.4.2. Calculation of Stability Properties

The stability properties (i.e., constancy, resistance, and recovery) of SIHUMIx were quantified on the basis of cytometric data. For each bioreactor, constancy was interpreted by a constancy space, which is a multi-dimensional dissimilarity space where the radius is determined by the variation of

chosen community states (deviation values determined by Canberra distance, CD). The constancy space was defined using samples from the two 24 hTTI and II using community states from the end of the adaptation phase (day 5) to the end of the experiment (day 15, n = 11), which resembles intrinsic community variation over time. The larger radius of the two constancy spaces from the two control bioreactors (i.e., 24 hTTI, tr = 0.1447, Supplementary Material Figure S2) was used as the threshold value to indicate the highest possible community deviation without TT changes.

Additionally, stability properties were calculated by resistance values (RS) (i.e., the ability of a community to stay unchanged) and recovery values (i.e., the ability of a community to return into the constancy space). For that, the community states at the end of the respective adaptation phases (reference state, SRef, day 5 per bioreactor) were successively compared with the community states during the following days of cultivation. The resulting CD values were used to calculate the resistant behavior and recovery strength of the microbial community following published guidelines [32].

2.5. *Metaproteomics*

2.5.1. Protein Extraction

An amount of 2 mL bioreactor liquid was taken, centrifuged (3200× g, 10 min, 4 °C), and the pellet was dissolved in 1 mL lysis buffer (10 mM Tris-HCl, NaCl 2 mg/mL, 1 mM PMSF, 4 mg/mL SDS). Bacteria were disrupted by bead beating (FastPrep-24, MP Biomedicals, Sanra Ana, CA, USA, 5.5 ms, 1 min, 3 cycles) followed by 15 min at 60 °C (Thermomixer comfort 5355, Eppendorf, Hamburg, Germany) and ultra-sonication (UP50H, Hielscher, Teltow, Germany, cycle 0.5, amplitude 60%). Protein concentration was determined with the bicinchoninic acid assay, according to the user manual (Pierce™ BCA Protein Assay Kit, Thermo Fischer Scientific, Waltham, MA, USA). Furthermore, 100 µg of protein was precipitated overnight at −20 °C with ice-cold acetone 1:5 (v/v) and centrifuged for 10 min at 14,000× g. The pellet was used for sodium dodecyl sulfate poly acryl amid one-dimensional gel electrophorese (SDS–PAGE). SDS-PAGE analysis, in-gel digestion, and protein purification with ZipTip®treatment were performed [36].

2.5.2. Liquid chromatography mass spectrometry (LC-MS/MS) Measurement

An amount of 5 µg peptide lysate was injected into nanoHPLC (UltiMate 3000 RSLCnano, Dionex, Thermo Fisher Scientific, Waltham, MA, USA). Peptide separation was performed on a C18-reverse-phase trapping column (C18 PepMap100, 300 µm × 5 mm, particle size 5 µm, nano viper, Thermo Fischer Scientific, Waltham, MA, USA), which was followed by a C18-reverse-phase analytical column (Acclaim PepMap® 100, 75 µm × 25 cm, particle size 3 µm, nanoViper, Thermo Fischer Scientific). Mass spectrometric analysis of peptides was performed on a Q Exactive HF mass spectrometer (Thermo Fisher Scientific, Waltham, MA, USA) coupled with a TriVersa NanoMate (Advion, Ltd., Harlow, UK) source in the liquid chromatography (LC) chip coupling mode. LC gradient, ionization mode, and the mass spectrometry mode were described [37].

2.5.3. Data Analysis

Raw data were processed with Proteome Discoverer (v 2.2, Thermo Fischer Scientific, Waltham, MA, USA). The search settings for the Sequest HT search engine were set to Trypsin (Full), Max. Missed Cleavage: 2, precursor mass tolerance: 10 ppm, fragment mass tolerance: 0.02 Da. The protein-coding sequences of the eight SIHUMIx strains were downloaded from UniProt (Available online: http://www.uniprot.org/), combined, and used as database resulting in 29,558 protein sequences. Individual *.fasta entries per species are given (Table S3). The false discovery rates (FDR) were determined with the node Percolator [38] embedded in Proteome Discoverer (v 2.2) and we set the FDR threshold at a peptide level of 5%. The same threshold was set for the protein FDR (5%). Redundant proteins from the protein-coding database were automatically grouped in protein groups by applying the strict parsimony principle. Only the protein groups that explain at least one unique identified peptide

were reported. Only the peptides that were not shared between different proteins or protein groups were used for the protein quantification through the Top3 approach implemented in the Proteome Discoverer (v 2.2). *GhostKOALA* was used to assign KEGG orthology (KO) numbers of KEGG to the identified functions of identified protein sequences. A protein report from Proteome Discoverer with assigned taxa and functional information from KEEG are provided (Supplementary Material S4). Only pathways with sufficient coverage (>10%) on the total amount per sample were used for statistical analysis. For specific pathway abundances, only pathways with sufficient relative abundance (>0.01%) per sample were evaluated. Visualization and statistical analysis were carried out with the GraphPad Prism (v. 8.0.2) using unpaired multiple t-tests per row. A Pearson correlation was performed with in-house written R scripts (*Hmisc* package using the *rcorr* function).

2.6. Metabolomics

2.6.1. Metabolite Extraction

For the analysis of short-chain fatty acids (SCFAs), the method of Han et al. was modified [33,39]. The sample was mixed with acetonitrile to a final concentration of 50% acetonitrile. SCFAs were derivatized with 0.5 volumes of 200 mM 3-nitrophenylhydrazine and 0.5 volumes of 120 mM N-(3-dimethylaminopropyl)-N′-ethylcarbodiimide hydrochloride in pyridine for 30 min at 40 °C. The mix was then diluted 1:50 in 10% acetonitrile.

2.6.2. LC-MS/MS Measurement and Data Analysis

An amount of 50 µL of the diluted SCFA derivatives was injected into the LC-MS/MS system. Chromatographic separation of SCFAs was performed on an Acquity UPLC BEH C18 column (1.7 µm, Waters, Eschborn, Germany) using H_2O (0.01% formic acid, FA) and acetonitrile (0.01% FA) as the mobile phases. The column flow rate was set to 0.35 mL/min and the column temperature was set at 40 °C. The gradient elution was performed as follows: 2 min at 15% B, 15%–50% B in 15 min, and then held at 100% B for 1 min. Lastly, the column was equilibrated for 3 min at 15% B. Mass spectrometric analysis of metabolites was performed QTRAP®5500 (AB Sciex, Framingham, MA, USA). For identification and quantitation, a scheduled multiple reaction monitoring (MRM) method was used, with specific transitions for every SCFA. Peak areas were determined in Analyst® Software (v. 1.6.2, AB Sciex) and areas for single SCFAs were exported. Normalization and statistics were performed with in-house written R scripts.

3. Results

3.1. Adaptation Phase of SIHUMIx under Continuous Cultivation Conditions

Bioreactors (n = 6) were inoculated with 1×10^9 cells/250 mL per species of the SIHUMIx bacteria and cultivated for five days (adaptation phase) until reaching a structural and functional constant state (Figure 2A) (Krause et al., in revision at the *Gut Microbes Journal*). To evaluate the species distribution of SIHUMIx, the community composition was analyzed based on the abundance of species-specific proteins [33,40]. In total (n = 90 samples), 7307 protein groups were identified. Protein group identification per sample is given (Supplementary Material Table S4). Within the first 24 h after inoculation, the relative abundance of *Clostridia* (*C. ramosum*, *C. butyricum*), *Lactobacillus* (*L. plantarum*), and *Bifidobacterium* (*B. longum*) clearly decreased, whereas the other SIHUMIx members, *Anerostipes* (*A. caccae*), *Bacteroides* (*B. thetaiotaomicron*), *Blautia* (*B. producta*) and *Escherichia* (*E. coli*), increased (Figure 2B). During the following four days, the abundance of *B. thetaiotaomicron* continued to increase, whereas the relative abundance of *A. caccae* and *E. coli* decreased. At the end of the adaptation phase (day 5), *B. thetaiotaomicron*, *B. producta*, *E. coli*, and *A. caccae* were the dominant members of SIHUMIx with 66%, 12%, 10.2%, and 2.7%, respectively.

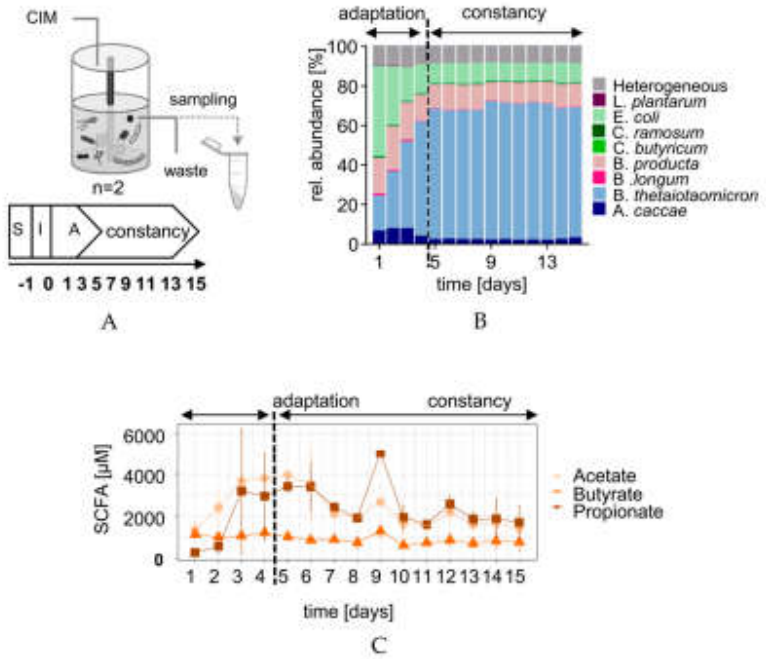

Figure 2. **(A)** Schematic overview of sample analysis to describe a stable functional state. *CIM* = Complex Intestinal Medium, S = sterile run, I = Inoculation, and A = adaptation. **(B)** The stacked bar graphs show taxa distribution over time (TT 24 h, $n = 2$) based on the relative protein abundance per species. **(C)** Absolute acetate, butyrate, and propionate concentrations over time.

To evaluate the metabolic activity of SIHUMIx, SCFA concentrations were measured daily (Figure 2C). The butyrate concentration was slightly higher on day one (1.1 mM) and stabilized on day five (1.02 mM). Acetate and propionate started at 1.3 mM and 0.3 mM, respectively, and increased until day five to 3.94 mM and 3.40 mM. At day 5, the concentration of acetate and propionate was 3.8 (SD = ±0.268) and 3.3 (SD = ±0.377) times higher when compared to butyrate.

3.2. *SIHUMIx Shows Slight Changes during Varying Transit Times*

The adaptation phase was followed by the intermediary phase in whichTTs were shifted (day 6 to 10). In two bioreactors, the TT was set to 12 h and, in another set of two bioreactors, it was set to 48 h, respectively. On day 11, the TTs were set to 24 h again for all bioreactors and maintained until the end of the experiment on day 15 (Figure 1). The bacterial cell number was determined (Figure 3A). Compared to the end of the adaptation phase, the cell numbers stayed unchanged for 12 hTT, but decreased slightly at 24 hTT and 48 hTT.

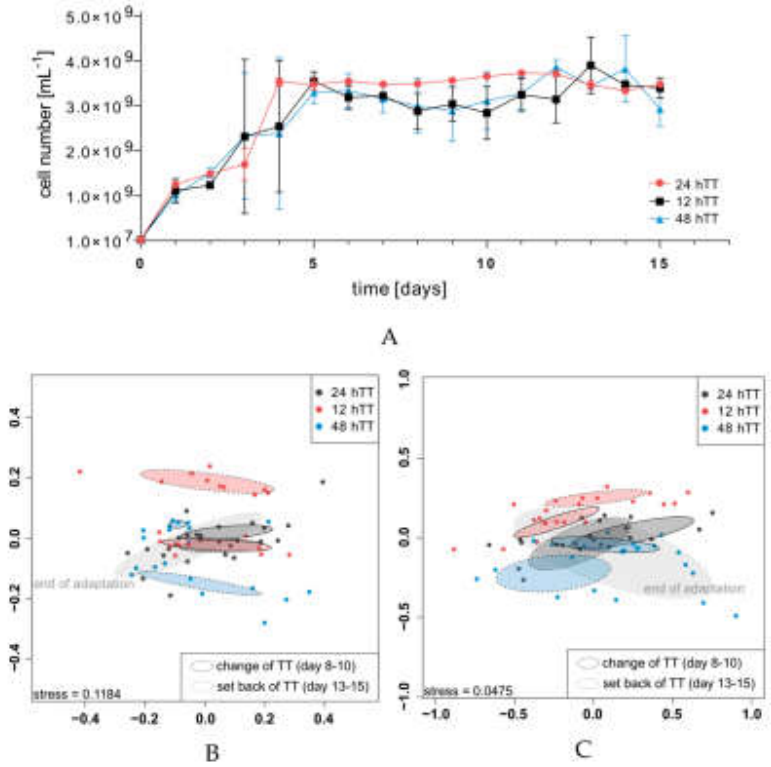

Figure 3. (**A**) Cell numbers of SIHUMIx. The NMDS plots show community dynamics during the experiment (Bray-Curtis dissimilarity) based on flow cytometry subpopulations (**B**) and absolute SCFA concentrations (**C**). The end of the adaptation of SIHUMIx is marked with a light grey ellipse. Control: dark grey ellipse with the dashed outline including days 8 to 10 and set back control: dark grey ellipse with the bold outline including days 13 to 15.

The impacts on the community structure and SCFA production were followed with two fingerprinting methods: flow cytometric fingerprinting based on flow cytometric data and short-chain fatty acid analysis based on the SCFA concentrations. With dissimilarity analysis (visualized as non-metric multidimensional scaling (NMDS) plots), the effects of different TTs on the community structures were indicated. The end of the adaptation phase of all six bioreactors was included as a landmark for the following changes of both the community structures and the metabolic activities (Figure 3B,C, grey ellipse without outline, "end of adaptation"). Grouping refers to the different phases of the experiment (see legend in Figure 2B,C). All the Bray-Curtis Dissimilarity's (BD) of flow cytometric data, which were used for the NMDS plotting, are given (Table S5). All groups were compared by pairwise ANOVA. R^2 and P values of all group comparisons are given (Table S6).

Flow cytometric fingerprinting showed that SIHUMIx was affected by the increase and decrease of the TT regarding the community structure (Figure 3B). A slight difference was visible within the control, referring to days 8 to 10 of the control bioreactors, and the setback phase of the control, referring to days 13 to 15 of the control bioreactors. This indicates that there was a time-dependent structural shift of the community since TT did not change. The constancy spaces were determined for the two

control bioreactors and a value of tr = 0.1447 (24 hTTI) was chosen as the accepted maximal intrinsic community variation (Figure S2). The proportion of the intrinsic variance between bioreactors and over time was small with regard to the result from pairwise ANOVA testing (control vs. set back control: R^2 = 0.61) even though the changes were found to be insignificant (P adjusted = 0.515, Supplementary Material Figure S6). In contrast, a comparison of the communities revealed that, within the changes in the TT, the communities changed significantly (P adjusted = 0.004) during 12 hTT and 48 hTT, which indicates a TT-dependent shift of the community structure. The proportion of intrinsic variance between 12 hTT and 48 hTT (R^2 = 6.36) was the highest calculated proportion of variance of all the calculated proportions of variances between the experimental groups. After the TT was set back to 24 h, the communities of the 12 hTT bioreactors reached a state comparable to the end of the adaptation. In contrast, after 48 hTT, the communities did not reach a state comparable to the end of the adaptation.

Additionally, short-chain fatty acid analysis revealed differences during the phases of varying TTs (Figure 3C). All Bray-Curtis Dissimilarity's of SCFA concentrations, which were used for the NMDS plots, are given (Table S5). All the groups were compared by pairwise ANOVA testing. The *P* values of all the group comparisons are given (Table S6). During 12 hTT and 48 hTT, the SCFA composition was significantly changed (R^2 = 7.33, P adjusted = 0.012), but reached a state comparable to the end of the adaptation afterward (end of adaptation vs. set back at 48 hTT R^2 = 1.87, P adjusted = 0.191, end of adaptation vs. setback 12 hTT R^2 = 1.93, P adjusted = 0.817). Only one further significant difference was found, namely between 12 hTT and the set back control (R^2 = 5.23, P adjusted = 0.035), but the proportion of variance between bioreactors was smaller compared to 12 hTT vs. 48 hTT.

Pairwise ANOVA analysis revealed less significant differences between the groups based on the SCFA concentrations when compared to those based on flow cytometric data.

3.3. *Stability Properties of SIHUMIx during Changed Retention Times*

To analyze the stability properties of SIHUMIx during varying TTs, the constancy values for each bioreactor were quantified based on flow cytometric data [32]. Constancy describes the ability of bacterial communities to stay essentially unchanged. Therefore, an artificial community state was defined by calculating the mean of cell abundances per each gate of the 19 gates upon all samples from day five (end of the adaptation phase) to day 15 (n = 11) for both bioreactors with 24 hTT.

To calculate the community constancy space, a multidimensional dissimilarity space was considered, described by variations of community states and determined by Canberra Distance (CD). The maximum CD value was used to define the radius of the constancy space.

The constancy value ranges between zero and one, while a smaller value represents a smaller community variation, which indicates a relatively high constancy. We found that the two communities of the control bioreactors, which were run with 24 hTT in all phases, showed the smallest constancy values (control bioreactor 24 hTTI CD = 0.1447, control bioreactor 24 hTTII CD = 0.1235) after 15 days of cultivation. All constancy values are shown (Figure S2). The higher constancy value of the control bioreactors (CD = 0.1447, control bioreactor 24 hTTI) was used to define the threshold for accepted intrinsic community variation under continuous cultivation conditions. This threshold was set to investigate whether a structural deviation of SIHUMIx during a transition change increases to higher values, which would point to instability.

To describe the stability of the communities (i.e., resistance to TT changes), the deviation values of each bioreactor in the different experimental phases were compared to their reference states. As a reference state, the last state of the adaptation (day 5) was set per each bioreactor. Then the community deviation was followed (Figure 4A). If the deviation of the community is higher than the threshold value of the constancy space, the community does change structurally.

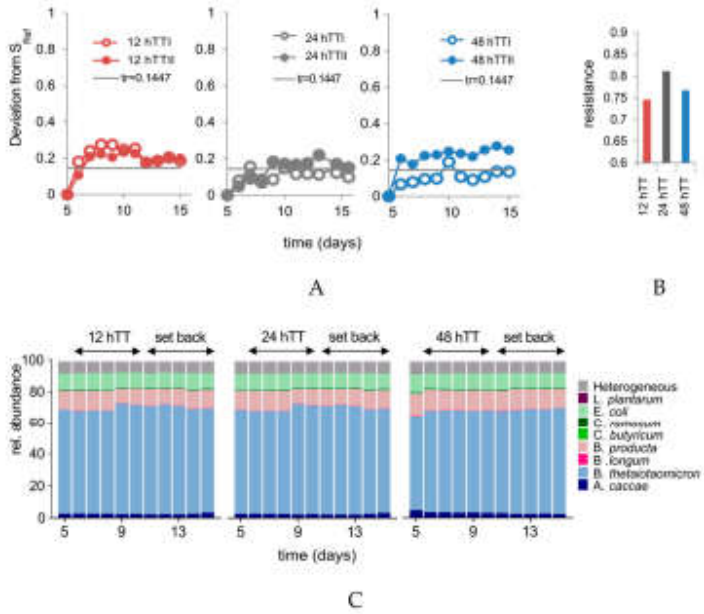

Figure 4. **(A)** The deviation of SIHUMIx from SRef. Tr = threshold of constancy space. Sref = reference state. **(B)** Resistance calculation based on flow cytometric data. **(C)** The stacked bar graphs show the taxa distribution of SIHUMIx (12 h/24 h/48 h, n = 2) based on the abundance of species-specific proteins during the phase of changed TT and during the set back of TT afterward.

The deviation values of the control bioreactors were close to the threshold value after 15 days of cultivation, which indicates that the community deviation was similar to the intrinsic variation, calculated by the constancy space. For 12 hTT, the community deviated, with a maximum value of 0.275 (bioreactor 12 hTTI, at day 8) and 0.233 (bioreactor 12 hTTII, at day 10). The community states of the samples from bioreactor 48 hTTI showed at day 10, with a maximum deviation value of 0.188, the state that has a deviation higher than the threshold. In contrast, even with the same settings, bioreactor 48 hTTII deviated from its reference state immediately and reached the highest deviation value of 0.2765 at day 14.

Furthermore, resistance (RS) values for all the bioreactors were calculated based on the deviation values. The RS values of all the bioreactors were within the range of 0.72 to 0.85, which indicates a relatively high resistance against changing TTs (all the resistance values are shown in the Supplementary Material, Figure S2). The mean RS values for the duplicate bioreactors with the same TTs are shown in Figure 4B. The control showed the highest RS (RS = 0.8114), which is followed by the 48 hTT (RS = 0.7674) and the 12 hTT (RS = 0.7459) bioreactors.

3.4. Changes in TT are Associated with Differences in Specific Pathways

To investigate whether the structural differences were associated with changes in species distribution or function, the metaproteomic analysis was performed. There were no changes in the taxa distribution of SIHUMIx in all the bioreactors since the end of the adaptation (day 5), despite the varied TTs (Figure 4C). Relative species abundances are given (Table S7).

Although relative species abundance was not affected (Figure 4C), differences were found in specific functions of SIHUMIx (Figure 5A). Differences were observed between 12 hTT and 48 hTT for

the following KEGG pathways: ribosome ($p = 0.0013$), chaperones and folding catalysts ($p = 0.0008$), RNA degradation ($p = 0.0311$), alanine, aspartate, and glutamate metabolism ($p = 0.002$), butanoate metabolism ($p = 0.0027$), amino sugar and nucleotide sugar metabolism ($p = 0.036$), propanoate metabolism ($p = 0.049$), arginine biosynthesis ($p = 0.0111$), phosphotransferase system (PTS) ($p = 0.004$), and peptidoglycan biosynthesis and degradation proteins ($p = 0.0016$). All the pathways were less abundant at 12 hTT compared to 48 hTT, except for the ribosome, which were more abundant at 12 hTT. On a species level, slight changes in relative abundances were found for 27 pathways identified in *A. caccae*, *B. thetaiotaomicron*, *B. producta*, and *E. coli*, which are the most abundant species in the SIHUMIx community (Figure 5B).

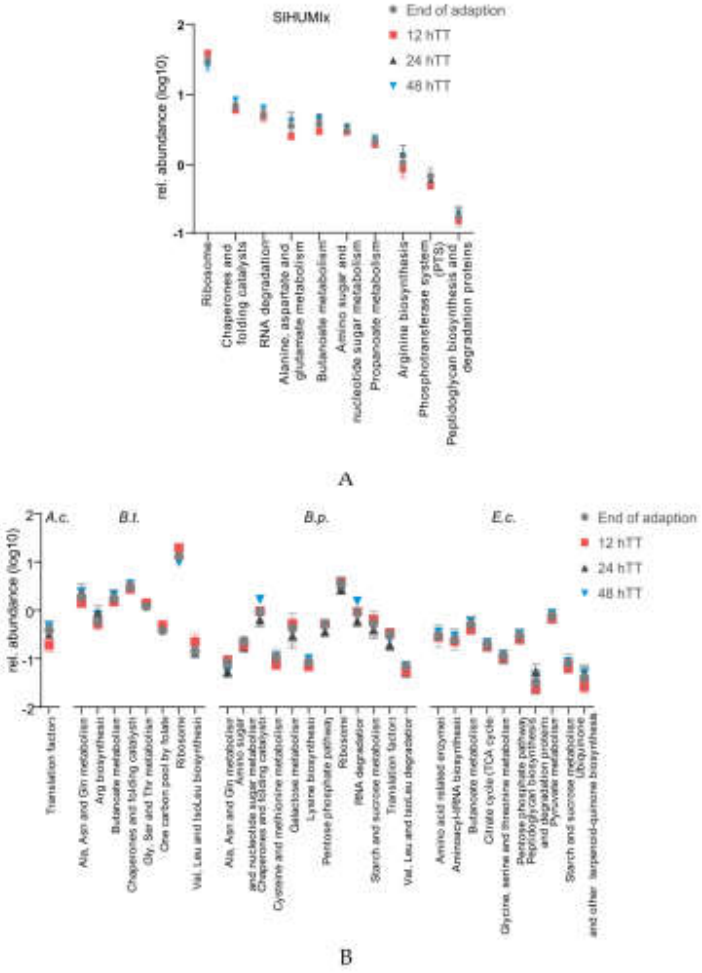

Figure 5. **(A)** Log transformed relative abundance of all proteins identified per pathway for SIHUMIx. **(B)** Relative pathway abundances of *A. caccae*, *B. thetaiotaomicron*, *B. producta*, and *E. coli* based on the average of six for the end of adaptation (day 5) or four for 12 h/24 h/48 h (day 9 and 10).

3.5. *Changes in TT are Associated with Differences in SCFA Concentrations*

In addition to differences in specific functions, SCFA concentrations changed during the varying TTs (Figure 6).

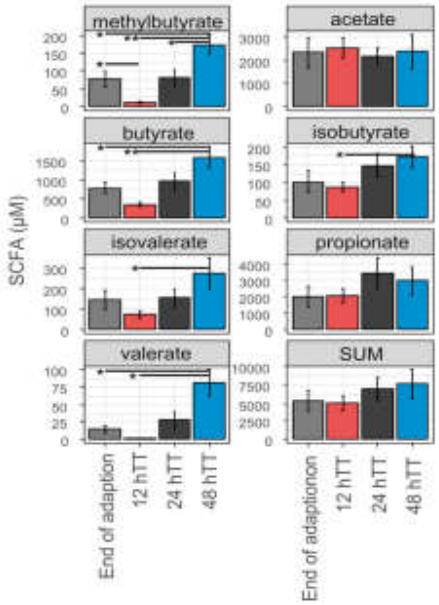

Figure 6. SCFA and branched-chain fatty acids (BCFA) concentrations under different transit times based on the average of six for the end of adaptation (day 5) or four for 12 h/24 h/48 h (day 9 and 10). *p* value was calculated with multiple *t*-test (using no *p*-value adjustment) between 12 hTT and 48hTT. * $p < 0.05$, ** $p < 0.001$.

The absolute concentrations of butyrate ($p = 0.0049$) and valerate ($p = 0.0404$) were lower at 12 hTT compared to 48 hTT. This was also true for the BCFA methylbutyrate ($p = 0.0012$), isobutyrate ($p = 0.039$), and isovalerate ($p = 0.0381$), which decreased at 12 hTT compared to 48 hTT. The amount of total SCFA and the concentration of acetate and propionate were not affected by changes in TT.

4. Discussion

The colon transit time (TT) has been described as a driving force that affects the composition and metabolism of complex intestinal communities, but the results differ between studies [15,16,20,21]. We recently established an extended simplified human intestinal microbiota (SIHUMIx) for bioreactor used to investigate physiological stressors on a species-specific level (Krause et al., in revision at the *Gut Microbes Journal*). Since the effects of varying TT on structure and function are not fully understood, we investigated the effects of three physiological colonic TT (48 h, 24 h, 12 h) on SIHUMIx. SIHUMIx was grown for 15 days in a colon simulating bioreactor system. Daily samples were analyzed with metaproteomics, SCFA analysis, and two fingerprinting techniques using flow cytometry data and SCFA concentrations to visualize the effect of changing TT on the community structure and function of SIHUMIx. This study shows that the structure of SIHUMIx was only slightly affected by changing TT and showed high stabilizing abilities after adapting to the bioreactor conditions. Functional changes

during changing TT are only partly in accordance with changes found for complex communities, i.e., it could be associated with the relative abundance changes of *B. thetaiotaomicron*, *B. producta*, and *E. coli*, which are the most abundant members of SIHUMIx.

4.1. SIHUMIx Shows Slight Changes During Varying Transit Times

TT in the bioreactor system can be influenced by differences in pump speed and clogging of the tubes. In order to prevent this (i), all medium pumps were calibrated before the experiments to assure no technical differences between the individual feed pumps and (ii) medium bottles were constantly stirred during the experiment to prevent particle formation.

The total cell number of SIHUMIx fluctuated during the whole experiment, but stayed mainly unchanged at 12 hTT, whereas the total cell numbers at the 24 hTT (control) and 48 hTT bioreactors slightly decreased during varying TTs (Figure 3A). The effect of the total cell numbers during 12 hTT is in contrast with studies conducted on complex bacterial communities [15]. In this study, the total cell numbers were not affected differently by varying TTs.

The different TTs also showed changes in the cytometric community structure using flow cytometric fingerprinting. During the phase of changed TT, communities of 48 hTT and 12 hTT were clearly different from each other but not to the control. To determine whether the structural differences in the SIHUMIx communities were higher than the normal community variation in the control at 24 hTT, the deviation of community states that the end of the adaptation was calculated. Accelerating the TT affected the community structure at 12 hTT. Both bioreactor communities deviated out of the constancy space. For the longer 48 hTT, the duplicate communities behaved differently. One of the 48 hTT bioreactors deviated from the reference state and out of the constancy space, whereas the other mostly stayed unchanged. Since only one replicate bioreactor deviated from the reference state, we assume that the microbial community in this bioreactor was not constant at day five. Although we expected that SIHUMIx reaches a constant state on day five (Krause et al., in revision at the *Gut Microbes Journal*), the adaptation phase should be prolonged to seven days in order to assure balanced growth in future studies.

In addition, with regard to larger structural deviations (Figure 4A) and significant community variations (Figure 3B,C), smaller resistance values were found in the groups of 12 hTT and 48 hTT but they were close to the values of controls. This shows that SIHUMIx is highly resistant against variation of TTs. During faster TTs, cell growth is likely to be supported since absolute cell numbers were also the highest at 12 hTT.

Bacterial cells modify their metabolism during the cell cycle and, thus, the community structure changes. Since flow cytometric fingerprinting is based on the measurement of cell size and DNA content, structural changes caused by different TTs can also be related to changes in the division states of community members or to a shift in species abundances. Metaproteomics revealed that species abundances stayed unchanged, which indicates that the communities were clearly not affected based on phylogenetic affiliation but by cell cycle activities. All the species, including the slow-growing bacterium *L. plantarum*, remained in the bioreactor system until the end of the experiment on day 15 [41].

4.2. Changes are Associated with Cell Division

In bacterial cell division, the final step is dependent on certain cell size. Bacterial cells need to at least double their biomass before division in order to prevent biomass losses. Individual cell sizes vary within a population and exhibit intrinsic variability, even under constant growth conditions [42]. Medium TT directly affects the availability of the medium ingredients. Carbon availability is higher at a shorter TT and, therefore, is likely to cause a functional change and faster growth. This functional change might be associated with changes in cell size and, hence, the time of division of cell subpopulations.

Functional differences were found for specific pathways in the KEGG sub-roles: translation, folding, sorting and degradation, membrane transport, and amino acid and glycan metabolism,

which are relevant for DNA replication and cell division (Figure 5A). During cell division, bacterial cells need to replicate two main components: the chromosomes and the peptidoglycan cell wall [43]. In fact, the glycan metabolism of SIHUMIx was affected differently during varying TTs. During the 12 hTT, the relative protein abundance of the pathways peptidoglycan biosynthesis and degradation proteins decreased. It is probable that, at 12 hTT, more alternative carbon and nitrogen sources were available and cell wall synthesis could be maintained without energy consumption recycling of peptidoglycans [44], but it is still unknown exactly how peptidoglycan chains are synthesized [43]. When bacteria are shifted from low to high nutrient availability, the expression of ribosomal RNA and ribosomal proteins is likely to accelerate [45]. Hence, in this study, the relative abundance of the proteins related to the KEGG pathway ribosome of SIHUMIx was higher at 12 hTT compared to 48 hTT. Apparently, this shift was slightly higher for *B. thetaiotaomicron* than *B. producta*. For other members of SIHUMIx, changes in relative abundances of ribosomal proteins were not assigned.

4.3. A Faster Transit Time Slightly Reduces Butyrate Metabolism of SIHUMIx And Favors Protein Fermentation

Short-chain fatty acid analysis revealed changes between 12 hTT and 48 hTT, even though changes on the functional level were smaller than those on the structural level. These changes were caused by a decrease in butyrate, methylbutyrate, isovalerate, and valerate concentrations at 12 hTT, whereas total SCFA concentrations were not significantly changed (Figure 6). In accordance with the SCFA analysis, the butyrate metabolism also decreased, which was shown by less protein abundance of butanoate metabolism at 12 hTT (Figure 5A). The reduction of butanoate metabolic proteins was specifically shown for *B. thetaiotaomicron* and *E. coli* (Figure 5B).

Furthermore, we found a decrease in the amino acid metabolism of SIHUMIx at 12 hTT by the less relative abundance of alanine, aspartate, and glutamate metabolism and arginine biosynthesis. Together with a reduced butanoate metabolism, this indicates reduced carbohydrate fermentation at faster TTs. In contrast to carbohydrate fermentation, the fermentation of proteins and amino acids resulted in the production of BCFA. The concentrations of the BCFA methylbutyrate, isovalerate, and isobutyrate increased (Figure 6), which indicates that protein fermentation was favored at faster TT. These findings are in accordance with previous results and strengthen the hypothesis that protein fermentation is favored with faster TT [46,47]. Functional changes in the pathway abundances of low abundant SIHUMIx bacteria were not detected. This is most likely due to the low proteome coverage of low abundant species (less than 1%), which is still a bottleneck in metaproteome analysis [48,49].

Fermentation end products are well studied, but the association between a specific substrate and SCFA formation is not well understood since several amino acids can be used for both SCFA and BCFA synthesis [50]. Although the absolute acetate concentration did not significantly increase at 12 hTT, correlation analysis revealed that acetate was slightly negatively correlated with the TT (Figure 7). The final steps of butyrate synthesis can be realized by two different enzymes: butyrate kinase, which uses butyryl-CoA, or butyryl-CoA:acetate-CoA transferase, which uses acetate to form butyrate. The latter has been suggested as the preferred route used by intestinal bacteria [51]. It has been shown that these enzymes are possessed simultaneously or depend on external metabolites [51,52]. It is likely that the decreased butyrate metabolism caused an increased acetate availability at 12 hTT.

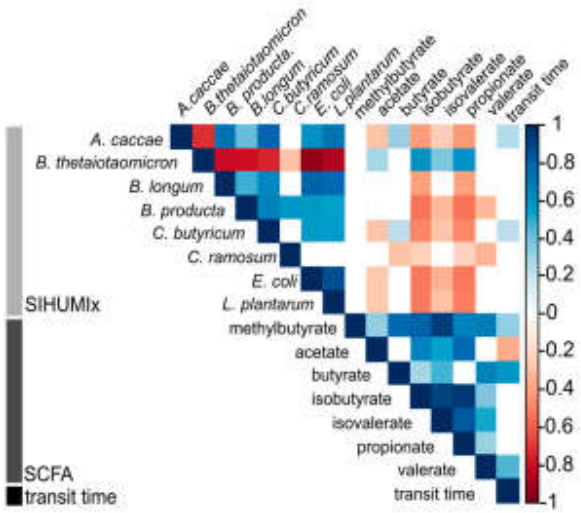

Figure 7. Correlation between relative species abundance, SCFA, and transit time.

4.4. B. thetaiotaomicron is Associated with SCFA and BCFA Production

Saccharolytic activity in the human intestine mainly concerns the breakdown of carbohydrates via the Embden-Meyerhof-Parnas pathway. At first, glucose is metabolized to pyruvate and further into SCFA. Genera that produce SCFA are known to be primarily *Bacterioides spp.*, *Lactobacillus spp.*, and *Bifidobacterium spp.* [8]. The correlation analysis of the SIHUMIx species abundance with the absolute concentrations of fermented SCFA products revealed that propionate could be strongly associated with *B. thetaiotaomicron* but not with *L. plantarum* or *B. longum* (Figure 7).

B. thetaiotaomicron was also positively correlated with isobutyrate and isovalerate. Isobutyrate and isovalerate can result from valine and leucine degradation. Both amino acids are utilized in the intestinal microbiota [53] Previous results correlated the production of BCFA only with low abundant species in a complex microbial community since they were found to be mainly responsible for protein degradation [21]. In our study, the production of BCFAs was correlated with the most abundant member of SIHUMIx *B. thetaiotaomicron*. However, only the production of propionate has been described to date [46]. At approximately 65%, *B. thetaiotaomicron* is the most abundant member of SIHUMIx. Mucus-associated bacterium *B. thetaiotaomicron* is the only member of SIHUMIx, with the ability to degrade mucin. Mucin is a glycoprotein, which can serve as a source for both carbohydrate and protein fermentation. This might provide an ecological advantage in nutrient accessibility and account for its high abundance [54,55]. Although mucin availability varied during the different TTs, the abundance of *B. thetaiotaomicron* was not affected.

5. Conclusions

Even though simplified bacterial communities are expected to be less stable against environmental stressors, SIHUMIx showed remarkable structural and functional resistance against varying physiological TTs. Moreover, correlation analysis revealed little correlation between species abundances or SCFA concentration and the TT, which indicates a high resistance of SIHUMIx against varying physiological TTs. Fingerprinting tools provided a fast and reproducible approach to assess microbial community dynamics and revealed slight changes in the community structure of SIHUMIx during

varying TTs. According to our metaproteomics data, these changes were associated with differences in membrane transport, glycan and protein metabolism, and, consequently, absolute SCFA and BCFA concentrations. *B. thetaiotaomicron* was identified to be affected in terms of butyrate metabolism, which has an important implication concerning intestinal health. Despite the limitation due to the relatively low abundant species, this study shows that the low complexity of SIHUMIx allowed the description of the effect of physiological stressors on a species-specific level.

Supplementary Materials: The following are available online at http://www.mdpi.com/2076-2607/7/12/641/s1, Figure S1: Master cell gate template for flow cytometric fingerprinting, Figure S2: Constancy space and resistance values per bioreactors based on flow cytometric data, Table S1: Additional information about SIHUMIx, Table S2: Growth media (Brain-Heart-Infusion, BHI), Complex intestinal medium, CIM), and growth conditions, Table S3: Protein-coding sequences per species, Table S4: Protein report of metaproteomic analysis, Table S5: Bray-Curtis Dissimilarity's of NMDS evaluation of flow cytometric data and SCFA concentrations, Table S6: P values from Pairwise ANOVA of flow cytometric data and SCFA concentrations, Table S7: Relative species abundance of SIHUMIx.

Author Contributions: Conceptualization, S.S.S., J.L.K., N.J., and M.v.B. Data curation, S.S.S., J.L.K., B.E., K.F.-W., F.S., and Z.L. Formal analysis, S.S.S. Funding acquisition, M.v.B., G.H., and J.L.K. Methodology, S.S.S., J.L.K., B.E., K.F.-W., and F.S. Supervision, S.M., N.J., U.R.-K., G.H., and M.v.B. Validation, S.S.S., J.L.K., Z.L., S.M., and U.R.-K. Visualization, S.S.S., J.L.K., and Z.L. Writing—original draft, S.S.S. and J.L.K. Writing—review & editing, B.E., K.F.-W., F.S., Z.L., S.M., N.J., U.R.-K., G.H., and M.v.B.

Funding: S.S.S. acknowledges funding by DFG SPP 1656. J.L.K. is thankful for funding by the German Federal Environmental Foundation (DBU) and M.v.B. is grateful for the partial funding by DFG Priority Program 2002.

Acknowledgments: We thank Michael Blaut (German Institute of Human Nutrition, Potsdam-Rehbruecke) for providing the SIHUMIx bacteria. We are thankful for technical assistance from Jeremy Knespel, Eva-Annamaria Stier, Kathleen Eismann, and Nicole Gröger and for culture medium supply from Martina Kolbe.

Conflicts of Interest: The authors declare no conflict of interest.

References

1. Almeida, A.; Mitchell, A.L.; Boland, M.; Forster, S.C.; Gloor, G.B.; Tarkowska, A.; Lawley, T.D.; Finn, R.D. A new genomic blueprint of the human gut microbiota. *Nature* **2019**, *568*, 499. [CrossRef] [PubMed]
2. Marques, F.Z.; Mackay, C.R.; Kaye, D.M. Beyond gut feelings: How the gut microbiota regulates blood pressure. *Nat. Rev. Cardiol.* **2017**, *15*, 20. [CrossRef] [PubMed]
3. Hemarajata, P.; Versalovic, J. Effects of probiotics on gut microbiota: Mechanisms of intestinal immunomodulation and neuromodulation. *Therap. Adv. Gastroenterol.* **2013**, *6*, 39–51. [CrossRef] [PubMed]
4. Den Besten, G.; van Eunen, K.; Groen, A.K.; Venema, K.; Reijngoud, D.J.; Bakker, B.M. The role of short-chain fatty acids in the interplay between diet, gut microbiota, and host energy metabolism. *J. Lipid Res.* **2013**, *54*, 2325–2340. [CrossRef] [PubMed]
5. Guzman-Rodriguez, M.; McDonald, J.A.K.; Hyde, R.; Allen-Vercoe, E.; Claud, E.C.; Sheth, P.M.; Petrof, E.O. Using bioreactors to study the effects of drugs on the human microbiota. *Methods* **2018**, *149*, 31–41. [CrossRef]
6. Morrison, D.J.; Preston, T. Formation of short chain fatty acids by the gut microbiota and their impact on human metabolism. *Gut Microbes* **2016**, *7*, 189–200. [CrossRef]
7. Hamer, H.M.; Jonkers, D.; Venema, K.; Vanhoutvin, S.; Troost, F.J.; Brummer, R.J. Review article: The role of butyrate on colonic function. *Aliment. Pharmacol. Ther.* **2008**, *27*, 104–119. [CrossRef]
8. Nyangale, E.P.; Mottram, D.S.; Gibson, G.R. Gut microbial activity, implications for health and disease: The potential role of metabolite analysis. *J. Proteome Res.* **2012**, *11*, 5573–5585. [CrossRef]
9. Baxter, N.T.; Schmidt, A.W.; Venkataraman, A.; Kim, K.S.; Waldron, C.; Schmidt, T.M. Dynamics of human gut microbiota and short-chain fatty acids in response to dietary interventions with three fermentable fibers. *mBio* **2019**, *10*, e02566-18. [CrossRef]
10. Lewis, S.J.; Heaton, K.W. Stool form scale as a useful guide to intestinal transit time. *Scand. J. Gastroenterol.* **1997**, *32*, 920–924. [CrossRef]
11. Vandeputte, D.; Falony, G.; Vieira-Silva, S.; Tito, R.Y.; Joossens, M.; Raes, J. Stool consistency is strongly associated with gut microbiota richness and composition, enterotypes and bacterial growth rates. *Gut* **2016**, *65*, 57–62. [CrossRef] [PubMed]

12. Sarosiek, I.; Selover, K.H.; Katz, L.A.; Semler, J.R.; Wilding, G.E.; Lackner, J.M.; Sitrin, M.D.; Kuo, B.; Chey, W.D.; Hasler, W.L.; et al. The assessment of regional gut transit times in healthy controls and patients with gastroparesis using wireless motility technology. *Aliment. Pharmacol. Ther.* **2010**, *31*, 313–322. [CrossRef] [PubMed]
13. Wang, Y.T.; Mohammed, S.D.; Farmer, A.D.; Wang, D.; Zarate, N.; Hobson, A.R.; Hellstrom, P.M.; Semler, J.R.; Kuo, B.; Rao, S.S.; et al. Regional gastrointestinal transit and ph studied in 215 healthy volunteers using the wireless motility capsule: Influence of age, gender, study country and testing protocol. *Aliment. Pharmacol. Ther.* **2015**, *42*, 761–772. [CrossRef]
14. Maurer, J.M.; Schellekens, R.C.; van Rieke, H.M.; Wanke, C.; Iordanov, V.; Stellaard, F.; Wutzke, K.D.; Dijkstra, G.; van der Zee, M.; Woerdenbag, H.J.; et al. Gastrointestinal ph and transit time profiling in healthy volunteers using the intellicap system confirms ileo-colonic release of colopulse tablets. *PLoS ONE* **2015**, *10*, e0129076. [CrossRef]
15. Child, M.W.; Kennedy, A.; Walker, A.W.; Bahrami, B.; Macfarlane, S.; Macfarlane, G.T. Studies on the effect of system retention time on bacterial populations colonizing a three-stage continuous culture model of the human large gut using fish techniques. *FEMS Microbiol. Ecol.* **2006**, *55*, 299–310. [CrossRef]
16. Tottey, W.; Feria-Gervasio, D.; Gaci, N.; Laillet, B.; Pujos, E.; Martin, J.F.; Sebedio, J.L.; Sion, B.; Jarrige, J.F.; Alric, M.; et al. Colonic transit time is a driven force of the gut microbiota composition and metabolism: In vitro evidence. *J. Neurogastroenterol. Motil.* **2017**, *23*, 124–134. [CrossRef]
17. Mitchell, R.J.; Kim, J.S.; Jeon, B.S.; Sang, B.I. Continuous hydrogen and butyric acid fermentation by immobilized clostridium tyrobutyricum ATCC 25755: Effects of the glucose concentration and hydraulic retention time. *Bioresour. Technol.* **2009**, *100*, 5352–5355. [CrossRef]
18. Payne, A.N.; Zihler, A.; Chassard, C.; Lacroix, C. Advances and perspectives in in vitro human gut fermentation modeling. *Trends Biotechnol.* **2012**, *30*, 17–25. [CrossRef]
19. Liu, Z.; Cichocki, N.; Hubschmann, T.; Suring, C.; Ofiteru, I.D.; Sloan, W.T.; Grimm, V.; Muller, S. Neutral mechanisms and niche differentiation in steady-state insular microbial communities revealed by single cell analysis. *Environ. Microbiol.* **2019**, *21*, 164–181. [CrossRef]
20. Macfarlane, G.T.; Macfarlane, S.; Gibson, G.R. Validation of a three-stage compound continuous culture system for investigating the effect of retention time on the ecology and metabolism of bacteria in the human colon. *Microb Ecol* **1998**, *35*, 180–187. [CrossRef]
21. Fehlbaum, S.; Chassard, C.; Haug, M.C.; Fourmestraux, C.; Derrien, M.; Lacroix, C. Design and investigation of polyferms in vitro continuous fermentation models inoculated with immobilized fecal microbiota mimicking the elderly colon. *PLoS ONE* **2015**, *10*, e0142793. [CrossRef] [PubMed]
22. Hinzke, T.; Kleiner, M.; Markert, S. Centrifugation-based enrichment of bacterial cell populations for metaproteomic studies on bacteria-invertebrate symbioses. *Methods Mol. Biol.* **2018**, *1841*, 319–334. [PubMed]
23. Starke, R.; Jehmlich, N.; Bastida, F. Using proteins to study how microbes contribute to soil ecosystem services: The current state and future perspectives of soil metaproteomics. *J. Proteomics* **2019**, *198*, 50–58. [CrossRef] [PubMed]
24. Becker, N.; Kunath, J.; Loh, G.; Blaut, M. Human intestinal microbiota: Characterization of a simplified and stable gnotobiotic rat model. *Gut Microbes* **2011**, *2*, 25–33. [CrossRef]
25. Rothe, M.; Blaut, M. Evolution of the gut microbiota and the influence of diet. *Benef. Microbes* **2013**, *4*, 31–37. [CrossRef]
26. Woting, A.; Pfeiffer, N.; Hanske, L.; Loh, G.; Klaus, S.; Blaut, M. Alleviation of high fat diet-induced obesity by oligofructose in gnotobiotic mice is independent of presence of bifidobacterium longum. *Mol. Nutr. Food Res.* **2015**, *59*, 2267–2278. [CrossRef]
27. Woting, A.; Pfeiffer, N.; Loh, G.; Klaus, S.; Blaut, M. Clostridium ramosum promotes high-fat diet-induced obesity in gnotobiotic mouse models. *MBio* **2014**, *5*, e01530-14. [CrossRef]
28. Slezak, K.; Krupova, Z.; Rabot, S.; Loh, G.; Levenez, F.; Descamps, A.; Lepage, P.; Dore, J.; Bellier, S.; Blaut, M. Association of germ-free mice with a simplified human intestinal microbiota results in a shortened intestine. *Gut Microbes* **2014**, *5*, 176–182. [CrossRef]
29. Weitkunat, K.; Schumann, S.; Petzke, K.J.; Blaut, M.; Loh, G.; Klaus, S. Effects of dietary inulin on bacterial growth, short-chain fatty acid production and hepatic lipid metabolism in gnotobiotic mice. *J. Nutr. Biochem.* **2015**, *26*, 929–937. [CrossRef]
30. Bauer, E.; Zimmermann, J.; Baldini, F.; Thiele, I.; Kaleta, C. Bacarena: Individual-based metabolic modeling of heterogeneous microbes in complex communities. *PLoS Comput. Biol.* **2017**, *13*, e1005544. [CrossRef]

31. Koch, C.; Muller, S. Personalized microbiome dynamics—Cytometric fingerprints for routine diagnostics. *Mol. Aspects Med.* **2018**, *59*, 123–134. [CrossRef] [PubMed]
32. Liu, Z.; Cichocki, N.; Bonk, F.; Gunther, S.; Schattenberg, F.; Harms, H.; Centler, F.; Muller, S. Ecological stability properties of microbial communities assessed by flow cytometry. *mSphere* **2018**, *3*, e00564-17. [CrossRef] [PubMed]
33. Wissenbach, D.K.; Oliphant, K.; Rolle-Kampczyk, U.; Yen, S.; Hoke, H.; Baumann, S.; Haange, S.B.; Verdu, E.F.; Allen-Vercoe, E.; von Bergen, M. Optimization of metabolomics of defined in vitro gut microbial ecosystems. *Int. J. Med. Microbiol.* **2016**, *306*, 280–289. [CrossRef] [PubMed]
34. Van Gelder, S.; Rohrig, N.; Schattenberg, F.; Cichocki, N.; Schumann, J.; Schmalz, G.; Haak, R.; Ziebolz, D.; Muller, S. A cytometric approach to follow variation and dynamics of the salivary microbiota. *Methods* **2018**, *134–135*, 67–79. [CrossRef] [PubMed]
35. Oksanen, J. *Multivariate Analysis of Ecological Communities in R: Vegan Tutorial*; University of Oulu: Oulu, Finland, 2007.
36. Starke, R.; Kermer, R.; Ullmann-Zeunert, L.; Baldwin, I.T.; Seifert, J.; Bastida, F.; von Bergen, M.; Jehmlich, N. Bacteria dominate the short-term assimilation of plant-derived n in soil. *Soil Biol. Biochem.* **2016**, *96*, 30–38. [CrossRef]
37. Haange, S.B.; Jehmlich, N.; Hoffmann, M.; Weber, K.; Lehmann, J.; von Bergen, M.; Slanina, U. Disease development is accompanied by changes in bacterial protein abundance and functions in a refined model of dextran sulfate sodium (dss)-induced colitis. *J. Proteome Res.* **2019**, *18*, 1774–1786. [CrossRef]
38. Käll, L.; Canterbury, J.D.; Weston, J.; Noble, W.S.; MacCoss, M.J. Semi-supervised learning for peptide identification from shotgun proteomics datasets. *Nat. Methods* **2007**, *4*, 923–925. [CrossRef]
39. Han, J.; Lin, K.; Sequeira, C.; Borchers, C.H. An isotope-labeled chemical derivatization method for the quantitation of short-chain fatty acids in human feces by liquid chromatography-tandem mass spectrometry. *Anal. Chim. Acta* **2015**, *854*, 86–94. [CrossRef]
40. Kleiner, M.; Thorson, E.; Sharp, C.E.; Dong, X.; Liu, D.; Li, C.; Strous, M. Assessing species biomass contributions in microbial communities via metaproteomics. *Nat. Commun.* **2017**, *8*, 1558. [CrossRef]
41. Storelli, G.; Defaye, A.; Erkosar, B.; Hols, P.; Royet, J.; Leulier, F. Lactobacillus plantarum promotes drosophila systemic growth by modulating hormonal signals through tor-dependent nutrient sensing. *Cell Metab.* **2011**, *14*, 403–414. [CrossRef]
42. Taheri-Araghi, S.; Bradde, S.; Sauls, J.T.; Hill, N.S.; Levin, P.A.; Paulsson, J.; Vergassola, M.; Jun, S. Cell-size control and homeostasis in bacteria. *Curr. Biol.* **2015**, *25*, 385–391. [CrossRef] [PubMed]
43. Egan, A.J.; Vollmer, W. The physiology of bacterial cell division. *Ann. N. Y. Acad. Sci.* **2013**, *1277*, 8–28. [CrossRef]
44. Reith, J.; Mayer, C. Peptidoglycan turnover and recycling in gram-positive bacteria. *Appl. Microbiol. Biotechnol.* **2011**, *92*, 1–11. [CrossRef] [PubMed]
45. Kief, D.R.; Warner, J.R. Hierarchy of elements regulating synthesis of ribosomal proteins in saccharomyces cerevisiae. *Mol. Cell Biol.* **1981**, *1*, 1016–1023. [CrossRef]
46. Adamberg, K.; Adamberg, S. Selection of fast and slow growing bacteria from fecal microbiota using continuous culture with changing dilution rate. *Microb Ecol. Health Dis.* **2018**, *29*, 1549922. [CrossRef] [PubMed]
47. Tottey, W.; Denonfoux, J.; Jaziri, F.; Parisot, N.; Missaoui, M.; Hill, D.; Borrel, G.; Peyretaillade, E.; Alric, M.; Harris, H.M.; et al. The human gut chip "hugchip", an explorative phylogenetic microarray for determining gut microbiome diversity at family level. *PLoS ONE* **2013**, *8*, e62544. [CrossRef] [PubMed]
48. Wenzel, L.; Heyer, R.; Schallert, K.; Löser, L.; Wünschiers, R.; Reichl, U.; Benndorf, D. Sds-page fractionation to increase metaproteomic insight into the taxonomic and functional composition of microbial communities for biogas plant samples. *Eng. Life Sci.* **2018**, *18*, 498–509. [CrossRef]
49. Hinzke, T.; Kouris, A.; Hughes, R.A.; Strous, M.; Kleiner, M. More is not always better: Evaluation of 1d and 2d-lc-ms/ms methods for metaproteomics. *Front. Microbiol.* **2019**, *10*, 238. [CrossRef]
50. Neis, E.P.; Dejong, C.H.; Rensen, S.S. The role of microbial amino acid metabolism in host metabolism. *Nutrients* **2015**, *7*, 2930–2946. [CrossRef]
51. Louis, P.; Duncan, S.H.; McCrae, S.I.; Millar, J.; Jackson, M.S.; Flint, H.J. Restricted distribution of the butyrate kinase pathway among butyrate-producing bacteria from the human colon. *J. Bacteriol.* **2004**, *186*, 2099–2106. [CrossRef]

52. Diez-Gonzalez, S.; Kaur, H.; Zinn, F.K.; Stevens, E.D.; Nolan, S.P. A simple and efficient copper-catalyzed procedure for the hydrosilylation of hindered and functionalized ketones. *J. Org. Chem.* **2005**, *70*, 4784–4796. [CrossRef] [PubMed]
53. Dai, Z.L.; Li, X.L.; Xi, P.B.; Zhang, J.; Wu, G.; Zhu, W.Y. Metabolism of select amino acids in bacteria from the pig small intestine. *Amino Acids* **2012**, *42*, 1597–1608. [CrossRef]
54. Salyers, A.A.; Vercellotti, J.R.; West, S.E.; Wilkins, T.D. Fermentation of mucin and plant polysaccharides by strains of bacteroides from the human colon. *Appl. Environ. Microbiol.* **1977**, *33*, 319–322. [PubMed]
55. Flint, H.J.; Scott, K.P.; Louis, P.; Duncan, S.H. The role of the gut microbiota in nutrition and health. *Nat. Rev. Gastroenterol. Hepatol.* **2012**, *9*, 577–589. [CrossRef] [PubMed]

Publication 3: The activation of mucosal-associated invariant T (MAIT) cells is affected by microbial diversity and riboflavin utilization *in vitro*

frontiers in Microbiology

ORIGINAL RESEARCH
published: 22 April 2020
doi: 10.3389/fmicb.2020.00755

The Activation of Mucosal-Associated Invariant T (MAIT) Cells Is Affected by Microbial Diversity and Riboflavin Utilization *in vitro*

*Jannike L. Krause[1], Stephanie S. Schäpe[2], Florian Schattenberg[3], Susann Müller[3], Grit Ackermann[5], Ulrike E. Rolle-Kampczyk[2], Nico Jehmlich[2], Arkadiusz Pierzchalski[1], Martin von Bergen[2,4] and Gunda Herberth[1]**

[1] Department of Environmental Immunology, Helmholtz-Centre for Environmental Research – UFZ Leipzig, Germany,
[2] Department of Molecular Systems Biology, Helmholtz-Centre for Environmental Research – UFZ, Leipzig, Germany,
[3] Department of Environmental Microbiology, Helmholtz-Centre for Environmental Research – UFZ, Leipzig, Germany,
[4] Faculty of Biosciences, Pharmacy and Psychology, Institute of Biochemistry, University of Leipzig, Leipzig, Germany,
[5] Alphaomega laboratory, Leipzig, Germany

OPEN ACCESS

Edited by:
Juarez Antonio Simões Quaresma,
Evandro Chagas Institute, Brazil

Reviewed by:
Pasquale Russo,
University of Foggia, Italy
Lionel Le Bourhis,
Institut National de la Santé et de la Recherche Médicale (INSERM), France

***Correspondence:**
Gunda Herberth
gunda.herberth@ufz.de

Specialty section:
This article was submitted to Microbial Immunology, a section of the journal Frontiers in Microbiology

Received: 14 February 2020
Accepted: 30 March 2020
Published: 22 April 2020

Citation:
Krause JL, Schäepe SS, Schattenberg F, Müller S, Ackermann G, Rolle-Kampczyk UE, Jehmlich N, Pierzchalski A, von Bergen M and Herberth G (2020) The Activation of Mucosal-Associated Invariant T (MAIT) Cells Is Affected by Microbial Diversity and Riboflavin Utilization in vitro. Front. Microbiol. 11:755. doi: 10.3389/fmicb.2020.00755

Recent research has demonstrated that MAIT cells are activated by individual bacterial or yeasts species that possess the riboflavin biosynthesis pathway. However, little is known about the MAIT cell activating potential of microbial communities and the contribution of individual community members. Here, we analyze the MAIT cell activating potential of a human intestinal model community (SIHUMIx) as well as intestinal microbiota after bioreactor cultivation. We determined the contribution of individual SIHUMIx community members to the MAIT cell activating potential and investigated whether microbial stress can influence their MAIT cell activating potential. The MAIT cell activating potential of SIHUMIx was directly related to the relative species abundances in the community. We therefore suggest an additive relationship between the species abundances and their MAIT cell activating potential. In diverse microbial communities, we found that a low MAIT cell activating potential was associated with high microbial diversity and a high level of riboflavin demand and vice versa. We suggest that microbial diversity might affect MAIT cell activation via riboflavin utilization within the community. Microbial acid stress significantly reduced the MAIT cell activating potential of SIHUMIx by impairing riboflavin availability through increasing the riboflavin demand. We show that MAIT cells can perceive microbial stress due to changes in riboflavin utilization and that riboflavin availability might also play a central role for the MAIT cell activating potential of diverse microbiota.

Keywords: human MAIT cells, gut microbiota, folate metabolism, microbial stress, riboflavin metabolism, SIHUMIx

INTRODUCTION

The intestinal microbiota, which clearly outnumbers the microbiota in other human habitats, shapes the immune system in various ways (Thaiss et al., 2016; Levy et al., 2017). In addition to its immunomodulatory properties, the intestinal microbiota is essential in various processes such as food digestion, colonization resistance and the synthesis of short chain fatty acids (SCFA) and

vitamins (Brestoff and Artis, 2013; Sender et al., 2016; Belkaid and Harrison, 2017; Levy et al., 2017). Environmental factors, such as diet, chemicals or drugs, influence the intestinal microbiota (Goodrich et al., 2016) and can thus increase the risk of disease initiation (Forbes et al., 2016). A reduction in microbial diversity, together with an increasing presence of mucosal-associated invariant T (MAIT) cells in the inflamed intestinal or adipose tissue have been reported from patients with inflammatory bowel diseases (IBD) ulcerative colitis and Crohn's disease (Serriari et al., 2014) or obesity (Magalhaes et al., 2015; Chiba et al., 2018).

Especially in IBD, the microbial diversity is unambiguously reduced. Also the number of *Firmicutes* and *Bacteroides* is decreased, while the frequency of *Actinobacteria* and *Proteobacteria* is increased. These changes in microbial diversity and composition as well as the acid fecal pH due to the faster gut transit time change the metabolic profile of intestinal microbiota (Moco et al., 2014) and might affect MAIT cells that accumulated in the intestinal mucosa of IBD patients (Chiba et al., 2018).

The majority of MAIT cells express the semi-invariant alpha chain 7.2 in their T-cell receptor (TCR), which is encoded by the TRAV1-2 gene. These TRAV1-2$^+$ MAIT cells are considered an innate-like T cell subset with effector memory-like phenotype (Dusseaux et al., 2011; Gherardin et al., 2016). The majority of these cells recognize microbial metabolites from the riboflavin biosynthesis pathway, but a small fraction of these TRAV1-2$^+$ MAIT cells also recognizes folate derivates after presentation on major histocompatibility complex I (MHC-I) related protein 1 (MR1) *in vitro* (Kjer-Nielsen et al., 2012; Corbett et al., 2014; Eckle et al., 2015; Gherardin et al., 2016). It has been shown that especially the riboflavin precursors 5-(2-oxopropylideneamino)-6-D-ribitylaminouracil (5-OP-RU) and 5-(2-oxoethylideneamino)-6-D-ribitylaminouracil (5-OE-RU) activate MAIT cells, whereas the folate derivates 6-formylpterin (6-FP) and N-acetyl-6-formylpterin (Ac-6-FP) inhibit MAIT cell activation *in vitro* (Kjer-Nielsen et al., 2012; Corbett et al., 2014). Moreover, MAIT cells can be activated independent of MR1 via cytokines (Ussher et al., 2014; van Wilgenburg et al., 2016). Microbial infections, but not commensal microbiota, are considered to trigger inflammation and thus induce the entire repertoire of MAIT cell effector function, but *in vivo* evidence is pending (Tastan et al., 2018). Nevertheless, MAIT cells are not able to distinguish commensal bacteria from pathogenic bacteria due to antigen recognition, and very little is known about the interaction of MAIT cells and the commensal microbiota (Berkson and Prlic, 2017). After activation, MAIT cells immediately produce effector molecules such as tumor necrosis factor (TNF), interferon gamma (IFNγ) and cytotoxic molecules like perforins or granzymes (Martin et al., 2009; Kurioka et al., 2015). In the human body, MAIT cells reside at barrier sites e.g., in the gut lamina propria (Treiner et al., 2003), the lung (Hinks, 2016), the female genital tract (Gibbs et al., 2017) and the skin (Teunissen et al., 2014). In addition, they are very common in the liver (Dusseaux et al., 2011) and account for to up to 10% of circulating T cells in peripheral blood (Tilloy et al., 1999). The localization of MAIT cell in combination with their ability to recognize and respond to microbial metabolites suggests a key role in host microbiota immune homeostasis and underlines their contribution to fight against infectious diseases.

Recent research has focused on the MAIT cell activating potential of individual commensal and pathogenic microorganisms from the human gut (Le Bourhis et al., 2013; Dias et al., 2017; Tastan et al., 2018). However, in the human body, MAIT cells encounter diverse microbiota and the response of MAIT cells to microbial communities rather reflects the physiologic situation. Thus, in this study we investigate the response of MAIT cells to microbial communities. Therefore, we first used the extended simplified human microbiota (SIHUMIx) model community to analyze the contribution of individual community members on MAIT cell activation. Second, we determined if microbial stress, here a short-term acid stress, affects the community composition or metabolism of SIHUMIx and thereby MAIT cell activation. Third, we investigated the MAIT cell response to microbiota with high diversity like fecal and colonic microbiota.

MATERIALS AND METHODS

The Model Community SIHUMIx

The extended simplified intestinal human microbiota (SIHUMIx) community was used to investigate the interaction of intestinal bacterial communities and MAIT cells. This model community shows major features of a human intestinal community (Becker et al., 2011) and allows the reproducible cultivation (Krause et al., 2020). SIHUMIx comprises of eight bacterial species *Anaerostipes caccae* (DSM 14662), *Bacteroides thetaiotaomicron* (DSM 2079), *Bifidobacterium longum* (NCC 2705), *Blautia producta* (DSM 2950), *Clostridium butyricum* (DSM 10702), *Clostridium ramosum* (DSM 1402), *Escherichia coli* K-12 (MG1655), and *Lactobacillus plantarum* (DSM 20174).

Cultivation of Bacteria

Cultivation of SIHUMIx Single Strains

All bacteria strains were anaerobically cultivated using the Hungate technique in Brain-Heart-Infusion (BHI) medium (**Supplementary Table S1**). After inoculation, the bacteria were incubated at 37°C and 175 rpm shaking for 24 h. Then, bacteria were fixed for MAIT cell stimulation assays or kept at room temperature for a maximum of 7 d for strain maintenance. For the purpose of bioreactor inoculation, the single strain bacteria were cultivated for 72 h in BHI medium.

Continuous Cultivation of SIHUMIx and Human Fecal Communities

To investigate the stimulation capacity of SIHUMIx under normal and stress conditions the SIHUMIx community was continuously cultivated in a Multifors 2 bioreactor (Infors, Switzerland, $N = 2$) as described in Krause et al. (2020) using complex intestinal medium [CIM, **Supplementary Table S2** (Krause et al., 2020)]. In addition, we cultivated human fecal microbiota alike the SIHUMIx community in triplicate bioreactors. In brief, growth conditions should reflect the colon of a healthy individual. After the sterile run, the bioreactors were

inoculated with an equal cell number of SIHUMIx strains or 1 mL fecal enrichment culture. Bacteria were cultivated under unimpeded culture conditions until day 14 (SIHUMIx) or day 16 (fecal microbiota). SIHUMIx additionally was exposed to an acid stress, therefore in duplicate bioreactors the pH was reduced from 6.5 to 5.5 on day 4 for 24 h. After sampling on day 5, the pH was reset to the original pH of 6.5 until the end of the cultivation.

Continuous Cultivation of Swine Colonic Bacteria

Colonic bacteria from two different, co-housed swine were continuously cultivated in duplicate multifors 2 bioreactors (Infors, Bottmingen Switzerland, $N = 4$) until metabolic stability was assumed (10× bioreactor turnover: day 21). Bacteria were cultivated in complex intestinal medium adapted to swine [swine CIM, **Supplementary Table S3**, adaption from (Tanner et al., 2014; McDonald et al., 2015)]. The cultivation temperature was set to 37°C and pH was adjusted to 6.5. Prior to inoculation, a sterile run was conducted under experimental conditions. We inoculated with the supernatant of 0.5 g colon content/vessel suspended in pre-warmed CIM. Colon content from pig 1 was used for bioreactor A and B; colon content from pig 2 was used to inoculate bioreactor C and D. After 24 h continuous cultivation was started continuous cultivation at a dilution rate of $D = 0.02$ [equal to a retention time of 48 h; (Wilfart et al., 2007)].

Bacteria Fixation

Bacterial cells were harvested (3.200 g, 5 min, 4°C) and fixed with 1% of formaldehyde for 1 min to preserve the cell structure and prevent bacteria lysis during freezing and thawing. Afterward, cells were washed three times with phosphate buffered saline (PBS, 140 mM NaCl, 10 mM Na_2HPO_4, 7 mM KH_2PO_4) to dilute out the formaldehyde. The cell number was determined using a Beckman Coulter Multisizer 3 cell counting system (Beckman Coulter, Brea, United States) and the cell number was adjusted to 3×10^9 cells/mL in IMDM medium (IMDM supplemented with 10% fetal calf serum, 25 mM HEPES, 50 μM β-mercaptoethanol and 100 U/mL Pencillin/Streptomycin). Bacteria pellets were frozen with IMDM supernatant at −80°C.

Purification of Peripheral Blood Mononuclear Cells

Blood from healthy donors was obtained from the blood donation service at the university hospital Leipzig, Germany. PBMCs were purified by gradient centrifugation on Ficoll-paque plus (GE Healthcare, Chicago, United States). PBMCs were gradually frozen in FCS with 10% DMSO at −80°C and stored at −150°C until use.

MAIT Cell Stimulation

The day before stimulation PBMCs were thawed and 1×10^6 of live PBMCs per well were seeded into 96-well plates. PBMCs were incubated over-night at 37°C and 5% CO_2. For stimulation, frozen bacteria pellets were mixed vigorously, diluted in IMDM, and used directly in a total volume of 200 μ L.

1×10^6 PBMCs were stimulated with 25 bacteria per cell (BpC) of all SIHUMIx single strains. The SIHUMIx 1:1 mix was generated by mixing equal cell numbers of the SIHUMIx strains. We used 25 BpC from the SIHUMIx 1:1 mix for stimulation. To calculate the average percentage of MAIT cell activation, we summarized the percentage of activated MAIT cells after single strain stimulation and divided by the number of strains.

PBMCs were stimulated with 200 BpC of complex communities that were cultivatied in the bioreactor, like SIHUMIx, the colonic and the fecal communities. The negative control remained unstimulated; the positive control was stimulated with 20 BpC *E. coli* K12.

To compare sample diversity, 200 BpC of *E. coli*, the SIHUMIx, the fecal and the colonic community were used for stimulation. To achieve an average MAIT cell response to SIHUMIx and the colonic communities, we pooled the bioreactor samples of both bioreactors on day 13 and day 14, respectively (recovered SIHUMIx communities). Likewise, we pooled all colonic communities A, B, C, and D on day 21 for MAIT cell stimulation assays.

MR1 antibody was incubated one hour before with PBMCs. Then bacteria were added for MAIT cell stimulation.

After two hours of stimulation 10 μg/mL Brefeldin A was added to prevent cytokine release. After a total of 6 h PBMCs were harvested for surface (CD3, CD8a, CD161, Va7.2) and intracellular staining (CD69, TNF, IFNg) followed by FACS analysis (FACS Canto II, Becton Dickinson and Company, Franklin Lakes, United States). Discrimination of dead cells was done by staining with Fixable Viability Dye eFluor 506. Antibodies were obtained from Biolegend and eBioscience (**Supplementary Table S4**). Data analysis was done with FlowJo v10 software. Data evaluation and hypothesis testing was done with GraphPad PRISM v7.04 software using one-way ANOVA.

Quantitation of Riboflavin in Bacterial Culture Supernatants

Supernatant samples were thawed at 37°C for 10 min. We extracted the metabolites with five volumes of a methanol:acetonitrile:water (2:3:1) mixture and added 10 μL internal standard. After addition of five volumes of extraction solvent samples were vortexed for 5 min and afterward sonicated in an ultrasound bath for 5 min. Debris was pelleted by centrifugation (14.000 rpm, 5 min, RT) and the supernatant was transferred to a fresh tube. The extract was dried in a SpeedVac vacuum concentrator (Eppendorf, Hamburg, Germany) and resuspended in 100 μL of mix of running solvent A and running solvent B (1:1).

For LC-MS/MS measurement 10 μL of the resuspended extract were injected into a HPLC-MS-System (RSLC Ultimate 3000 Thermo Fisher coupled with Q-Trap 5500 AB Sciex). Metabolites were separated on ACQUITY UPLC BEH 300 C18 (1,7 μm, Waters, Milford, United States) with a flow rate of 0.3 mL/min in a gradient of running solvent A (0.1% formic acid in water) and running solvent B (0.1% formic acid in methanol): 0.5 min 100% A, 0.6–4 min 0–100% B, hold 3 min, 3 min 100% A. The Q-Trap was set up to positive MRM mode (Riboflavin MRM: parent ion: 377, product ions: 243, 198, and 172; Internal Standard MRM: parent ion: 383, product ions: 249, 202, and 175). Bar plots were generated with the GraphPad PRISM v7.04 software.

Quantitation of Folate in Bacterial Culture Supernatants

Supernatant of bacterial cultures was used for the measurement of total folate concentration with the electrochemiluminescence immunoassay Elecsys Folate (Roche, Basel, Switzerland) according to manufacturer's instructions.

Metaproteome and Proteome Analysis

Bacteria pellets were thawed and dissolved in the 1000 µL lysis buffer (10 mM Tris–HCl, NaCl 2 mg/mL, 1 mM PMSF, 4 mg/mL SDS). Cells were disrupted by 1. Bead beating (FastPrep-24, MP Biomedicals, Santa Ana, United States: 5.5 ms, 1 min, 3 cycles), 2. 15 min incubation at 60°C (Thermomixer comfort 5355, Eppendorf, Germany) and 3. Ultra-sonication UP50H, Hielscher, Teltow, Germany; cycle 0.5, amplitude 60%). Protein concentration was determined with bicinchoninic acid assay according to the user manual (Pierce BCA Protein Assay Kit, Thermo Fisher Scientific, Waltham, United States). 100 µg of protein were precipitated overnight in acetone 1:5 (V/V) at -20°C and centrifuged (10 min, 14,000 × *g*). The precipitate was used for SDS-PAGE analysis, in-gel digestion and protein purification with ZipTip treatment (Starke et al., 2016).

Measurement was performed as described (Krause et al., 2020). 5 µg peptide lysate was injected into nanoHPLC (UltiMate 3000 RSLCnano, Dionex, Thermo Fisher Scientific, Waltham, United States). Peptide separation was performed on a C18-reverse phase trapping column (C18 PepMap100, 300 µm × 5 mm, particle size 5 µm, nano viper, Thermo Fischer Scientific, Waltham, United States), followed by a C18-reverse phase analytical column (Acclaim PepMap§ 100, 75 µm × 25 cm, particle size 3 µm, nanoViper, Thermo Fisher Scientific, Waltham, United States). Mass spectrometric analysis of peptides was performed on a Q Exactive HF mass spectrometer (Thermo Fisher Scientific, Waltham, United States) coupled to a TriVersa NanoMate (Advion, Ltd., Harlow, United Kingdom) source in LC chip coupling mode. LC gradient, ionization mode, and mass spectrometry mode are described (Haange et al., 2019).

Raw data were processed with Proteome Discoverer (v 2.2, Thermo Fischer Scientific, Waltham, United States). Search settings for Sequest HT search engine were set to: Trypsin (Full), Max. Missed Cleavage: 2, precursor mass tolerance: 10 ppm, fragment mass tolerance: 0.02 Da. Protein grouping was enabled, with protein group requiring at least one unique peptide. For single species the protein coding sequences of the eight SIHUMIx strains were downloaded from UniProt[1]. For SIHUMIx protein coding sequences of all eight were combined and used as database resulting in 29,558 protein sequences. For complex microbiota protein coding sequences of all "bacteria" were downloaded from UniProt (13.05.2017; http://www.uniprot.org/) resulting in 15,214,675 protein coding sequences. Protein identification was performed as descried (Schäpe et al., 2019). In brief, the false discovery rates (FDR) were determined with the node Percolator (Käll et al., 2007) embedded in Proteome Discoverer (v 2.2) and we set the FDR threshold at peptide and protein level at 5%. Only protein groups were assigned that explains at least one unique identified peptide.

GhoastKOALA was used to assign KO numbers of KEGG to identified functions of identified protein sequences. Visualization and statistical analysis were done with GraphPad Prism (v. 8.0.2) using unpaired multiple *t*-tests per row.

[1]http://www.uniprot.org/

16 S rRNA Gene Analysis

For DNA extraction, bacteria pellets were thawed and one volume of bacteria slurry was mixed with 30 volumes of sterile 10% Chelex (wt/vol) solution. Samples were incubated in a ThermoMixer (Eppendorf, Hamburg, Germany) at 95°C for 45 min and 1000 rpm shaking. Afterward the suspension was centrifuged for 3 min at 11,000 *g* and the supernatant, containing the DNA, was transferred into a fresh, sterile tube and stored at -20°C. High throughput 16S amplicon generation, sequencing and analysis was done by StarSeq GmbH (Mainz, Germany). The 16S gene region V3 to V4 was amplified with the primers 341F and 806bR, sequencing was performed on an Illumina MiSeq DNA sequencer (Illumina, San Diego, United States).

Microbial Flow Cytometry

The bacteria suspension was centrifuged (3,200 × g, 10 min, and 4°C) and cells were fixed in 2% formaldehyde [stock: 8% formaldehyde pH 7, diluted with PBS (6 mM Na_2HPO_4, 1.8 mM NaH_2PO_4 and 145 mM NaCl in bi-distilled water, pH 7)] at RT for 30 min. The bacteria were pelleted (3,200 × g, 10 min, and 4°C) and resuspended in 70% ethanol for long-term storage at −20°C.

After a minimum of one day at −20°C, single strain bacteria and SIHUMIx were stained with 0.24 µM 4′,6-di-amidino-2-phenyl-indole (DAPI, Sigma-Aldrich, St-Louis, United States) overnight according to the protocol from Koch et al. (2013). The fecal and colonic bacteria were homogenized by ultra-sonication and stained with 0.68 µM 4′,6-di-amidino-2-phenyl-indole (DAPI, Sigma-Aldrich, St-Louis, United States) overnight. Measurement and data analysis were performed as in Krause et al. (2020).

Statistical Analysis

Bar plots report the mean and standard deviation. Comparison of groups were done using GraphPad Prism version 8.3.0 (La Jolla, CA, United States) using Student's t-test or ordinary one-way ANOVA for unpaired data with Dunnett's or Tukey *post hoc* test for multiple comparisons as specified in the figure legends. Significance was defined at $P < 0.05$. The calculation of Bray-Curtis-Dissimilarities was done in R using the metaMDS function from the vegan package (Dixon, 2003), data were visualized in a heatmap using the heatmap.2 function.

RESULTS

The Model Community SIHUMIx Comprises of MAIT Cell Activating and Non-activating Strains

To characterize the response of MAIT cells to intestinal bacterial communities and the contribution of individual strains, we utilized the extended simplified human microbiota model community (SIHUMIx). SIHUMIx is a defined bacterial community of eight species commonly found in the human intestine: *A. caccae*, *B. thetaiotaomicron*, *B. longum*, *B. producta*, *C. butyricum*, *C. ramosum*, *E. coli* K-12 and *L. plantarum* (Becker et al., 2011). First, we evaluated the activating potential of the individual community members and therefore individually stimulated peripheral blood mononuclear cells (PBMCs) with these bacterial strains (**Figures 1A–D**, $n = 6$). In this study, all bacteria were treated with formaldehyde and stored at −80°C prior to PBMC stimulation. Nevertheless, the cellular structure of the bacteria was largely preserved and bacterial lysis during the freeze-thaw-cycle was prevented (total and viable bacteria cell numbers: **Supplementary Figure S1** and viability staining images: **Supplementary Figure S2**).

Furthermore, we identified TRAV1-2$^+$ MAIT cells by the expression of CD3$^+$, CD8a$^+$, CD161$^+$, and the TCR Vα 7.2$^+$ surface receptors within the alive single cell lymphocytes (hereafter called MAIT cells, **Figure 1A**). CD69$^+$/TNF$^+$ expressing MAIT cells were defined as activated MAIT cells (**Figure 1B**). Upon co-incubation, the bacterial strains *B. thetaiotaomicron*, *E. coli*, and *L. plantarum* activated MAIT cells in decreasing order and significantly increased the percentage of CD69$^+$/TNF$^+$ MAIT cells compared to the unstimulated control (**Figure 1C**, one-way-ANOVA, $n = 6$). *B. thetaiotaomicron* e.g., activated 34.0% of MAIT cells ($P < 0.0001$). The remaining strains *A. caccae*, *B. longum*, *B. producta*, *C. butyricum*, and *C. ramosum* were not able to activate MAIT cells.

Resent research showed that MAIT cell activating bacteria possess at least the enzyme ribD/G from the riboflavin biosynthesis pathway (Corbett et al., 2014; Kurioka et al., 2015; Soudais et al., 2015). Other *in vitro* studies proved that the majority of MAIT cells recognize riboflavin metabolites and after recognition become activated (Corbett et al., 2014). Nevertheless, a small proportion of MAIT cells recognizes folate derivates (Gherardin et al., 2016). Since these metabolites are difficult to quantify, we measured the riboflavin and folate concentration in the culture supernatant as a proxy. After blank subtraction, a positive Δ vitamin concentration indicated vitamin secretion into the culture medium, whereas a negative value indicated vitamin uptake from the culture medium.

Exclusively for the MAIT cell activating bacterial strains, *B. thetaiotaomicron*, *E. coli* and *L. plantarum*, we observed positive Δ riboflavin concentrations (**Figure 1D**, raw data: **Supplementary Table S5** and **Supplementary Figure S3A**) suggesting the ability of riboflavin biosynthesis and secretion. *B. thetaiotaomicron* had the highest Δ riboflavin concentration combined with the highest potential to activate MAIT cells. Both, the ability to activate MAIT cells and the Δ riboflavin concentration in the culture supernatant were lower for *E. coli* and the lowest for *L. plantarum* compared to *B. thetaiotaomicron*. Additionally, we observed negative Δ riboflavin concentrations for all non-activating bacterial strains indicating riboflavin uptake from the culture medium (**Figure 1D**). The Δ folate concentrations were positive after blank subtraction for all bacterial strains independent of their MAIT cell activating potential and exceeded the riboflavin concentration (**Figure 1E**, raw data: **Supplementary Table S6** and **Supplementary Figure S3B**). Our results indicate that the MAIT cell activating SIHUMIx strains, *B. thetaiotaomicron*, *E. coli*, and *L. plantarum*, are capable of riboflavin biosynthesis and secretion, whereby the non-activating SIHUMIx strains seem not to be able to synthesize riboflavin and thus might take up riboflavin from the medium.

We next analyzed the enzymatic repertoire to synthesize riboflavin of the SIHUMIx strains to confirm our findings regarding the ability to synthesize riboflavin and/or folate. Therefore, we combined shotgun proteomics with a proteome and genome based data base search in the UniProt and KEGG database (**Figure 2**). We detected protein abundance levels assigned to riboflavin biosynthesis with proteomics in *B. thetaiotaomicron*, *E. coli*, and *L. plantarum*. Using the database search, we also found proteins from the riboflavin biosynthesis pathway for *A. caccae* and *C. butyricum* (**Supplementary Table S7**). The remaining bacterial strains did not possess enzymes from the riboflavin biosynthesis pathway. However, only the MAIT cell activating bacterial strains *B. thetaiotaomicron*, *E. coli*, and *L. plantarum* proved to have all enzymes for riboflavin biosynthesis. Moreover, we detected proteins for riboflavin uptake (except *C. ramosum*) and riboflavin conversion into the cofactors flavin mononucleotide (FMN) and flavin adenine dinucleotide (FAD) in all SIHUMIx strains expect (**Figure 2**). Indeed, the MAIT cell activating SIHUMIx strains as only had the necessary enzymes for riboflavin biosynthesis. In contrast, the non-activating SIHUMIx strains possessed incomplete riboflavin biosynthesis pathways combined with the enzymatic equipment for riboflavin uptake and conversion. With regard to folate, we observed an increase in Δ folate combined with a close to full enzyme coverage of the folate biosynthesis pathways for all SIHUMIx strains, except *C. ramosum*, indicating the ability to produce and secret folate (**Supplementary Table S8** and **Supplementary Figure S4**).

To understand the contribution of individual bacterial strains to the MAIT cell activating potential of bacterial communities, we stimulated MAIT cells with an artificial SIHUMIx community, the SHIUMIx 1:1 mix. In this SIHUMIx 1:1 mix, all strains were mixed from single strain cultures at equivalent abundances (SIHUMIx 1:1 mix, **Figure 3A**). We compared the MAIT cell activating potential of SIHUMIx 1:1 mix to a calculated value. This calculated value represents the average MAIT cell response after MAIT cell stimulation with the individual SIHUMIx strains (**Figure 1A**). The MAIT cell activating potential of SIHUMIx 1:1 mix was equal to the calculated MAIT cell response (**Figure 3B**, $n = 4$, unpaired t-test, ns). Therefore, we assume a correlation between the relative species abundances in the community and the MAIT cell activating potential of the community.

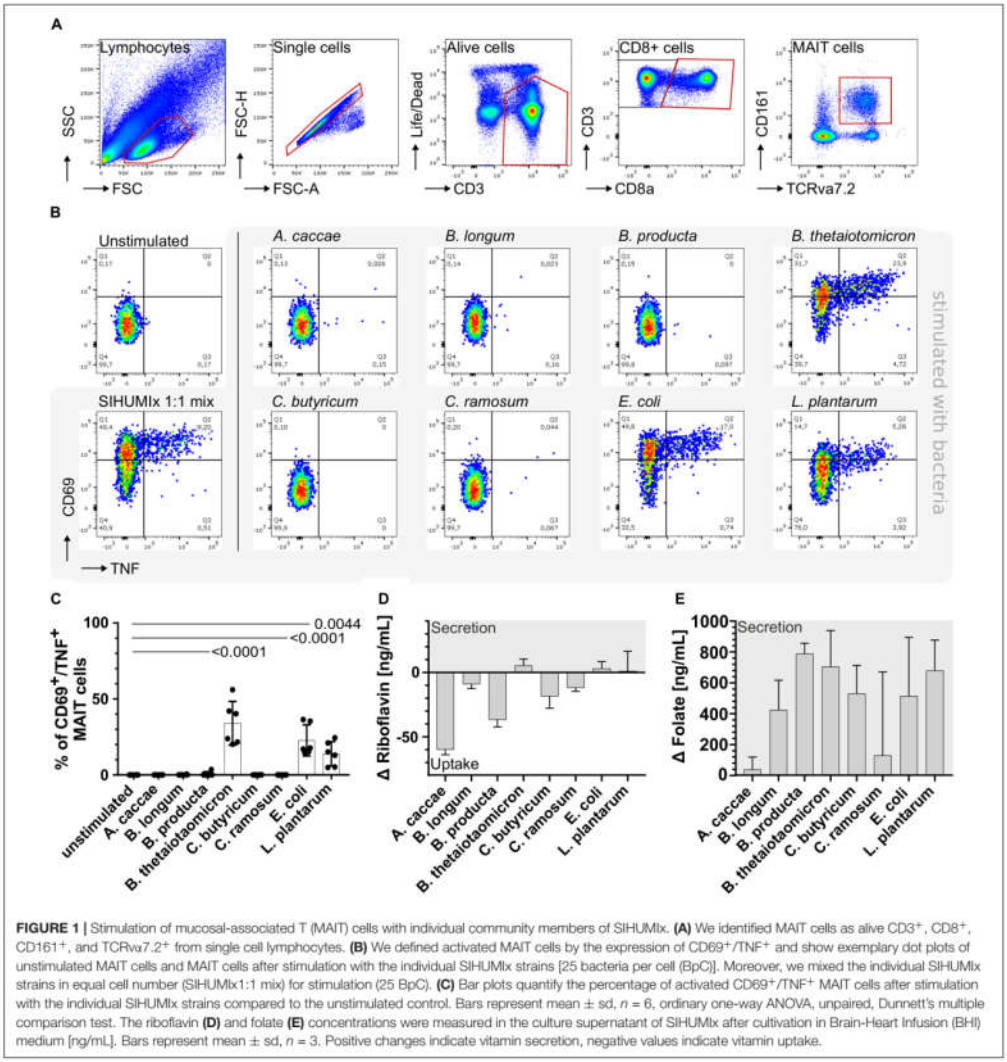

FIGURE 1 | Stimulation of mucosal-associated T (MAIT) cells with individual community members of SIHUMIx. **(A)** We identified MAIT cells as alive $CD3^+$, $CD8^+$, $CD161^+$, and $TCRva7.2^+$ from single cell lymphocytes. **(B)** We defined activated MAIT cells by the expression of $CD69^+/TNF^+$ and show exemplary dot plots of unstimulated MAIT cells and MAIT cells after stimulation with the individual SIHUMIx strains [25 bacteria per cell (BpC)]. Moreover, we mixed the individual SIHUMIx strains in equal cell number (SIHUMIx1:1 mix) for stimulation (25 BpC). **(C)** Bar plots quantify the percentage of activated $CD69^+/TNF^+$ MAIT cells after stimulation with the individual SIHUMIx strains compared to the unstimulated control. Bars represent mean ± sd, $n = 6$, ordinary one-way ANOVA, unpaired, Dunnett's multiple comparison test. The riboflavin **(D)** and folate **(E)** concentrations were measured in the culture supernatant of SIHUMIx after cultivation in Brain-Heart Infusion (BHI) medium [ng/mL]. Bars represent mean ± sd, $n = 3$. Positive changes indicate vitamin secretion, negative values indicate vitamin uptake.

Acid Stress Affects the MAIT Cell Activating Potential by Altering Microbial Riboflavin Metabolism

MAIT cells and microbiota convene at the body's barrier sites, where environmental factors or stressors can affect the microbiota (Goodrich et al., 2016). We aimed to investigate if microbial stress can affect the MAIT cell activating potential of microbiota and thereby can directly influence MAIT cell activation. Since patients with active ulcerative colitis can show a lower colonic pH as part of the disease (Nugent et al., 2001; Moco et al., 2014), we cultivated the SIHUMIx model community *in vitro* and induced an acute acid stress of pH 5.5 (Krause et al., 2020), experimental set-up: **Supplementary Figure S5**). Thereafter, we compared the MAIT cell activating potential of the unstressed and the acid stressed SIHUMIx community.

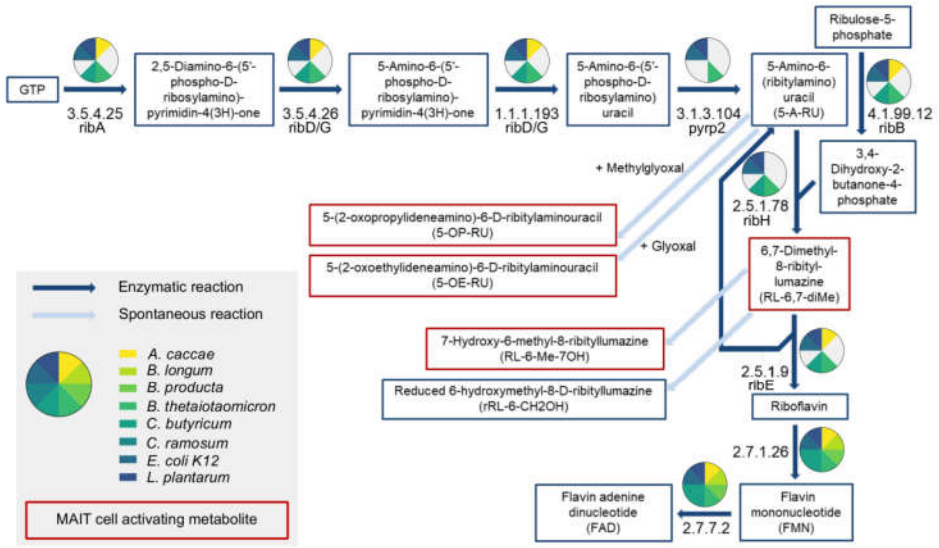

FIGURE 2 | Riboflavin biosynthesis pathway analysis of SIHUMIx bacterial strains. Enzymes from the riboflavin biosynthesis pathway are coded by their EC number. The colors used in the pie charts indicate detected proteins of corresponding bacterial strains. Metabolites that activate MAIT cells after presentation on MHC I related protein 1 (MR1) are marked in red.

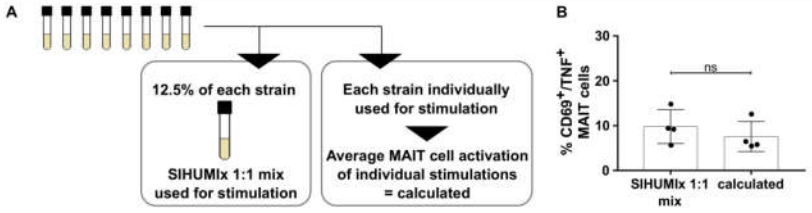

FIGURE 3 | Contribution of individual SIHUMIx strains to the MAIT cell activating potential. **(A)** Study design: Left – Mixture of individual SIHUMIx strains in equal cell numbers (SIHUMIx 1:1 mix) were used for stimulation. Right – Individual SIHUMIx strains were used for stimualtion. **(B)** We compared the MAIT cell activating potential of the SIHUMIx 1:1 mix community to the calculated MAIT cell activating potential based on the individual activating potential of each SIHUMIx strain (mean ± sd, $n = 4$, unpaired t-test).

During adaptation to the culture conditions in the bioreactor system on day 1 and day 2, the MAIT cell activating potential of SIHUMIx was highest and dropped slightly on day 3 in both, the unstressed and the stressed SIHUMIx community (**Figure 4**). In the unstressed SIHUMIx, the MAIT cell activating potential remained constant until the end of the experiment after day 3 (**Figure 4A**, $n = 3$, one-way ANOVA). Under acid stress SIHUMIx lost the potential to activate MAIT cells on day 5 (**Figure 4B,C**, $n = 3$, one-way ANOVA, P are listed in **Supplementary Table S9**). After resetting the pH to the original value, the MAIT cell activating potential recovered to the initial MAIT cell activating potential on day 13 and day 14 (**Figure 4B,C**, $n = 3$).

Changes in the relative species abundances of SIHUMIx might cause the reduced MAIT cell activating potential under acid stress. Therefore, we performed metaproteomics to elucidate the community composition. Based on the relative species abundances day 1, day 5, and day 14 segregated in a principal component analysis (**Supplementary Figure S6**) although the community compositions on day 1, day 5 and day 14 were similar (**Figure 5A** and **Supplementary Table S10**). Nevertheless, our data revealed an increase in the low abundant bacterial strains

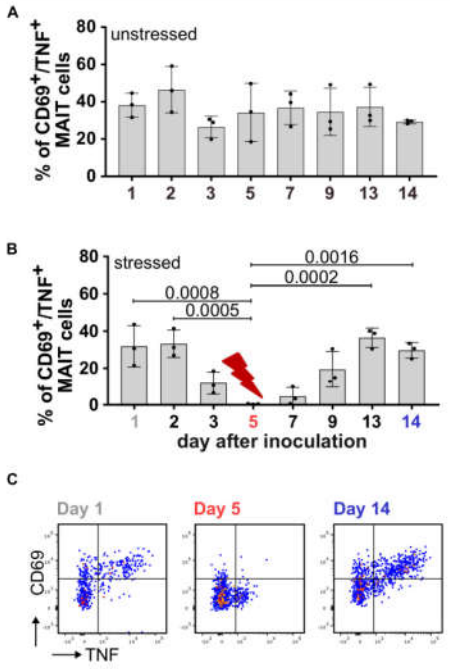

FIGURE 4 | The MAIT cell activating potential of SIHUMIx is lost during acid stress. We cultivated SIHUMIx community in bioreactors (n = 4) for 14 d. On day 5, bacteria were exposed to a short-term acid stress (n = 2), whereas others remained untreated (n = 2). **(A)** Bar plots quantify the percentage of $CD69^+/TNF^+$ activated MAIT cells after stimulation with pooled SIHUMIx communities from unstressed bioreactors and **(B)** bioreactors that were exposed to a short-term acid stress on days 1, 2, 3, 5, 7, 9, 13, and 14. Bars represent mean ± sd (n = 3, unpaired data, ordinary one-way ANOVA, Tukey *post hoc* test for multiple comparisons). **(C)** We show exemplary dot plots of $CD69^+/TNF^+$ activated MAIT cells after stimulation with SIHUMIx from the stressed bioreactors on day 1 (initial), day 5 (acid stress) and day 14 (recovered) with 200 bacteria per cell (BpC).

B. longum, *C. ramosum* and *L. plantarum* under acid stress (day 5) compared to the communities on day 1 and day 14 (**Supplementary Figure S7**).

From our findings, we expected an additive relation between the relative species abundances (community composition) and the MAIT cell activating potential in the model community SIHUMIx (**Figure 3B**). Thus, we compared the activating potential of bioreactor grown SIHUMIx communities on day 1, day 5, and day 14 (**Figure 5B**, day 1/5/14 BR) to SIHUMIx mix communities (**Figure 5C**, day 1/5/14 mix). We aimed to test if the increased relative species abundances of *B. longum*, *C. ramosum*, and *L. plantarum* were causative for the reduced MAIT cell activating potential under acid stress. The mix communities were generated from single strain cultures equal to the community composition on day 1, day 5, and day 14 observed by metaproteomics (**Figure 5A** and **Supplementary Table S10**).

The acid stressed SIHUMIx community (day 5) from the bioreactor had a significantly lower potential to activate MAIT cells compared to the analogous mix-community (**Figure 5D**, unpaired t-test, $P = 0.0199$). In contrast, the unstressed bioreactor communities on day 1 and day 14 as well as their corresponding mix-communities, showed a similar MAIT cell activating potential (**Figure 3D**, unpaired t-test, ns). These results suggest that acute acid stress barely affected the community composition and that the slight changes in community composition did not account for the reduced MAIT cell activating potential under acid stress.

Since riboflavin and folate metabolites might determine the MAIT cell activating potential, we measured the concentration of both these vitamins as proxy for the metabolites. After blank subtraction, we observed high initial Δ riboflavin concentrations during adaptation, which significantly dropped on day 3 and equaled zero. Under acute acid stress, the Δ riboflavin concentration significantly dropped further and reached a minimum on day 7. After the stress ended, the Δ riboflavin concentration recovered to zero and became similar to the concentration on day 3 (**Figure 5E** and **Supplementary Table S11**, one-way ANOVA: P are listed in **Supplementary Table S12**). In contrast to riboflavin, folate was detected in high concentrations independent of the acid stress (**Figure 5F** and **Supplementary Table S11**, one-way ANOVA: P are listed in **Supplementary Table S13**). Furthermore, we considered global functional effects, but we did not observe other changes in the communities' metabolism related to the acid stress (**Supplementary Figure S8**). We found, that microbial acid stress barely affected the community composition and metabolism of SIHUMx but altered the riboflavin utilization toward an increased riboflavin uptake from the medium.

The MAIT Cell Activating Potential of Diverse Colonic Communities

To test the impact of more diverse communities on MAIT cell activation, we continuously cultivated colonic communities from swine colon content in bioreactors A, B, C, and D (community A, B, C, and D). The colonic communities A, C, and D had a similar MAIT cell activating potential (**Figure 6A**, n = 4, A = 5.9%, C = 5.67%, D = 5.9% $CD69^+/TNF^+$ MAIT cells, one-way ANOVA, ns). In contrast, the potential to activate MAIT cells was almost twice as high for community B (**Figure 6A**, n = 4, 12.3% $CD69^+/TNF^+$ MAIT cells, one-way ANOVA, ns).

Since the community composition in the model community SIHUMIx on the one hand and microbial riboflavin metabolism on the other hand correlated with the MAIT cell activating potential, we performed metaproteomics to unravel the community composition. The communities A, B, C, and D were distinct on phylum (**Figure 6B** and **Supplementary Table S14**) and family level (**Supplementary Figure S9** and **Supplementary Table S15**). The phyla *Proteobacteria*, *Firmicutes* and *Bacteroides* dominated in all colonic communities, whereas the phylum *Actinobacteria* was low abundant. In contrast to the

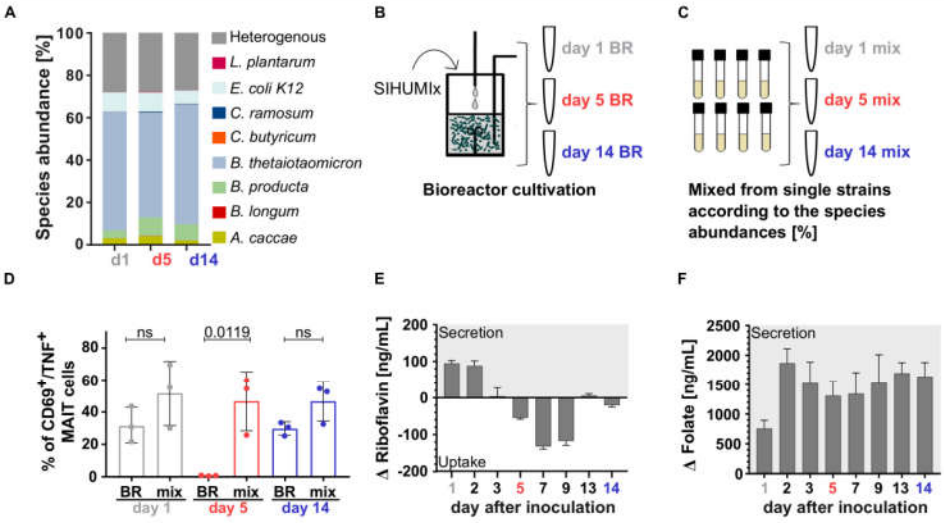

FIGURE 5 | Acid stress mainly affected microbial riboflavin utilization and thereby MAIT cell activation. **(A)** The relative species abundances of SIHUMIx on day 1, day 5, and day 14 observed by metaproteomics was similar. **(B)** We stimulated MAIT cell with SIHUMIx communities on days 1, 5, and 14 cultivated in the bioreactor (BR) and **(C)** with mix communities based on the relative species abundances observed by metaproteomics. These were prepared from individual cultures on days 1, 5, and 14. **(D)** The unstressed bioreactor communities (BR) on day 1 and day 14 had a similar MAIT cell activating potential as their corresponding mix communities (mix), whereas on day 5 the BR community under acid stress significantly lost its MAIT cell activating potential (mean ± sd, $n = 3$, unpaired t-test). Quantitation of **(E)** riboflavin and **(F)** folate in the culture supernatant of SIHUMIx after bioreactor cultivation [ng/mL]. Bars represent mean ± sd, $n = 3$. Positive changes indicate vitamin secretion, negative values indicate vitamin uptake.

other communities, community B showed a high abundance of *Firmicutes* (**Figure 6B**). In line with this, the Bray-Curtis (BC) dissimilarity of community B was highest compared to the other communities based on the family abundances. Community A, C, and D showed a lower BC dissimilarity to each other than to community B (**Figure 6C** and **Supplementary Table S16**), proving community B to be different.

Riboflavin measurement unraveled that all colonic communities A, B, C, and D after blank subtraction had negative Δ riboflavin concentrations indicating riboflavin uptake from the culture medium (**Figure 6D**, $n = 3$, mean ± sd, one-way ANOVA, raw data: **Supplementary Table S17** and **Supplementary Figure S10**). Of note, community B had the highest MAIT cell activating potential and used significantly less riboflavin than the communities A, C, and D (**Figure 6D**, $n = 3$, mean ± sd, GraphPad Prism, version: 8.3.0, one-way ANOVA, Tukey correction for multiple comparisons, P listed in **Supplementary Table S18**).

In Vitro MAIT Cell Activation Is Inversely Related to Microbial Diversity

Since a loss of microbial diversity and/or species richness in the intestine is associated with a variety of diseases (Mosca et al., 2016), we compared the MAIT cell response to microbial samples with different diversity. We used (i) diverse communities from cultivated human feces and swine colon content, (ii) the SIHUMIx model community composed of eight species, and (iii) the bacterial strain *E. coli*, a known MAIT cell activator. Microbial diversity was determined with two orthogonal methods: 16S rRNA gene analysis and microbial flow cytometry. For 16S rRNA gene analysis, the number of families were compared (**Figure 7A**, **Supplementary Figure 11**), whereas in microbial flow cytometry, the number of sub-populations in the corresponding cell gates were used to describe species richness (**Supplementary Figure S12**). Based on 16S rRNA sequencing, the fecal and the colonic communities both had the highest microbial diversity (number of families: 19 and 12, number of sub-populations: 21 and 31, respectively). The microbial diversity of SIHUMIx was significantly lower (number of families: 6, number of sub-populations: 19) and it was lowest for *E. coli* (number of families: 1, number of sub-populations: 5, representing different growth states, one-way ANOVA, $n = 3$, mean ± sd, P are listed in **Supplementary Table S19**). With regard to the MAIT cell activating potential, we observed the lowest potential to activate MAIT cells for the fecal and the colonic community (**Figures 7B,C**, $n = 3$, 5.4 and 2.8% $CD69^+/TNF^+$ MAIT cells, respectively). The SIHUMIx community had a slightly higher MAIT cell activating potential (8.0% $CD69^+/TNF^+$ MAIT cells), and *E. coli* showed the highest potential to activate MAIT

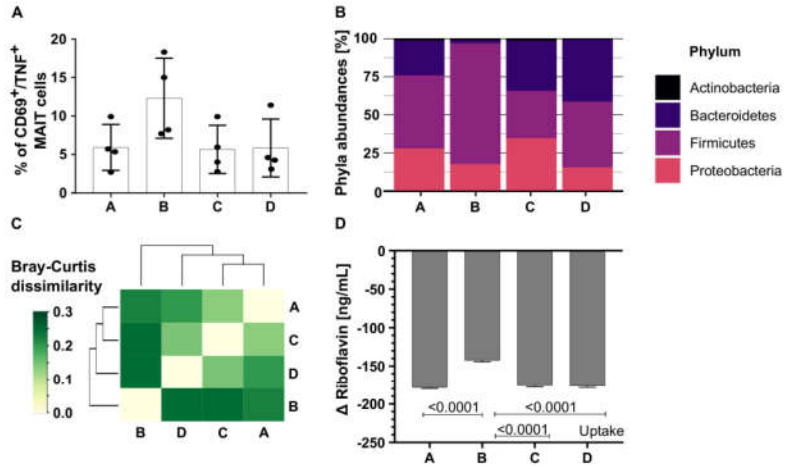

FIGURE 6 | The MAIT cell activating potential of diverse colonic microbiota. We cultivated four colonic communities in continuous bioreactors. **(A)** Bar plots quantify the percentage of $CD69^+/TNF^+$ activated MAIT cells after stimulation with the colonic communities A, B, C, and D (200 bacteria per cell). Bars represent mean ± sd, $n = 4$, ordinary one-way ANOVA, unpaired, *Tukey post hoc* test for multiple comparisons. **(B)** Phyla abundances of the colonic communities A, B, C, and D based on metaproteomics. **(C)** The matrix illustrates the Bray-Curtis dissimilarities between the communities A, B, C, and D. Dark green indicates high dissimilarity between community pairs, light green indicates low dissimilarity. **(D)** The riboflavin concentration was measured in the culture supernatant of all four colonic communities [ng/mL]. Bars represent mean ± sd, $n = 3$. Positive changes indicate riboflavin secretion, negative values indicate riboflavin uptake.

cells (25.57% $CD69^+/TNF^+$ MAIT cells), respectively (one-way ANOVA, $n = 3$, mean ± sd, P are listed in **Supplementary Table S20**). The addition of anti-MR1 antibody significantly blocked the activation of MAIT cells. This suggests MR1-mediated antigen presentation (**Supplementary Figure S13**).

The microbiota were cultivated in different culture media. Therefore, we compared the riboflavin utilization with the Δ riboflavin concentration relative to the medium (**Figure 7D**). A negative Δ riboflavin value indicated riboflavin uptake, whereby a positive Δ riboflavin value suggested riboflavin secretion. For the fecal, the colonic and the SIHUMIx community, riboflavin was taken up from the medium. However, the fecal and the colonic community took up more riboflavin than SIHUMIx and *E. coli* (**Figure 7E**, one-way ANOVA, $n = 3$, mean ± sd, P are listed in **Supplementary Table S21**). For *E. coli* we observed a positive Δ riboflavin concentration, suggesting riboflavin biosynthesis and secretion. The riboflavin utilization of *E. coli* and SIHUMIx were similar but differed from the fecal and the colonic community. We observed that the riboflavin demand increased with microbial diversity.

DISCUSSION

In physiological context, MAIT cells probably interact with diverse microbiota, but the interaction of MAIT cells and diverse microbiota is still unexamined. Therefore, we have analyzed the response of MAIT cells to microbial communities. We used the extended simplified human microbiota (SIHUMIx) model community to investigate the contribution of individual community members to MAIT cell activation and investigated the MAIT cell response to diverse microbiota. Moreover, we analyzed whether acute microbial stress can indirectly affect MAIT cell activation.

MAIT cells recognize activating riboflavin metabolites and to a lower extent inhibitory folate metabolites after presentation on MR1. Thus, we speculated that riboflavin as well as folate concentrations secreted by individual bacteria strains might indicate the MAIT cell activating potential of the bacteria. The SIHUMIx bacteria cover the phyla *Bacteroides* (*B. thetaiotaomicron*), *Proteobacteria* (*E. coli*), *Actinobacteria* (*B. longum*), and *Firmicutes* (*A. caccae, B. producta, C. butyricum, C. ramosum*, and *L. plantarum*), for which has recently been shown that they activate MAIT cells in decreasing order (Tastan et al., 2018). In line with their results, *B. thetaiotaomicron* had the highest MAIT cell activating potential and at the same time secreted the highest amount of riboflavin into the medium. *E. coli* showed an intermediate and *L. plantarum* a low MAIT cell activating potential with simultaneously decreasing riboflavin secretion. For these MAIT cell activating bacterial strains, metaproteome data (proteome analysis and UniProt database) as well as genome data (KEGG database) proved the ability to synthesize riboflavin and thus the possible existence of MAIT cell activating metabolites (**Figure 2** and **Supplementary Table S11**). On contrary, all strains unable to activate MAIT cells did not possess the full riboflavin biosynthesis pathway. The

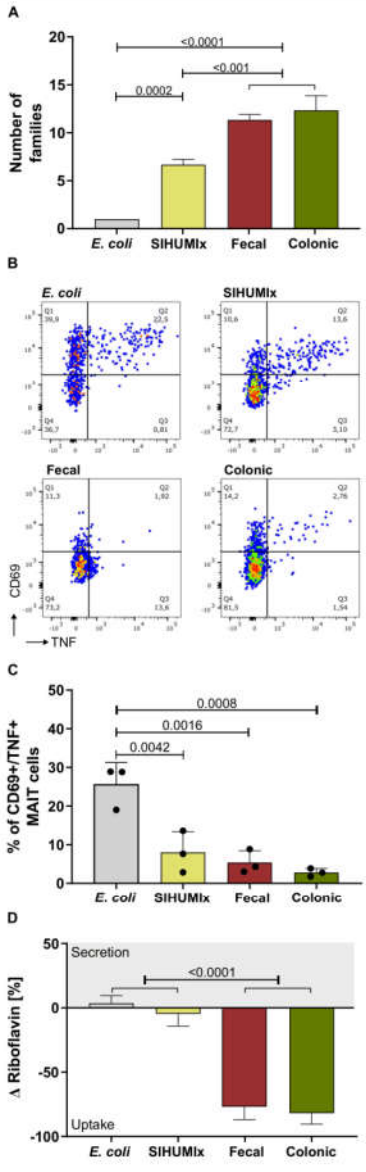

FIGURE 7 | Comparing the MAIT cell activating potential with regard to microbial diversity. **(A)** We quantified microbial diversity by metaproteomics and therefore evaluated the number of families in human fecal communities, *(Continued)*

FIGURE 7 | Continued
swine colonic communities, the SIHUMIx community and *E. coli*. **(B)** The exemplary dot plots show the percentage of $CD69^+/TNF^+$ activated MAIT cells after stimulation with fecal, colonic, SIHUMIx communities and *E. coli*. 200 bacteria per cell (BpC). **(C)** The bar plots quantify the percentage of $CD69^+/TNF^+$ activated MAIT cells after stimulation with fecal, colonic and SIHUMIx communities, and *E. coli*. Bars represent mean ± sd, $n = 3$, ordinary one-way ANOVA, Tukey *post hoc* test for multiple comparisons. **(D)** The riboflavin concentration was measured in the culture supernatant after microbiota cultivation [ng/mL]. Bars represent mean ± sd ($n = 3$). Positive changes indicate riboflavin secretion, negative values indicate riboflavin uptake.

enzyme RibD/G (EC: 3.5.4.26/1.1.1.193) was reported in the two non-activating SIHUMIx strains *A. caccae* and *C. butyricum*. This enzyme has been identified as key enzyme for the synthesis of 5-A-RU (Kjer-Nielsen et al., 2018), however, pryp2 (EC: 3.1.3.104) is essential to perform the last enzymatic transformation toward 5-A-RU and is missing in the SIHUMIx strains *A. caccae* and *C. butyricum*.

A minority of MAIT cells can recognize folate metabolites (Gherardin et al., 2016), which are MAIT cell inhibitors *in vitro* (Kjer-Nielsen et al., 2012; Corbett et al., 2014). On contrary, the majority of TRAV1-2^+ MAIT cells recognizes riboflavin metabolites via their TCR. Nevertheless, the activating riboflavin and the inhibitory folate metabolites compete for the MR1 binding site thereby impacting on MAIT cell activation independent of the TCR repertoire. *In vitro* studies show that the most potent inhibitory folate metabolite, Ac-6-FP, must exceed the molar concentration of 5-OP-RU, the strongest MAIT cell activator from the riboflavin pathway, by 10^6 to inhibit the activating effect of 5-OP-RU (Corbett et al., 2014; Eckle et al., 2015). The folate concentration exceeded the riboflavin concentration in all the bacterial single strains from the SIHUMIx community. To determine the contribution of individual community members to the MAIT cell activating potential of a community, we stimulated MAIT cells with a SIHUMIx 1:1: mix. This SIHUMIx 1:1 mix contained all strains in equivalent numbers. We observed that the MAIT cell activating potential of the artificial SIHUMIx 1:1 mix equals the mean MAIT cell activating potential of the individual community members. Moreover, the folate/riboflavin ratio did not correlate with the MAIT cell activating potential of the SIHUMIx single strains (**Supplementary Figure S3**). It remains to be elucidated whether bacteria do not produce the inhibitory folate photo-degradation product 6-FP in culture e.g., due to darkness or whether 6-FP plays a minor role in MAIT cell activation. Indeed, we and others suppose a direct association between MAIT cell activation and riboflavin secretion on the single strain level at least under unimpeded conditions (Tastan et al., 2018).

Intestinal bacteria supply the host with a variety of B-vitamins and cross-feed nutrients with other species in the gut (LeBlanc et al., 2013; Magnusdottir et al., 2015; Rodionov et al., 2019). Genome analysis (2,228 genomes) unraveled that all bacteria from the phyla *Bacteroides* and *Proteobacteria* were prototrophic for riboflavin (Rodionov et al., 2019). Besides, bacteria from these phyla invariably were shown to activate MAIT cells in

our study and others (Tastan et al., 2018). 60% of all *Firmicutes* and *Actinobacteria* in the study of Rodionov et al. (2019) were unable to synthesize riboflavin and should therefore be unable to activate MAIT cells, which is in line with our data. Nevertheless, riboflavin is essential for all organisms to synthesize flavin mononucleotide (FMN) and flavin adenine dinucleotide (FAD) and thus has to be taken up (Gutiérrez-Preciado et al., 2015; García-Angulo, 2017). Accordingly, the reduced riboflavin concentration in the culture supernatant of the non-MAIT cell activating bacterial strains *A. caccae, B. longum, B. producta, C. butyricum*, and *C. ramosum* suggests riboflavin uptake and thereby riboflavin auxotrophy. We show that the non-activating SIHUMIx strains lack the riboflavin biosynthesis pathway completely or in parts and in parallel possess the enzymatic equipment for riboflavin uptake and conversion to FAD and FMN. Riboflavin biosynthesis is strongly dependent on extracellular riboflavin and the individual demand of microbial species (Gutiérrez-Preciado et al., 2015). Furthermore, extracellular riboflavin favors riboflavin import and in parallel inhibits riboflavin biosynthesis (García-Angulo, 2017), which presumably bypasses the synthesis of MAIT cell activating metabolites. We suggest that the MAIT cell activating potential of individual species, but also microbial communities, depends on the availability of riboflavin in the culture medium and on the culture conditions, which together determine the need for riboflavin biosynthesis. In support of this, culture conditions have recently been identified to alter the MAIT cell activating potential of *E. coli* (Schmaler et al., 2018).

Opposed to the situation in single strains, all microbial communities (fecal, colonic, SIHUMIx) cultivated in our study removed riboflavin from the culture medium and still had the potential to activate MAIT cells. However, the MAIT cell activating potential decreased with increasing community diversity. Especially in symbiotic or commensal interactions, like those found in the intestine, secretion of metabolites such as riboflavin are important for symbiosis establishment, maintenance and microbial cross-feeding (LeBlanc et al., 2013; Rowland et al., 2018; Rodionov et al., 2019). Within communities, the expression of enzymes from the riboflavin biosynthesis pathway (FMN riboswitch) is regulated in various ways. E.g., riboflavin can suppress the expression of genes coding for riboflavin biosynthesis enzymes to maintain an energy efficient riboflavin biosynthesis. It is suggested, that the majority of riboflavin is used by bacteria that do not actively produce the vitamin (Gutiérrez-Preciado et al., 2015; Rowland et al., 2018). Thus, in diverse communities, we suggest that some prototrophic bacteria supply riboflavin and possess MAIT cell activating metabolites, whereas many other bacteria take up riboflavin and do not produce MAIT cell activating metabolites.

To investigate if microbial stress can affect the MAIT cell activation downstream, we exposed the model community SIHUMIx to an acute acid stress. One major advantage of the SIHUMIx model community is the reproducible development and quick adaptation to the bioreactor system (Krause et al., 2020). During the adaptation phase to the bioreactor system, the Δ riboflavin concentration leveled around zero, which suggests an even riboflavin balance and accounts for riboflavin cross-feeding in an energy efficient manner (LeBlanc et al., 2013; Magnusdottir et al., 2015). Under acute acid stress, the SIHUMIx community lost its MAIT cell activating potential. However, we did not observe changes in community composition, but the communities' riboflavin demand increased. Adaptation to stress shifts energy and nutrient flows, since microbial function or survival are threatened. Shifting from growth to survival-related metabolism sustains survival under acute stress, whereas changes in community composition are thought to occur as a response to long-term stress (Schimel et al., 2007). In *E. coli* flavoenzymes are involved in a variety of processes, e.g., oxidative stress response, which is directly associated with acid stress and presumably survival-related metabolism (Maurer et al., 2005; García-Angulo, 2017). FMN and FAD are used for the synthesis of flavoenzymes, which make up to 2% of coded genes (Gutiérrez-Preciado et al., 2015). The SIHUMIx strains possess riboflavin transporter and enzymes for riboflavin conversion to flavin cofactors (FMN and FAD), irrespective of their ability to synthesize riboflavin themselves (**Supplementary Table S11**). We propose that acid stress non-specifically affected the SIHUMIx community and stimulated riboflavin uptake for the synthesis of flavoenzymes in order to survive. Furthermore, we assume that the prototrophic SIHUMIx strains (*B. thetaiotaomicron, E. coli*, and *L. plantarum*) directly utilized their MAIT cell activating metabolites for riboflavin synthesis or completely stopped riboflavin biosynthesis in order to use GTP for survival. Either way, the prototrophic strains lose their MAIT cell activating potential during the stress response. The exact mechanism of riboflavin biosynthesis under stress should be investigated in the future. In addition, the riboflavin auxotrophic bacterial strains had an elevated demand for riboflavin and thus increased riboflavin uptake from the medium to synthesize flavoenzymes, which became visible in the decreased riboflavin concentration. After the acute acid stress ended, the MAIT cell activating potential of SIHUMIx as well as the riboflavin concentration recovered. Since the availability of riboflavin precursors was affected under acute acid stress, we hypothesize that riboflavin can serve as a microbial stress sensor, which mediates microbial stress to MAIT cells at least under acute stress conditions. IBD patients indeed can have a low colonic pH (Nugent et al., 2001), but here blood MAIT cells were chronically activated (Serriari et al., 2014). In contrast to IBD, in the bioreactors we introduced an acute stress for 24 h, whereas in IBD the gut is chronically inflamed.

With regard to diverse microbial communities, we observed that the most potent colonic community with regard to MAIT cell activation at the same time had the lowest riboflavin demand. In this community, the phylum *Firmicutes* dominated with ∼80% phyla abundance over the other phyla. In conflict with our result, Tastan et al. designated bacteria from the phylum *Firmicutes* low or no MAIT cell stimulators (Tastan et al., 2018). However, genome analysis predicted a functional riboflavin biosynthesis pathway to ∼50% of analyzed *Firmicutes*, indicating at least a 50% potential to activate MAIT cells (Gutiérrez-Preciado et al., 2015; Magnusdottir et al., 2015; Rodionov et al., 2019). Taxonomic analysis alone was insufficient to estimate the MAIT cell activating potential of the communities. However, concluding

from our results riboflavin utilization seems to be a good approximation for the MAIT cell activating potential of microbial communities *in vitro*.

Especially the MAIT cell activating potential of bacterial single strains is directly related to the riboflavin secretion. Our data indicate that the MAIT cell activating potential of microbial communities on the one hand correlated with the riboflavin demand and on the other hand with microbial diversity. A high microbial diversity was associated with a higher demand of riboflavin combined with a low MAIT cell activating potential. Furthermore, we show that acute microbial stress can indirectly affect the MAIT cell activation downstream *in vitro* via riboflavin metabolism. Therefore, we hypothesize that microbial stress can be mediated to MAIT cells via riboflavin utilization.

DATA AVAILABILITY STATEMENT

The raw data supporting the conclusions of this article will be made available by the authors, without undue reservation, to any qualified researcher.

AUTHOR CONTRIBUTIONS STATEMENT

JK and GH conceptualized the study. JK cultivated the bacteria in bioreactors, wrote the manuscript's first draft, prepared the single strain bacteria and performed the immunologic experiments and prepared the samples for microbial flow cytometry. UR-K was responsible for riboflavin analysis. GH and GA contributed to the folate analysis. SS accomplished metaproteome analysis and together with NJ analyzed the data. FS performed flow cytometric measurement of all microbial samples and together with SM evaluated the data. GH, AP, SM, and MB provided helpful discussions and revised the manuscript.

ACKNOWLEDGMENTS

We thank Jeremy Knespel and Nicole Gröger for technical assistance and Martina Kolbe for the supply with complex intestinal medium. Furthermore, we thank the German Federal Environmental Foundation for financial support of Jannike Lea Krause. Stephanie Serena Schäpe is grateful for support from a DFG-grant within the Priority Program 1656, and Martin von Bergen acknowledges partial funding by DFG Priority Program 2002.

SUPPLEMENTARY MATERIAL

The Supplementary Material for this article can be found online at: https://www.frontiersin.org/articles/10.3389/fmicb.2020.00755/full#supplementary-material

REFERENCES

Becker, N., Kunath, J., Loh, G., and Blaut, M. (2011). Human intestinal microbiota: characterization of a simplified and stable gnotobiotic rat model. *Gut Microbes* 2, 25–33. doi: 10.4161/gmic.2.1.14651

Belkaid, Y., and Harrison, O. J. (2017). Homeostatic immunity and the microbiota. *Immunity* 46, 562–576. doi: 10.1016/j.immuni.2017.04.008

Berkson, J. D., and Prlic, M. (2017). The MAIT conundrum – how human MAIT cells distinguish bacterial colonization from infection in mucosal barrier tissues. *Immunol. Lett.* 192, 7–11. doi: 10.1016/j.imlet.2017.09.013

Brestoff, J. R., and Artis, D. (2013). Commensal bacteria at the interface of host metabolism and the immune system. *Nat. Immunol.* 14, 676–684. doi: 10.1038/ni.2640

Chiba, A., Murayama, G., and Miyake, S. (2018). Mucosal-Associated invariant T cells in autoimmune diseases. *Front. Immunol.* 9:1333. doi: 10.3389/fimmu.2018.01333

Corbett, A. J., Eckle, S. B. G., Birkinshaw, R. W., Liu, L., Patel, O., Mahony, J., et al. (2014). T-cell activation by transitory neo-antigens derived from distinct microbial pathways. *Nature* 509, 361–365. doi: 10.1038/nature13160

Dias, J., Leeansyah, E., and Sandberg, J. K. (2017). Multiple layers of heterogeneity and subset diversity in human MAIT cell responses to distinct microorganisms and to innate cytokines. *Proc. Natl. Acad. f Sci. U.S.A.* 114, E5434–E5443. doi: 10.1073/pnas.1705759114

Dixon, P. (2003). VEGAN, a package of R functions for community ecology. *J. Veg. Sci.* 14, 927–930. doi: 10.1111/j.1654-1103.2003.tb02228.x

Dusseaux, M., Martin, E., Serriari, N., Peguillet, I., Premel, V., Louis, D., et al. (2011). Human MAIT cells are xenobiotic-resistant, tissue-targeted, CD161hi IL-17-secreting T cells. *Blood* 117, 1250–1259. doi: 10.1182/blood-2010-08-303339

Eckle, S. B. G., Corbett, A. J., Keller, A. N., Chen, Z., Godfrey, D. I., Liu, L., et al. (2015). Recognition of Vitamin B precursors and byproducts by mucosal associated invariant T cells. *J. Biol. Chem.* 290, 30204–30211. doi: 10.1074/jbc.R115.685990

Forbes, J. D., Van Domselaar, G., and Bernstein, C. N. (2016). The gut microbiota in immune-mediated inflammatory diseases. *Front. Microbiol.* 7:1081. doi: 10.3389/fmicb.2016.01081

García-Angulo, V. A. (2017). Overlapping riboflavin supply pathways in bacteria. *Crit. Rev. Microbiol.* 43, 196–209. doi: 10.1080/1040841X.2016.1192578

Gherardin, N. A., Keller, A. N., Woolley, R. E., Le Nours, J., Ritchie, D. S., Neeson, P. J., et al. (2016). Diversity of T cells restricted by the MHC class I-related molecule MR1 facilitates differential antigen recognition. *Immunity* 44, 32–45. doi: 10.1016/j.immuni.2015.12.005

Gibbs, A., Leeansyah, E., Introini, A., Paquin-Proulx, D., Hasselrot, K., Andersson, E., et al. (2017). MAIT cells reside in the female genital mucosa and are biased towards IL-17 and IL-22 production in response to bacterial stimulation. *Mucosal Immunol.* 10, 35–45. doi: 10.1038/mi.2016.30

Goodrich, J. K., Davenport, E. R., Beaumont, M., Jackson, M. A., Knight, R., Ober, C., et al. (2016). Genetic determinants of the gut microbiome in UK twins. *Cell Host Microbe* 19, 731–743. doi: 10.1016/j.chom.2016.04.017

Gutiérrez-Preciado, A., Torres, A. G., Merino, E., Bonomi, H. R., Goldbaum, F. A., and García-Angulo, V. A. (2015). Extensive identification of bacterial riboflavin transporters and their distribution across bacterial species. *PLoS One* 10:e0126124. doi: 10.1371/journal.pone.0126124

Haange, S.-B., Jehmlich, N., Hoffmann, M., Weber, K., Lehmann, J., von Bergen, M., et al. (2019). Disease development is accompanied by changes in bacterial protein abundance and functions in a refined model of dextran sulfate sodium (DSS)-induced colitis. *J. f Proteome Res.* 18, 1774–1786. doi: 10.1021/acs.jproteome.8b00974

Hinks, T. S. C. (2016). Mucosal-associated invariant T cells in autoimmunity, immune-mediated diseases and airways disease. *Immunology* 148, 1–12. doi: 10.1111/imm.12582

Käll, L., Canterbury, J. D., Weston, J., Noble, W. S., and MacCoss, M. J. (2007). Semi-supervised learning for peptide identification from shotgun proteomics datasets. *Nat. Methods* 4, 923–925. doi: 10.1038/nmeth1113

Kjer-Nielsen, L., Corbett, A. J., Chen, Z., Liu, L., Mak, J. Y., Godfrey, D. I., et al. (2018). An overview on the identification of MAIT cell antigens. *Immunol. Cell Biol.* 96, 573–587. doi: 10.1111/imcb.12057

Kjer-Nielsen, L., Patel, O., Corbett, A. J., Le Nours, J., Meehan, B., Liu, L., et al. (2012). MR1 presents microbial vitamin B metabolites to MAIT cells. *Nature* 491, 717–723. doi: 10.1038/nature11605

Koch, C., Günther, S., Desta, A. F., Hübschmann, T., and Müller, S. (2013). Cytometric fingerprinting for analyzing microbial intracommunity structure variation and identifying subcommunity function. *Nat. Protoc.* 8, 190–202. doi: 10.1038/nprot.2012.149

Krause, J. L., Schaepe, S. S., Fritz-Wallace, K., Engelmann, B., Rolle-Kampczyk, U., Kleinsteuber, S., et al. (2020). Following the community development of SIHUMIx – a new intestinal *in vitro* model for bioreactor use. *Gut Microbes* 1–14. doi: 10.1080/19490976.2019.1702431

Kurioka, A., Ussher, J. E., Cosgrove, C., Clough, C., Fergusson, J. R., Smith, K., et al. (2015). MAIT cells are licensed through granzyme exchange to kill bacterially sensitized targets. *Mucosal Immunol.* 8, 429–440. doi: 10.1038/mi.2014.81

Le Bourhis, L., Dusseaux, M., Bohineust, A., Bessoles, S., Martin, E., Premel, V., et al. (2013). MAIT cells detect and efficiently lyse bacterially-infected epithelial cells. *PLoS Pathog.* 9:e1003681. doi: 10.1371/journal.ppat.1003681

LeBlanc, J. G., Milani, C., de Giori, G. S., Sesma, F., van Sinderen, D., and Ventura, M. (2013). Bacteria as vitamin suppliers to their host: a gut microbiota perspective. *Curr. Opin. Biotechnol.* 24, 160–168. doi: 10.1016/j.copbio.2012.08.005

Levy, M., Blacher, E., and Elinav, E. (2017). Microbiome, metabolites and host immunity. *Curr. Opin. Microbiol.* 35, 8–15. doi: 10.1016/j.mib.2016.10.003

Magalhaes, I., Pingris, K., Poitou, C., Bessoles, S., Venteclef, N., Kiaf, B., et al. (2015). Mucosal-associated invariant T cell alterations in obese and type 2 diabetic patients. *J. Clin. Invest.* 125, 1752–1762. doi: 10.1172/JCI78941

Magnusdottir, S., Ravcheev, D., de Crécy-Lagard, V., and Thiele, I. (2015). Systematic genome assessment of B-vitamin biosynthesis suggests co-operation among gut microbes. *Front. Genet.* 6:148. doi: 10.3389/fgene.2015.00148

Martin, E., Treiner, E., Duban, L., Guerri, L., Laude, H., Toly, C., et al. (2009). Stepwise development of MAIT cells in mouse and human. *PLoS Biol.* 7:e1000054. doi: 10.1371/journal.pbio.1000054

Maurer, L. M., Yohannes, E., Bondurant, S. S., Radmacher, M., and Slonczewski, J. L. (2005). pH regulates genes for flagellar motility, catabolism, and oxidative stress in *Escherichia coli* K-12. *J. Bacteriol.* 187, 304–319. doi: 10.1128/JB.187.1.304-319.2005

McDonald, J. A. K., Fuentes, S., Schroeter, K., Heikamp-deJong, I., Khursigara, C. M., de Vos, W. M., et al. (2015). Simulating distal gut mucosal and luminal communities using packed-column biofilm reactors and an in vitro chemostat model. *J. Microbiol. Methods* 108, 36–44. doi: 10.1016/j.mimet.2014.11.007

Moco, S., Candela, M., Chuang, E., Draper, C., Cominetti, O., Montoliu, I., et al. (2014). Systems biology approaches for inflammatory bowel disease: emphasis on gut microbial metabolism. *Inflamm. Bowel Dis.* 20, 2104–2114. doi: 10.1097/MIB.0000000000000116

Mosca, A., Leclerc, M., and Hugot, J. P. (2016). Gut microbiota diversity and human diseases: should we reintroduce key predators in our ecosystem? *Front. Microbiol.* 7:455. doi: 10.3389/fmicb.2016.00455

Nugent, S. G., Kumar, D., Rampton, D. S., and Evans, D. F. (2001). Intestinal luminal pH in inflammatory bowel disease: possible determinants and implications for therapy with aminosalicylates and other drugs. *Gut* 48, 571–577. doi: 10.1136/gut.48.4.571

Rodionov, D. A., Arzamasov, A. A., Khoroshkin, M. S., Iablokov, S. N., Leyn, S. A., Peterson, S. N., et al. (2019). Micronutrient requirements and sharing capabilities of the human gut microbiome. *Front. Microbiol.* 10:1316. doi: 10.3389/fmicb.2019.01316

Rowland, I., Gibson, G., Heinken, A., Scott, K., Swann, J., Thiele, I., et al. (2018). Gut microbiota functions: metabolism of nutrients and other food components. *Eur. J. Nutr.* 57, 1–24. doi: 10.1007/s00394-017-1445-8

Schäpe, S. S., Krause, J. L., Engelmann, B., Fritz-Wallace, K., Schattenberg, F., Liu, Z., et al. (2019). The simplified human intestinal microbiota (SIHUMIx) shows high structural and functional resistance against changing transit times in in vitro bioreactors. *Microorganisms* 7:641. doi: 10.3390/microorganisms7120641

Schimel, J., Balser, T. C., and Wallenstein, M. (2007). Microbial stress-response physiology and its implications for ecosystem function. *Ecology* 88, 1386–1394. doi: 10.1890/06-0219

Schmaler, M., Colone, A., Spagnuolo, J., Zimmermann, M., Lepore, M., Kalinichenko, A., et al. (2018). Modulation of bacterial metabolism by the microenvironment controls MAIT cell stimulation. *Mucosal Immunol.* 11, 1060–1070. doi: 10.1038/s41385-018-0020-9

Sender, R., Fuchs, S., and Milo, R. (2016). Revised estimates for the number of human and bacteria cells in the body. *PLoS Biol.* 14:e1002533. doi: 10.1371/journal.pbio.1002533

Serriari, N.-E., Eoche, M., Lamotte, L., Lion, J., Fumery, M., Marcelo, P., et al. (2014). Innate mucosal-associated invariant T (MAIT) cells are activated in inflammatory bowel diseases: MAIT cells in IBD. *Clin. Exp. Immunol.* 176, 266–274. doi: 10.1111/cei.12277

Soudais, C., Samassa, F., Sarkis, M., Le Bourhis, L., Bessoles, S., Blanot, D., et al. (2015). In Vitro and In Vivo analysis of the gram-negative bacteria–derived riboflavin precursor derivatives activating mouse MAIT cells. *J. Immunol.* 194, 4641–4649. doi: 10.4049/jimmunol.1403224

Starke, R., Kermer, R., Ullmann-Zeunert, L., Baldwin, I. T., Seifert, J., Bastida, F., et al. (2016). Bacteria dominate the short-term assimilation of plant-derived N in soil. *Soil Biol. Biochem.* 96, 30–38. doi: 10.1016/j.soilbio.2016.01.009

Tanner, S. A., Zihler Berner, A., Rigozzi, E., Grattepanche, F., Chassard, C., and Lacroix, C. (2014). In Vitro continuous fermentation model (PolyFermS) of the swine proximal colon for simultaneous testing on the same gut microbiota. *PLoS One* 9:e94123. doi: 10.1371/journal.pone.0094123

Tastan, C., Karhan, E., Zhou, W., Fleming, E., Voigt, A. Y., Yao, X., et al. (2018). Tuning of human MAIT cell activation by commensal bacteria species and MR1-dependent T-cell presentation. *Mucosal Immunol.* 11, 1591–1605. doi: 10.1038/s41385-018-0072-x

Teunissen, M. B. M., Yeremenko, N. G., Baeten, D. L. P., Chielie, S., Spuls, P. I., de Rie, M. A., et al. (2014). The IL-17A-Producing CD8 + T-Cell population in psoriatic lesional skin comprises mucosa-associated invariant T cells and conventional T cells. *J. Investig. Dermatol.* 134, 2898–2907. doi: 10.1038/jid.2014.261

Thaiss, C. A., Zmora, N., Levy, M., and Elinav, E. (2016). The microbiome and innate immunity. *Nature* 535, 65–74. doi: 10.1038/nature18847

Tilloy, F., Treiner, E., Park, S.-H., Garcia, C., Lemonnier, F., de la Salle, H., et al. (1999). An invariant T cell receptor α chain defines a novel TAP-independent major histocompatibility complex class Ib–restricted α/β T cell subpopulation in mammals. *J. Exp. Med.* 189, 1907–1921. doi: 10.1084/jem.189.12.1907

Treiner, E., Duban, L., Bahram, S., Radosavljevic, M., Wanner, V., Tilloy, F., et al. (2003). Selection of evolutionarily conserved mucosal-associated invariant T cells by MR1. *Nature* 422, 164–169. doi: 10.1038/nature01433

Ussher, J. E., Bilton, M., Attwod, E., Shadwell, J., Richardson, R., de Lara, C., et al. (2014). CD161 ++ CD8 + T cells, including the MAIT cell subset, are specifically activated by IL-12+IL-18 in a TCR-independent manner: innate immunity. *Eur. J. Immunol.* 44, 195–203. doi: 10.1002/eji.201343509

van Wilgenburg, B., Scherwitzl, I., Hutchinson, E. C., Leng, T., Kurioka, A., Kulicke, C., et al. (2016). MAIT cells are activated during human viral infections. *Nat. Commun.* 7:11653. doi: 10.1038/ncomms11653

Wilfart, A., Montagne, L., Simmins, H., Noblet, J., and van Milgen, J. (2007). Digesta transit in different segments of the gastrointestinal tract of pigs as affected by insoluble fibre supplied by wheat bran. *Br. J. Nutr.* 98, 54–62. doi: 10.1017/S0007114507682981

Conflict of Interest: GA was employed by Alphaomega laboratory.

The remaining authors declare that the research was conducted in the absence of any commercial or financial relationships that could be construed as a potential conflict of interest.

Publication 4: Mucosal-associated invariant T-Cell (MAIT) activation is altered by chlorpyrifos- and glyphosate-treated commensal gut bacteria

JOURNAL OF IMMUNOTOXICOLOGY
2020, VOL. 17, NO. 1, 10–20
https://doi.org/10.1080/1547691X.2019.1706672

Taylor & Francis
Taylor & Francis Group

RESEARCH ARTICLE

OPEN ACCESS Check for updates

Mucosal-associated invariant T-Cell (MAIT) activation is altered by chlorpyrifos- and glyphosate-treated commensal gut bacteria

Anne Mendler[a], Florian Geier[a], Sven-Bastiaan Haange[b], Arkadiusz Pierzchalski[a], Jannike Lea Krause[a], Ivonne Nijenhuis[c], Jean Froment[b], Nico Jehmlich[b], Urs Berger[d], Grit Ackermann[e], Ulrike Rolle-Kampczyk[b], Martin von Bergen[b,f] and Gunda Herberth[a]

[a]Department of Environmental Immunology, Helmholtz Centre for Environmental Research Leipzig – UFZ, Leipzig, Germany; [b]Department of Molecular Systems Biology, Helmholtz Centre for Environmental Research Leipzig – UFZ, Leipzig, Germany; [c]Department of Isotope Biogeochemistry, Helmholtz Centre for Environmental Research Leipzig – UFZ, Leipzig, Germany; [d]Department of Analytical Chemistry, Helmholtz Centre for Environmental Research Leipzig – UFZ, Leipzig, Germany; [e]Alphaomega laboratory, Delitzsch, Germany; [f]Institute of Biochemistry, University of Leipzig, Leipzig, Germany

ABSTRACT

Mucosal-associated invariant T-cells (MAIT) can react to metabolites of the vitamins riboflavin and folate which are produced by the human gut microbiota. Since several studies showed that the pesticide chlorpyrifos (CPF) and glyphosate (GLP) can impair the gut microbiota, the present study was undertaken to investigate the impact of CPF and GLP treatment on the metabolism of gut microbiota and the resulting bacteria-mediated modulation of MAIT cell activity. Here, *Bifidobacterium adolescentis* (*B. adolescentis*), *Lactobacillus reuteri* (*L. reuteri*), and *Escherichia coli* (*E. coli*) were treated with CPF (50–200 µM) or GLP (75–300 mg/L) and then used in MAIT cell stimulation assays as well as in vitamin and proteome analyses. All three bacteria were nonpathogenic and chosen as representatives of a healthy human gut microflora. The results showed that *E. coli* activated MAIT cells whereas *B. adolescentis* and *L. reuteri* inhibited MAIT cell activation. CPF treatment significantly increased *E. coli*-mediated MAIT cell activation. Treatment of *B. adolescentis* and *L. reuteri* with CPF and GLP weakened the inhibition of MAIT cell activation. Riboflavin and folate production by the test bacteria was influenced by CPF treatment, whereas GLP had only minor effects. Proteomic analysis of CPF-treated *E. coli* revealed changes in the riboflavin and folate biosynthesis pathways. The findings here suggest that the metabolism of the analyzed bacteria could be altered by exposure to CPF and GLP, leading to an increased pro-inflammatory immune response.

ARTICLE HISTORY
Received 30 September 2019
Revised 27 November 2019
Accepted 16 December 2019

KEYWORDS
MAIT cells; gut microbiota; pesticides; glyphosate; chlorpyrifos

Introduction

Commensal bacteria in the human gut provide important functions for the host including protection against pathogens, nutrient digestion, production of metabolites as well as the modulation of host immune responses (Sekirov et al. 2010). Furthermore, microbiota of the gut have also been recognized as a source of vitamins which cannot be synthesized by the human body. Amongst these, riboflavin and folate (Vitamins B_2 and B_9) have been shown to be produced by probiotic bacteria in the human gut, as well as by food-associated lactic acid bacteria (Hill 1997; Pompei et al. 2007; LeBlanc, et al. 2011, 2013). For example, *Bifidobacterium adolescentis* (*B. adolescentis*), *Lactobacillus reuteri* (*L. reuteri*), and *Escherichia coli* (*E. coli*) have each been shown to contribute to folate production (Santos et al. 2008; LeBlanc et al. 2011; Rossi et al. 2011; Thiaville et al. 2016). This vitamin is implicated in DNA replication, repair, and methylation, as well as in amino acid biosynthesis (LeBlanc et al. 2013). Besides folate, riboflavin production has been described in a number of strains of *L. reuteri* and *E. coli* (Fischer et al. 1996; Wang et al. 2015; Thakur et al. 2016). Riboflavin is essential as it is the precursor of the co-enzymes flavin mononucleotide and flavin adenine dinucleotide – both of which are both involved in redox reactions (LeBlanc et al. 2013).

Recent studies have shown that metabolites of riboflavin and folate can regulate the activity of a novel innate-like T cell subtype, the mucosal-associated invariant T (MAIT)-cells. The latter is a T-cell type that is highly abundant in human blood and mucosal tissues like the liver and gut (Kjer-Nielsen et al. 2012; Reantragoon et al. 2013). MAIT cells are characterized by a semi-invariant T-cell receptor (TCR) (Vα7.2 in humans) restricted to a non-classical MHC Class I-related (MR1) molecule and by expression of CD161 (Reantragoon et al. 2013). Precursors of bacterial riboflavin biosynthesis can activate MAIT cells. In contrast, folate metabolites inhibit MAIT cell activity by covalently binding to MR1, thereby blocking cell activation by riboflavin precursors (Eckle et al. 2014; Kjer-Nielsen et al. 2018). After activation, MAIT cells produce pro-inflammatory cytokines (i.e. tumor necrosis factor [TNF]-α and interferon [IFN]-γ) and cytolytic proteins (i.e. perforin and granzyme B) (Chiba et al. 2018; Rudak et al. 2018).

CONTACT Gunda Herberth gunda.herberth@ufz.de Department of Environmental Immunology, Helmholtz Centre for Environmental Research – UFZ, Permoserstraße 15, Leipzig 04318, Germany

Supplemental data for this article can be accessed here.

An imbalance between activating and inhibiting metabolites may impact the function of MAIT cells. This in turn could lead to chronic activation of these cells and as a consequence, to increased production of inflammatory cytokines. Indeed, MAIT cells have been found in the inflamed tissues of patients with Crohn's disease, multiple sclerosis, rheumatoid arthritis and asthma (Serriari et al. 2014; Carolan et al. 2015; Chiba et al. 2018; Lezmi and Leite-de-Moraes 2018). Likewise, a disturbance of the gut microbiota (dysbiosis) is involved in the same pathologies (Serriari et al. 2014). This leads to the assumption that bacterial homeostasis is linked to immune homeostasis, and although not exclusively, it might be reflected by a modulation in MAIT cell activity.

Environmental contaminants, including pesticides that can reach the human gut via food ingestion might potentially impact on gut homeostasis. Chlorpyrifos (CPF) is one of the most frequently used broad-spectrum insecticides. It is used to control a multitude of insects during the cultivation of grains, cotton, vegetable crops, lawns, and ornamental plants (Thengodkar and Sivakami 2010) and is also used in some instances in veterinary medicine (Marquez Giron et al. 2017). It was recently shown that CPF causes gut microbiota dysbiosis in mice, rats and zebrafish (Zhao et al. 2016; Fang et al. 2018; Wang et al. 2019). Glyphosate (GLP) is a commonly used broad-spectrum herbicide that is applied globally for weed control (Green 2018; van Bruggen et al. 2018). GLP and the GLP-based herbicide Roundup were shown to be able to perturb the gut microbiota of honey bees, mice, and rats (Aitbali et al. 2018; Mao et al. 2018; Motta et al. 2018); however, other studies have shown no effect (Nielsen et al. 2018). There is still an ongoing debate about the effects of glyphosate on the microbiota. Due to this combination of frequent usage and possible effects on microbiota, the present study was undertaken to investigate the potential impact of the pesticides CPF and GLP on select commensal bacteria.

Recently, it was shown that the microenvironment can impact the bacterial metabolism leading to a modification of MAIT cell activation (Schmaler et al. 2018). Thus, the hypothesis here was that pesticide-induced changes in bacterial metabolism might alter the riboflavin and/or folate production by these microorganisms, thereby impacting the activation of MAIT cells. In the current study, the bacterial strains *L. reuteri*, *B. adolescentis* and *E. coli* were investigated as their health-promoting effects are well described (Malchow 1997; Kruis et al. 2004; Lee et al. 2008; Khokhlova et al. 2012; Wu et al. 2017; Mu et al. 2018), as have been their capacity to produce riboflavin and folate.

In the context of MAIT cells, *E. coli* has been described as being able to activate MAIT cells whereas *L. reuteri* has an inhibitory effect (Dias et al. 2016; Johansson et al. 2016; Schmaler et al. 2018). With regard to *B. adolescentis*, there is no data currently available regarding MAIT cell activation or inhibition. However, due to its already-described folate-producing activities, it was assumed here that this strain might inhibit MAIT cell activation. Thus, the aim of the present study was to evaluate whether MAIT cell-activating bacteria as well as MAIT cell-inhibiting bacteria might be affected by CPF or GLP treatment.

Materials and methods

Stock solutions

Chlorpyrifos (CPF) (Cheminova, Lemvig, Denmark) was dissolved in DMSO (Appli-Chem, Darmstadt, Germany) as a 200 mM stock solution and then stored at room temperature. Commercially-available glyphosate (GLP; in the formulation Roundup LB Plus; Monsanto Agrar Germany, Düsseldorf, Germany) containing 360 g GLP/L was diluted in bacteria culture medium and stored at 4 °C. Acetyl-6-formylpterin (Ac-6-FP, Schircks Laboratories, Bauma, Switzerland) was dissolved in 17 mM NaOH to make a 5 mM stock solution and then stored at −20 °C.

Bacteria preparation

Escherichia coli DH5α (ThermoFisher Scientific, Waltham, MA, USA) was cultured for 16 hr in LB medium Miller (Carl Roth GmbH, Karlsruhe, Germany) at 37 °C with shaking at 175 rpm. The starter culture was then diluted 1:50 with fresh LB medium Miller. Both *Bifidobacterium adolescentis* E298b Variant c (DSM-20086) and *Lactobacillus reuteri* M6220-5A (DSM-28673) (both from DSMZ, Braunschweig, Germany) were cultured in Bifidobacteria medium and MRS medium, respectively (Supplementary Table S1) under anaerobic conditions for 3 d (pre-culture) at 37 °C and 175 rpm, then diluted 1:50 in fresh culture medium and grown for an additional 48 hr. After this culture time (16 hr for *E. coli* and 48 hr for *B. adolescentis* and *L. reuteri*) all bacterial strains were treated for 16 hr with CPF (at final concentrations of 50, 100, or 200 µM), GLP (final concentrations of 75, 150, or 300 mg/L), or the respective solvents without CPF or GLP. The bacteria were then fixed at room temperature in 1% Formaldehyde (ThermoFisher) for 10 min (*E. coli*) or 5 min (*B. adolescentis* and *L. reuteri*). After washing three times with phosphate-buffered saline (PBS; pH 7.4), the bacteria were counted using a Multisizer 3 Coulter Counter (Beckman Coulter, Indianapolis, IN) and also frozen as aliquots at −80 °C (Supplementary Table S1). Identically-treated bacteria from three independent preparations were pooled to avoid batch effects and used for the MAIT cell stimulation assays (see below).

Delayed growth toxicity assay for bacterial viability

Bacteria were treated with CPF or GLP as above. In these studies, 0.4 M NaOH was used as a positive control for inducing bacterial cell death. At the end of the 16-hr period, the now-treated bacteria were diluted in fresh bacteria culture medium and then grown an additional 6 hr (*E. coli*) or 24 hr (*B. adolescentis* and *L. reuteri*). Optical density of the culture suspensions was then measured at 600 nm in a UV-1800 Spectrophotometer (Shimadzu, Kyoto, Japan).

MAIT cell activation assays

Pseudonymous buffy coat samples from six healthy volunteers were obtained from the blood bank at the University of Leipzig. All participants had given written informed consent. The study was approved by the Ethics Committee of the University of Leipzig (Ref. #079-15-09032015). Peripheral blood mononuclear cells (PBMC) were isolated from the buffy coats by density-gradient centrifugation using Ficoll-Paque Plus (GE Healthcare, Little Chalfont, UK). Cells were stored in liquid nitrogen until needed in the stimulation assays.

For the assay, PBMC were cultured in IMDM (GlutaMax supplement, Fisher Scientific, Schwerte, Germany) supplemented with 10% fetal bovine serum (FBS, Biochrom, Berlin, Germany),

1X Pen-Strep Solution (Biowest, Nuaillé, France), and 50 µM β-mercaptoethanol (AppliChem). The cells were plated at 10^6 cells/well in U-bottom 96-well microplates (Greiner Bio-One, Frickenhausen, Germany). After incubation overnight at 37 °C in a 5% CO_2 incubator, the cells were stimulated for 6 hr with bacteria. Brefeldin A (10 µg/mL) (Sigma, St. Louis, MO) was added to all wells for the final 4 hr of this culture period.

Prior experiments determined the optimal bacterial concentration of E. coli for MAIT cell activation. These assays showed that 25–50 bacteria (*E. coli*) per cell) led to a clear MAIT cell activation (Supplementary Figure S1). For all future experiments we chose 30 bacteria (*E. coli*) per cell (BpC). This level enabled increases and decreases of activation by pesticide-treated *E. coli* to be demonstrated (data not shown). Accordingly, a concentration of 30 BpC *E. coli* was used in the present MAIT cell activation studies. On the other hand, due to a general lack of information about MAIT cell-activating capacities for *B. adolescentis* and *L. reuteri*, a higher concentration of 100 BpC of each strain was used here to provoke MAIT cell activation.

To visualize any inhibition of MAIT cell activation, PBMC were seeded as above. Prior to the assays, titration experiments were conducted to determine the appropriate amount of *B. adolescentis* and *L. reuteri* to achieve inhibition of MAIT cell activation of ≈50% (Supplementary Figure S2). A level of 50% inhibition enable detection of either an increase of inhibition by pesticide-treated *B. adolescentis* and *L. reuteri* (i.e. leading to lower cytokine production) or a decrease of inhibition (i.e. leading to higher cytokine production). In this assay, the PBMC were pre-stimulated with untreated or CPF- or GLP-treated *B. adolescentis* (20 BpC) or *L. reuteri* (6 BpC) for 1 hr or left untreated (i.e. without bacteria). As a positive control for inhibition of MAIT cell activation, PBMC were pre-stimulated with Ac-6-FP (50 µM) for 1 hr. Thereafter, to all wells, untreated *E. coli* (30 BpC) was added and the cells were cultured for 6 hr. As above, 10 µg/mL Brefeldin A was added to all wells for the final 4 hr of the incubation period.

Antibody staining and flow cytometry

After *in vitro* stimulation, PBMC were stained with Fixable Viability Dye eFluor™ 506 (eBioscience, Frankfurt/Main, Germany) for dead cell exclusion, followed by cell surface staining for 30 min at room temperature (Supplementary Table S2). Thereafter, the cells were fixed in FACS™ lysing Solution (BD) and permeabilized using FACS™ Permeabilizing Solution 2 (BD Biosciences, San Jose, CA). Finally, the cells were intracellularly stained for 30 min at room temperature (Supplementary Table S2), and then analyzed in a BD FACSCanto™ II cytometer with FACS Diva software version 8.0.1 (BD Biosciences, San Jose, CA, USA). Flow cytometry data were analyzed with FlowJo Version 10.2 (FlowJo, Ashland, OR). A minimum of 150,000 viable T-cells/sample was acquired. The lymphocytes among the human PBMC were identified by means of FSC-A and SSC-A. MAIT cells were identified (as $CD3^+CD8a^+CD161^+TCRV\alpha7.2^+$) after exclusion of doublets and dead cells.

Note: $CD8a^+$ MAIT cells are termed "MAIT cells" hereafter for simplicity. TNFα and IFNγ production in these cells was also quantified (Supplementary Figure S3).

Riboflavin and folate analysis

To measure riboflavin and folate content, bacterial cell pellets of untreated and pesticide-treated bacteria ($n = 3$ independent experiment for each treatment) were lysed using CelLytic B Plus Kit (Sigma), according to manufacturer instructions - without adding the supplied Protease Inhibitor Cocktail. The riboflavin concentration was analyzed by LC-MS/MS whereas the total folate content was measured with the electrochemiluminescence immunoassay Elecsys Folate (Roche, Basel, Switzerland) (see Supplementary Methods).

Proteomic analysis

Samples of *E. coli* ($n = 6$) that had been untreated (solvent\vehicle) or treated with CPF (50–200 µM) were lysed using a Fastprep (FastPrep-24, MP Biomedicals, Eschwege, Germany). The proteome was then analyzed by LC-MS/MS (see Supplementary Methods).

Statistical analysis

In vitro stimulation assays were performed with cells from six donors in three independ-ent experiments, and data were normalized to the cytokine production in untreated *E. coli*. Folate and riboflavin analysis was conducted three times; raw data and solvent control normalized data are presented. All data are presented as means ± SEM. A one-way analysis of variance (ANOVA) was used to analyze the effect of chemical treatment in the *in vitro* assays and in the vitamin analyses. All analyses were performed using Prism v.7.04 (GraphPad Software, San Diego, CA, USA). A p-value $< .05$ was considered statistically significant.

For the proteomic studies, CPF-treated *E. coli* pellets of six independent experiments were used. Transforming and normalization of the protein intensity data to label free quantification (LFQ) values was performed by an in-house written R script. Intensities were $\log_2$-transformed and normalized by the transformed median intensities of the sample multiplied by the median of the $\log_2$ transformed medians of all samples. LFQ values were correlated with the CPF concentration with PERMANOVA using the corrplot package from R. Exact n numbers for all experiments are indicated below the respective figures. A p-value $< .05$ was considered statistically significant.

Results

MAIT cell activation

In the present study, MAIT cells were stimulated with fixed *E. coli*, *B. adolescentis* or *L. reuteri* in single stimulation assays and activation then assessed via measures of intracellular TNFα und IFNγ production. Stimulation with *E. coli* led to an increased number of TNFα- and IFNγ-producing MAIT cells (Figures 1(A,B)). The frequencies of *E. coli*-induced TNFα- and IFNγ-producing MAIT cells averaged 32.0 [± 4.9]% and 9.8 [± 1.5]%, respectively; unstimulated MAIT cells did not produce TNFα and IFNγ. Stimulation with *B. adolescentis* and *L. reuteri* did not induce TNFα and IFNγ production by MAIT cells, even at high concentrations of 100 BpC.

Since *B. adolescentis* and *L. reuteri* did not induce MAIT cell activation, these bacteria were assessed for potentials to inhibit activation by *E. coli*. The appropriate amount of *B. adolescentis* and *L. reuteri* was determined in titration experiments to achieve an inhibition of ≈50%; this was obtained using 20 bacteria per cell (BpC) *B. adolescentis* and 6 BpC *L. reuteri* (Supplementary Figure S2). The results show that in the co-stimulation assays, *B. adolescentis* and *L. reuteri* both reduced *E. coli*-induced MAIT cell activation (Figure 2(A)). A co-presence of *B. adolescentis* led

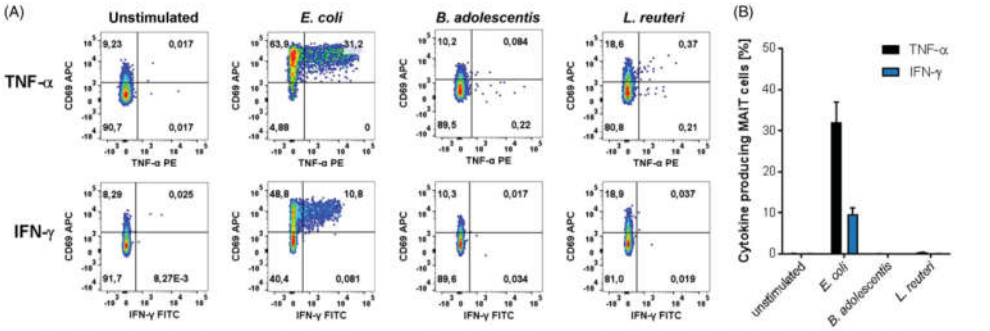

Figure 1. MAIT cell activation after single stimulation with different bacterial strains. PBMC were stimulated with fixed *Escherichia coli* (*E. coli*, 30 BpC), *Bifidobacterium adoles-centis* (*B. adolescentis*, 100 BpC) or *Lactobacillus reuteri* (*L. reuteri*, 100 BpC) for 6 hr. MAIT cells ($CD3^+CD8a^+CD161^+TCRV\alpha7.2^+$ populations) were detected by flow cytometry. Activation was measured via intracellular staining of TNFα and IFNγ production. Results are given as percentage of gated MAIT cell populations. (A) Representative dot-plots of bacteria-stimulated MAIT cells from $n = 6$ (unstimulated, *E. coli*) or $n = 2$ (*B. adolescentis*, *L. reuteri*) donors; summarized (mean ± SEM) in (B).

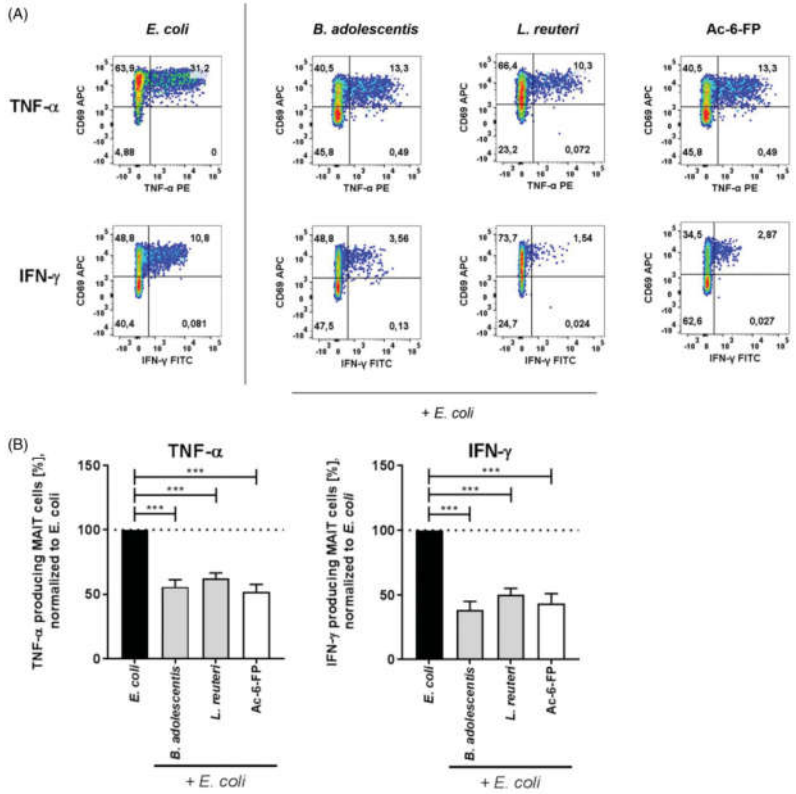

Figure 2. Inhibition of *E. coli*-induced MAIT cell activation by *B. adolescentis*, *L. reuteri*, or the folate metabolite acetyl-6-formylpterin (Ac-6-FP). PBMC were stimulated with fixed *E. coli* alone (30 BpC) or co-stimulated with fixed *E. coli* (30 BpC) and fixed *B. adolescentis* (20 BpC), *L. reuteri* (6 BpC) *or* Ac-6-FP (50 μM) for 6 hr. MAIT cells ($CD3^+CD8a^+CD161^+$ $TCRV\alpha7.2^+$ populations) were detected by flow cytometry. Activation of cells was measured via intracellular staining of TNFα and IFNγ production. Results given as percentage of gated MAIT cell population. (A) Representative dot-plots of bacteria and Ac-6-FP stimulated MAIT cells from $n = 6$ donors. (B) Summarized data after normalization to the single stimulation with *E. coli*. $N = 6$, mean ± SEM, one-way ANOVA. $^{***}p < .001$ vs. *E. coli*.

to 44.2% and 61.6% fewer TNFα- and IFNα-producing MAIT cells (compared to levels with *E. coli* alone), respectively (Figure 2(B)). Similar results were obtained in the *L. reuteri* co-stimulation assays (Figure 2(B)). The folate metabolite, Ac-6-FP (positive control for MAIT cell inhibition) also reduced *E. coli*-induced MAIT cell activation by nearly 50%.

Modulation of MAIT cell activity by pesticide-treated bacteria

To see whether pesticide-treated bacteria impacted activation\inhibition of MAIT cells, the bacterial strains were treated with CPF or GLP for 16 hr prior to fixation. Data from the growth assay revealed that neither CPF nor GLP had lethal effects on these bacterial strains at the levels used here (Supplementary Table S3). Subsequently, the pesticide-treated bacteria were used in MAIT cell stimulation assays and the numbers of cytokine-producing cells was then normalized to controls without CPF or GLP treatment. The data show that CPF treatment (200 µM) of *E. coli* induced a significantly higher number of TNFα ($p = .011$)- and IFNγ ($p = .002$)-producing MAIT cells compared to that by untreated *E. coli* controls (Figures 3(A,B)). GLP treatment (150 mg/L) of *E. coli* led to an increase in TNFα-producing MAIT cells ($p = .017$), but did not significantly alter IFNγ production by these cells.

As stimulation of MAIT cells with CPF- or GLP-treated *B. adolescentis* or *L. reuteri* did not induce IFNγ or TNFα production (data not shown), these CPF- or GLP-treated bacteria were tested in co-stimulation assays together with untreated *E. coli*. In all cases, the number of TNFα- and IFNγ-producing MAIT cells was normalized to the response induced by the untreated *E. coli* alone. The results showed that CPF-treatment of *B. adolescentis* reduced the extent of inhibition of MAIT cell activation compared to that by untreated *B. adolescentis* (Figure 4(B)). A similar pattern was observed with IFNγ production. In contrast, GLP treatment of *B. adolescentis* did not cause significant changes in impact on MAIT cell activation compared to that seen with untreated *B. adolescentis*.

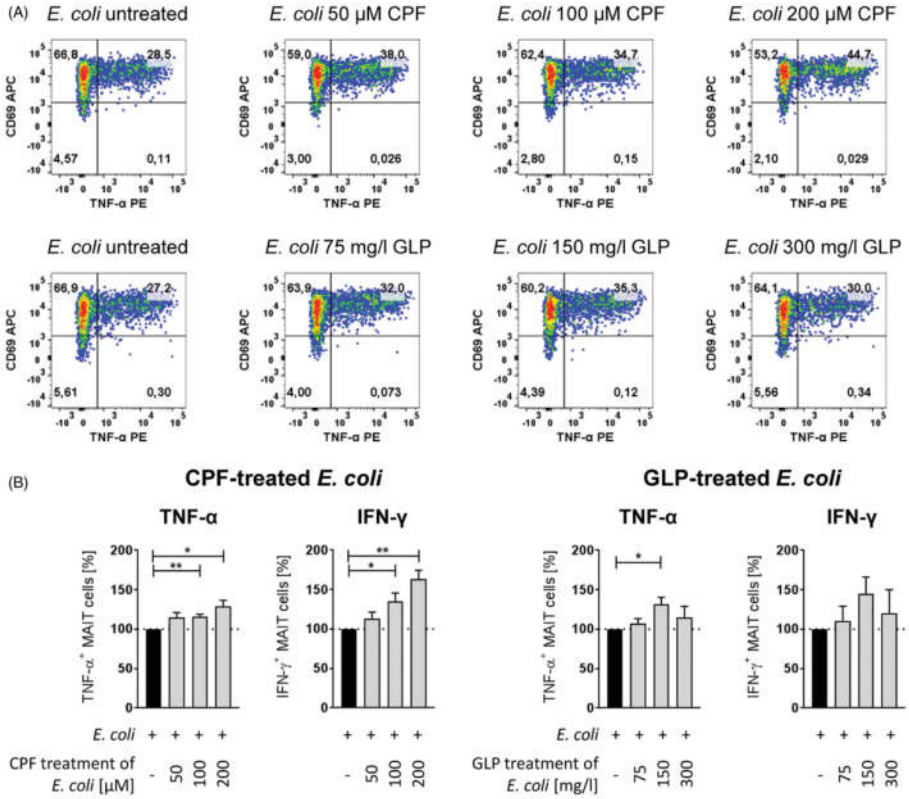

Figure 3. MAIT cell activation by chlorpyrifos (CPF)- or glyphosate (GLP)-treated *E. coli*. PBMC were stimulated with fixed CPF- and GLP- treated *E. coli* (30 BpC) for 6 hr. MAIT cells ($CD3^+CD8a^+CD161^+TCRV\alpha7.2^+$ populations) were detected by flow cytometry. Activation of cells was measured via intracellular staining of TNFα and IFNγ production. Results are given as percentage of gated MAIT cell population. (A) Representative dot-plots of MAIT cells stimulated with *E. coli* (control) and CPF- or GLP-treated *E. coli* from $n = 6$ donors. (B) Summarized data for the stimulation with CPF- and GLP-treated *E. coli* after normalization to the control (untreated *E. coli*), $n = 6$, mean ± SEM, one-way ANOVA. $^*p < .05$, $^{**}p < .01$ vs. control.

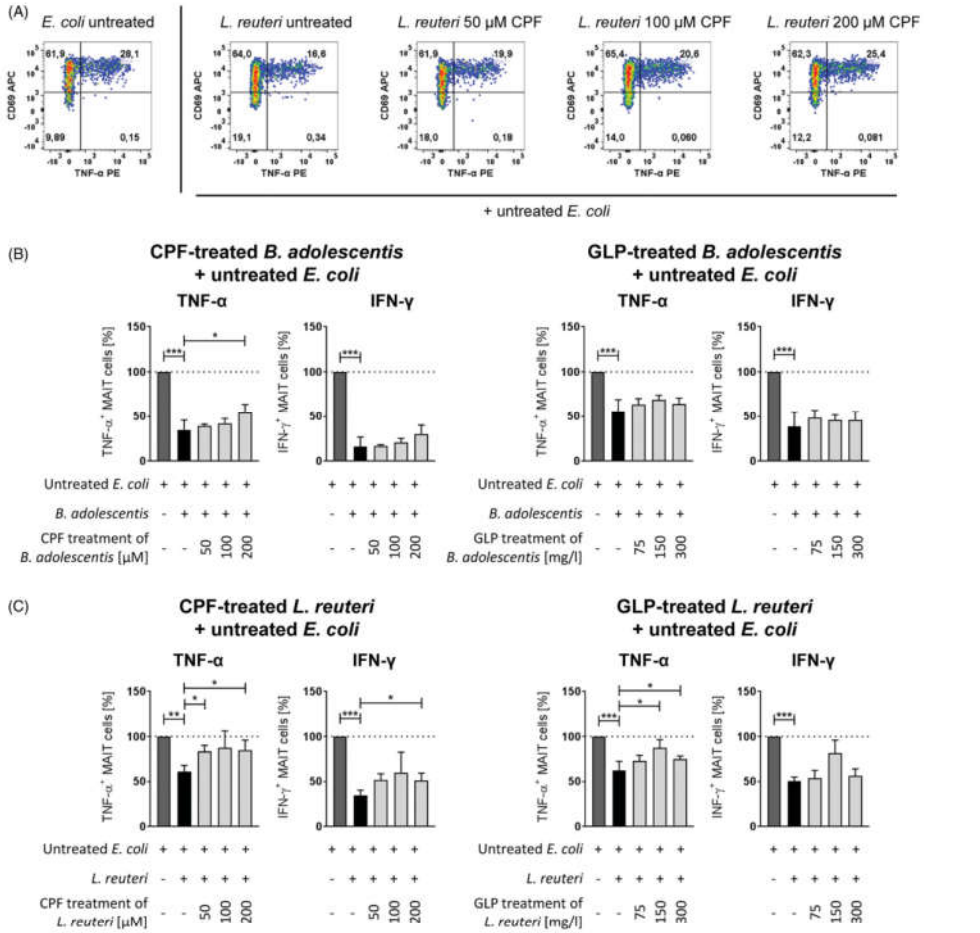

Figure 4. Modulation of *Escherichia coli* (*E. coli*)-induced MAIT cell activation by CPF- or GLP-treated *B. adolescentis* and *L. reuteri*. PBMC were co-stimulated for 6 hr with untreated fixed *E. coli* (30 BpC) and fixed CPF- or GLP-treated (or untreated) (A) *B. adolescentis* (20 BpC) or (B) *L. reuteri* (6 BpC). MAIT cells ($CD3^+CD8a^+CD161^+TCRV\alpha7.2^+$ populations) were detected by flow cytometry. Activation of cells was measured via intracellular staining of TNFα and IFNγ production. Results are given as percentage of gated MAIT cell population. (A) Representative dot-plots of cells (from $n = 6$ donors) stimulated with untreated *E. coli* (control) and in co-stimulation with CPF-treated or untreated *L. reuteri*. (B) Summarized data for co-stimulation with CPF- and GLP-treated *B. adolescentis and L. reuteri* after normalization to control (un-treated *E. coli*). Dark gray bars show response to untreated *E. coli*. Black bars represent untreated co-stimulation control (untreated *B. adolescentis* or *L. reuteri* + untreated *E. coli*), $n = 6$, mean ± SEM, one-way ANOVA. $^*p < .05$, $^{**}p < .01$ vs. control.

In contrast, CPF treatment of *L. reuteri* significantly changed the ability of these bacteria to modulate MAIT cell activation by untreated *E. coli*. Specifically, it was seen that levels of both TNFα- and IFNγ-producing MAIT cells were significantly increased compared to that seen after co-stimulation with the untreated *L. reuteri* (Figures 4(A,C)). Compared with CPF, treatment with GLP led to *L. reuteri* that could induce a slightly higher number of TNFα-producing MAIT cells in the co-stimulation assays than non-GLP treated *L. reuteri* (Figure 4(C)). However, this effect was not observed with regard to IFNγ-producing cells.

Bacterial vitamin production upon CPF and GLP exposure

Concentrations of riboflavin and folate (as end-products of respective biosynthesis pathways) were measured as proxies for the already-known MAIT cell-activating and -inhibiting metabolites. Raw data for untreated as well as CPF- and GLP-treated bacteria are provided in Supplementary Table S4. To better assess the influence of CPF and GLP treatment on folate and riboflavin production, all results were normalized to untreated control values. Regarding ribo-flavin production, a high concentration was seen in *E. coli* whereas the concentrations in the

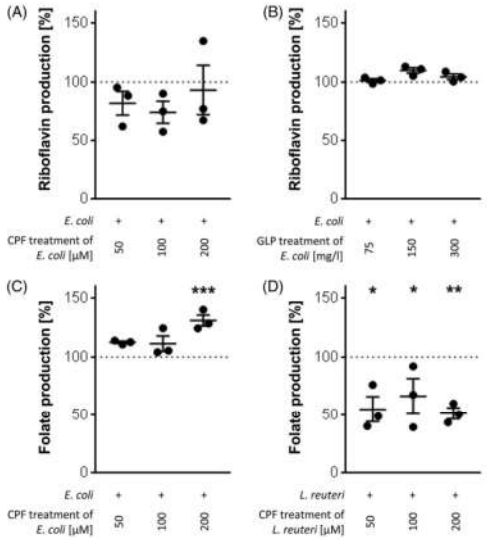

Figure 5. Riboflavin and folate production by CPF- and GLP-treated bacteria. Riboflavin production was measured in *E. coli* lysates after treatment with increasing levels of (A) CPF and (B) GLP. Folate production was analyzed in bacterial lysates of (C) *E. coli* and (D) *L. reuteri* after CPF treatment. Riboflavin and folate production were normalized to the control (bacteria without chemical treatment). $N = 3$, mean ± SEM, one-way ANOVA. $^{*}p < .05$, $^{**}p < .01$, $^{***}p < .001$ vs. control.

lysates of *B. adolescentis* and *L. reuteri* were rather low. CPF treatment (at 100 µM) of the *E. coli* led to lower riboflavin production (Figure 5(A), Supplementary Table S4); in contrast, after GLP treatment (150 mg/L), production trended higher (Figure 5(B)). With *B. adolescentis* and *L. reuteri*, riboflavin production was not affected by CPF or GLP treatment.

Folate was detected in all bacterial strains, with *E. coli* exhibiting the highest production. CPF treatment led to a significantly higher folate concentration in *E. coli* compared to the control (Figure 5(C)). However, *E. coli* folate production was not affected by GLP (Supplementary Table S4). The CPF or GLP treatment did not alter *B. adolescentis* folate production. With *L. reuteri*, there was nearly 50% lower formation of folate after CPF treatment (compared to the control) whereas GLP treatment imparted no significant effect (Figure 5(D)).

Proteomic analysis of CPF-treated E. coli

The strongest effect of pesticide treatment regarding MAIT cell activation was seen with CPF-treated *E. coli*. Therefore, proteomic analysis was performed after CPF treatment of this strain. LC-MS/MS based shotgun proteomics of CPF-treated *E. coli* revealed 2033 proteins in total, with very similar numbers of proteins per treatment group and sample (Supplementary Figure S4-A). NMDS modeling control based on *E. coli* protein label-free quantification (LFQ) values revealed a trend ($p = .082$, PERMANOVA) in separation of the global proteomes of the three treatment groups and the control (Supplementary Figure S4-C). Pair-wise NMDS modeling showed significant separation between samples treated with the highest CPF concentration (200 µM) and the control ($p = .027$, PERMANOVA), but not at the lower CPF concentrations (Supplementary Figures S3-D, -E, and -F). The LFQ protein values were correlated with the concentration of CPF. In total, 317 *E. coli* proteins significantly correlated ($p < .05$) with CPF concentration; 180 were negatively-correlated to CPF concentration while 137 exhibited positive correlation (Supplementary Figure S4-B). All known *E. coli* proteins of the folate biosynthesis pathway were detected. Two proteins had significant negative correlation to CPF concentration, i.e. *p*-aminobenzoate synthetase component I (PabB, K01665, $r = -0.5942$, $p = .0022$) and dihydropteroate synthase (FolP, K00796, $r = -0.5216$, $p = .0090$) (Figure 6(A)). Furthermore, all *E. coli* proteins known to belong to the riboflavin biosynthesis pathway were identified. Riboflavin synthase (RibE, K00783, $r = -0.5667$, $p = .0038$) was observed to have a negative correlation to CPF concentration (Figure 6(B)).

Discussion

The hypothesis of the present investigation was that pesticides might alter the immuno-modulatory function of commensal bacterial strains. To test this hypothesis, MAIT cells were examined since it is known that activation of these cells is modulated by bacterial metabolites of the B vitamin pathway. Three commensal bacterial strains, *E. coli*, *B. adolescentis* and *L. reuteri*, were selected and the frequently-used pesticides CPF and GLP were chosen for their treatment. MAIT cell activation was assessed via induction of intracellular cytokine production after stimulation of PBMC with treated or untreated bacteria. Concentrations of riboflavin and folate were measured in bacterial lysates after CPF or GLP treatment. Additionally, a proteomic analysis was performed with CPF-treated *E. coli*.

For this study, pesticide concentrations were chosen that were used in recent publications concerning microbiota. Harishankar et al. (2013) showed that CPF at a dose of ≤ 285 µM was tolerated by all tested strains. Therefore, concentrations in a similar range (i.e. 50–200 µM) were used here. Regarding the GLP concentrations, published data are rather diverse, i.e. 5 mg/L–5 g/L (Shehata et al. 2013; Motta et al. 2018; Nielsen et al. 2018). However, sufficient concentra-tions of aromatic amino acids in the bacterial environment can strongly limit the effect of GLP on bacteria (and prevent anti-microbial effects [Nielsen et al. 2018]). Therefore, in the present study, media containing aromatic amino acids (to mitigate anti-microbial effects) and GLP concentrations of 75–300 mg/L were employed.

Certainly, there might be unknown (non-toxicity related) effects of GLP and CPF on bacterial metabolism leading to an alteration of MAIT cell activation. For humans, acceptable daily intakes (ADI) of these compounds are 0.01 mg CPF/kg and 1.0 mg GLP/kg (according to WHO [2004 and 2016, respectively]). In a 70 kg human with 1.2 L gut volume, this corresponds to a 25–100 (CPF)- and 1.25–5.00 (GLP)-fold lower dose compared to the levels employed in the current study. Though the levels used here exceeded these ADI, the underlying aim was to analyze if these pesticides impact the bacterial metabolism at all. Hence, a high-dose and short-term exposure (i.e. 16 hr) paradigm was used. It would be of great interest to investigate long-term low-dose exposures in future experiments, since contaminated foods might be ingested over years.

Here, toxicity assays for both pesticides were first performed to ensure bacterial viability. These assays revealed that the concentrations of CPF (50–200 µM) and GLP (75–300 mg/L) used did not inhibit growth of *E. coli*, *B. adolescentis* and *L. reuteri*.

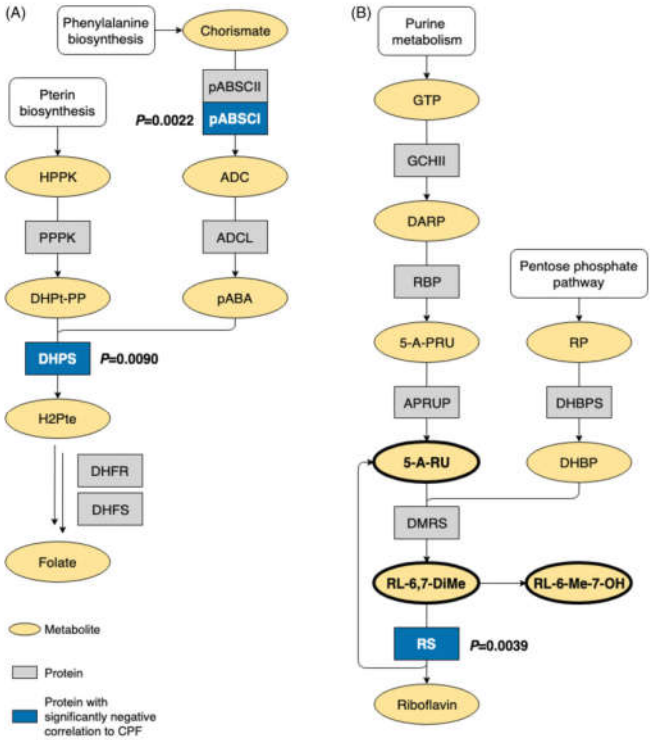

Figure 6. Folate and riboflavin metabolism of CPF-treated *E. coli*. The *E. coli* proteome was analyzed in bacteria that were either untreated (solvent) or CPF-treated (50-200 µM) for 16 hr. Proteins of the (A) folate and (B) riboflavin biosynthesis pathways are represented by rectangles and are either gray (protein detected but not influenced by CPF treatment) or blue (protein exhibits significant negative correlation with CPF, $p < .05$). p-Values are indicated when a significant correlation with CPF treatment was seen. Metabolites are represented by yellow ellipses. MAIT cell activating metabolites in riboflavin pathway are in bold. 5-A-PRU, 5-amino-6-(5-phosphoribosylamino)-uracil; 5-A-RU, 5-amino-6-D-ribitylaminouracil; ADC, 4-amino-4-deoxychoris-mate; ADCL, 4-amino-4-deoxychorismate lyase; APRUP, 5-amino-6-(5-phospho-D-ribityl-amino)-uracil phosphatase; DARP, 2,5-diamino-6-(5-phosphoribosylamino)-4-pyrimi-dinone; DHBP, 3,4-dihydroxy-2-butanone-4-phosphate; DHBPS, 3,4-dihydroxy-2-butanone-4-phosphate synthase; DHFR, dihydrofolate reductase; DHFS, dihydrofolate synthase/folyl-poly-glutamate synthase; DHPS, dihydropteroate synthase; DHPt-PP, 6-hydroxymethyl-7,8-dihydrop-terin diphosphate; H2Pte, 7,8-dihydropteroate; DMRS, 6,7-dimethyl-8-ribityllumazine synthase; GCHII, guanosine-5-triphosphate cyclohydrolase II; GTP, guanosine-5-triphosphate; HPPK, 6-hydroxymethyl-7,8-dihydropterin; pABA, *p*-aminobenzoate; pABSCI, pABA synthetase compo-nent I; pABSCII, pABA synthetase component II; PPPK, 6-hydroxymethyl-7,8-dihydropterin pyrophosphokinase; RBP, riboflavin biosynthesis protein; RL-6,7-DiMe, 6,7-dimethyl-8-D-ribityllumazine; RL-6-Me-7-OH, 7-hydroxy-6-methyl-8-D-ribityllumazine; RP, ribulose-5-phosphate; RS, riboflavin synthase.

These outcomes differ slightly from those in earlier studies that showed that GLP (at some concentrations) could impair the growth of *E. coli* (5000 mg/L) and *B. adolescentis* (75 mg/L), as well as some *Lactobacilli* strains (600 mg/L) (Shehata et al. 2013). Those effects were caused by inhibition of 5-enolpyruvylshiki-mate-3-phosphate synthase, leading to insufficient amounts of aromatic amino acid formation by the bacteria (Motta et al. 2018). As already noted, all bacteria culture media used in the present study contained aromatic amino acids as part of the yeast extract (Supplementary Table S1) (Martini et al. 1979). Therefore, apart from the concentrations here being lower than the "toxic ones" in the Shehata et al. study, one could assume that the findings of a lack of GLP-mediated toxicity here could have been due to sufficient concentrations of aromatic amino acids being present in the culture media. Regarding CPF, it has been shown that *E. coli* can grow even in the presence of high concentrations of CPF (up to 4 mM), tolerate CPF for up to 15 days, and contribute to the degradation of the agent itself (Harishankar et al. 2013). Because of the lack of "lethality" of the test pesticides here, it can be concluded that the observed effects on MAIT cell activation here were not due to reduced bacterial viability but rather likely via secondary effects of the pesticides on bacterial metabolism (which in turn affected formation of known MAIT cell inhibiting and activating metabolites).

The present study findings also revealed that CPF-treated *E. coli* induced a significantly higher number of TNFα- and IFNγ-producing MAIT cells. This enhanced MAIT cell activation might be due to the presence of more activating bacterial metabolites, less inhibiting bacterial metabolites, or a combination of both. To prove this, the *E. coli* proteome was evaluated after CPF treatment.

Exposure to 200 µM CPF caused significant alterations in the global *E. coli* proteome that were not observed at lower concentrations (Supplementary Figure S4-F). In addition, the proteomic analysis of the CPF-treated *E. coli* revealed a significantly negative correlation of CPF treatment with riboflavin synthase (RS,

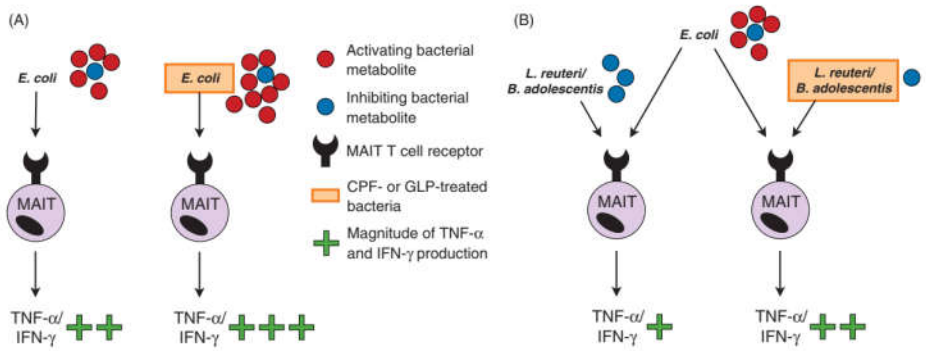

Figure 7. Schematic of MAIT cell stimulation assays with untreated and CPF- or GLP-treated *E. coli*, *B. adolescentis*, and *L. reuteri*. (A) MAIT cells stimulated with untreated *E. coli* or CPF- or GLP-treated *E. coli* (orange) in single stimulation assays. (B) MAIT cells were stimulated with untreated *B. adolescentis* or *L. reuteri* or CPF- or GLP-treated *B. adolescentis* or *L. reuteri* (orange) in single stimulation or co-stimulation assays with untreated *E. coli*. MAIT cells ($CD3^+CD8a^+CD161^+TCRV\alpha7.2^+$ populations) were detected by flow cytometry. Activation measured via intracellular staining of TNFα and IFNγ production. Green crosses show levels of TNFα and IFNγ production. Amount of activating and inhibiting bacterial metabolites is indicated as red and blue circles, respectively.

Figure 6(B)), a key enzyme of the riboflavin biosynthesis pathway. Down-regulation of this enzyme can lead to reduced riboflavin production. In line with this, there was a trend for reduced riboflavin production by CPF-treated *E. coli* in the current study. Since expression of all other enzymes of the riboflavin biosynthesis pathway did not correlate with CPF treatment, the down-regulation of this enzyme could have conceivably led to an accumulation of MAIT cell-activating riboflavin metabolites. As a consequence, CPF-treated *E. coli* may cause stronger MAIT cell activation, leading to an enhanced number of activated cells and as was noted, increases in TNFα and IFNγ production.

In addition to activating riboflavin metabolites, the levels of inhibitory folate metabolites synthesized by *E. coli* might have been altered by CPF. The proteomic analysis showed that expression of a key enzyme of folate biosynthesis, dihydropteroate synthase (DHPS), was significantly negative correlated with CPF treatment. Reduced DHPS levels could lead to lower folate production by the treated *E. coli*. Oddly, significantly stronger folate production by *E. coli* after CPF treatment was observed (Supplementary Table S1). Previous studies have shown that the DHPS is competitively feedback inhibited by its own product dihydropteroate, and by folate and some of its related molecules (Prabhu et al. 1997; Vinnicombe and Derrick 1999). Therefore, the observed negative correlation of this enzyme with CPF treatment in *E. coli* might be due to product inhibition by folate itself, since folate production is higher in CPF-treated *E. coli*.

Despite the increased folate content after CPF treatment, it is difficult to estimate whether levels of MAIT cell-inhibiting folate metabolites were altered. Though speculative, it might be that degradation of folate to MAIT cell-inhibiting metabolites was impaired by CPF, leading to lower amounts of these metabolites – and as a consequence, to an enhanced number of activated MAIT cells. In addition, MAIT TCR exhibits an increased affinity to MR1 presenting activating riboflavin metabolites compared to MR1 with inhibiting folate metabolites (Patel et al. 2013). Thus, one might assume that the observed enhanced MAIT cell activation by CPF-treated *E. coli* was probably mostly driven by an accumulation of the riboflavin metabolites.

In comparison to CPF, GLP treatment had a smaller influence on the *E. coli*-mediated MAIT cell activation but did not affect vitamin production. This led us to assume that this pesticide may not (or only slightly) impact upon *E. coli* metabolism.

Regarding the other bacterial strains, the current study showed that untreated as well as CPF- or GLP-treated *B. adolescentis* and *L. reuteri* did not induce MAIT cell activation *per se*, but inhibited *E. coli* induced activation (in co-stimulation assays). Thus, the main question this generated was whether CPF- and GLP-treatment might change the inhibitory capacity of these strains during co-stimulation with untreated *E. coli*. The findings showed there was a moderate increase in TNFα- but not IFNγ-producing MAIT cells after co-stimulation with GLP-treated *L. reuteri* compared to with untreated *L. reuteri*. CPF-treated *L. reuteri* led to a significant increase of both TNFα- and IFNγ-producing MAIT cells, indicating a reduced MAIT cell inhibiting capacity after treatment. CPF-treated *B. adolescentis* also led to a significant increase of TNFα- and a trend of an increase in IFNγ-producing MAIT cells in co-stimulation assays. Taken together, the findings let us assume that CPF treatment especially might impact bacterial metabolite formation by *B. adolescentis* and *L. reuteri*, leading to alterations in the inhibition of MAIT cell activation (Figure 7).

Concerning riboflavin production by *B. adolescentis* and *L. reuteri*, no changes were observed after CPF or GLP treatment (Supplementary Table S1). Since the concentration of riboflavin in the bacterial lysates of these strains was in general very low, production of folate might be more important for these bacteria. Indeed, analyses of folate content showed that the observed reduction in levels of MAIT cell inhibition by CPF-treated *L. reuteri* was accompanied by significantly lower folate production. This might lead to smaller amounts of inhibitory folate metabolites, depending on any impact of the pesticides on regulation of folate degradation by *L. reuteri*. Regardless of how precisely CPF and GLP treatment of *B. adolescentis* and *L. reuteri* led to a reduction of their normal inhibition of MAIT cell activation, these changes in immuno-regulatory impact of these bacteria resulted in increased numbers of TNFα- and IFNγ-producing MAIT cells. In a live host, this would suggest a directing of immune responses toward more inflammation.

Limitations

The authors are keenly aware that a key limitation of the current study was that the experiments were performed with peripheral blood cells (PBMC) and not with MAIT cells from the gut where pesticides would be presumed to act first in an exposed host. Because gut MAIT cells have differences in activation marker expression (relative to those on PBMC) (Booth et al. 2015), differing reactions of gut MAIT cells to CPF- and GLP-treated bacteria cannot be as yet be ruled out. It is also important to mention that the current data represents results in a simple model (cultured bacteria/cells). Regardless, these outcomes should promote further studies in more complex bacterial communities and also in intact animal models.

Conclusions

The results of the current study indicate that CPF – and to lesser extent GLP – might alter bacterial metabolism, leading to imbalances in levels of activating\inhibiting bacterial metabo-lites that could impact on inflammatory immune responses. Inflammation is associated with a variety of non-communicable diseases including multiple sclerosis, inflammatory bowel disease, obesity and asthma, and alterations in MAIT cell function and distribution are also known to be associated with these diseases. Therefore, the present findings lead us conclude that bacterial treatment with CPF and GLP, resulting in an enhanced inflammatory cytokine production by MAIT cells, might potentially contribute to the development and/or progression of inflammatory immune system-based diseases.

Acknowledgements

The authors thank Michaela Loschinski, Florian Tschernikl, Nicole Gröger, Susann Reißhauer, and Franziska Erber for their excellent assistance in the laboratory. Jannike Lea Krause is thankful forfunding by the German Federal Environmental Foundation (DBU).

Disclosure statement

The authors report no conflicts of interest. The authors alone are responsible for the content of this manuscript.

ORCID

Ulrike Rolle-Kampczyk http://orcid.org/0000-0002-7728-6284
Martin von Bergen http://orcid.org/0000-0003-2732-2977

References

Aitbali Y, Ba-M'hamed S, Elhidar N, Nafis A, Soraa N, Bennis M. 2018. Glyphosate based-herbicide exposure affects gut microbiota, anxiety and depression-like behaviors in mice. Neurotoxicol. Teratol. 67:44–49.

Booth J, Salerno-Goncalves R, Blanchard T, Patil S, Kader H, Safta A, Morningstar L, Czinn S, Greenwald B, Sztein M. 2015. Mucosal-associated invariant T-cells in the human gastric mucosa and blood: Role in *Helicobacter pylori* infection. Front Immunol. 6:466.

Carolan E, Tobin LM, Mangan BA, Corrigan M, Gaoatswe G, Byrne G, Geoghegan J, Cody D, O'Connell J, Winter DC, et al. 2015. Altered distribution and increased IL-17 production by mucosal-associated invariant T-cells in adult and childhood obesity. J Immunol. 194(12):5775–5780.

Chiba A, Murayama G, Miyake S. 2018. Mucosal-associated invariant T-cells in autoimmune diseases. Front Immunol. 9:1333.

Dias J, Sobkowiak M, Sandberg J, Leeansyah E. 2016. Human MAIT-cell responses to *Escheri-chia coli*: Activation, cytokine production, proliferation, and cytotoxicity. J. Leukocyte Biol. 100(1):233–240.

Eckle S, Birkinshaw R, Kostenko L, Corbett A, McWilliam H, Reantragoon R, Chen Z, Gherardin N, Beddoe T, Liu L, et al. 2014. A molecular basis underpinning the T-cell receptor heterogeneity of mucosal-associated invariant T-cells. J. Exp. Med. 211(8):1585–1600.

Fang B, Li J, Zhang M, Ren F, Pang G. 2018. Chronic chlorpyrifos exposure elicits diet-specific effects on metabolism and the gut microbiome in rats. Food Chem. Toxicol. 111:144–152.

Fischer M, Eberhardt S, Richter G, Krieger C, Gerstenschlager I, Bacher A. 1996. Biosynthesis of riboflavin. Bifunctional pyrimidine deaminase/reductase of *Escherichia coli* and *Bacillus subtilis*. Biochem. Soc. Trans. 24(1): 35S–35S.

Green J. 2018. The rise and future of glyphosate and glyphosate-resistant crops. Pest Manag Sci. 74(5):1035–1039.

Harishankar M, Sasikala C, Ramya M. 2013. Efficiency of the intestinal bacteria in the degradation of the toxic pesticide, chlorpyrifos. Biotech. 3: 137–142.

Hill M. 1997. Intestinal flora and endogenous vitamin synthesis. Eur. J. Cancer Prev. 6:43–45.

Johansson M, Björkander S, Mata Forsberg M, Qazi K, Salvany Celades M, Bittmann J, Eberl M, Sverremark-Ekström E. 2016. Probiotic *Lactobacilli* modulate *Staphylococcus aureus*-induced activation of conventional and unconventional T-cells and NK Cells. Front Immunol. 7:273.

Khokhlova E, Smeianov V, Efimov B, Kafarskaia L, Pavlova S, Shkoporov A. 2012. Anti-inflammatory properties of intestinal Bifidobacterium strains isolated from healthy infants. Microbiol. Immunol. 56(1):27–39.

Kjer-Nielsen L, Corbett A, Chen Z, Liu L, Mak J, Godfrey D, Rossjohn J, Fairlie D, McCluskey J, Eckle S. 2018. An overview on the identification of MAIT cell antigens. Immunol Cell Biol. 96(6):573–587.

Kjer-Nielsen L, Patel O, Corbett A, Le Nours J, Meehan B, Liu L, Bhati M, Chen Z, Kostenko L, Reantragoon R, et al. 2012. MR1 presents microbial vitamin B metabolites to MAIT cells. Nature. 491(7426):717–723.

Kruis W, Fric P, Pokrotnieks J, Lukás M, Fixa B, Kascák M, Kamm M, Weismueller J, Beglinger C, Stolte M, et al. 2004. Maintaining remission of ulcerative colitis with the probiotic *E. coli* Nissle 1917 is as effective as with standard mesalazine. Gut. 53(11):1617–1623.

LeBlanc J, Laiño J, del Valle M, Vannini V, van Sinderen D, Taranto M, de Valdez G, de Giori G, Sesma F. 2011. B-group vitamin production by lactic acid bacteria: Current knowledge and potential applications. J. Appl. Microbiol. 111(6):1297–1309.

LeBlanc J, Milani C, de Giori G, Sesma F, van Sinderen D, Ventura M. 2013. Bacteria as vitamin suppliers to their host: A gut microbiota perspective. Curr. Opin. Biotechnol. 24(2):160–168.

Lee D, Jang S, Kim M, Kim J, Chung M, Kim K, Ha N. 2008. Anti-proliferative effects of *Bifidobacterium adolescentis* SPM0212 extract on human colon cancer cell lines. BMC Cancer. 8(1):310.

Lezmi G, Leite-de-Moraes M. 2018. Invariant natural killer T- and mucosal-associated invariant T-cells in asthmatic patients. Front Immunol. 9:1766.

Malchow H. 1997. Crohn's Disease and *Escherichia coli*: A new approach in therapy to maintain remission of colonic Crohn's Disease? J. Clin. Gastroenterol. 25(4):653–658.

Mao Q, Manservisi F, Panzacchi S, Mandrioli D, Menghetti I, Vornoli A, Bua L, Falcioni L, Lesseur C, Chen J, et al. 2018. The Ramazzini Institute 13-week pilot study on glyphosate and Roundup administered at human-equivalent dose to Sprague Dawley rats: Effects on the microbiome. Environ Health. 17(1):50

Marquez Giron S, Aguirre Ramirez N, Palacio Baena J. 2017. Bioconcentration of chlorpyrifos in roots and foliage of plants of *Cenchrus clandestinus* (Hochst. ex chiov.) morrone, cultured in green house. Rev Fac Nac Agron. 70:64524.

Martini A, Miller M, Martini A. 1979. Amino acid composition of whole cells of different yeasts. J Agric Food Chem. 27(5):982–984.

Motta E, Raymann K, Moran N. 2018. Glyphosate perturbs the gut microbiota of honey bees. Proc Natl Acad Sci Usa . 115(41):10305–10310.

Mu Q, Tavella V, Luo X. 2018. Role of *Lactobacillus reuteri* in human health and diseases. Front Microbiol. 9:757.

Nielsen L, Roager H, Casas M, Frandsen H, Gosewinkel U, Bester K, Licht T, Hendriksen N, Bahl M. 2018. Glyphosate has limited short-term effects on commensal bacterial community composition in the gut environment due to sufficient aromatic amino acid levels. Environ. Pollut. 233:364–376.

Patel O, Kjer-Nielsen L, Le Nours J, Eckle S, Birkinshaw R, Beddoe T, Corbett A, Liu L, Miles J, Meehan B, et al. 2013. Recognition of vitamin B metabolites by mucosal-associated invariant T-cells. Nat Commun. 4:2142

Pompei A, Cordisco L, Amaretti A, Zanoni S, Matteuzzi D, Rossi M. 2007. Folate production by bifidobacteria as a potential probiotic property. Appl Environ. Microbiol. 73(1):179–185.

Prabhu V, Lui H, King J. 1997. Arabidopsis dihydropteroate synthase: General properties and inhibition by reaction product and sulfonamides. Phytochemistry. 45(1):23–27.

Reantragoon R, Corbett AJ, Sakala IG, Gherardin NA, Furness JB, Chen Z, Eckle SB.G, Uldrich AP, Birkinshaw RW, Patel O, et al. 2013. Antigen-loaded MR1 tetramers define T-cell receptor heterogeneity in mucosal-associated invariant T-cells. J. Exp. Med. 210(11):2305–2320.

Rossi M, Amaretti A, Raimondi S. 2011. Folate production by probiotic bacteria. Nutrients. 3(1):118–134.

Rudak P, Choi J, Haeryfar S. 2018. MAIT cell-mediated cytotoxicity: Roles in host defense and therapeutic potentials in infectious diseases and cancer. J Leukoc Biol. 104(3):473–486.

Santos F, Wegkamp A, de Vos W, Smid E, Hugenholtz J. 2008. High-Level folate production in fermented foods by the B12 producer *Lactobacillus reuteri* JCM1112. Appl. Environ. Microbiol. 74(10):3291–3294.

Schmaler M, Colone A, Spagnuolo J, Zimmermann M, Lepore M, Kalinichenko A, Bhatia S, Cottier F, Rutishauser T, Pavelka N, et al. 2018. Modulation of bacterial metabolism by the microenvironment controls MAIT cell stimulation. Mucosal Immunol. 11(4):1060–1070.

Sekirov I, Russell S, Antunes L, Finlay B. 2010. Gut microbiota in health and disease. Physiol. Rev. 90(3):859–904.

Serriari N, Eoche M, Lamotte L, Lion J, Fumery M, Marcelo P, Chatelain D, Barre A, Nguyen-Khac E, Lantz O, et al. 2014. Innate mucosal-associated invariant T (MAIT)-cells are activated in inflammatory bowel diseases. Clin Exp Immunol. 176(2):266–274.

Shehata A, Schrodl W, Aldin A, Hafez H, Kruger M. 2013. The effect of glyphosate on potential pathogens and beneficial members of poultry microbiota *in vitro*. Curr Microbiol. 66(4):350–358.

Thakur K, Tomar S, De S. 2016. Lactic acid bacteria as a cell factory for riboflavin production. Microb Biotechnol. 9(4):441–451.

Thengodkar R, Sivakami S. 2010. Degradation of chlorpyrifos by an alkaline phosphatase from cyanobacterium *Spirulina platensis*. Biodegradation. 21(4):637–644.

Thiaville J, Frelin O, García-Salinas C, Harrison K, Hasnain G, Horenstein N, Díaz de la Garza R, Henry C, Hanson A, de Crécy-Lagard V. 2016. Experimental and metabolic modeling evidence for a folate-cleaving side-activity of ketopantoate hydroxymethyltransferase (PanB). Front Microbiol. 7:431.

van Bruggen A, He M, Shin K, Mai V, Jeong K, Finckh M, Morris J. 2018. Environmental and health effects of the herbicide glyphosate. Sci. Total Environ. 616:255–268.

Vinnicombe H, Derrick J. 1999. Dihydropteroate synthase from *Streptococcus pneumoniae*: Characterization of substrate binding order and sulfonamide inhibition. Biochem. Biophys. Res. Commun. 258(3):752–757.

Wang X, Shen M, Zhou J, Jin Y. 2019. Chlorpyrifos disturbs hepatic metabolism associated with oxidative stress and gut microbiota dysbiosis in adult zebrafish. Comp. Biochem. Physiol. C Toxicol. Pharmacol. 216:19–28.

Wang X, Wang Q, Qi Q. 2015. Identification of riboflavin: Revealing different metabolic characteristics between *Escherichia coli* BL21(DE3) and MG1655. FEMS Microbiol. Lett. 362:pii fnv071.

World Health Organization (WHO). 2004. Reference for chlorpyrifos: report of pesticide residues in food. Geneva: WHO.

World Health Organization (WHO). 2016. Reference for glyphosate: report of pesticide residues in food. Geneva: WHO.

Wu W, Wang Y, Zou J, Long F, Yan H, Zeng L, Chen Y. 2017. *Bifidobacterium adolescentis* protects against necrotizing enterocolitis and up-regulates TOLLIP and SIGIRR in premature neonatal rats. BMC Pediatr. 17(1):1.

Zhao Y, Zhang Y, Wang G, Han R, Xie X. 2016. Effects of chlorpyrifos on the gut microbiome and urine metabolome in mouse (*Mus musculus*). Chemosphere. 153:287–293.

Publication 5: Quantification of glyphosate and AMPA from microbiome reactor fluids

Received: 30 May 2019 | Revised: 20 November 2019 | Accepted: 20 November 2019
DOI: 10.1002/rcm.8668

RESEARCH ARTICLE

Rapid Communications in Mass Spectrometry WILEY

Quantification of glyphosate and aminomethylphosphonic acid from microbiome reactor fluids

Katarina Fritz-Wallace[1] | Beatrice Engelmann[1] | Jannike L. Krause[2] | Stephanie S. Schäpe[1] | Judith Pöppe[3] | Gunda Herberth[2] | Uwe Rösler[3] | Nico Jehmlich[1] | Martin von Bergen[1,4] | Ulrike Rolle-Kampczyk[1]

[1]Department of Molecular Systems Biology, Helmholtz Centre for Environmental Research-UFZ, Leipzig, Germany

[2]Department of Environmental Immunology, Helmholtz Centre for Environmental Research-UFZ, Leipzig, Germany

[3]Institute for Animal Hygiene and Environmental Health, Freie Universität Berlin, Berlin, Germany

[4]Institute of Biochemistry, Faculty of Life Sciences, University of Leipzig, Leipzig, Germany

Correspondence
U. Rolle-Kampczyk, Department of Molecular Systems Biology, Helmholtz Centre for Environmental Research-UFZ, Leipzig, Germany.
Email: ulrike.rolle-kampczyk@ufz.de

Funding information
Bundesministerium für Ernährung und Landwirtschaft; Deutsche Bundesstiftung Umwelt; Deutsche Forschungsgemeinschaft, Grant/Award Number: SPP 1656; DBU; BMEL, Grant/Award Number: 2815HS018

Rationale: Glyphosate is one of the most widely used herbicides and it is suspected to affect the intestinal microbiota through inhibition of aromatic amino acid synthesis via the shikimate pathway. *In vitro* microbiome bioreactors are increasingly used as model systems to investigate effects on intestinal microbiota and consequently methods for the quantitation of glyphosate and its degradation product aminomethylphosphonic acid (AMPA) in microbiome model systems are required.

Methods: An optimized protocol enables the analysis of both glyphosate and AMPA by simple extraction with methanol:acetonitrile:water (2:3:1) without further enrichment steps. Glyphosate and AMPA are separated by liquid chromatography on an amide column and identified and quantified with a targeted tandem mass spectrometry method using a QTRAP 5500 system (AB Sciex).

Results: Our method has a limit of detection (LOD) in extracted water samples of <2 ng/mL for both glyphosate and AMPA. In complex intestinal medium, the LOD is 2 and 5 ng/mL for glyphosate and AMPA, respectively. These LODs allow for measurement at exposure-relevant concentrations. Glyphosate levels in a bioreactor model of porcine colon were determined and consequently it was verified whether AMPA was produced by porcine gut microbiota.

Conclusions: The method presented here allows quantitation of glyphosate and AMPA in complex bioreactor fluids and thus enables studies of the impact of glyphosate and its metabolism on intestinal microbiota. In addition, the extraction protocol is compatible with an untargeted metabolomics analysis, thus allowing one to look for other perturbations caused by glyphosate in the same sample.

1 | INTRODUCTION

Glyphosate is one of the most commonly used herbicides worldwide, and since the introduction of glyphosate-resistant crops in 1996 its use has dramatically increased.[1] Although possible health effects of glyphosate are vigorously discussed, there have been no credible reports of proven adverse effects of glyphosate on human and animal health.[1]

Glyphosate was originally designed and patented as an antibiotic. It inhibits the enzyme 5-enolpyruvylshikimate-3-phosphate synthase

Katarina Fritz-Wallace and Beatrice Engelmann contributed equally

(EPSPS), which is present in most bacteria as part of the shikimate pathway, and disrupts the production of aromatic amino acids.[2] As the shikimate pathway is present in higher plants, glyphosate was found to be an efficient general herbicide.[3] Since the shikimate pathway is absent in humans and animals, there is no mechanistic explanation for the observed effects of glyphosate on the redox status in mammalian cells[4-6] or its possible carcinogenicity.[7]

However, several microorganisms express a glyphosate-sensitive EPSPS, and thus the molecule may influence the gut microbiome of animals[8] and thereby mediate an adverse effect on a host. A recent study showed that glyphosate affects honey bees by altering their microbial community composition, and this may be a threat to bee health due to a greater susceptibility to pathogens.[9] For the mammalian microbiome, Lozano et al found a gender-specific effect on the composition of intestinal microbiota in rats[10] and Mao et al revealed effects in rats on the bacterial composition in the F1 generation.[11]

Apart from the inhibitory effect of glyphosate on EPSPS, some microorganisms are able to metabolize glyphosate. The first biodegradation route relies on the cleavage of the C&bond;P bond by carbon–phosphorus lyase, resulting in sarcosine and inorganic phosphorus. The second glyphosate degradation route is widespread and better understood. Glyphosate oxidoreductase catalyzes the cleavage of the C—N bond yielding aminomethylphosphonic acid (AMPA) and glyoxylate. While glyoxylate can be used as an energy substrate, AMPA is often exported to the extracellular space, as it can only be degraded by a few microorganisms.[12] Wang et al showed the degradation of glyphosate into amino acids in a water–sediment system,[13] suggesting a role of sediment during microbial degradation. In systems where AMPA is not further degraded, it may serve as an indicator for glyphosate degradation.[14] In order to study the effects of glyphosate on the microbiome, but also to estimate the actual exposure of the herbicide, methods for accurate quantitation in complex matrices are required.

One option for the determination of glyphosate concentrations is by enzyme-linked immunosorbent assay.[15] However, due to the higher flexibility of chromatographic methods in conjunction with mass spectrometry (MS), this approach is more widely used. The identification and quantitation of pesticides and herbicides from different matrices using gas chromatography or liquid chromatography (LC) coupled to MS have been proven to be precise[16-18] and thus useful. Due to the polar nature of glyphosate and the need to quantify small concentrations, there are reports of a variety of approaches, which all have specific advantages and drawbacks.

Chromatographic methods usually require purified samples, and therefore several extraction techniques for glyphosate and related metabolites have been developed. Due to the requirement for low detection limits, various enrichments based on solid-phase extraction (SPE) have been used.[19,20] SPE enables the enrichment of compounds from large sample volumes allowing for the detection of lower original concentrations of glyphosate. Mostly, SPE has been reported for the purification of glyphosate in a combination of different steps. However, every step in sample preparation potentially reduces reproducibility. Furthermore, as far as we know, there have been no reports of glyphosate extraction with SPE from complex bioreactor media.

One widely used method is based on the derivatization of the glyphosate molecule with fluorenylmethyloxycarbonyl chloride. The derivatization enables detection based on the fluorescence of the derivatized molecule.[21] Although LC/MS allows a more specific detection than UV, standard reversed-phase LC/MS on a C18 column of non-derivatized glyphosate cannot be applied due to the polar nature of the molecule. Hence, alternatives to the standard reversed-phase LC are needed. However, so far, literature reporting this has been sparse.[22] One alternative approach has used hydrophobic interaction LC coupled to MS for the analysis of glyphosate in various food items.[23]

Currently, glyphosate quantification methods have been established in water, soil, food products and body fluids such as urine and breast milk.[20,23-26] To the best of our knowledge, there are no studies reporting the quantitation of glyphosate from bacterial culture media used in bioreactors. Bioreactors can be used to simulate conditions found in the intestinal tract of animals and humans *in vitro*, but the media are accordingly complex. The options of *in vitro* gut fermentation models range from simple batch cultures to single- and multistage continuous flow models.[27] The latter permit a close evaluation while operating under well-defined culture conditions.[28] Environmental parameters such as temperature, anaerobiosis, pH and flow rate of the medium are closely monitored and controlled. However, changes in the microbiota community structure following inoculation are difficult to adjust.[29] When using liquid inoculation, a rapid washout of less competitive bacteria is generally experienced, restricting the experiment time to less than 4 weeks.[30]

In contrast to *in vivo* conditions, bioreactors are usually based on a homogeneous diet which realistically does not occur in microbiome hosts, especially not in humans. Another potential limitation is the missing interaction of the microbiome with the immune or neuroendocrine system of the host.[30] Nevertheless, the innovative technology of gut fermentation models facilitates a higher throughput of different conditions such as community structure and diet. In addition, exposure to other substances such as xenobiotics can be analyzed.[31] In view of social and ethical aspects, human studies are primarily limited to the analysis of fecal samples which do not necessarily reflect the community structure and function in the colon.[32]

The effect of herbicides like glyphosate on the microbiome of pigs is relevant as stock animals are exposed to higher amounts of glyphosate due to the higher maximum residue levels in animal feed. It has been reported that glyphosate concentrations in tested companion animal feed were higher than in human diets.[33] The impacts of a high exposure of pig colonic microbiota to glyphosate are currently unknown.

The aims of the study reported here were therefore (i) to develop a time- and cost-effective and reliable method for the extraction of glyphosate and its degradation product AMPA from a complex

bioreactor medium, (ii) to quantify glyphosate and AMPA at exposure-relevant concentrations from a complex intestinal medium and (iii) to be able to combine the measurement with an untargeted approach in order to allow for a high degree of multiplicity.

2 | MATERIALS AND METHODS

2.1 | Chemicals and reagents

Acetonitrile, methanol, ammonium acetate and ammonium hydroxide were all purchased from Sigma Aldrich (St Louis, MO, USA). All solvents for MS were of analytical grade purity. Experimental water (resistivity of 18.2 MΩ cm) was purified using a Milli-Q system (Millipore, Milford, MA, USA).

Roundup® unkrautfrei LB plus (Monsanto Agrar Deutschland GmbH, PZN 024142–00), simply called "Roundup" in the following text, was used as the glyphosate-based product to be analyzed. A standard stock solution of Roundup (10 μg/mL) was prepared in Milli-Q water.

Glyphosate (*N*-(phosphonomethyl)glycine) was obtained from Glentham Life Sciences Ltd (Corsham, UK) and AMPA was purchased from Sigma Aldrich (Darmstadt, Germany). Standard stock solutions for both (10 μg/mL) were prepared in Milli-Q water and stored at −20°C. Working dilutions were prepared in Milli-Q water immediately before use.

Phosphate-buffered saline (PBS) constituents NaCl, Na_2HPO_4 and KH_2PO_4 were all purchased from Merck (Darmstadt, Germany). Complex intestinal medium (CIM) pig, CIM human and brain–heart infusion (BHI) medium were used as matrices. Chemical compositions and corresponding suppliers of these bioreactor media are included in Tables S1–S3 (supporting information).

2.2 | Bioreactor model of swine colon

Three parallel 250 mL vessels (A, B and C) of a Multifors2 bioreactor system (Infors, Bottmingen, Switzerland) were inoculated with 0.5 g of colonic bacteria from two 8- to 9-week-old German Landrace pigs on day 0 (pig 1, bioreactors A and B; pig 2, bioreactor C). The bacteria were cultivated under anaerobic conditions, with constant stirring at 150 rpm and at 37°C. The pH was kept at 6.5 by automatic addition of 1 M NaOH and an average retention time of 48 h was chosen.[30] To prevent washing out of slow-dividing bacteria, continuous cultivation was started on day 1 with a dilution rate of 0.02. The bioreactors were then run for 25 days. After ten bioreactor turnovers, the communities were considered as stable. Thus, days 20 to 22 were considered as the control phase, as the community should not change unless there are external perturbations. The treatment phase lasted from days 23 to 25 when the bioreactors were treated with 10.7 mM Roundup. Roundup was directly spiked into the bioreactor vessels, and simultaneously the medium supply was changed to a medium containing 10.7 mM Roundup.

2.3 | Sampling and extraction

For biomass determination, 1 mL of bioreactor medium was pelleted (3200 *g*, 4°C, 10 min). The supernatant was discarded and the bacteria pellets were washed twice with PBS (140 mM NaCl, 10 mM Na_2HPO_4, 7 mM KH_2PO_4). The pellets were dried completely in a vacuum concentrator (MicroCenvac NB-503CIR, Acondor) at 45°C. Bacterial dry weight was determined using a precision scale (AC 210S, Sartorius).

Samples for glyphosate measurement were taken daily at 24 h intervals on days 20 to 25. The bacterial suspension was centrifuged (5000 *g*, 5 min, 4°C) and the supernatant was stored at −80°C until sample preparation. Extraction of glyphosate and AMPA was performed by adding 1000 μL of methanol:acetonitrile:water (2:3:1) to 100 μL of specimen. Samples were vortexed for 5 min, sonicated for 5 min and finally centrifuged at 14 000 × *g* for 10 min at room temperature. The supernatant was dried in a vacuum centrifuge (Concentrator Plus, Eppendorf AG Hamburg, Germany). The dried extract was dissolved in 100 μL of Milli-Q water and immediately used for LC/MS/MS analysis. The procedure was the same for all matrices, in particular water and the bioreactor media CIM pig, BHI and CIM human.

Samples with a concentration above the upper limit of quantitation were diluted with the appropriate media.

2.4 | Replicates

For the validation of the LC/MS method, we used five repeat injections as technical replicates. In order to show the robustness of the extraction method we used three biological replicates (i.e. three different bioreactors). From each bioreactor three aliquots were extracted separately and finally each extract was measured twice.

2.5 | LC/MS/MS analysis for selected reaction monitoring (SRM) method

For the analysis of glyphosate and AMPA using LC/MS/MS, 10 μL of resuspended extract was injected onto a BEH amide column (2.1 × 100 mm, 1.7 μm; Waters, Milford, MA, USA). The autosampler was kept at 10°C and the column oven was run at 30°C. The following solvents were used for the LC program. Solvent A: 66% H_2O, 33% acetonitrile, 10 mM ammonium acetate, 0.04% ammonium hydroxide, pH 9; solvent B: 10% H_2O, 90% acetonitrile, 10 mM ammonium acetate, 0.04% ammonium hydroxide, pH 9. The LC program was performed at a constant flow rate of 0.4 mL/min. The injection volume was 10 μL. Both glyphosate and AMPA were eluted with 0% B which was initially used to equilibrate the column. Afterwards, the column was cleaned with a gradient from 0% B to 100% B within 2.5 min. Then 100% B was held for 2 min and finally there was an equilibration step at 0% B for 3.4 min. Identification and quantitation of AMPA and glyphosate were based on specific SRM

traces for both analytes measured using a QTRAP® 5500 (Sciex, Framingham, MA, USA) in negative mode electrospray ionization. The ionization source settings were as follows: ion spray voltage, −4.5 kV; temperature, 450°C; curtain gas flow rate, 35 arbitrary units; collision gas, medium; ion source gases, 40 and 60 arbitrary units. The transitions and the specific corresponding declustering potentials and collision energies are provided in Table 1. Parameters were evaluated *a priori* using flow injection analysis. Data acquisition and analysis were performed in Analyst® software (version 1.6.2, Sciex).

2.6 | Method validation

The method was applied to water as a reference matrix and to various complex bioreactor media. Standard curves for all matrices were prepared with spiked amounts of glyphosate and AMPA and with addition of known amounts of Roundup for the measurement of bioreactor samples. The standards were then extracted in the same way as described above (section 2.3).

Method validation included the measurement of specificity, linearity, limit of detection (LOD), lower limit of quantification (LOQ), accuracy and precision (intra- and inter-assay variation). The specificity of the method was evaluated by comparing a blank matrix sample and a glyphosate and AMPA spiked sample (50 ng/mL). Standard curves were generated by a linear regression ($y = ax + b$) for all four matrices. The linearity was assessed at six concentrations, 2, 5, 20, 40, 200 and 500 ng/mL ($n = 5$), in all four matrices. The signal-to-noise ratio required for LOD and LOQ determination was established using the signal-to-noise script implemented in Analyst 1.6.2 software. A time window of 30 s before the peak of interest was defined as noise and the peak itself was selected in a time window of 0.1 min and defined as the signal. LOD and LOQ were estimated by the lowest concentration of spiked sample with a signal-to-noise ratio of at least 3 and 10, respectively. The accuracy (defined as the percentage recovery) and precision (defined as intra-assay variation and inter-assay variation measured as relative standard deviation (RSD)) were calculated at different concentration levels in each matrix. We considered a recovery of 70–120% as acceptable.

TABLE 1 SRM transitions and settings for glyphosate and AMPA measurement

Q1 *m/z*	Q3 *m/z*	Time (ms)	ID	DP (V)	CE (V)
110.0	79	50	AMPA_1	−60	−60
110.0	63	50	AMPA_2	−60	−60
168.0	79	50	Glypho_1	−110	−110
168.0	63	50	Glypho_2	−30	−30
168.0	150	50	Glypho_3	−30	−30
168.0	124	50	Glypho_4	−30	−30
168.0	81	50	Glypho_5	−30	−30

2.7 | Untargeted metabolomics

Extraction of bioreactor samples for untargeted metabolomics was performed as described in section 2.3.

For LC/MS/MS measurement, 10 µL of resuspended extract was injected into a high-performance LC quadrupole time-of flight instrument (6540 UHD Accurate-Mass Q-TOF LC/MS, Agilent Technologies, Santa Clara, CA, USA). Metabolites were separated on a C18 column at a flow rate of 0.3 mL/min with the following gradient of running solvent A (0.1% formic acid in water) and running solvent B (2% isopropanol, 0.1% formic acid in acetonitrile): 0–5 min, 1% B; 5.1–20 min, 1–100% B; 20.1–25 min, 1% B. The mass spectrometer was set up in centroid mode and in screening mode allowing the detection of ions with a mass-to-charge ratio of between 60 and 1000. After each full scan the most intense ion (threshold 200 counts) was subjected to fragmentation.

For data analysis, raw files (.d) were converted to mzML files using ProteoWizard.[34] Following the principles described by Alonso et al, the spectral processing was carried out using XCMS adapted for use via Galaxy.[35-37] The workflow included a peak picking step (using the xcmsSet script) followed by a grouping step and retention time alignment (using xcmsGroup and xcmsRetcor scripts). Settings for xcmsSet script were as follows: extraction method for peak identification, centWave; maximum tolerated ppm *m/z* deviation, 25; minimum and maximum peak width, 10 and 35 s; signal-to-noise threshold, 10; minimum difference in *m/z* for peaks with overlapping retention time, 0.05. The workflow finished with a fillPeak script and CAMERA annotate. This resulted in a feature matrix that was used for statistical analysis. The peaks were filtered using a blank subtraction. Medium blanks were subtracted from corresponding samples (pure medium without Roundup was subtracted from bioreactor samples which did not contain Roundup; medium supplemented with Roundup was subtracted from bioreactor samples treated with Roundup). Normalization and calculation of statistics were done in R.

3 | RESULTS AND DISCUSSION

3.1 | Rapid extraction and measurement of glyphosate and AMPA

In order to estimate effects of glyphosate, e.g. on a microbiome, a reliable method for the extraction and quantitation of glyphosate and its degradation product AMPA is required. In Figure 1 an optimized workflow for the analysis of glyphosate is presented. We used a simple one-step extraction protocol, which facilitates fast and reproducible results. A mix of methanol, acetonitrile and Milli-Q water was added to the sample. After vortexing, sonication and centrifugation, the supernatant was dried in a vacuum centrifuge. The glyphosate- and AMPA-containing residue was reconstituted in water for measurement. Separation of compounds was carried out on an amide column using a gradient of diluted acetonitrile at basic pH. Although the compounds of interest elute during the isocratic

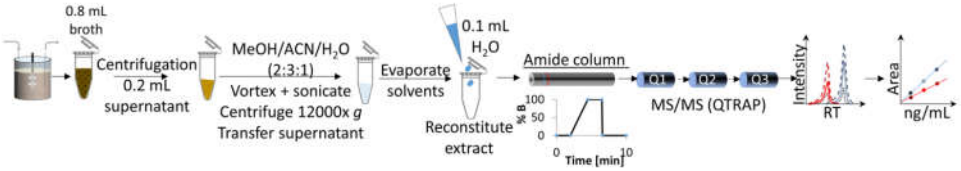

FIGURE 1 Exemplary workflow for the quantification of AMPA and glyphosate from bioreactor samples. After centrifugation of the culture broth, 100 µL of supernatant is used for the extraction with methanol, acetonitrile and water. After vortexing, sonication and centrifugation, the supernatant (containing glyphosate and AMPA) is dried in a vacuum centrifuge and finally the extract is reconstituted with 100 µL of water. AMPA and glyphosate are chromatographically separated on a BEH amide column and masses are determined with SRM using a QTRAP 5500 system (for details, see section 2)

part of the LC run, the gradient was needed to clean the column. Separation of glyphosate and AMPA was achieved (Figure 2) and unambiguous assignment of analytes due to different ion masses enabled reliable quantification.

The optimized parameters for MS/MS are described in section 2. Full-scan MS and the corresponding product ion scan for glyphosate and AMPA were performed in negative ionization mode. In full-scan MS, glyphosate produced a $[M-H]^-$ ion at m/z 168.0; the corresponding transition with the highest intensity was m/z 168.0 → 63.0 which was used for quantification. The $[M-H]^-$ ion of AMPA was at m/z 110, and the transition used for quantification was m/z 110.0 → 63.0.

3.2 | Method validation

In order to assess the applicability of this LC/MS method, standards of glyphosate and AMPA were diluted in water and analyzed. The absence of interfering peaks at the retention time of both analytes in all blank matrix samples verified the specificity of the method. A representative chromatogram of different blanks and spiked sample (in water and CIM pig) is shown in Figure S1 (supporting information). The linear response for glyphosate and AMPA ranged from 2 to

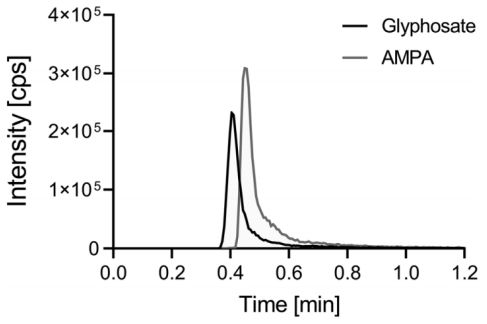

FIGURE 2 Exemplary chromatogram of the detection of glyphosate and AMPA standards with hydrophobic interaction LC/MS/MS

500 ng/mL in water with an average SEM of 3.15% for glyphosate and 3.69% for AMPA with four technical replicates (Figure S2, supporting information). In the studied range there was a linear correlation between intensity and concentration with R^2 values of 0.9994 and 0.9998 for glyphosate and AMPA, respectively.

A common problem with the analysis of glyphosate and AMPA is the extraction from complex matrices. Standard curves for AMPA and glyphosate were prepared in water as reference and in different complex bioreactor media (CIM pig, CIM human and BHI medium). Both analytes were spiked into the media and extracted with a mix of acetonitrile, methanol and Milli-Q water. This mixture precipitates most of the proteins and at the same time enables solubilization of small polar molecules. In addition, this mixture is used for the extraction of metabolites in our untargeted metabolomics workflow. Thus, the same composition was used in order to combine untargeted metabolomics with the targeted analysis of glyphosate within the same sample. Furthermore, the drying step concentrates compounds, while omitting the need for SPE methods. The absence of interfering peaks at the retention time of both analytes in all blank matrix samples verified the specificity of the method. A representative chromatogram of both blank and spiked sample is shown in Figure S1 (supporting information).

The linearity of the glyphosate standard curves was sufficient in the range 2 to 500 ng/mL (R^2 = 1) for water, 2 to 500 ng/mL (R^2 = 0.9995) for CIM pig, 5 to 500 ng/mL (R^2 = 0.9998) for CIM human and 10 to 500 ng/mL (R^2 = 0.9991) for BHI medium. The standard curve of extracted AMPA from water showed linearity in the range 2 to 500 ng/mL (R^2 = 0.9998). Linearity was achieved from 5 to 500 ng/mL (R^2 = 0.9999) in CIM pig and from 5 to 500 ng/mL (R^2 = 0.9999) in CIM human. AMPA measurement in BHI was rather difficult showing a linearity only between 10 and 500 ng/mL (R^2 = 0.9923). Probably, the nutritional composition of BHI hinders AMPA quantification at low concentration levels. Standard curves of both analytes in CIM pig are displayed in Figure 3 and standard curves measured in CIM human and BHI medium are shown in Figure S3 (supporting information).

All calibration curves were established for five technical replicates per concentration. The focus here was on validation of the LC/MS method; thus, each sample was injected five times. LOD and LOQ, defined as the lowest concentration that can be discriminated from

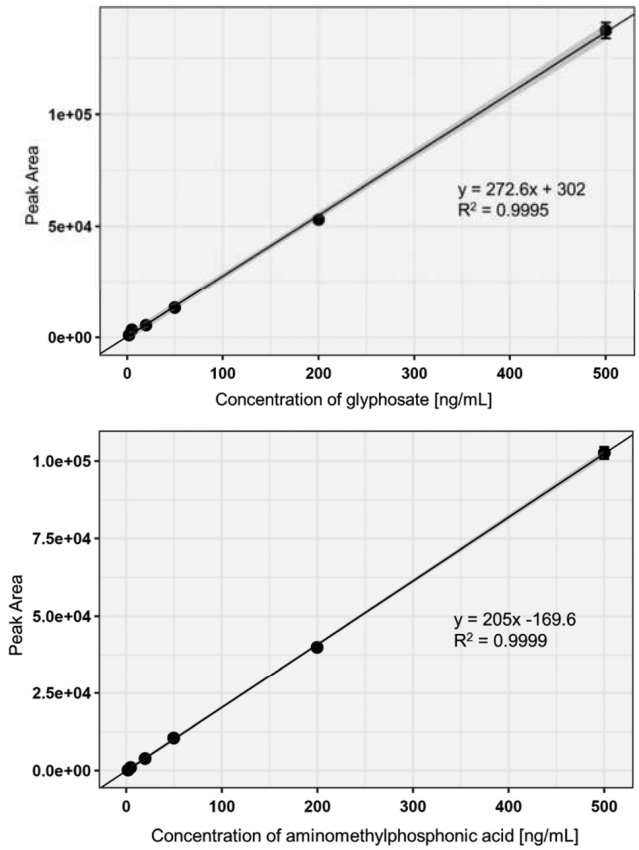

FIGURE 3 Calibration curves (n = 5) of glyphosate and AMPA in the range 2–500 ng/mL extracted from CIM pig

the background with a signal-to-noise ratio greater than 3 and 10, respectively, are presented in Table 2 for all tested matrices. As expected, LOD and LOQ were lowest for both AMPA and glyphosate when extracted from water. For glyphosate, a LOD of 0.5 ng/mL and a LOQ of 2 ng/mL were obtained. LOD and LOQ for AMPA were 0.5 and 1 ng/mL, respectively. Detection and quantification limits for glyphosate and AMPA were higher in the investigated bioreactor media (Table 2). The recovery rates are presented as mean percentages for 5 and 50 ng/mL in Table 3. For glyphosate and AMPA, the recovery rates ranged from 95.3% to 101.0% in water, from 95.4% to 227.0% in CIM pig and from 79.1% to 106.5% in CIM human. Spiked concentration of 5 ng/mL showed a recovery of 227.0% in CIM pig, failing the desired recovery. Considering the precision of the calibration curve, this measurement can be seen as an outlier.

TABLE 2 Determined LOD and LOQ of glyphosate and AMPA in all tested matrices

	Glyphosate (ng/mL)		AMPA (ng/mL)	
Matrix	LOD	LOQ	LOD	LOQ
Water	0.5	2	0.5	1
CIM	2	20	5	20
CIM human	5	20	5	20
BHI medium	10	50	10	50

Both analytes fulfilled the accuracy criterion range of 70–120% in water and two of the used bioreactor media, indicating that the presented method can be considered as reliable and reproducible. In BHI medium the signal-to-noise ratio was lower than 3 at 5 ng/mL and the recovery of glyphosate and AMPA was therefore only calculated at 50 ng/mL.

Values of RSD of less than 20% and 10% (n = 4) were defined as acceptable precisions for inter-assay and intra-assay variation, respectively. For glyphosate and AMPA, the RSD was calculated for 5 and 50 ng/mL (Table 3). In general, inter-assay variation was better

TABLE 3 Percentage recovery, intra-assay variation and inter-assay variation of glyphosate and AMPA in all analyzed matrices

Extraction matrix	Water				CIM				CIM human				BHI	
	Glyphosate		AMPA		Glyphosate		AMPA		Glyphosate		AMPA		Glyphosate	AMPA
Spiked concentration (ng/mL)	5	50	5	50	5	50	5	50	5	50	5	50	50	50
Recovery (%)	101.0	100.7	99.7	95.3	227.0	95.4	117.7	103.5	79.1	106.5	78.9	101.2	102.1	121.5
Intra-assay variation, RSD (%)	6.3	10.2	7.6	8.1	3.3	4.4	1.2	2.5	8.4	6.9	1.1	4.5	3.8	2.8
Inter-assay variation, RSD (%)	12.2	9.14	19.3	17.8	5.6	8.5	12.3	8.5	1.7	6.2	5.9	4.7	5.2	15.8

for glyphosate measurement, ranging from 1.7% to 12.3% compared with 4.7% to 19.3% for AMPA measurement across all analyzed matrices. The intra-assay variation was slightly better for AMPA measurement (1.1–8.1%) than for glyphosate measurement (3.3–10.2%). For all analyzed matrices, the RSD for inter-assay and intra-assay variation was lower than 20% and 10%, respectively (Table 3).

Previously reported approaches for detection of glyphosate include gas chromatography, high-performance liquid chromatography, ion chromatography as well as MS-coupled methods. Often, derivatization is required for analysis, thus adding a time-consuming step. In the last few years an increasing number of methods have been published omitting the tedious derivatization step.[20,38] However, pre-purification of the sample via an SPE cartridge or other enrichment strategies is often included.[20]

LC/MS/MS omits the need for a derivatization step, thus improving recovery and reproducibility. Our aim was to establish a simple extraction step without enrichment, derivatization or filtration. In order to achieve lower LOD and LOQ, direct injection methods have been applied. However, due to matrix interferences, direct injection methods are only applicable for relatively clean matrices, such as water or simple water-based matrices.[25,38,39] A glyphosate detection limit of 0.25 ng/mL has been reported in water samples without extraction but with a filtering step.[25] In urine, Sierra-Diaz et al could quantify concentrations of 0.363 µg/mL.[32] These methods are not likely to be applicable to bioreactor fluids due to their complexity and an extraction step will be needed. Our method provides this extraction step while still maintaining high recovery and reproducibility for the measurement of glyphosate and AMPA.

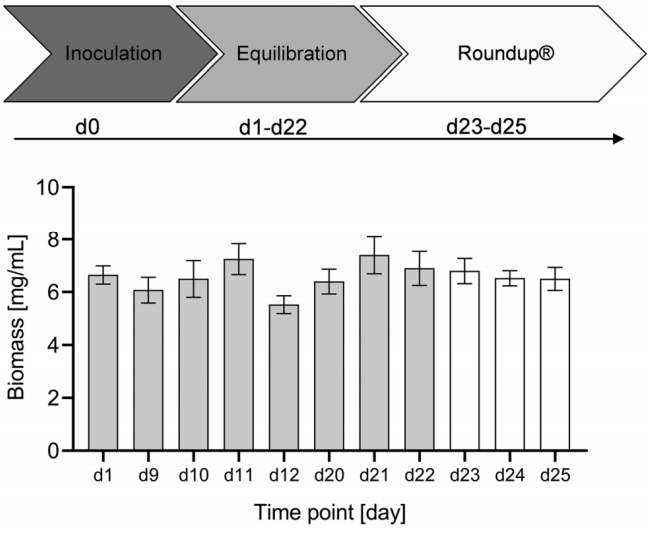

FIGURE 4 Determined mean biomass concentrations ±SEM per day are displayed. Three parallel 250 mL vessels of a bioreactor system were inoculated with 0.5 g of colonic bacteria from two 8- to 9-week-old German Landrace pigs on day 0. After 22 days of equilibration, Roundup (1.8 g/L) was spiked into the bioreactors (days 23 to 25)

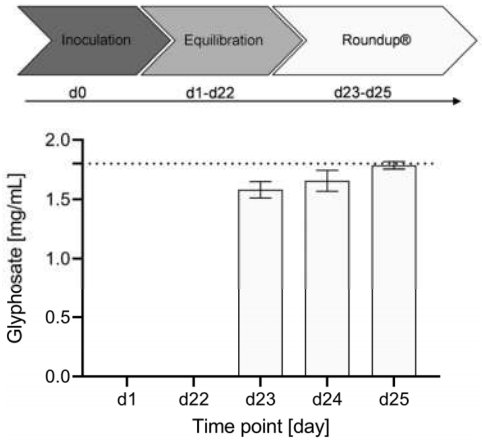

FIGURE 5 Experimental setup with measured glyphosate concentrations in bioreactor samples. After addition of glyphosate to a final concentration of 1.8 mg/mL (dotted line), a mean concentration of 1.68 mg/mL (day 23–25) was detected

3.3 | Application

In recent years, glyphosate quantification has been established in different matrices including water, soil and food.[20,23,24,26] Nevertheless, it was claimed that the current methodology for glyphosate analysis is not sufficient, stating that monitoring should be intensified.[33] Since there is an interest in the effect of glyphosate on the metabolism of intestinal microbiota, we applied the method to quantify glyphosate and AMPA in bioreactor media. The addition of Roundup to bioreactors containing porcine colonic bacteria was monitored. The bacterial communities were equilibrated for 21 days, which is equivalent to ten bioreactor turnovers. Then Roundup was spiked into the bioreactors directly after sampling and the medium supply was also exchanged to a medium including Roundup. Samples were drawn daily during the control phase (days 20 to 22) and the treatment phase (days 23 to 25). As the concentration of glyphosate added to the bioreactor was higher than accounted for by the calibration curve, samples were diluted with fresh medium before extraction to get the concentration within the linear range. Although Roundup was applied in a high concentration equal to 10.7 mM or 1.8 mg/mL glyphosate, an effect on the biomass could not be observed (Figure 4). The absence of an effect on biomass does not

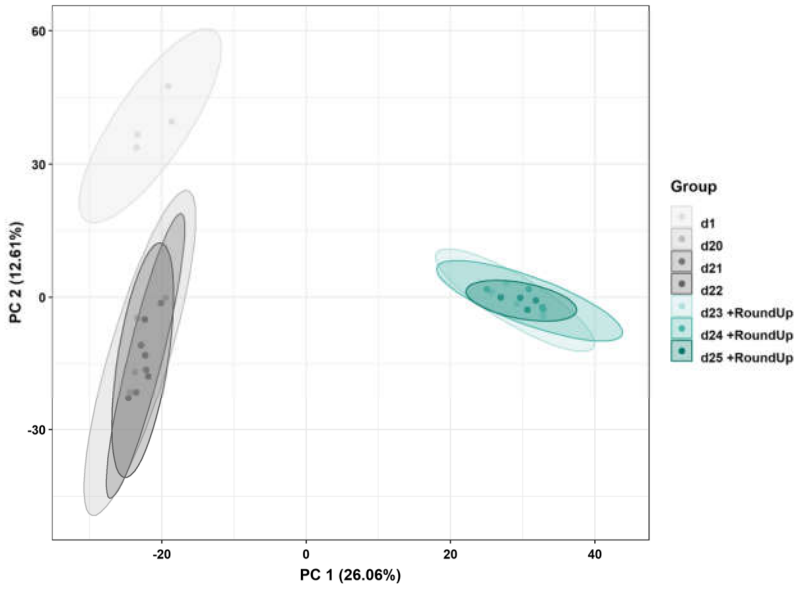

FIGURE 6 Principal component analysis of all bioreactor media samples. Each dot represents one bioreactor and color indicates the group. Each ellipse displays the 95% confidence interval per group. Performance was done using blank-subtracted and median-normalized data. Grouping is based on the day of cultivation: day 1, 24 h after inoculation; days 20–22, controls; days 23–25, Roundup addition. PC, principal component

exclude the possibility of a functional disturbance in the community. After the addition of glyphosate a mean concentration of 1.68 mg/mL (days 23–25) was detected (Figure 5), corresponding to a recovery of 93%. In the samples up to day 22 no glyphosate could be detected. AMPA was detected in the analyzed bioreactor fluid on days 23–25. However, the peak areas for AMPA were similar to those for Roundup itself, suggesting a missing metabolism of glyphosate by the intestinal microbiota during the treatment phase.

Medium complexity is a relevant topic in bioreactor cultivation because compositions of media are crucial for bacterial cultivation in batch culture and chemostat models.[40] At this point we can detect and quantify glyphosate and its main degradation product AMPA at exposure-relevant concentrations in different bacterial culture media, representative of complex culture compositions.

3.4 | Extraction method is compatible with untargeted metabolomics

Untargeted metabolomics was used to evaluate the metabolic profile of the medium before and after the addition of Roundup. Metabolic profiles of pure medium with and without Roundup were subtracted from those of the appropriate bioreactor samples to ensure that detected differences were based on the addition of Roundup itself.

Unsupervised principal component analysis of the metabolic profile was conducted to get an impression of the overall variations between the samples (Figure 6). Identification of metabolites was omitted as this was not the aim of this study, but rather to show the compatibility with the untargeted metabolomics method. Each dot represents one bioreactor medium sample and the color indicates the group. Control samples of days 20 to 22 and the samples of the days in which Roundup was supplemented to the bioreactor medium are separated based on the first two principal components. The difference between day 1 and all other later time points without Roundup was expected. In a model community, SIHUMIx takes five days to stabilize the community, and this can also be observed in the metabolic profile. Once the community is stable small perturbations like the transit time only slightly affect the community.[41,42] However, the more complex community arising from pig colon content is expected to be even more stable against external influences.

Although there was no effect on the biomass, the metabolic profile is influenced by the addition of Roundup. As Roundup is a mixture of various chemicals, the effect of glyphosate is inconclusive. However, this is not the aim of this study, but rather to show the compatibility of the two different methods. Although glyphosate could be detected in the untargeted approach, the sensitivity is not sufficient for determination of low glyphosate concentrations and thus renders necessary the targeted approach presented here.

4 | CONCLUSIONS

We present a simple method for the extraction of glyphosate and its degradation product AMPA from complex matrices such as bioreactor media. Identification and quantification were realized using a targeted LC/MS/MS method, which enables the quantification of glyphosate and AMPA at exposure-relevant concentrations. Due to the simple sample extraction and preparation procedure, the methodology allows for the possibility of robust and high-throughput detection and quantification. Negative mode electrospray ionization with SRM gives excellent sensitivity and selectivity. The establishment of the technique for other related matrices and media is still ongoing.

This extraction method is compatible with untargeted profiling of metabolites, enabling the quantification of glyphosate and AMPA and the characterization of the metabolome from the same samples, thus combining hypothesis-generating workflows with the quantification of glyphosate and AMPA. This is especially relevant, as it is still uncertain as to whether glyphosate has mechanisms of action independent of EPSPS.

ACKNOWLEDGEMENTS

MvB and URK are grateful for funding by the BMEL-funded GlyphoBac Project (2815HS018). JLK is funded by the DBU (German Federal Environmental Foundation) and SSS is grateful for the support from Deutsche Forschungsgemeinschaft SPP 1656. The authors also thank Nicole Gröger for her excellent technical support and Sven-Bastiaan Haange for beneficial discussions.

ORCID

Katarina Fritz-Wallace https://orcid.org/0000-0002-2317-9387

REFERENCES

1. Myers JP, Antoniou MN, Blumberg B, et al. Concerns over use of glyphosate-based herbicides and risks associated with exposures: A consensus statement. *Environ Health*. 2016;15(1):19. https://doi.org/10.1186/s12940-016-0117-0
2. Amrhein N, Schab J, Steinrucken HC. The mode of action of the herbicide glyphosate. *Naturwissenschaften*. 1980;67(7):356-357.
3. Jaworski EG. Mode of action of N-phosphonomethylglycine. Inhibition of aromatic amino-acid biosynthesis. *J Agric Food Chem*. 1972;20(6):1195-1198. https://doi.org/10.1021/jf60184a057
4. Mesnage R, Renney G, Seralini GE, Ward M, Antoniou MN. Multiomics reveal non-alcoholic fatty liver disease in rats following chronic exposure to an ultra-low dose of Roundup herbicide. *Sci Rep*. 2017;7(1):39328. https://doi.org/10.1038/srep39328
5. Kasuba V, Milic M, Rozgaj R, et al. Effects of low doses of glyphosate on DNA damage, cell proliferation and oxidative stress in the HepG2 cell line. *Environ Sci Pollut Res Int*. 2017;24(23):19267-19281. https://doi.org/10.1007/s11356-017-9438-y
6. Martini CN, Gabrielli M, Brandani JN, Vila M d C. Glyphosate inhibits PPAR gamma induction and differentiation of preadipocytes and is able to induce oxidative stress. *J Biochem Mol Toxicol*. 2016;30(8):404-413. https://doi.org/10.1002/jbt.21804
7. De Roos AJ, Blair A, Rusiecki JA, et al. Cancer incidence among glyphosate-exposed pesticide applicators in the agricultural health study. *Environ Health Perspect*. 2005;113(1):49-54. https://doi.org/10.1289/ehp.7340
8. Dai P, Yan Z, Ma S, et al. The herbicide glyphosate negatively affects midgut bacterial communities and survival of honey bee during larvae reared in vitro. *J Agric Food Chem*. 2018;66(29):7786-7793. https://doi.org/10.1021/acs.jafc.8b02212

9. Motta EVS, Raymann K, Moran NA. Glyphosate perturbs the gut microbiota of honey bees. *Proc Natl Acad Sci U S A*. 2018;115(41):10305-10310. https://doi.org/10.1073/pnas.1803880115
10. Lozano VL, Defarge N, Rocque LM, et al. Sex-dependent impact of Roundup on the rat gut microbiome. *Toxicol Rep*. 2018;5:96-107. https://doi.org/10.1016/j.toxrep.2017.12.005
11. Mao Q, Manservisi F, Panzacchi S, et al. The Ramazzini institute 13-week pilot study on glyphosate and Roundup administered at human-equivalent dose to Sprague Dawley rats: Effects on the microbiome. *Environ Health*. 2018;17(1):50. https://doi.org/10.1186/s12940-018-0394-x
12. la Cecilia D, Maggi F. Analysis of glyphosate degradation in a soil microcosm. *Environ Pollut*. 2018;233:201-207. https://doi.org/10.1016/j.envpol.2017.10.017
13. Wang S, Liu B, Yuan D, Ma J. A simple method for the determination of glyphosate and aminomethylphosphonic acid in seawater matrix with high performance liquid chromatography and fluorescence detection. *Talanta*. 2016;161:700-706. https://doi.org/10.1016/j.talanta.2016.09.023
14. Sviridov AV, Shushkova TV, Ermakova IT, Ivanova EV, Epiktetov DO, Leont'evskii AA. Microbial degradation of glyphosate herbicides (review). *Appl Biochem Microbiol*. 2015;51(2):183-190. https://doi.org/10.1134/S0003683815020209
15. Berg CJ, King HP, Delenstarr G, Kumar R, Rubio F, Glaze T. Glyphosate residue concentrations in honey attributed through geospatial analysis to proximity of large-scale agriculture and transfer off-site by bees. *PLoS ONE*. 2018;13(7):e0198876. https://doi.org/10.1371/journal.pone.0198876
16. Grimalt S, Dehouck P. Review of analytical methods for the determination of pesticide residues in grapes. *J Chromatogr A*. 2016;1433:1-23. https://doi.org/10.1016/j.chroma.2015.12.076
17. Masia A, Suarez-Varela MM, Llopis-Gonzalez A, Pico Y. Determination of pesticides and veterinary drug residues in food by liquid chromatography-mass spectrometry: A review. *Anal Chim Acta*. 2016;936:40-61. https://doi.org/10.1016/j.aca.2016.07.023
18. Souza Tette PA, Rocha Guidi L, de Abreu Gloria MB, Fernandes C. Pesticides in honey: A review on chromatographic analytical methods. *Talanta*. 2016;149:124-141. https://doi.org/10.1016/j.talanta.2015.11.045
19. Borjesson E, Torstensson L. New methods for determination of glyphosate and (aminomethyl)phosphonic acid in water and soil. *J Chromatogr A*. 2000;886(1-2):207-216. https://doi.org/10.1016/S0021-9673(00)00514-8
20. Nagatomi Y, Yoshioka T, Yanagisawa M, Uyama A, Mochizuki N. Simultaneous LC–MS/MS analysis of glyphosate, glufosinate, and their metabolic products in beer, barley tea, and their ingredients. *Biosci Biotechnol Biochem*. 2013;77(11):2218-2221. https://doi.org/10.1271/bbb.130433
21. Sancho J, Hérnandez F, López F, Hogendoorn E, Dijkman E, Pv Z. Rapid determination of glufosinate, glyphosate and AMPA in environmental water samples. *J Chromatogr A*. 1996;737(1):75-83. https://doi.org/10.1080/03067319608027052
22. Nielsen LN, Roager HM, Casas ME, et al. Glyphosate has limited short-term effects on commensal bacterial community composition in the gut environment due to sufficient aromatic amino acid levels. *Environ Pollut*. 2018;233:364-376. https://doi.org/10.1016/j.envpol.2017.10.016
23. Li X, Xu J, Jiang Y, Chen L, Xu Y, Pan C. Hydrophilic-interaction liquid chromatography (HILIC) with DAD and mass spectroscopic detection for direct analysis of glyphosate and glufosinate residues and for product quality control. *Acta Chromatogr*. 2009;21(4):559-576. https://doi.org/10.1556/AChrom.21.2009.4.4
24. Emily Guo FR. Survey of glyphosate residues in honey, corn and soy products. *J Environ Anal Toxicol*. 2014;05(01):249. https://doi.org/10.4172/2161-0525.1000249
25. Okada E, Coggan T, Anumol T, Clarke B, Allinson G. A simple and rapid direct injection method for the determination of glyphosate and AMPA in environmental water samples. *Anal Bioanal Chem*. 2019;411(3):715-724. https://doi.org/10.1007/s00216-018-1490-z
26. Silva V, Montanarella L, Jones A, et al. Distribution of glyphosate and aminomethylphosphonic acid (AMPA) in agricultural topsoils of the European Union. *Sci Total Environ*. 2018;621:1352-1359. https://doi.org/10.1016/j.scitotenv.2017.10.093
27. Payne AN, Zihler A, Chassard C, Lacroix C. Advances and perspectives in in vitro human gut fermentation modeling. *Trends Biotechnol*. 2012;30(1):17-25. https://doi.org/10.1016/j.tibtech.2011.06.011
28. Wissenbach DK, Oliphant K, Rolle-Kampczyk U, et al. Optimization of metabolomics of defined in vitro gut microbial ecosystems. *Int J Med Microbiol*. 2016;306(5):280-289. https://doi.org/10.1016/j.ijmm.2016.03.007
29. Macfarlane GT, Macfarlane S. Models for intestinal fermentation: Association between food components, delivery systems, bioavailability and functional interactions in the gut. *Curr Opin Biotechnol*. 2007;18(2):156-162. https://doi.org/10.1016/j.copbio.2007.01.011
30. Macfarlane GT, Macfarlane S, Gibson GR. Validation of a three-stage compound continuous culture system for investigating the effect of retention time on the ecology and metabolism of bacteria in the human colon. *Microb Ecol*. 1998;35(2):180-187. https://doi.org/10.1007/s002489900072
31. Guzman-Rodriguez M, McDonald JAK, Hyde R, et al. Using bioreactors to study the effects of drugs on the human microbiota. *Methods*. 2018;149:31-41. https://doi.org/10.1016/j.ymeth.2018.08.003
32. Haange SB, Oberbach A, Schlichting N, et al. Metaproteome analysis and molecular genetics of rat intestinal microbiota reveals section and localization resolved species distribution and enzymatic functionalities. *J Proteome Res*. 2012;11(11):5406-5417. https://doi.org/10.1021/pr3006364
33. Zhao J, Pacenka S, Wu J, et al. Detection of glyphosate residues in companion animal feeds. *Environ Pollut*. 2018;243(Pt B):1113-1118. https://doi.org/10.1016/j.envpol.2018.08.100
34. Chambers MC, Maclean B, Burke R, et al. A cross-platform toolkit for mass spectrometry and proteomics. *Nat Biotechnol*. 2012;30(10):918-920. https://doi.org/10.1038/nbt.2377
35. Alonso A, Marsal S, Julia A. Analytical methods in untargeted metabolomics: State of the art in 2015. *Front Bioeng Biotechnol*. 2015;3:23. https://doi.org/10.3389/fbioe.2015.00023
36. Smith CA, Want EJ, O'Maille G, Abagyan R, Siuzdak G. XCMS: Processing mass spectrometry data for metabolite profiling using nonlinear peak alignment, matching, and identification. *Anal Chem*. 2006;78(3):779-787. https://doi.org/10.1021/ac051437y
37. Giacomoni F, Le Corguille G, Monsoor M, et al. Workflow4Metabolomics: A collaborative research infrastructure for computational metabolomics. *Bioinformatics*. 2015;31(9):1493-1495. https://doi.org/10.1093/bioinformatics/btu813
38. Hao C, Morse D, Morra F, Zhao X, Yang P, Nunn B. Direct aqueous determination of glyphosate and related compounds by liquid chromatography/tandem mass spectrometry using reversed-phase and weak anion-exchange mixed-mode column. *J Chromatogr A*. 2011;1218(33):5638-5643. https://doi.org/10.1016/j.chroma.2011.06.070
39. Sierra-Diaz E, Celis-de la Rosa AD, Lozano-Kasten F, et al. Urinary pesticide levels in children and adolescents residing in two agricultural communities in Mexico. *Int J Environ Res Public Health*. 2019;16(4):562. https://doi.org/10.3390/ijerph16040562
40. Tramontano M, Andrejev S, Pruteanu M, et al. Nutritional preferences of human gut bacteria reveal their metabolic idiosyncrasies.

Nat Microbiol. 2018;3(4):514-522. https://doi.org/10.1038/s41564-018-0123-9

41. Krause JL, Schaepe SS, Fritz-Wallace K, et al. Following the community development of SIHUMIx - a new intestinal in vitro model for bioreactor use. *Gut Microbes*. 2020:1-14. https://doi.org/10.1080/19490976.2019.1702431
42. Schäpe SS, Krause JL, Engelmann B, et al. The Simplified Human Intestinal Microbiota (SIHUMIx) shows high structural and functional resistance against changing transit times in in vitro bioreactors. *Microorganisms*. 2019;7(12):641. https://doi.org/10.3390/microorganisms7120641

SUPPORTING INFORMATION

Additional supporting information may be found online in the Supporting Information section at the end of this article.

How to cite this article: Fritz-Wallace K, Engelmann B, Krause JL, et al. Quantification of glyphosate and aminomethylphosphonic acid from microbiome reactor fluids. *Rapid Commun Mass Spectrom*. 2020;34:e8668. https://doi.org/10.1002/rcm.8668

Publication 6: The glyphosate formulation Roundup® LB plus influences the global metabolome of pig gut microbiota *in vitro*

Science of the Total Environment xxx (xxxx) 140932

Contents lists available at ScienceDirect

Science of the Total Environment

journal homepage: http://ees.elsevier.com

The glyphosate formulation Roundup® LB plus influences the global metabolome of pig gut microbiota *in vitro*

Jannike L. Krause [a,1,*], Sven-Bastiaan Haange [b,1], Stephanie S. Schäpe [b], Beatrice Engelmann [b], Ulrike Rolle-Kampczyk [b], Katarina Fritz-Wallace [b,d], Zhipeng Wang [b], Nico Jehmlich [b], Dominique Türkowsky [b], Kristin Schubert [b], Judith Pöppe [e], Katrin Bote [e], Uwe Rösler [e], Gunda Herberth [a], Martin von Bergen [b,c]

[a] *Helmholtz-Centre for Environmental Research - UFZ, Department of Environmental Immunology, Leipzig, Germany*
[b] *Helmholtz-Centre for Environmental Research - UFZ, Department of Molecular Systems Biology, Leipzig, Germany*
[c] *Institute of Biochemistry, Faculty of Biosciences, Pharmacy and Psychology, University of Leipzig, Germany*
[d] *National Center for Tumor Diseases - NCT, Dresden, Germany*
[e] *Institute for Animal Hygiene and Environmental Health, Freie Universität Berlin, Berlin, Germany*

ARTICLE INFO

Article history:
Received 3 June 2020
Received in revised form 6 July 2020
Accepted 11 July 2020
Available online xxx
Editor: Jay Gan

Keywords
16S
Metaproteome
Meta-metabolome
Continuous *in vitro* culture
Bioreactor
Microbiome

ABSTRACT

Glyphosate is the world's most widely used herbicide, and its potential side effects on the intestinal microbiota of various animals, from honeybees to livestock and humans, are currently under discussion. Pigs are among the most abundant livestock animals worldwide and an impact of glyphosate on their intestinal microbiota function can have serious consequences on their health, not to mention the economic effects. Recent studies that addressed microbiota-disrupting effects focused on microbial taxonomy but lacked functional information.Therefore, we chose an experimental design with a short incubation time in which effects on the community structure are not expected, but functional effects can be detected. We cultivated intestinal microbiota derived from pig colon in chemostats and investigated the acute effect of 228 mg/d glyphosate acid equivalents from Roundup® LB plus, a frequently applied glyphosate formulation. The applied glyphosate concentration resembles a worst-case scenario for an 8–9 week-old pig and relates to the maximum residue levels of glyphosate on animal fodder. The effects were determined on the functional level by metaproteomics, targeted and untargeted meta-metabolomics, while variations in community structure were analyzed by 16S rRNA gene profiling and on the single cell level by microbiota flow cytometry. Roundup® LB plus did not affect the community taxonomy or the enzymatic repertoire of the cultivated microbiota in general or on the expression of the glyphosate target enzyme 5-enolpyruvylshikimate-3-phosphate synthase in detail. On the functional level, targeted metabolite analysis of short chain fatty acids (SCFAs), free amino acids and bile acids did not reveal significant changes, whereas untargeted meta-metabolomics did identify some effects on the functional level. This multi-omics approach provides evidence for subtle metabolic effects of Roundup® LB plus under the conditions applied.

1. Introduction

Since 2015, the debate about possible health risks of glyphosate for humans and livestock has come into the medial focus (Tarazona et al., 2017). Glyphosate-based herbicides are the most frequently used pesticide group worldwide (Benbrook, 2016) with applications ranging from agricultural to non-agricultural applications (Hanke et al., 2010). Consequently, it enters the organisms after the consumption of contaminated food or fodder (Licht and Bahl, 2019; Claus et al., 2016). In humans, but also in cows and rats, glyphosate is primarily taken up *via* the diet (Brewster et al., 1991) and therefore the intestinal microbiota is especially prone to exposure. Glyphosate targets the enzyme 5-enolpyruvylshikimate-3-phosphate synthase (EPSPS) from the shikimate pathway and thus blocks the synthesis of the aromatic amino acids tyrosine, phenylalanine and tryptophan (Amrhein et al., 1980). As only organism group, animals lack the shikimate pathway and thus the EPSPS. Hence, to date glyphosate is considered safe for humans and animals (Myers et al., 2016). Similar to plants, most microorganisms use the shikimate pathway to synthesize aromatic amino acids. Two classes of the EPSPS exist in bacteria: the glyphosate sensitive class I EPSPS (Funke et al., 2009) and the glyphosate insensitive class II EPSPS (Priestman et al., 2005). Glyphosate has antimicrobial properties (US patent 7771736 B2) and thus could potentially affect growth of sensitive species *e.g.* in the intestine. Several studies have investigated the effect of glyphosate acid or glyphosate-based formulations on the intestinal microbiota (Tsiaoussis et al., 2019) *in vivo* and *in vitro* studies at different concentrations and in different species, not surprisingly leading to contrary results.

In vivo studies pose four major challenges when assessing microbiota-modulating effects. First, host effects can distort the conclusions drawn from ana-

* Corresponding author.
martin.vonbergen@ufz.de
E-mail address: jannike-lea.krause@ufz.de (J.L. Krause)
[1] Authors contributed equally

https://doi.org/10.1016/j.scitotenv.2020.140932

lyzing the taxonomic or functional parameters of the microbiota (Payne et al., 2012). Second, cage-effects coming from animal housing and exposure in separate treatment groups can facilitate the misinterpretation of results. Third, the characterization of the initial microbiota, to discriminate treatment-related community shifts from normal variation, is often neglected. Fourth, microbiota at different facilities from different animal strains might respond differently (Macpherson and McCoy, 2015). One option to address these challenges is to use *in vitro* cultivation systems with defined cultivation parameters. This allows the long-term cultivation of microbiota and the investigation of acute or chronic microbiota modulating effects coming from the exposure itself (Payne et al., 2012).

Healthy intestinal microbiota shows a high inter-individual taxonomic variability between individual hosts, though they share the same "healthy" functional repertoire (Qin et al., 2010; Turnbaugh et al., 2007). Thus, microbial communities can shift in their distribution of taxa and still exhibit "healthy" functional properties for the host. Consequently, these alterations might be considered neutral, beneficial or harmful, depending on their contribution to a diseased state (Levy et al., 2017; Lozupone et al., 2012). Therefore, concentrating on the functional repertoire is essential to identify non-healthy states (Levy et al., 2017; Lozupone et al., 2012). The effect of glyphosate on microorganisms was investigated *in vitro* on pure bacterial batch cultures from poultry (Shehata et al., 2013) and continuous cultures of bovine rumen microbiota (Riede et al., 2016). However, the latter study primarily focused on taxonomic changes upon glyphosate exposure.

Over the past decade, culture-independent methods like metagenomics, metatranscriptomics, metaproteomics, meta-metabolomics (hereafter metabolomics) and cytomics have been developed to investigate functional and structural properties in microbiota. Metagenomics captures the potential physiology of a microbiota but lacks the discrimination between live and dead cells (Xu, 2006). Even though the metagenome-based prediction of functionality has improved, there is still a great need to verify the potential activity by analyzing the functional activity (Franzosa et al., 2015). Metatranscriptomics allows time-point specific insights into the transcriptional regulation of the microbiota, but still lacks the functional proof (Bashiardes et al., 2016), whereas metaproteomics provides real functional information and furthermore provides information on the taxonomy by analyzing microbial enzymes (Heintz-Buschart and Wilmes, 2018; von Bergen et al., 2013). Metabolomics complements metaproteomics by measuring the metabolites arising from enzymatic activity (Yadav et al., 2018). Cytomics captures microbial community structure variations on the single-cell level by measuring optical characteristics, but does not resolve functional processes performed in individual bacterial cells (Koch et al., 2013).

With our approach, we circumvent possible challenges from *in vivo* exposure and analyze the effects of Roundup® LB plus on continuously cultivated pig colonic microbiota. We analyzed the taxonomic distribution as a baseline analysis and focused on functional effects by the application of a comprehensive multi-omics approach. Therefore, in this study, we acutely exposed pig microbiota to Roundup® LB plus at a reasonable high concentration of 228 mg/d glyphosate equivalents. The species composition was assessed by 16 S RNA gene profiling and the enzymatic repertoire and the subsequent metabolites by metaproteomics and metabolomics.

2. Materials and methods

2.1. Chemicals and reagents

Acetonitrile, methanol, ammonium acetate and ammonium hydroxide were purchased from Sigma Aldrich (St.Louis, MO, USA). Solvents for mass spectrometry were of analytical grade purity. Experimental water (resistivity 18.2 MΩcm) was purified using a Milli-Q-System (Millipore, Milford, MA, USA).

For *in vitro* exposure of intestinal microbiota, the glyphosate-based herbicide Roundup® LB plus (Monsanto Agrar Deutschland GmbH, PZN 250524, approval number 024142-60) was used. Roundup® LB plus is a mixture of water (42.5%), glyphosate isopropylamine salt (41.5%), and

For glyphosate quantitation, a standard stock solution of Roundup® LB plus (10 μg/mL) was prepared in Milli-Q water. Glyphosate (N-(phosphonomethyl)-glycine) was obtained from Glentham Life Sciences Ltd. (Wiltshire, UK). Standard stock solutions (10 μg/mL) were prepared in Milli-Q water and stored at −20 °C. Working dilutions were prepared in Milli-Q-water before use.

2.2. Bioreactor model of pig colonic microbiota

Colon content of two 8 to 9 week old male German Landrace pigs (Landesamt für Gesundheit und Soziales, number H0005/18) was sampled, directly put under anaerobic conditions (AnaeroGen 2.5 L; Thermo Scientific) and stored at −80 °C.

Four parallel and independent 250 mL bioreactor vessels of a Multifors 2 bioreactor system (Infors, Bottmingen Switzerland) were set-up under anaerobic conditions with sterile complex intestinal medium adjusted to pig (CIM, Supplemental Table 1). Anaerobic conditions were maintained by constant gassing of bioreactor vessels and reservoir bottles with sterile nitrogen. Cultivation temperature was set to 37 °C and pH was adjusted to 6.5 by automatic addition of 1 M sodium hydroxide. Constant stirring at 150 rpm prevented settling of bacteria. The bioreactors were run under experimental conditions for 24 h to prove sterility (sterile run: S, Fig. 1A).

Colon content was thawed anaerobically (37 °C, 60 min) and slurry equal to 1 g colon content was mixed with the double amount of pre-warmed CIM. Coarse material was given 2 min of settling and then the whole supernatant was used to inoculate two bioreactors with bacteria suspension from 0.5 g colon content per bioreactor. The community was given 24 h to establish and then continuous cultivation started at a dilution rate of D = 0.02 (residence time of 48 h, (Wilfart et al., 2007)). The communities were cultivated for a total of 25 days. After ten bioreactor turn-over (day 21 ± 1), the bioreactor system were considered to be at steady-state (McNeil and Harvey, 2008) and the days 20–22 resemble the control phase. After sampling on day 22, the communities were exposed to Roundup® LB plus. Therefore, Roundup® LB plus war spiked into the bioreactor vessels and supplied with the medium feed to maintain the defined concentration during the treatment phase days 23 to 25 (Fig. 1A).

The applied concentration was chosen on the basis of the calculated maximal dietary burden of 2.85 mg/kg body weight per day recorded by EFSA (Authority, 2018). This value was applied to an 80 kg pig resulting in a daily exposure of 228 mg glyphosate. This study aims to identify microbiota-modulating properties of the frequently applied glyphosate-formulation Roundup® LB plus and hence the amount of 228 mg/d glyphosate-equivalents from Roundup® LB plus (1.8 mg/mL in feed medium) was fed into the bioreactors.

Samples were taken in a multiple of 24 h, starting with an initial sampling after one day and during the control and treatment phase. For 16S rRNA gene profiling, short chain fatty acid (SCFA) analysis, untargeted metabolomics and metaproteomics samples were centrifuged (5000*g*, 5 min, 4 °C). Cell pellets without supernatant were stored directly at −20 °C for 16S rRNA gene profiling and metaproteomics, whereas the supernatants for metabolomics were stored at −80 °C.

2.3. Microbiota flow cytometry

Immediately after sampling, bacteria were pelleted (3200 ×*g*, 10 min, and 4 °C) and preserved in 2% formaldehyde (stock: 8% formaldehyde at pH 7, diluted with PBS (6 mM Na_2HPO_4, 1.8 mM NaH_2PO_4 and 145 mM NaCl in bi-distilled water, pH 7)) at RT for 30 min. Afterward, the bacteria were centrifuged (3200g, 10 min, and 4 °C) and fixed in 70% ethanol for long-term storage at −20 °C.

After a minimum of one day at −20 °C, the bacteria were washed with PBS, treated by ultra-sonication, OD adjusted ($OD_{\lambda 700nm}$ ($d_{cuvette}$ = 0.5 cm) = 0.035), treated for 20 min at RT with permeabilization buffer containing 0.11 M citric acid and 4.1 mM Tween20 and stained with 0.68 μM 4′,6-di-amidino-2-phenyl-indole (DAPI, Sigma-Aldrich, St-Louis, USA) overnight in the dark. Measurement and

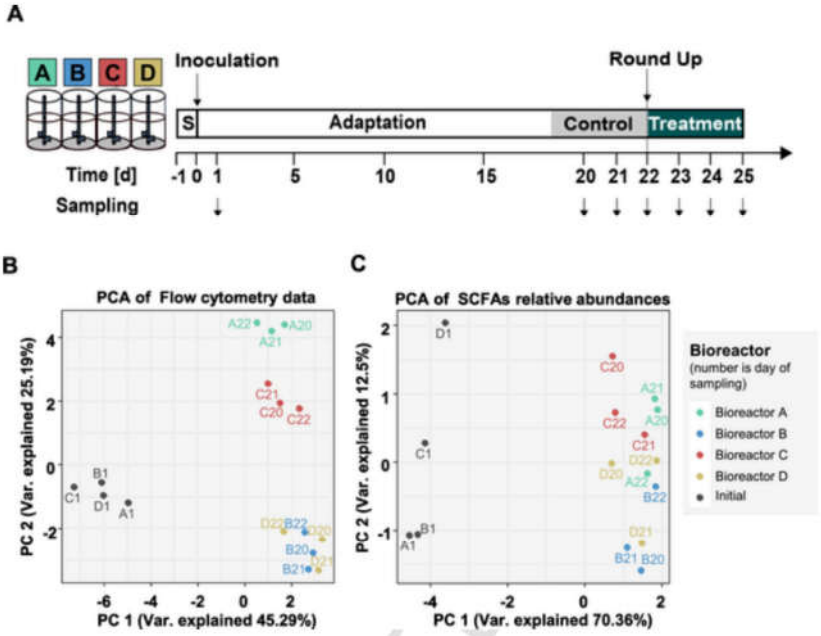

Fig. 1. Experimental setup and analysis of community steady-state before Roundup treatment. **A:** After the sterile run (S) all bioreactors A, B, C and D were inoculated with pig colonic microbiota and given time for adaptation. **B:** Whether the communities reached a steady state was determined before treatment by principal component analysis (PCA) of microbiota flow cytometry data and short chain fatty acid abundances.

changed neutral density filter for side scatter (ND 1.9). Raw cytometric data and gate templates can be found at flow repository ID: FR-FCM-Z2L4 under: https://flowrepository.org.

2.4. Targeted glyphosate measurements

The analysis of glyphosate and AMPA by LC-MS/MS was done as previously described (Fritz-Wallace et al., 2020). In brief, 10 µL of the resuspended extract were injected onto a BEH Amide column (2.1 × 100 mm, 1.7 µm) supplied by Waters (Milford, USA). Chromatographic separation was performed with a gradient of solvent A (66% H_2O, 33% acetonitrile, 10 mM ammonium acetate, 0.04% ammonium hydroxide; pH 9) and solvent B (10% H_2O, 90% acetonitrile, 10 mM ammonium acetate, 0.04% ammonium hydroxide; pH 9). The LC was run at a constant flow rate of 0.4 mL/min. Initial equilibration for 2 min with 0% B, within 2.5 min gradient from 0 to 100% solvent B, hold 100% solvent B for 2 min, back to 0% solvent B for 3.4 min. MRM measurement of glyphosate was done on a QTRAP® 5500 (AB Sciex, Framingham, USA) in negative ionization mode. Data acquisition and analysis were performed in Analyst® Software (AB Sciex, Framingham, USA, version 1.6.2).

2.5. 16S rRNA gene profiling

Bacteria pellets were thawed and one volume of bacteria slurry was mix with 30 volumes of sterile 10% Chelex (*w/v*) solution. After incubation in a ThermoMixer® (Eppendorf, Hamburg, Germany) at 95 °C for 45 min and 1000 rpm shaking samples were centrifuged for 3 min at 11,000*g*. The DNA containing supernatant was transferred into a fresh, sterile tube and stored at −20 °C.

The 16S gene region V3 to V4 was amplified with the primers 341F and 806bR, sequencing was performed on an Illumina MiSeq DNA sequencer (Illumina, San Diego, USA). 16S amplicon generation, sequencing and analysis were done by StarSeq GmbH (Mainz, Germany). Raw data analysis was done by StarSeq GmbH (Mainz, Germany) following their standard data analysis pipeline. Briefly, raw data were de-multiplexed, quality checked by FastQC, primers trimmed. Paired-end reads were joined, low-quality reads were removed reads were corrected, chimeras removed and Amplicon Sequence Variants (ASVs) were obtained by the deblur workflow. Taxonomy was annotated to the ASVs using the SILVA 138 database (Quast et al., 2013). The reads counts per ASV with taxonomic annotation were normalized, by dividing the read counts by sum of sequence in the given sample and multiplying by the minimum sum across all samples using the R scripts from Rhea (Lagkouvardos et al., 2017). In addition, relative abundances of each ASV and taxa were calculated using Rhea (Lagkouvardos et al., 2017)

2.6. Metaproteomics

As described previously (Schape et al., 2019), thawed bacteria pellets were dissolved in the 1000 µL lysis buffer (10 mM Tris-HCl, NaCl 2 mg/mL, 1 mM PMSF, 4 mg/mL SDS). For cell disruption following steps were applied: 1. bead beating (FastPrep-24, MP Biomedicals, Santa Ana, USA: 5.5 ms, 1 min, 3 cycles), 2. 15 min incubation at 60 °C (Thermomixer comfort 5355, Eppendorf, Germany) and 3. Ultra-sonication (UP50H, Hielscher, Teltow, Germany; cycle 0.5, amplitude 60%). The protein concentrationwas determined with bicinchoninic acid assay according to the manufacturer's instructions (Pierce™ BCA Protein Assay Kit, Thermo Fisher Scientific, Waltham, USA). 100 µg protein was precipitated in acetone 1:5 (*v/v*) at −20 °C overnight and then centrifuged (10 min, 14,000 xg). The precipitate was dissolved in Laemmli buffer and used for SDS-PAGE analysis, in-gel digestion and protein purification with ZipTip® treatment (Haange et al., 2019).

Five µg peptide lysate was injected into nanoHPLC (UltiMate 3000 RSLCnano, Dionex, Thermo Fisher Scientific, Waltham, USA). Peptides were sepa-

rated on a C18 reverse-phase trapping column (C18 PepMap100, 300 μm × 5 mm, particle size 5 μm, nano viper, Thermo Fischer Scientific, Waltham, USA), followed by a C18 reverse-phase analytical column (Acclaim PepMap® 100, 75 μm × 25 cm, particle size 3 μm, nanoViper, Thermo Fisher Scientific, Waltham, USA). Mass spectrometric analysis of peptides was performed on a Q Exactive HF mass spectrometer (Thermo Fisher Scientific, Waltham, USA) coupled to a TriVersa NanoMate (Advion, Ltd., Harlow, UK) source in LC chip coupling mode. LC gradient, ionization mode, and mass spectrometry mode are described elsewhere (Haange et al., 2019). Raw data were processed with Proteome Discoverer (vr2.2, Thermo Fischer Scientific, Waltham, USA). Search settings for the Sequest HT search engine were set to: trypsin (full), max. Missed cleavage: 2, precursor mass tolerance: 10 ppm, fragment mass tolerance: 0.02 Da. Protein grouping was enabled, with protein group requiring at least one unique peptide. For complex microbiota, protein-coding sequences of all bacteria were downloaded from UniProt (13.05.2017; http://www.uniprot.org/) resulting in 15,214,675 protein-coding sequences. Protein identification was performed as descried in (Schape et al., 2019).

2.7. Untargeted metabolomics

Supernatants were thawed at 37 °C for 5–10 min. For metabolites extraction, five volumes of methanol:acetonitrile:water (2:3:1) were added to the supernatant and samples were vortexed for 5 min. Afterwards, the samples were sonicated for 5 min and centrifuged at 18000 ×*g* for 5 min. Supernatants were transferred into fresh tubes and dried under vacuum (SpeedVac™, Eppendorf, Hamburg, Germany). Dried pellets were resuspended in 100 μL of a 1:1 mix of running solvent A (0.1% formic acid in water) and B (2% isopropanol, 0.1% formic acid in acetonitrile).

10 μL extract was injected into an HPLC-QToF instrument from Agilent Technologies (6540 UHD Accurate-Mass Q-TOF LC/MS instrument) for LC-MS/MS measurement. Metabolites were separated on a C18 column (flow rate: 0.3 mL/min) with the following gradient of running solvent A, and running solvent B: 0–5.5 min 1% B, 5.5–20 min 1%–100% B, 20–22 min 100% B, 22.-22.5 min 100%–1% B and 22.5–25 min 1% B. The QToF was set up in centroid mode and in screening mode allowing the detection of ions with a mass to charge ratio between 60 and 1000. After a full scan, the most intense ion (threshold 200 counts) was fragmented.

Raw files (.d) were imported into Progenesis QI 2.1 software (Waters, Milford, USA). Different ionization modes were processed separately. Isotope and adduct fusion were applied and covered $[M + H]^+$, $[M + ACN + H]^+$, $[M + H\text{-}H2O]^+$ in positive mode and $[M\text{-}H]^-$, $[M\text{-}H20\text{-}H]^-$ for negative mode, respectively. The next steps included alignment of ion chromatograms in t_R direction based on a reference chromatogram chosen automatically from the data set. The following peak picking was done using default sensitivity settings. Database search was performed using ChemSpider as identification method with *E. coli* metabolome database, fecal metabolome database and KEGG as input selection. Precursor and fragment mass tolerance were set to 20 ppm and 10 ppm, respectively. Only precursor peaks with corresponding fragment spectra were kept. Normalized peak areas and possible identifications were exported. For quality control purposes, peaks detected in medium and medium with added Roundup® LB plus were excluded from the corresponding samples (D1-D22: medium; D23-D25: medium with added Roundup® LB plus). Samples were grouped according to their treatment with Roundup® LB plus. Only peaks with valid values in at least 50% of replicates in both groups were considered for further analysis.

2.8. Targeted bile acid analysis

Bile acids were quantified as previously described (Haange et al., 2020). Briefly, for bile acid measurements the bile acids kit (Biocrates Life Sciences AG, Innsbruck, Austria) was used as outlined in the manufacturer's instructions. In short, 10 μL samples were used for the assay on a 96-well plate format. All isobaric bile acids were separated by HPLC with a flow rate of 0.4 mL/min and at a column pressure 11 min. Eluting bile acids were measured online with a triple quadrupole mass spectrometer (MS/MS) using an electrospray source in negative mode. For the quantitation, a calibration set with seven concentration levels and a mixture of 10 internal standards was used (Siskos et al., 2017).

2.9. Targeted short-chain fatty acids (SCFA) analysis

As described previously (Schape et al., 2019), supernatants were thawed at 37 °C for 5–10 min. The samples were mixed with acetonitrile to a final concentration of 50% acetonitrile. SCFAs were derivatized for 30 min at 40 °C with 0.5 volumes of 200 mM 3-nitrophenylhydrazine and 0.5 volumes 120 mM N-(3-dimethylaminopropyl)-N'-ethylcarbodiimide hydrochloride in pyridine. For LC-MS/MS measurement, the mix was diluted 1:50 in 10% acetonitrile.

50 μL diluted SCFA derivatives were injected into the LC-MS system. SCFAs were separated on an Acquity UPLC BEH C18 column (1.7 μm) (Waters, Milford, USA) with solvent A: 0.01% formic acid in water and solvent B: 0.01% formic acid in acetonitrile as mobile phases. The column flow rate was set to 0.35 mL/min, the column temperature to 40 °C. The gradient elution was done as follows: 2 min at 15% solvent B, 15–50% B in 15 min, then held at 100% solvent B for 1 min. Subsequently, the column was equilibrated for 3 min at 15% solvent B. For identification and quantitation, a scheduled Multiple Reaction Monitoring method was used, with specific transitions for every SCFA. Peak areas were determined in Analyst software and areas for single SCFAs were exported. Normalization and statistics were done in R.

2.10. Targeted analysis of amino acids

Free physiological amino acids were quantified on day 1 and day 22 before Roundup® LB plus treatment and on day 23 to 25 during exposure of the bacteria in all bioreactors. Therefore, 100 μL of culture supernatant and blank medium were used for metabolite extraction.

The extraction of amino acids was carried out according to the user guide of EZ:faast kit (KH0-7337, Phenomenex, US). Briefly, seven concentration points (0, 10, 20, 50, 100, 150, 200 nmol/mL) of standard amino acids from SD1 and SD2 were used for calibration. Both of the standards and samples were mixed with 100 μL internal standards, followed by solid-phase extraction, derivatization, and liquid/liquid extraction. The samples were re-dissolved in 100 μL of a 1:1 mix of solvent A/solvent B (solvent A: 10 mM ammonium formate in water, solvent B: is 10 mM ammonium formate in methanol). The derivatized amino acids were analyzed by MRM method on a QTRAP 5500® instrument (AB Sciex, Framingham. USA) after separation on an EZ:faast AAA-MS column (250 × 2.0 mm) with a 17 min gradient at a flow rate of 0.25 mL/min as suggested in the manual.

The data analysis was carried out in the Analyst software (AB Sciex, Framingham, USA, version: 1.6.2). Briefly, the intensity of amino acids from both the standards and samples were normalized by the internal standard intensity. Linear regression curves were calculated on each standard amino acid. To improve the reliability, four replicates of each standard amino acid were used to generate the regression curve to calculate the concentration of amino acids in the samples.

2.11. Statistical analysis of omics data

Alpha-diversity, principal component analysis (PCA) and non-metric multi-dimensional scaling (NMDS) dissimilarity analysis were done in R (Ihaka and Gentleman, 1996) using the basic functions and the vegan package (Dixon, 2003). Statistics were done in R using in-house written scripts as previously described (Haange et al., 2020). Briefly, the statistical tests used were for complete sample data analysis PERMANOVA using the adonis function in the vegan R package (Dixon, 2003), and for single variables Kruskal-Wallis group test followed by a posthoc pairwise Dunn test. Where appropriate (number of tests >20), *P*-values were corrected for multi-testing by the Benjamini-Hochberg method (Benjamini and Hochberg, 1995). K-means were calcu-

lated in R using the kmeans function. Heatmaps were constructed with pheatmap R package and all other figures were constructed using the R package ggplots2 (Wickham, 2011).

3. Results

3.1. Bioreactors microbiota model communities reached constant state before roundup-exposure

Four pig colonic microbiota (A to D) were cultivated under anaerobic conditions in continuous bioreactors (Fig. 1A). Since it was shown before that the functional and the taxonomic level of microbial communities can develop independently during adaptation or upon perturbation (Krause et al., 2020; Liu et al., 2018), we assessed community development during the control phase per bioreactor on the structural and functional level, respectively. Structural development was determined by microbial flow cytometry (Fig. 1B), depicting bacterial cell division and growth states. Functional development was examined by SCFA analysis (Fig. 1C), which are the main fermentation products of the intestinal microbiota. After ten full medium exchanges (day 21 ± 1), the communities did not change considerable with regard to both community structure and function. However, flow cytometric analysis of the microbial community indicated differences in the community on the taxonomic level.

We defined a three-day control phase (day 20 to day 22) before Roundup® LB plus treatment and thereafter exposed the microbial communities to 228 mg/d glyphosate acids equivalent during the treatment phase from day 23 to day 25 (Fig. 1A).

3.2. Exposure to Roundup® LB plus did not affect taxonomic community composition

To assess influences of Roundup® LB plus treatment on the community structure of the microbiota, we conducted 16S rRNA gene profiling. Previously, it has been shown that *in vitro* model systems can reveal effects of toxins on the microbiota in short time frames, which would only be observed after weeks in animal models (Li et al., 2019).Compared to the initial communities (day 1) the alpha diversity (Fig. 2A, Shannon effective) increased ($P = 0.0124$). Roundup® LB plus exposure (days 23, 24 and 25) did not alter the microbial alpha diversity compared to the steady-state microbiota in the control phase (days 20, 21 and 22). This was also true for the species richness based on ASV numbers (Supplemental Fig. 1A) and the evenness (Supplemental Fig. 1B).

NMDS dissimilarity analysis was performed on the ASV level to determine global taxonomic differences between samples. As already indicated by microbial flow cytometry, the microbial communities clustered according to the bioreactors from which they originated (Fig. 2B, PERMANOVA $P = 0.001$). However, the communities did not cluster according to whether they were exposed to Roundup® LB plus or not and showing no or little effect on the taxonomic community composition. For a more in-depth look, we analyzed the microbial family distribution. The communities on day 1 from the same inoculum (communities A + B *vs.* communities C + D) were very similar (Fig. 2C). In the initial communities A and B, *Enterobacteriaceae* were the most relative abundant family on day 1, followed by *Lactobacillaceae*, *Bifidobacteriaceae* and *Coriobacteriaceae,* with other families only making up a minor part of the communities. In the initial communities C and D, the most abundant families were *Enterobacteriaceae*, *Lactobacillaceae*, *Lachnospiraceae* and *Bifidobacteriaceae*. During the adaptation phase, the family distribution changed considerably, resulting in the development of four different microbial communities A, B, C and D. On day 20 to 22, the most relative abundant families in all communities were in the order of abundance *Ruminococcaceae*, *Lachnospiraceae*, *Enterobacteraceae* and *Prevotellaceae* (Fig. 2C) though in community B and D *Prevotellaceae* were scarce. In the communities C and D *Bacteroidaceae* were one of the most prominent families. The mean relative distribution of bacterial families of all four communities showed no significant Roundup LB plus associated shifts on day 23 to day 25. In order to identify smaller effects of Roundup LB plus on individual families of intestinal microbiota independent of the bioreactor, we calculated the fold change of family abundances compared to the last day of the control phase (day 22) for each of the respective bioreactor. No significant increase or decrease in fold change of the six most abundant microbial families could be detected due to Roundup LB plus (Fig. 2D). A shift in the ratio of Bactoidetes to Firmicutes has previously been decribed as an indicator for dysbiosis. (Yan et al., 2011; Joly et al., 2013). Therefore similar to above, we calculated the fold-change of the Bacteroidetes to Firmicutes ratio between each day to day 22, and no significant shift was observed for this fold change before and after Roundup-exposure (Supplemental Fig. 1C).

3.3. Roundup® LB plus did not influence the active enzymatic repertoire

Metaproteomics analysis is based on protein content, which quickly responds to changes within one hour (Shamir et al., 2016). Thus, this method analyzes the active enzymatic repertoire of microbial communities and determines taxa distribution, highlighting the metabolic more active taxa (Kleiner et al., 2017).

On the functional active taxonomic level, 50% of the relative intensity was due to protein groups annotated as heterogeneous (Fig. 3A). Heterogeneous protein groups are classified as bacterial proteins but cannot be annotated to a single bacterial family. Mostly this happens because of conserved protein sequence regions between taxa. The relative intensity of protein groups, which could be attributed to specific bacterial families (Fig. 3A), followed the profile of 16S rRNA gene sequencing data (Fig. 2C) to a close degree. Following our expectations and the results from 16S rRNA gene profiling, metaproteomics revealed no influence of Roundup® LB plus on the taxonomic distribution in the microbial communities.

Following this, metaproteomics data were used to reveal the functional repertoire of the microbial communities. The NMDS dissimilarity analysis revealed no global influence of Roundup® LB plus on the metabolic pathways of the communities (Fig. 3B). A more detailed view revealed that the communities A to D possessed a very similar enzymatic repertoire, based on observed KEGG subroles (Fig. 3C). The most prevalent KEGG subroles were *carbohydrate metabolism* followed by *translation*, *energy metabolism*, *transport and catabolism* as well as *amino acid metabolism*. These subroles showed no discernable effect due to the exposure. To ascertain that the general KEGG subrole did not overlook effects, we analyzed in more detail individual KEGG metabolic pathways. Here we concentrated on the amino acid pathways, since glyphosate inhibits aromatic amino acid synthesis *via* the shikimate pathway (Fig. 3D). As above, for each community we looked at the fold-changes compared to day 22, just before Roundup-exposure, to remove the variation from the individual bioreactor communities. We neither observed significant effects of Roundup-exposure on the fold changes of amino acid-related enzymes in general nor on enzymes involved in the synthesis of aromatic amino acids, arginine or lysine synthesis (Fig. 3D). Furthermore, the 5-enolpyruvylshikimate-3-phosphate synthase (EPSPS), the enzyme specifically inhibited by glyphosate, did not alter in fold change after Roundup-exposure (Fig. 3D).

3.4. Roundup® LB plus had a slight influence on the metabolome of the microbiota

Since neither the taxonomic community structure nor the enzymatic repertoire of the microbial communities revealed any significant influence of Roundup-exposure, we analyzed the metabolome of the microbiota. Metabolomics is very sensitive and able to detect small functional changes upon stress, though is not able to pinpoint these to specific taxa (Mumtaz et al., 2017).

Since short chain fatty acids (SCFAs) are the major metabolite group produced by the intestinal microbiota and that are essential for the host, we decided to do a targeted analysis of nine SCFAs. The SCFA profile of each community changed between day 1 and the later days (day 20–25) but was not altered by Roundup-exposure (days 20–22 *vs.* days 23–25, Fig. 4A). We additionally analyzed the fold changes of absolute SCFA concentrations per bioreactor individually and plotted the mean and standard deviation. Our analysis re-

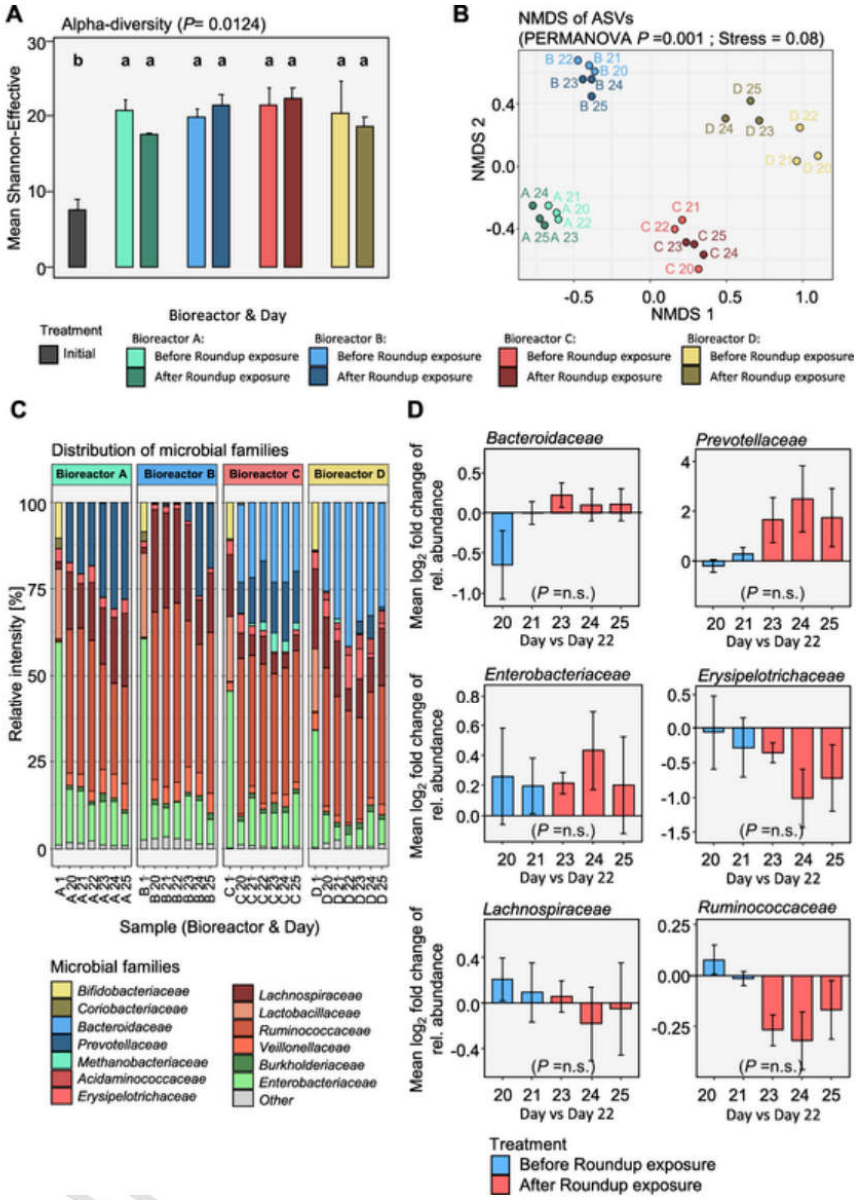

Fig. 2. 16S rRNA gene profiling data. **A:** Alpha-diversity of the microbiota on ASV level by bioreactor and treatment phase. When Krustal-Wallis test is significant then bars labelled with different letters are significantly to each other ($P < 0.05$). **B:** Beta diversity based on non-metric multidimensional scaling (NMDS) of samples before and after Roundup exposure. Sample names: Letter represents the bioreactor and the number the sampling day. *P* calculated by PERMANOVA. **C:** Relative distribution of microbial families at each sampling day. **D:** Mean $\log_2$ fold changes of relative abundance of selected bacterial families from each sampling day to day 22 (directly before Roundup exposure). Error is SEM, *P* calculated by Kruskal-Wallis with pairwise posthoc test done by Dunn test, n.s. non-significant.

vealed no significant effect of Roundup-exposure on SCFA abundances (Fig. 4B).

Following SCFA analysis, we performed untargeted metabolomics on the microbial communities' culture supernatant to capture global effects on the metabolome. We filtered for peaks, which were observed before and after Roundup exposure, to remove peaks attributed to the different Roundup® LB plus constituents. After this filtering, we included 104 peaks for NMDS analysis. NMDS dissimilarity analysis showed a significant shift in the metabolite

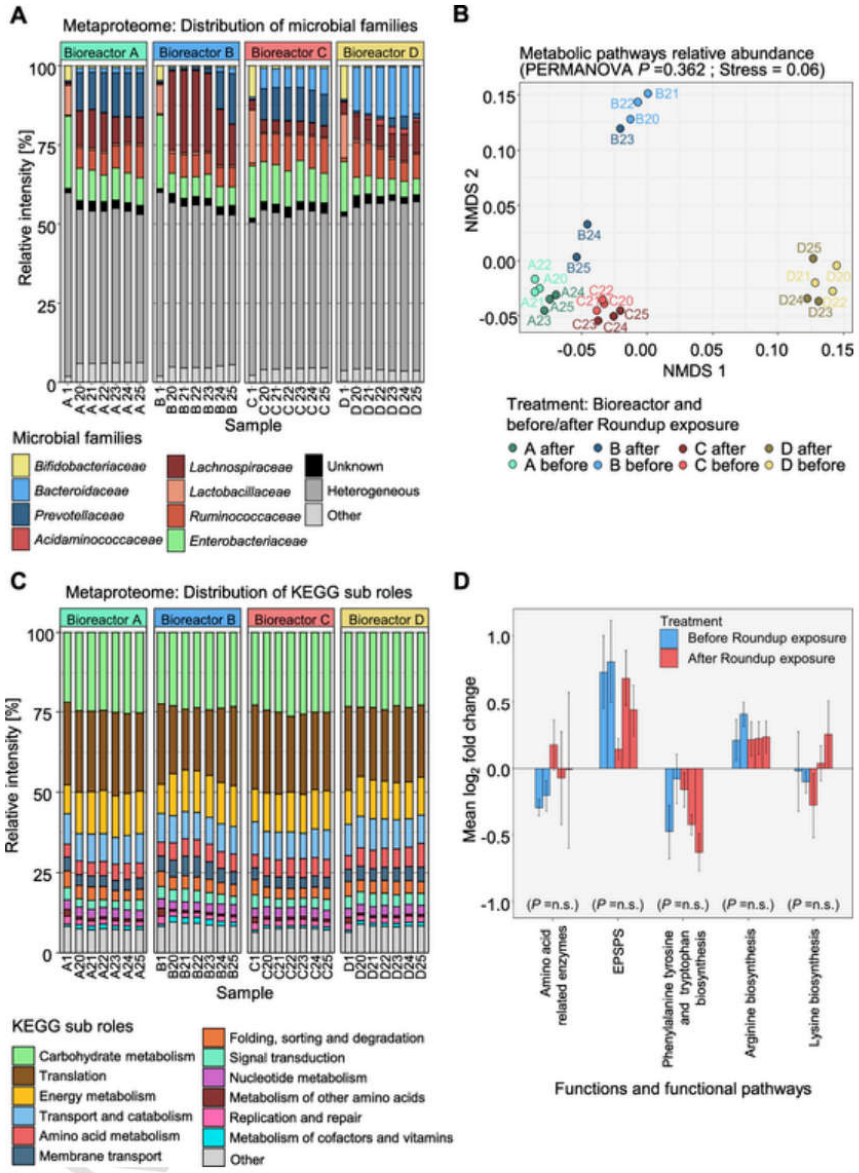

Fig. 3. Metaproteomics data. **A:** Distribution of microbial families based on summed measured relative intensities of protein groups assigned to the family. Heterogeneous: protein groups assigned to multiple microbial families. **B:** Beta-diversity of samples by NMDS dissimilarity analysis based on relative abundance of KEGG metabolic pathways. **C:** Distribution of KEGG metabolic subroles based on summed measured relative intensities of protein groups assigned to the family. **D:** Mean $\log_2$ fold changes of summed relative protein group intensities assigned to 5-enolpyruvylshikimate-3-phosphate synthase (EPSPS) and selected amino acid metabolic pathways from each sampling day to day 22 (directly before Roundup exposure). Error is SEM, *P* calculated by Kruskal-Wallis with pairwise posthoc test done by Dunn test, n.s. non-significant.

profile between before (day 20–22) and after (day 23–25) Roundup-exposure, though the metabolite profiles seemed to also cluster by bioreactor (Fig. 4C). A more detailed look at the untargeted metabolome before and after Roundup-exposure revealed a clustering of communities peak intensities by bioreactor and, interestingly, by exposure (Fig. 4D). To pinpoint these specific changes in the untargeted metabolic measurements, we did a k-means clustering analysis on the filtered peaks (Fig. 5A). We were able to identify two clusters with responding metabolite profiles (Fig. 5B, clusters 1 and 2). The 16 peaks from the

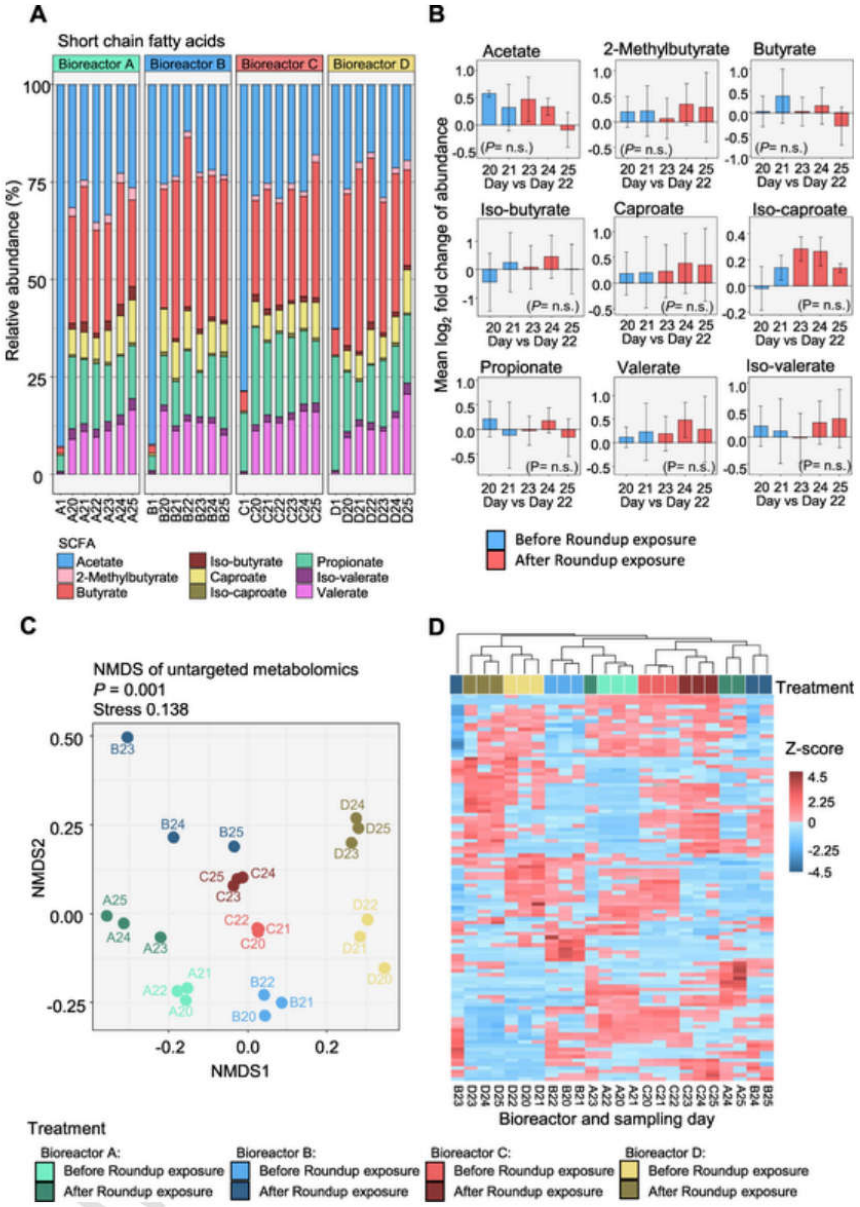

Fig. 4. Metabolomics data. **A:** Relative abundance of short chain fatty acids (SCFAs) **B:** Mean Log_2 fold changes of SCFA absolute abundance from each sampling day to day 22 (just before Roundup exposure). Error is SEM; *P* calculated by Kruskal-Wallis with pairwise posthoc test done by Dunn test, n.s. non-significant. **C:** NMDS plot of bioreactor samples based on untargeted metabolomics with *P* calculated by PERMANOVA. **D:** heat map of the corresponding peak intensities.

first cluster (Fig. 5B, purple) exhibited an increase in peak intensity after Roundup-exposure, thereby encompassing compounds with higher abundance after Roundup-exposure. The second cluster (Fig. 5B, turquoise), including 16 peaks, showed a decrease in peak intensity and therefore a lower abundance of the corresponding compounds after Roundup-exposure. We were able to annotate several peaks from the two clusters. In cluster 1, one peak was putatively identified as pyridoxamine, a form of vitamin B6, and a second as imidazolepropionic acid, a histidine intermediate. In cluster 2, we were able to puta-

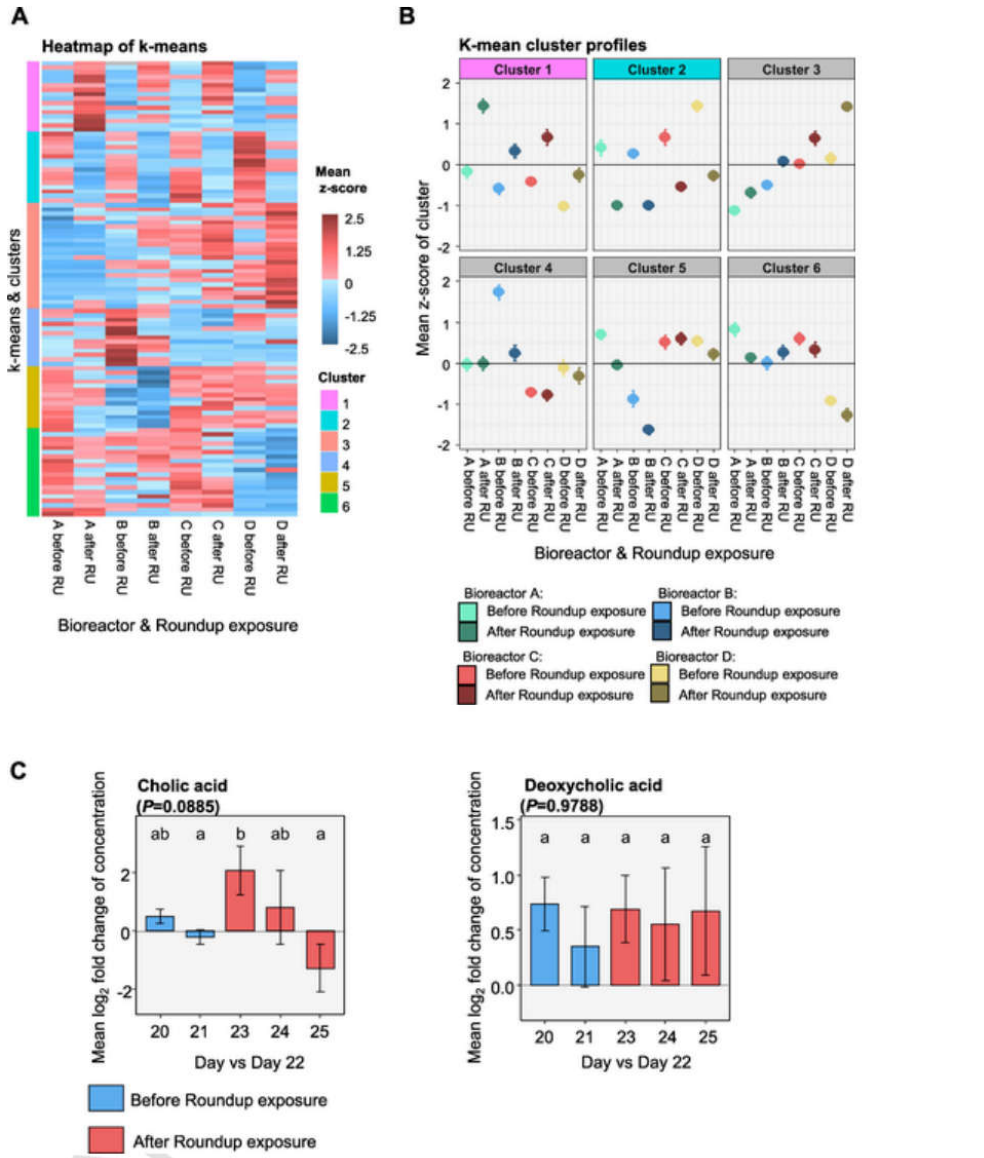

Fig. 5. Metabolomics data. **A**: K-means of peaks identified by untargeted metabolomics. **B**: Clustering profile of the k-means, only using those peaks identified in samples before and after Roundup (RU) exposure. **C**: Mean Log2 fold changes of cholic acid concentration **D**: Mean Log2 fold changes of deoxycholic. Bile acids were measured by targeted metabolomics and compared from each sampling day to day 22 (just before Roundup exposure). Error is SEM; P calculated by Kruskal-Wallis with pairwise posthoc test done by Dunn test.

tively annotate one peak to cholic acid (CA), a bile acid. This finding led us to do an in-depth targeted analysis of bile acids. We were able to identify and quantify 12 bile acids (Supplemental Table 8). Interestingly, based on fold change analysis to day 22, we found a hint (P = .0885) that CA increased after the first day (day 23) of Roundup-exposure and then decreased on the third day (day 25) (Fig. 5C).

3.5. The microbial communities did not metabolize glyphosate in Roundup® LB plus

To check whether glyphosate is metabolized by the microbiota and therefore potentially loses its inhibitory properties on the biosynthesis of aromatic amino acid pathways we determined the concentration of glyphosate in the me-

dia. Our targeted measurements revealed no glyphosate in the samples before Roundup-exposure, which was expected, and no change in the concentration of glyphosate in the communities during Roundup-exposure compared to the media provided. This indicates that glyphosate was not metabolized by the microbiota (Fig. 6A).

3.6. The concentration of aromatic amino acids in the microbial communities did not change after Roundup® LB plus exposure

A reason for the lack of influence of Roundup® LB plus on the microbial communities could be that there is a sufficiently high concentration of aromatic amino acids present in the culture medium. This would negate the need for

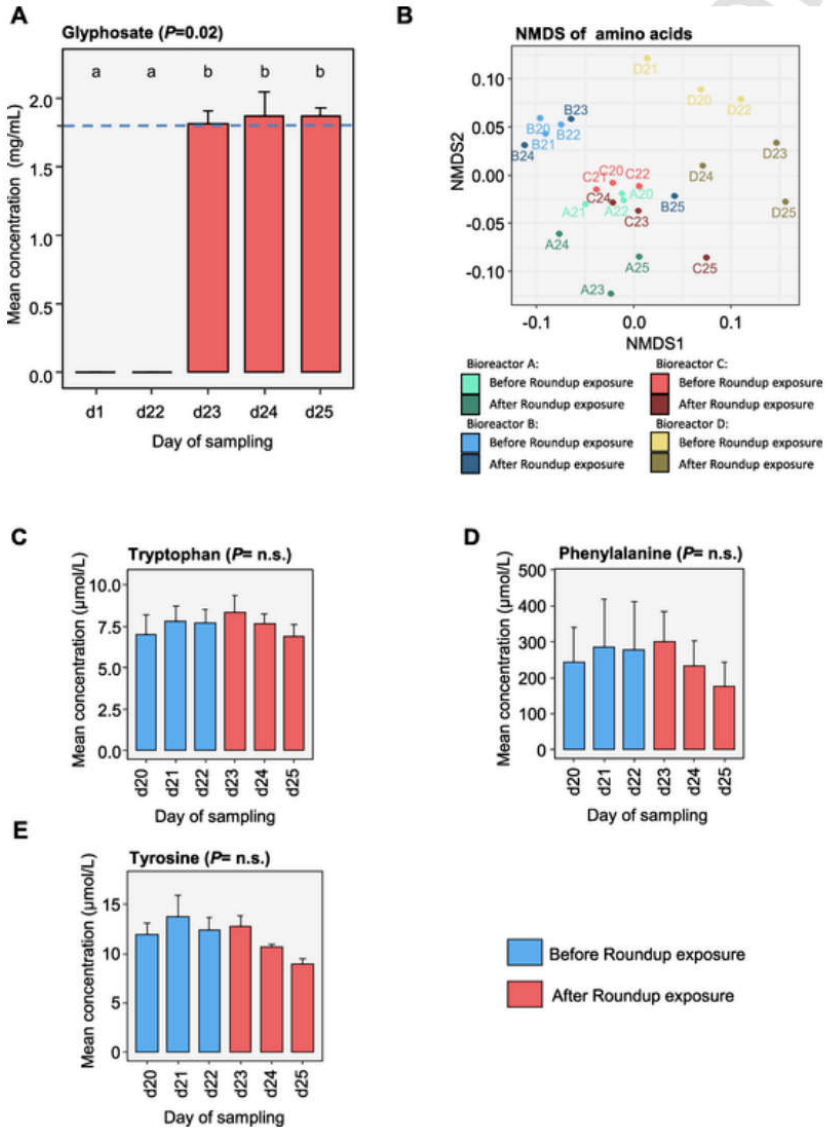

Fig. 6. Glyphosate and amino acid concentration quantified in culture medium. **A**: Detected mean Glyphosate concentration with blue dotted line concentration of Glyphosate (1.8 mg/mL) in the medium prepared for day 23 to day 25. When Krustal-Wallis test is significant then bars labelled with different letters are significantly to each other ($P < 0.05$). **B**: NMDS-dissimilarity analysis of measured amino acid concentrations. Measured mean concentration of phenylalanine (**C**), tryptophan (**D**) and tyrosine (**E**) in samples. Error is SEM, P calculated by Kruskal-Wallis test (for amino acids P corrected for multi-testing by Benjamnini-Hochberg method) with pairwise posthoc Dunn test. (For interpretation of the references to colour in this figure legend, the reader is referred to the web version of this article.)

their synthesis by the microbes. A targeted measurement of amino acids in the medium and in the microbial community samples revealed that aromatic amino acid concentrations were high in pure medium and were being utilized from the medium during cultivation (Supplemental Fig. 2). An NMDS analysis of amino acid concentrations at days 20–25 did not reveal any clustering by Roundup-exposure (Fig. 6B). Furthermore, no significant change in the concentration of tryptophan (Fig. 6C), phenylalanine (Fig. 6D) and tyrosine (Fig. 6E) after Roundup-exposure was observed. This was also true for all other measured amino acids (Supplemental Table 5).

Between days 20 and 25, average aromatic amino acid concentration for each bioreactor was lowest for tryptophan followed by tyrosine, while the concentration of phenylalanine was at least a factor of ten higher (Table 1.)

4. Discussion

Several studies have investigated the effect of glyphosate exposure on the intestinal microbiota *in vitro* and *in vivo* using different organisms. Likewise, from the *in vivo* studies, preferentially using rats, and from the *in vitro* studies the results are contrasting (Riede et al., 2016; Nielsen et al., 2018; Lozano et al., 2018). Furthermore, most of these studies focused on glyphosate-related taxonomic changes, with only two studies analyzing community function at all. Riede et al. (2016) did not identify adverse effects on the ruminal metabolism (Riede et al., 2016). Mesnage et al. (2019, non-reviewed preprint), on the contrary, observed taxonomic changes in the rat caecal microbiota combined with an increase in intermediate metabolites from the shikimate pathway (Mesnage et al., 2019). Because contrasting results shape the debate of potential risks coming from glyphosate exposure, we sought to investigate the microbiota-modulating effects of the most frequently used glyphosate formulation Roundup® LB plus on the function of intestinal microbiota in more detail, using a high concentration. The pig microbiota is an interesting model system because on the one hand, pigs are a livestock species with economic relevance and on the other hand, the pig microbiota is more similar to humans than the intestinal microbiota of other model organisms, such as rodents (Roura et al., 2016). Consequently, analyzing the microbiota-modulating effects of glyphosate on the pig microbiota allows the extrapolation to the human microbiota.

The complex intestinal culture medium in our study was adapted to the pig colon environment (Krause et al., 2020; Tanner et al., 2014). It is well known that microbiota quickly respond to a perturbation on the functional level (Medicine Io, 2003) and, if pressure is high enough, also by shifting towards another stable taxonomic community state (Levy et al., 2017). Therefore, we acutely exposed the microbiota to a high glyphosate concentration by the addition of Roundup® LB plus. However, adult pigs weight over 100 kg, which is associated with a higher fodder uptake and consequently a higher exposure to glyphosate.

Table 1
Mean concentrations (μM) of aromatic amino acids before (days 20–22) and after Roundup exposure (days 23–25). Error is SEM.

Bioreactor	Sampling days	Phenylalanine	Tryphtophane	Tyrosine
A	20–22 (no RU)	101.8 ± 4.2	9.9 ± 0.1	12.2 ± 0.2
	23–25 (RU)	198.7 ± 10.3	9.8 ± 0.6	12.1 ± 1.2
B	20–22 (no RU)	198.3 ± 1	5.6 ± 0.2	9.7 ± 0.3
	23–25 (RU)	205.7 ± 47.5	6.8 ± 0.2	9.4 ± 0.6
C	20–22 (no RU)	143 ± 3.3	7.9 ± 0.2	12.1 ± 0.2
	23–25 (RU)	111.8 ± 34.9	7.4 ± 0.5	11.1 ± 1.5
D	20–22 (no RU)	631.3 ± 41.8	6.6 ± 0.5	16.9 ± 1.3
	23–25 (RU)	435.0 ± 45.6	6.4 ± 0.3	10.6 ± 0.4

The effect of Roundup-exposure in the concentration applied in this study was only slight. These effects cannot singularly be attributed to glyphosate, since Roundup® LB plus contains 16% unknown surface active ingredients. In addition, our data indicate that the colonic microbiota did not metabolize glyphosate. Roundup-exposure neither changed the community taxonomic structure nor the enzymatic repertoire of the microbiota within the three days of exposure. Furthermore, neither the concentration of SCFAs, main products of microbial metabolism, nor the concentration of any of the 29 analyzed amino acids was altered. However, a few metabolite peaks were detected at altered abundance by untargeted metabolomics after Roundup-exposure. Of these, only a minority could be annotated to putative compounds, with one peak annotated to cholic acid. The targeted bile acid measurement did show a trend in the decrease in cholic acid after Roundup-exposure. Certain members of the intestinal microbiota are known to deconjugate or dehydroxylate bile acids, and thereby enhancing their toxicity towards other bacteria (Islam et al., 2011; Yokota et al., 2012). Moreover, converted bile acids are involved in signaling between microbiota and host. Alterations to the bile acid profile were reported to affect the metabolism of the host *via* the farnesoid X receptor (Ryan et al., 2014), which controls bile acid synthesis but also glucose and lipid metabolism in the liver. The liver was observed to be one of the major targets affected by ultra-low dose of glyphosate in a two-year study on rats, exhibiting lipotoxic stress and further biochemical and anatomical damage (Mesnage et al., 2015).

The observed metabolic alterations, which did not correspond to significant changes on the proteome level, can be explained by two arguments. First, the metaproteome coverage might not be sufficient for detecting the changes, which might result from rather high community complexity. We have recently shown that community complexity is the most crucial factor determining proteome coverage in metaproteomics (Lohmann et al., 2020). Second, glyphosate or other compounds in Roundup® LB plus, including surfactants, which could possibly harm the intestinal bacteria (Mesnage and Antoniou, 2017) might interfere with other enzymes than the primary target EPSPS. The mode of action of glyphosate is based on its structural similarity to phosphoenolpyruvate (PEP), the physiological substrate of EPSPS. Both compounds compete for EPSPS binding. However, PEP is involved in many other important metabolic processes, such as glycolysis, gluconeogenesis, the synthesis of secondary metabolites or the phosphotransferase sugar uptake system (Kanehisa and Goto, 2000). Thus, the interference by glyphosate could be even broader, as already suggested by a recent study of Ford et al. (2017) (Ford et al., 2017).

Thermal proteome profiling (TPP) would be a powerful tool to screen the proteome more specifically for proteins interacting with glyphosate (and its metabolites), degrading it or being adversely affected. In the past, this method identified off-targets of active ingredient of drugs (Savitski et al., 2014), but also pollutant degrading enzymes and regulators thereof in bacteria (Türkowsky et al., 2019). TPP might open up a new, interesting perspective for testing of pesticides for health and environmental safety in general.

The contradictory findings of *in vivo* studies might result from a low lab-to-lab reproducibility that derives from the existence of different microbiota in the housing facilities (Hugenholtz and de Vos, 2018) and the different experimental procedures and glyphosate formulations. *E.g.*, Dechartres et al. (2019) daily fed rat dams 5 mg/kg body weight per day glyphosate isopropylamine salt or glyphosate equivalents from Roundup® 3Plus for 30 days and investigated the maternal behavior and neuroplasticity in the hippocampus. However, they barely observed significant effects on maternal behavior or the neurological end-points investigated in their study. In contrast to glyphosate isopropylamine salt, Roundup® 3Plus significantly altered the taxonomy of the intestinal microbiota in their study, indicating that substances from the formulation applied in their study might be causative for the taxonomic alterations detected (Dechartres et al., 2019). Lozano et al. (2018) identified sex-dependent shifts in taxonomy after long-term high doses of glyphosate (2.5 g/L) from R Grand Travaux Plus exposure *via* drinking water. In this study, the chronic and high

trasting findings (Lozano et al., 2018). Although the exact composition of both, R Grand Travaux Plus and Roundup LB plus, are unknown, for R Grand Travaux Plus a contamination with heavy metals has been reported (Defarge et al., 2018). This, as well as potential differences in the formulation might add on to the different observations. A more recent study by Mesnage et al. (2019) investigated the effects of three different concentrations of pure glyphosate and MON 52276 on the rat microbiome for 90 days (maximal concentration of 175 mg/kg body weight). They included taxonomic and functional analysis using a multi-omics approach. Contrary to our results, they observed slight effects on the microbial taxonomic distribution together with large inter-individual variation, which limits the reliability of the data. Alike to our study, they reported only slight effects on the metabolome in rats, with 12 of 744 metabolites being significantly altered. This corresponds to 1.6% of all metabolites. Among these metabolites, they observed an increase in shikimate and 3-dehydroshikimate, which they assigned to the inhibition of the EPSPS, the target enzyme of glyphosate from the shikimate pathway (Mesnage et al., 2019). In a further study, Nielsen et al. orally treated rats with 25 mg/kg bodyweight glyphosate or from the glyphosate formulations Glyfonova® 450 Plus for 14 days. They observed very little influence on the intestinal microbiota. The authors suggest that the availability of high concentrations of aromatic amino acids in the rat gut inhibit the synthesis of aromatic amino acids *via* the shikimate pathway. This might subsequently nullify an inhibition of the EPSPS by glyphosate (Nielsen et al., 2018), similar to our study, in which high amino acid concentrations were measured in pure medium. However, as Mesnage et al. indicated in their study, there may be effects on the intermediate metabolites upstream the EPSPS caused by glyphosate.

The shikimate pathway is regulated on various levels. One way of regulation is transcriptional attenuation (Pittard and Yang, 2008). A second way of regulation is negative feedback gene regulation, where the gene expression of the shikimate operon is controlled by a tryptophan sensitive (TrpR) and a tyrosine sensitive (TyrR) repressor (Pittard and Yang, 2008; Schoner and Herrmann, 1976). These repressors bind to their respective amino acid and mask the operator, thereby inhibiting transcription (Tabaka et al., 2008). Transcription inhibition commences at 10 μM of tyrosine or tryptophan, respectively (Baasov and Knowles, 1989). Another mechanism for controlling aromatic amino acid synthesis is allosteric feedback inhibition of the 3-Deoxy-D-arabinoheptulosonate 7-phosphate (DHAP) synthase. The DHAP synthase catalyzes the first enzymatic conversion in the shikimate pathway. Allosteric inhibition reaches its maximum in the presence of 100 μM of any of the aromatic amino acids (Rodriguez et al., 2014). Tyrosine and tryptophan in our study were present at concentrations, which would inhibit the DHAP synthase synthesis by transcriptional attenuation while the concentration of phenylalanine reached the concentrations where allosteric inhibition would be at maximum (see Table 1). This is in line with our finding that Roundup-exposure did not affect the abundance of protein groups of the shikimate pathway, including the EPSPS, since the medium was a model for the contents of the pig gut and therefore rich in amino acids. An inhibited shikimate pathway would result in a reduced production of aromatic amino acids, thus weakening or negating transcriptional inhibitory control. This would lead to an increase in the translation of the proteins of this pathway, which was not observed in this study. Taken together, these findings suggest that the concentrations of aromatic amino acids in the microbiota cultures were high enough to suppress the synthesis of the aromatic amino acids. The microbes were sourcing the aromatic amino acids from the media in sufficient quantities already before but also during Roundup- exposure. However, other animals, *e.g.* non-vertebrates with a less diverse microbiota or with lower aromatic amino acid levels in the gut might be susceptible to glyphosate exposure, as was proven for honey bees (Motta et al., 2018).

Since the microbial culture medium was closely modelled on the intestinal lumen content of the pig colon (Tanner et al., 2014), we would expect a similar *in vivo* response of the intestinal microbiota to Roundup-exposure as observed in our study.

5. Conclusions

An impact of the glyphosate-based herbicide Roundup® LB plus on the intestinal microbiota of pig was not confirmed at the applied glyphosate concentration. We did not observe changes on the taxonomic level and only showed minor alterations on the functional level. Nevertheless, we cannot exclude the susceptibility of microbiota in susceptible timeframes or combination with other destabilizing factors, such as medication, a shift in diet or disease. Moreover, glyphosate itself, produced glyphosate metabolites or components from the formulation after resorption from the intestine might react with other target proteins and should be included in future investigations.

CRediT authorship contribution statement

Jannike L. Krause: Conceptualization, Writing - original draft, Writing - review & editing, Formal analysis, Visualization. **Sven-Bastiaan Haange:** Writing - original draft, Writing - review & editing, Formal analysis, Visualization. **Beatrice Engelmann:** Writing - review & editing. **Ulrike Rolle-Kampczyk:** Supervision. **Katarina Fritz-Wallace:** Writing - review & editing. **Zhipeng Wang:** Writing - review & editing. **Nico Jehmlich:** Conceptualization, Supervision. **Dominique Türkowsky:** Writing - review & editing. **Kristin Schubert:** Supervision. **Uwe Rösler:** Funding acquisition. **Gunda Herberth:** Supervision. **Martin von Bergen:** Conceptualization, Writing - review & editing, Supervision, Funding acquisition.

Declaration of competing interest

The authors declare that they have no known competing financial interests or personal relationships that could have appeared to influence the work reported in this paper.

Acknowledgments

Jannike Lea Krause is thankful for funding by the German Federal Environmental Foundation (DBU). Sven-Bastiaan Haange, Uwe Roesler, Judith Pöppe and Katrin Bote and Martin von Bergen are grateful for the funding by Federal Ministry of Food and Agriculture (BMEL) through the research project "Glypho-Bak" (Project number: 2815HS018). Stephanie Schäpe is grateful for support from a DFG-grant within the Priority Program 1656. We thank Florian Schattenberg for cytometric measurement of microbiota and help and discussion during data analysis. We thank Nicole Gröger and Jeremy Knespel for their excellent technical assistance and Martina Kolbe for medium supply.

Appendix A. Supplementary

Supplementary data to this article can be found online at https://doi.org/10.1016/j.scitotenv.2020.140932.

References

Amrhein, N, Schab, J, Steinrücken, H C, 1980. The mode of action of the herbicide glyphosate. Naturwissenschaften 67, 356–357.
Authority, E F S, 2018. Evaluation of the impact of glyphosate and its residues in feed on animal health. EFSA J. 16, e05283.
Baasov, T, Knowles, J R, 1989. Is the first enzyme of the shikimate pathway, 3-deoxy-D-arabino-heptulosonate-7-phosphate synthase (tyrosine sensitive), a copper metalloenzyme? J. Bacteriol. 171, 6155–6160.
Bashiardes, S, Zilberman-Schapira, G, Elinav, E, 2016. Use of metatranscriptomics in microbiome research. Bioinform Biol. Insights 10, 19–25.
Benbrook, C M, 2016. Trends in glyphosate herbicide use in the United States and globally. Environ. Sci. Eur. 28, 3.
Benjamini, Y, Hochberg, Y, 1995. Controlling the false discovery rate - a practical and powerful approach to multiple testing. J Roy Stat Soc B Met 57, 289–300.
Brewster, D W, Warren, J, Hopkins, W E, 1991. Metabolism of glyphosate in Sprague-Dawley rats: tissue distribution, identification, and quantitation of glyphosate-derived materials following a single oral dose. Fundam. Appl. Toxicol. 17, 43–51.
Claus, S P, Guillou, H, Ellero-Simatos, S, 2016. The gut microbiota: a major player in the toxicity of environmental pollutants? NPJ Biofilms Microbiomes 2, 16003.
Dechartres, J, Pawluski, J L, Gueguen, M M, Jablaoui, A, Maguin, E, Rhimi, M, et al., 2019. Glyphosate and glyphosate-based herbicide exposure during the peripartum period affects maternal brain plasticity, maternal behaviour and microbiome. J. Neuroendocrinol. 31, e12731.

Publication 7: Bisphenol A, bisphenol F and bisphenol S directly modulate MAIT cell activation

MAIT cell activation is modulated by bisphenol exposure

Authors

JL Krause[1], B Engelmann[2], U Rolle-Kampczyk[2], Ulisses Nunes da Rocha[3], A Pierzchalski[1], M von Bergen[2, 4], G Herberth[1]

[1] Helmholtz-Centre for Environmental Research - UFZ, Department of Environmental Immunology, Leipzig, Germany

[2] Helmholtz-Centre for Environmental Research - UFZ, Department of Molecular Systems Biology, Leipzig, Germany

[3] Helmholtz-Centre for Environmental Research - UFZ, Department of Environmental Microbiology, Leipzig, Germany

[4] Institute of Biochemistry, Faculty of Biosciences, Pharmacy and Psychology, University of Leipzig, Germany

Corresponding author:

Gunda Herberth, Permoser Straße 15, 04318 Leipzig; phone: +49 341 235 1547;

Fax: +49 341 235 1787; email: gunda.herberth@ufz.de

Abstract

Aims: This study elucidates the microbiota-mediated and the direct effects of bisphenol exposure on mucosal-associated invariant T (MAIT) cells.

Methods and Results: Two common bacterial species from the human intestinal microbiota, *Bacteroides thetaiotaomicron* and *Escherichia coli,* as well as human fecal microbiota have been exposed to bisphenol (Bp) A, BpF and BpS in batch culture. Effects on microbial growth, viability and metabolism have been determined. The microbiota show different susceptibility toward bisphenol exposure. The exposed microbiota have been utilized to stimulate MAIT cells to identify microbiota-mediated MAIT cell modulation. BpA and BpF-exposure, but not BpS-exposure, resulted in a decreased ability to activate MAIT cell in *Bacteroides thetaiotaomicron* and *Escherichia coli.* The fecal microbiota maintained the ability to activate MAIT cells despite BpA- and BpF-exposure

Conclusion: Phylogenetic and metaproteomic analysis revealed the predominance of sulfatereducing bacteria belonging to the family Desulfobulbaceae within a toluene degrading microbial

consortium.

Significance and Impact of Study: This is the first study which investigates the microbiota-mediated effects of BpX-expsoure on specialized immune cells, i.e. MAIT cells.

Keywords:

BpA, BpF, BpS, human intestinal microbiota, in vitro model, batch culture

Introduction

Bisphenol A (BpA) has been detected globally in human urine, serum, cord blood and breast milk during epidemiologic studies (reviewed in Vanderberg 2007, Geens 2012, Huang 2018,page 975), which indicates chronical human exposure. BpA is among the chemicals with the highest production volume worldwide (Vandenberg et al., 2007). In 2015, 7.7 million tons of BpA have been produced worldwide, but the production volume will continue to increase in the coming years (Lehmler et al., 2018). The majority of BpA is used for the

production of polycarbonate plastics and epoxy resins (European Food Safety Authority, 2015). Among many other applications polycarbonate plastics are used in food contact applications, such as food and liquid containers, plastic plates and mugs, microwave-proof plastic boxes, cook- and tableware or water reservoirs in water dispensers (European Food Safety Authority, 2015). Epoxy resins have a similarly broad range of end-uses, e.g. in dental sealants and as protective lining in water pipes, water storage tanks, food cans and in the lids of glass jars (ref). Monomeric BpA can leach from polycarbonate and epoxy resins (Geens et al., 2012). According to the EU EFSA, more than 90 % of BpA detected in human urine was assumed to derive from exposure *via* the oral route (European Food Safety Authority, 2015). The intestinal microbiota, the mucosa and mucosa-associated immune cells are potentially exposed to these compounds.

However, only within the last decade linkage of BpA-exposure to impaired reproduction and other health effects regarding human development and metabolism (Rochester, 2013; Vandenberg et al., 2013) led to a more restrictive regulation of BpA. I.e., BpA was banned for use in baby bottles within the European Union in 2011 (EC 2011s from Almeida) and the tightened the regulation of BpA utilization in consumer products (reviewed Almeida et al., 2018). In 2017, BpA was listed as substance of very high concern (SVHC, ED/30/2017) within the European Union and put on the candidate list for annex XIV (authorization list) of the REACH regulation. Substances from the authorization list have to be authorized by the ECHA for specific applications and manufacturers have to prove the socioeconomic benefit from the utilization of SVHC versurs the chemicals risk (ref ECHA). In addition, the tolerable daily intake (TDI) concentration has been lowered from 50 µg/kg bodyweight to 4 µg/kg bodyweight in the European Union (EU). Nevertheless, other countries, like the US and Japan still apply a TDI of 50 µg/kg bodyweight (Almeida et al., 2018).

The stricter regulations have contributed to the increasing use of BpA-analogues (Eladak et al., 2015). To date, 16 BpA-analoques are utilized in industrial applications, which all share the common structure of two hydroxyphenyl moieties (Chen et al., 2016). Due to the shared structural features a similar health risk can be assumed (Rochester and Bolden,

2015). This has been reported with regard to estrogenicity, for which Eldaek et al. (2015) already showed that BpF and BpS pose a similar risk. The BpA analogues bisphenol F (BpF) and bisphenol S (BpS) are increasingly used in polycarbonate plastics and epoxy resins (Huang, 2018), which is reflected by the detection of BpA-like levels of BpF and BpS in human urine (Zhou et al., 2014). To date, BpS-derived riks is under assessment with REACH as chemical with high priority (https://echa.europa.eu/de/substance-information/-/substanceinfo/100.001.13). However, the risk of BpF is not evaluated within the EU, although similar properties of BpF compared to BpA and BpS can be assumed Since BpA was shown to influence the human intestinal microbiota on the taxonomic level (Lai et al., 2016), the microbiota-modulating effects of BpA-analogues, BpF and BpS have to be determined.

The intestinal microbiota is a densely populated ecosystem and essential for food digestion, colonization resistance and the *de novo* synthesis or modification of metabolites, such as short chain fatty acids (SCFAs) and vitamins (Belkaid and Harrison, 2017; Brestoff and Artis, 2013; Levy et al., 2017; Sender et al., 2016). Microbial metabolites affect the immune system in various ways (Levy et al., 2017; Thaiss et al., 2016). Indirect effects on the immune system may be mediated by the microbiota, since specialized immune cells, such as mucosal-associated invariant T (MAIT) cells, recognize microbial metabolites. These metabolites derive from the riboflavin (vitamin B2) biosynthesis pathway or the folate (vitamin B9) biosynthesis pathway and are presented to MAIT cells *via* the MHC class 1-related protein 1 (MR1) (Corbett et al., 2014; Eckle et al., 2015; Gherardin et al., 2016; Kjer-Nielsen et al., 2012). *In vitro* studies showed that the riboflavin precursors 5-(2-oxopropylideneamino)-6-D-ribitylaminouracil (5-OP-RU) and 5-(2-oxoethylideneamino)-6-D-ribitylaminouracil (5-OE-RU) activate MAIT cells, whereas the folate derivate 6-formylpterin (6-FP) and its synthetic analogue N-acetyl-6-formylpterin (Ac-6-FP) inhibit MAIT cell activation (Corbett et al., 2014; Kjer-Nielsen et al., 2012).

MAIT cell properties render these cells potentially susceptible to microbiota-mediated effects of chemical exposure. Furthermore, environmental factors, such as diet, chemicals

or drugs, influence the intestinal microbiota (Goodrich et al., 2016) and can thus increase the risk of disease initiation (Forbes et al., 2016). A reduction in microbial diversity, together with an increasing presence of mucosal-associated invariant T (MAIT) cells in the inflamed intestinal or adipose tissue have been reported from patients with inflammatory bowel diseases (IBD) ulcerative colitis and Crohn's disease (Serriari et al., 2014) or obesity (Chiba et al., 2018; Magalhaes et al., 2015). Therefore, the effects of chemical exposure on the intestinal microbiota and downstream on MAIT cells should be elucidated.

First, we cultivated two common members of the human intestinal microbiota, i.e. *Bacteroides thetaiotaomicron* (Comstock and Coyne, 2003) and *Escherichia coli* (Martinson et al., 2019), as well as human fecal microbiota in batch and exposed these to the bisphenols BpA, BpF and BpS at three different concentrations. With regard to the exposed microbiota, we analyzed overall microbial growth, microbial viability and microbial metabolism. Second, we used the exposed microbiota to investigate indirect effects of bisphenol exposure on specialized immune cells that recognize microbial metabolites, the mucosal-associated invariant T cells (MAIT cells). Third, we determined the direct effects of bisphenol exposure on the activation of MAIT cells *in vitro.*

Results

Bisphenol exposure affects microbial growth and viability

The major route of bisphenols (BpX) exposure in humans is oral uptake (European Food Safety Authority, 2015), which leads to a direct exposure of the intestinal microbiota. Hence, we investigated the microbiota-modulating effects of Bisphenol A (BpA), Bisphenol F (BpF) and Bisphenol S (BpS) and exposed human fecal microbiota and two common bacterial species from the intestine, *Bacteroides thetaiotaomicron* and *Escherichia coli*. We applied BpA, BpF and BpS at three concentrations based on the actual European tolerable daily intake (TDI) for BpA: 4 µg/kg bodyweight (2.27 µg/mL), 50 µg/kg bodyweight (28.32 µg/mL) and 625 µg/kg bodyweight (353.96 µg/mL). Modulation of microbiota was

129 first assessed by analyzing microbial growth (optical density 600 nm - OD_{600}, Figure 1 A)
130 and quantification of microbial viability (Figure 1. B). The results are shown as n-fold value
131 of the untreated control and statistical analysis refer to the corresponding solvent control.

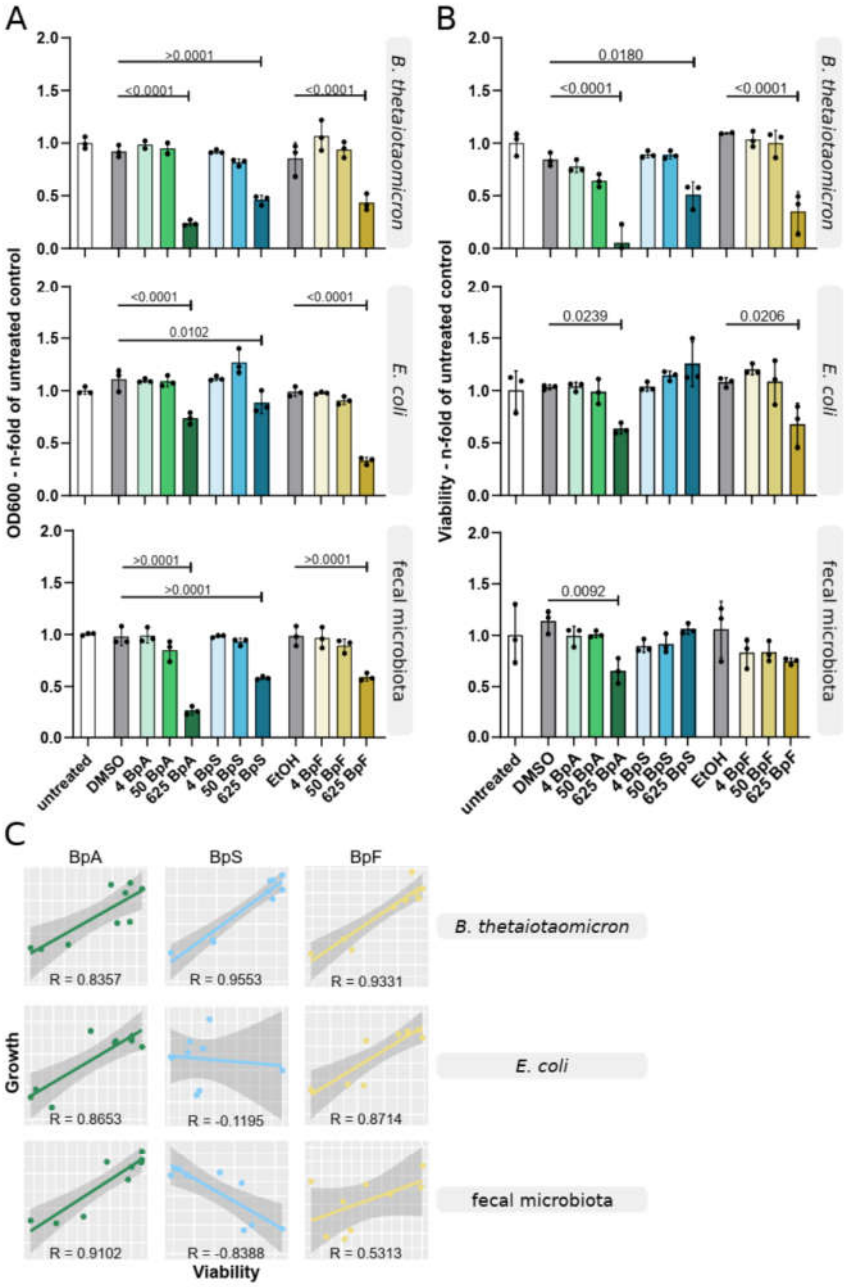
A
B
C
OD600 - n-fold of untreated control
Viability - n-fold of untreated control
B. thetaiotaomicron
E. coli
fecal microbiota
>0.0001
<0.0001
0.0102
0.0180
0.0239
0.0206
0.0092
untreated
DMSO
4 BpA
50 BpA
625 BpA
4 BpS
50 BpS
625 BpS
EtOH
4 BpF
50 BpF
625 BpF
BpA
BpS
BpF
Growth
Viability
R = 0.8357
R = 0.9553
R = 0.9331
R = 0.8653
R = -0.1195
R = 0.8714
R = 0.9102
R = -0.8388
R = 0.5313

Figure 1.

Neither the DMSO nor the ethanol (EtOH) solvent control affected microbial growth or viability, indicating that the effects on microbial growth and viability resulted from the BpX-exposure. Growth of *B. thetaiotaomicron* was significantly reduced upon exposure at 625 BpX, independent of the applied compound (Figure 1, n=3, ordinary one-way ANOVA, Tukey's test for multiple comparisons, *P* values are summarized in supplementary file 1: Tab. S1 and S2). The effects on growth and viability were positively correlated for *B. thetaiotaomicron* with a Pearson correlation coefficient R > 0.8. For *B. thetaiotaomicron* growth and viability were reduced by BpX with effect strength form high to low by BpA < BpF < BpS (Figure 1 C). Growth of E. coli was significantly declined due to BpX-exposure at 625. We observed a significant reduction of microbial viability upon exposure to 625 BpA and 625 BpF, but not for 625 BpS (n=3, one-way ANOVA, Tukey's test for multiple comparisons, *P* values are summarized in supplementary file XXX, Tab. SXXX). Growth and viability correlated with regard to BpA- and BpF-expsoure (Pearson correlation coefficient R> 0.8), but not for BpS (Pearson correlation coefficient R= -01195, Figure 1 C). Growth and viability of *E. coli* were most severely altered by BpF < BpA < BpS. Similar to the single strain cultures, the exposure to 625 BpX signifianctly decreased microbial growth, but microbial viability only mirrored the results from BpA. Here, growth and viability correlated (Pearson correlation coefficient R> 0.8). For BpF and BpS no effects on microbial viability were observed. No correlation of growth and viability was detected for BpF (Pearson correlation coefficient R< 0.5) and a negative correlation of growth and viability was observed for BpS (Figure 1 C). The fecal microbiota were most strongly affected by BpA < BpF < BpS based on microbial growth and viability.

Exposure to BpA affected microbial metabolism in a dose-dependent manner

Since microbial growth and viability were affected by BpX-exposure, we next evaluated the effects on microbial metabolism. Global changes were visualized by NMDS analysis of untargeted metabolomics data using the Bray-Curtis (BC) distance (Figure 2 A). The BC distance indicates similarity between sample points in the NMDS analysis. Furthermore, BC

161 similarity was used to determine the effect strength resulting from the BpX-exposure by
162 comparing the BC similarity of every sample to the untreated control (Figure 2 B).

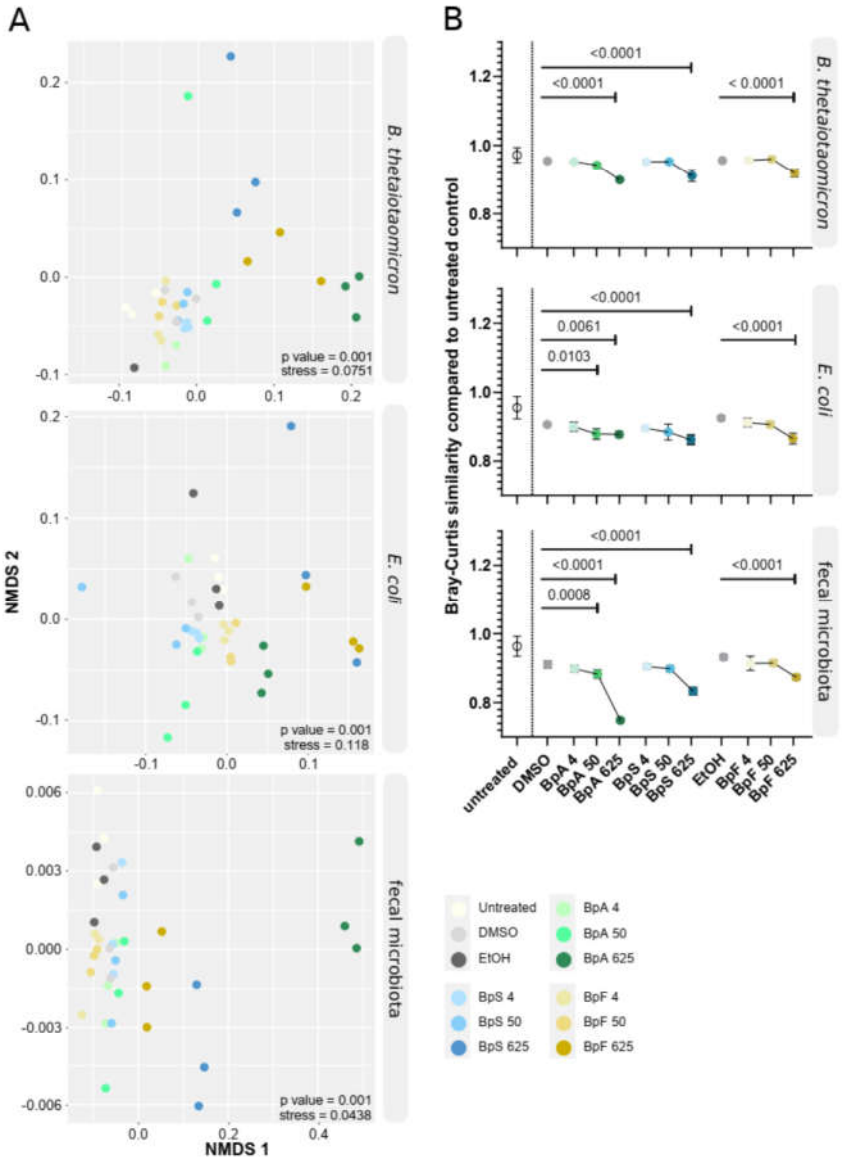

163

164 Figure 2

165 The addition of either DMSO or ethanol affected the microbial metabolome compared to
166 untreated control in all microbiota (Fig. 2A and 2B, n=3, mean± sd, one-way ANOVA, *P*-
167 values: supplemental Table XXX). The BC similarity of BpX-exposed samples were
168 compared to the corresponding solvent control. The metabolomes of *B. thetaiotaomicron*,
169 *E. coli* and the fecal microbiota responded in a dose dependent manner to the exposure
170 with BpA. BpA exposure induced non-significant changes at 4 BpA for all microbiota, but
171 significant alterations in the metabolome of *E. coli* and the fecal microbiota at 50 BpA and
172 625 BpA. At the highest concentration of 625 BpX all compounds significantly affected the
173 microbial metabolome of all microbiota (n=3, mean± sd, one-way ANOVA, *P*-values:
174 supplemental Tab. XXX). Ranking of effect strength with regard to the global metabolome
175 unraveled an effect from high to low by BpA < BpF < BpS for all microbiota.

176 Furthermore, we analyzed the effects of BpX on the absolute abundance of nine short-
177 chain fatty acids (SCFAs) by the fecal microbiota, since SCFAs constitute a group of
178 essential microbiota-derived metabolites that potentially influence the host in various ways
179 (den Besten et al., 2013). Global changes were visualized by NMDS analysis, using the
180 Bray-Curtis (BC) distance (Figure 3 A). The BC distance was used to determine the effect
181 strength by comparing the BC similarity of every sample to the untreated control (Figure
182 3 B).

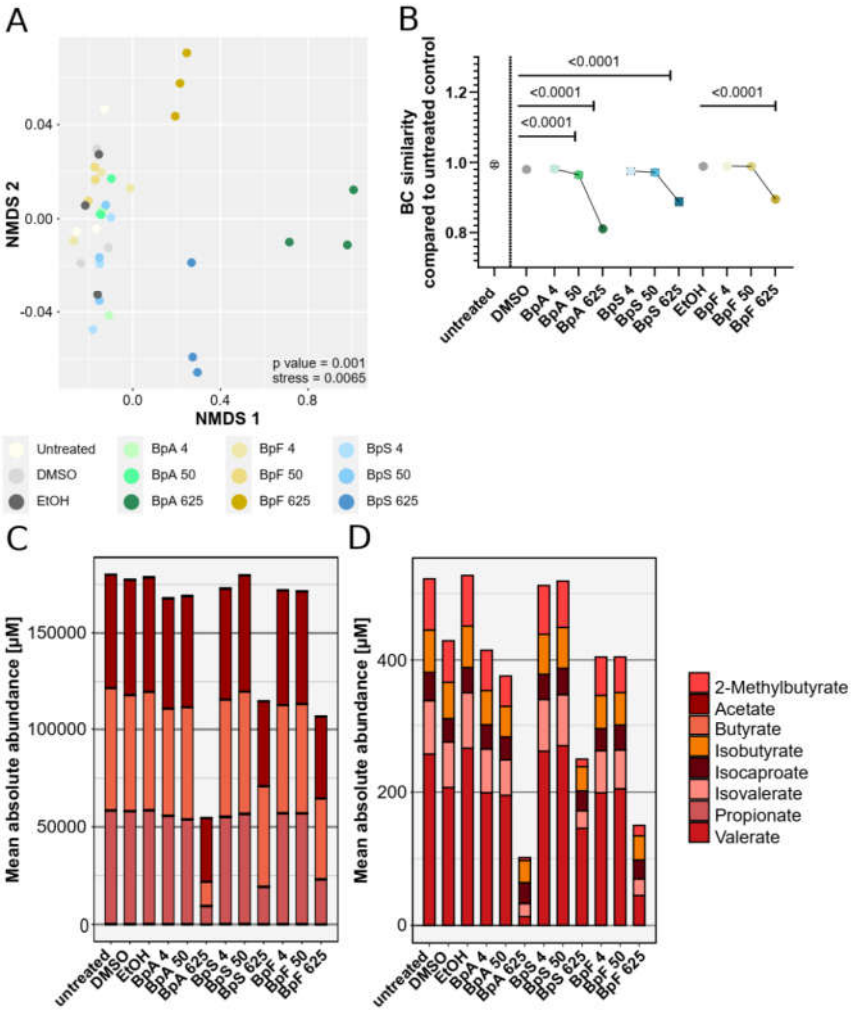

183

184 Figure 3

185 Similar to the effects on the global metabolome, NMDS analysis of SCFAs indicated that
186 high concentrations of BpX modified the microbial SCFA-profile (Figure 3 A). Compared to
187 the corresponding solvent control, the SCFA-profile was significantly affected after
188 exposure to 50 BpA and 625 BpA, whereby BpF and BpS significantly altered the SCFA-
189 profile at the highest concentration only (n=3, mean± sd, one-way ANOVA, *P*-values:
190 supplemental Table XXX). The mean absolute SCFA abundances were clearly reduced by
191 BpX in high concentrations regardless of the compound, simultaneously the proportion of

192 acetate increased (supplementary Fig. XXX). The effect strength decreased from BpA <
193 BpF < BpS.

194 ***Bisphenols impaired the MAIT cell-activating potential of individual bacterial***
195 ***strains***

196 MAIT cells are unconventional T cells that can be activated by microbiota-derived riboflavin
197 metabolites. Since BpX-exposure modified the microbial metabolome, we investigated
198 whether BpX-exposure indirectly affected MAIT cell activation via an altered microbial
199 metabolism.

200 We identified MAIT cells as alive single cell lymphocytes expressing CD3, CD8a, CD161 and
201 the semi-invariant T cell receptor (TCR) vα7.2 (Figure 4 A). In this study, activated MAIT
202 cells were quantified by the expression the CD69 and the simultaneous upregulation of
203 tumor necrosis factor (TNF) production (Figure 4 B).

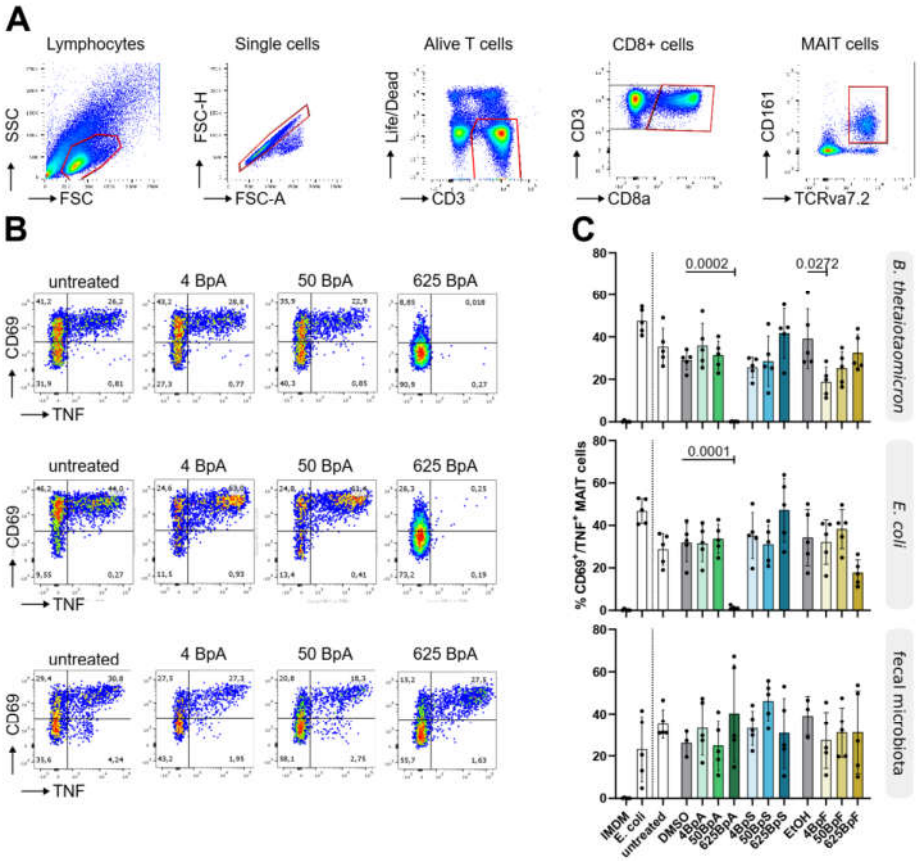

Figure 4

Although microbial growth and metabolism were altered at 625 BpX, the MAIT cell-activating potential of *B. thetaiotaomicron* was only reduceed at 625 BpA and interestingly at 4 BpF. For BpF and BpS the MAIT cell activating potential slightly increased with rising BpX concentration. Similarly, the MAIT cell-activating potential of *E. coli* was significantly lowered at 625 BpA as the only concentration and tendentially reduced at 625 BpF. As for *B. thetaiotaomicron* the MAIT cell-activating potential of *E. coli* seemed to increase with increasing concentration of BpS, but not for BpF. Despite the effects on microbial growth and metabolism, we did not observe effects on the MAIT cell-activating potential of the fecal microbiota.

To elucidate the degree of relatedness of the measured parameters, i.e. microbial growth and viability, the effect on microbial metabolism and the downstream effects on MAIT cell activation, we performed correlation analysis (Figure 5)

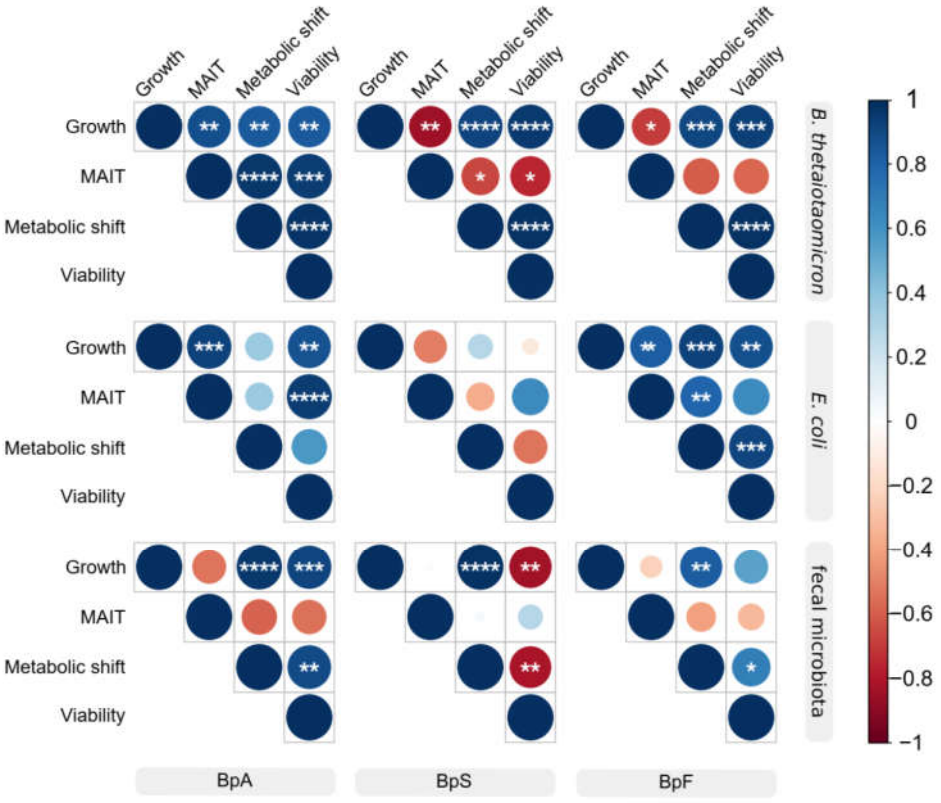

Figure 5

BpX-exposure affects the community structure in a dose-dependent manner

Since the fecal microbiota resemble a complex microbial community, we investigated BpX-related changes in taxonomy by 16S rRNA gene analysis.

Direct exposure to bisphenols did not affect cell viability, but modulated the MAIT cell response

BpX can affect microbial growth, viability and metabolism. Therefore, we also investigated the direct effects of BpX-exposure on human PBMCs with a focus on MAIT cell modulation. Therefore, MAIT cells were stimulated with 20 BpC *E. coli* in the presence of BpX.

First, we determined the percentage of alive $CD3^+$ cells to unravel potential cytotoxic effects of BpX-exposure (Figure 6).

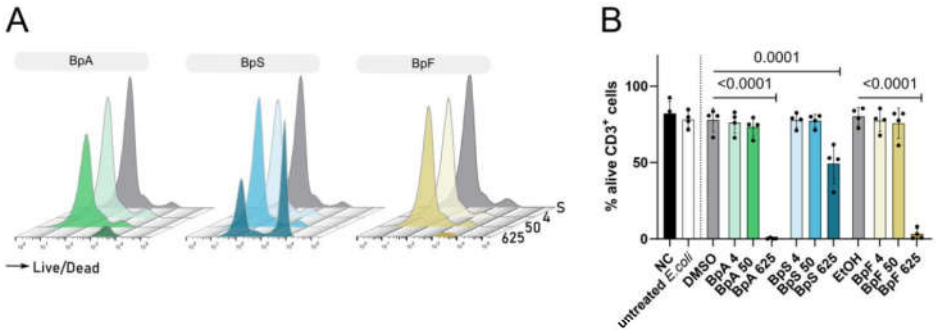

Figure 6

Due to cytotoxicity the number of alive $CD3^+$ cells was significantly reduced at a concentration of 625 BpX, whereby BpS less severely impaired $CD3^+$ viability. In contrast, treatment of microbiota with 4 BpX and 50 BpX did not affect the viability of $CD3^+$ cells.

Second, we determined the modulation of MAIT cell activation within the viable fraction of $CD3^+$ cells.

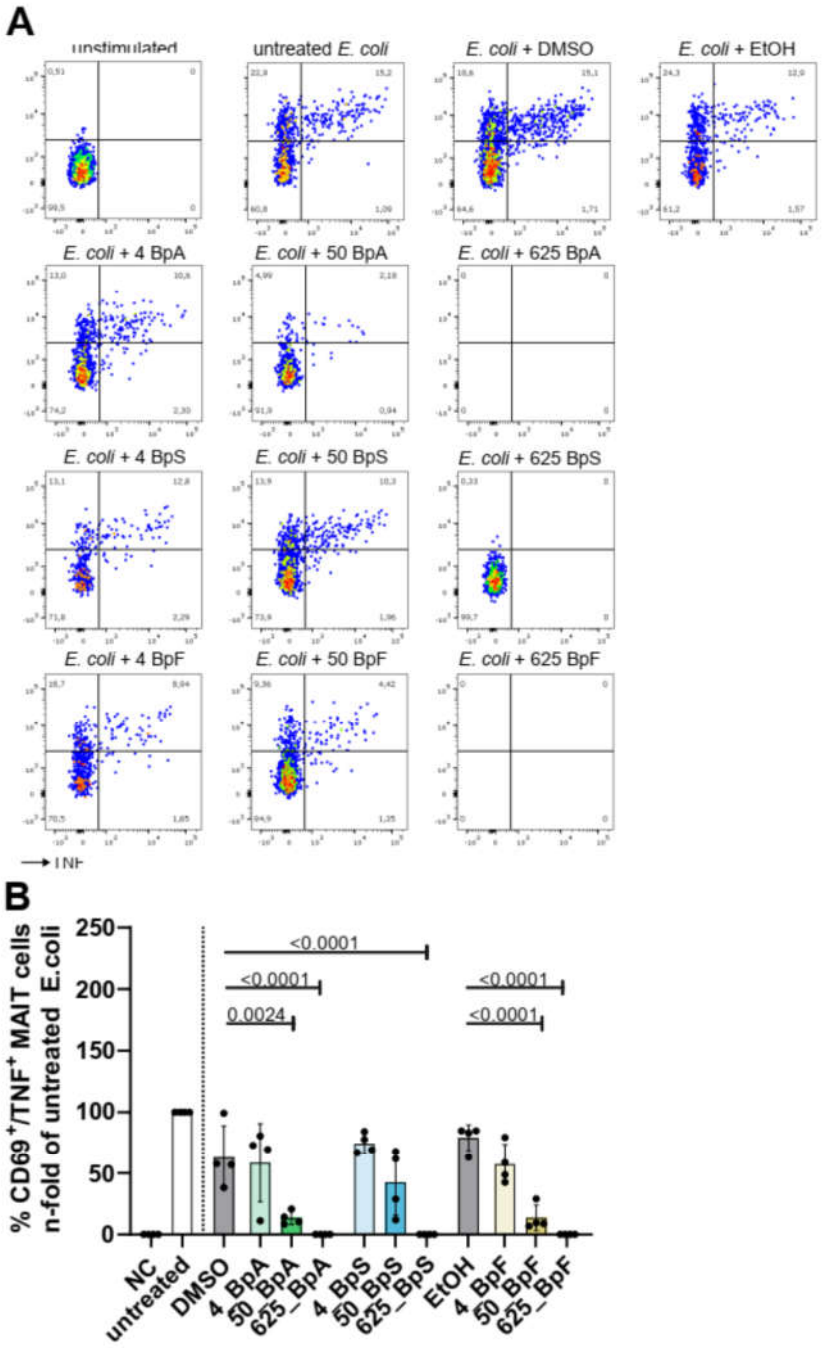

238

239 Figure 7

16

MAIT cell activation was reduced upon exposure to 50 BpA and 50 BpF, whereby BpS at the same concentration only slightly impaired MAIT cell activation.

Discussion

Methods

Preparation of fecal microbiota for reproducible batch cultivation

The inoculum was prepared from pooled fecal material of four lean (normal BMI), male subjects at the age of 25-35, without antibiotic therapy within six months prior to donation. After defecation, samples were kept anaerobic within 10 min and stored at -20 °C. Samples were thawed under anaerobic conditions (37 °C, 60 min) and ~0.125 g per donor (n=4) were inoculated into 50 mL Brain-Heart Infusion (BHI) medium (supplementary Tab. XXX – medium composition). The enrichment cultures were grown at 37 °C, 175 rpm shaking for a maximum of 24 h until stationary phase (supplementary Fig. XXX growth curves) and then bacteria were transferred into fresh BHI medium for another enrichment step. From the 9^{th} enrichment culture, 25% glycerol stocks were frozen at -20 °C and used as inoculum.

Bisphenol (BpX) exposure of microbiota in batch culture

Pre-warmed BHI was inoculated with fecal microbiota with a start OD600 of 0.4, the individual bacterial strains *E. coli* and *B. thetaiotaomicron* were inculated from an overnight culture at a start OD_{600} of 0.15 to 0.2. Since intestinal microbiota in the physiologic situation are constantly supplied with food, the microbiota were exposed during exponential growth.

Therefore, the bacteria were grown to early- to mid-exponential phase at 37 °C and 175 rpm shaking and then treated with bisphenols (BpX, Fig. S1). We applied BpX (Sigma-

263 Aldrich, St. Louis, US) in three concentrations based on the tolerable daily intake (TDI) of
264 bisphenol A (BpA). The BpX concentrations correspond to the actual TDI (4 µg/kg body
265 weight) and the TDI before 2015 (50 µg/kg body weight, European Food Safety Authority,
266 2015). We extrapolated these two concentrations to a high concentration of 625 µg/kg
267 body weight. Referring to the chemical approval in the EU, we calculated chemical uptake
268 for an average European male with 70 kg body weight and an average amount of stool
269 with 126.3 g (Rendtorff, 1967). Information on solvent and final molar concentrations are
270 summarized in supplementary Tab. XXX. For BpX treatment and solvent controls, we
271 applied the chemicals with a final concentration of 0.5 % solvent. The untreated control
272 remained untreated, but was opened so that all cultures were treated identically.

273 The bacteria were incubated for a total of 24 h. Upon centrifugation (3200 g, 5 min, 4 °C),
274 cell-free culture samples for metabolomics were stored at -80 °C, pellets for DNA-
275 extraction cell were stored at -20 °C.

276 ***Determination of microbial viability***

277 Microbial viability of 24 h old cultures was quantified using the microbial viability assay kit
278 (MVA, Dojindo EU GmbH, Munich, Germany) according to the manufacturer's instructions.

279 ***Preparation of microbiota for MAIT cell stimulation***

280 As described previously, bacteria were fixed and frozen prior to utilization in MAIT cell
281 stimulation assays (Krause et al., 2020). In brief: Equal volumes of culture of each replicate
282 were pooled per treatment. Bacteria cells were harvested by centrifugation, fixed in 1 %
283 formaldehyde for 1 min, washed three times with phosphate buffered saline (PBS) and
284 finally resuspended in IMDM medium. The cell number was determined using a Quantom
285 TX cell counting system (Beckman Coulter, Brea, USA) and cell numbers were adjusted in
286 IMDM medium. Bacteria pellets were frozen with supernatant and stored at -80 °C.

Purification of Peripheral Blood Mononuclear Cells (PBMCs)

We obtained blood from healthy donors from the blood donation service at the university hospital Leipzig, Germany. PBMCs were purified by gradient centrifugation on Ficoll-paque plus (GE Healthcare, Chicago, USA) and gradually frozen in FCS with 10% DMSO at -80 °C. PBMCs were stored at -150 °C until use.

MAIT cell stimulation assay

PBMCs were thawed at 37 °C for 10 min and seeded 1 x 10^6 of live PBMCs/well in IMDM into 96-well plates. PBMCs recovered over-night at 37 °C and 5 % CO_2.

To investigate the immune modulatory effects of bisphenols (BpX), we thawed the frozen BpX-exposed bacteria pellets, mixed them vigorously, and used 200 bacteria per cell (BpC) in a final volume of 200 µL for stimulation. The negative control remained unstimulated; the positive control was stimulated with 20 BpC *E. coli* K12.

After two hours, we added 10 µg/mL Brefeldin A to prevent cytokine release. After a total of 6 h PBMCs we stained surface (CD3, CD8a, CD161, Va7.2) and intracellular markers (CD69, TNF, IFNg) for FACS analysis (FACS Canto II, Becton Dickinson and Company, Franklin Lakes, USA). We discriminated dead cells by Fixable Viability Dye eFluor™ 506 staining. Antibodies/stains were obtained from Biolegend and eBioscience (supplementary Tab. S15). Data analysis was done with FlowJo® v10 software. Data evaluation and hypothesis testing was done with GraphPad PRISM v7.04 software using one-way ANOVA.

Quantitation of riboflavin in bacterial culture supernatants

Bacteria cells were pelleted by centrifugation (3.200 g, 5 min, 4 °C) and supernatants were stored at -80 °C for metabolome analysis. Samples were thawed at 37 °C for 5 -10 min. Metabolites were extracted with 5 volumes of a methanol:acetonitrile:water (2:3:1) mixture and 10 µL internal standard were added. After addition of 5 volumes of extraction solvent samples were vortexed for 5 min and sonicated in an ultrasound bath for additional 5 min. After centrifugation at 14000 rpm for 5 min the supernatant was transferred to a

313 fresh tube and dried in a SpeedVac™ vacuum concentrator (Eppendorf, Hamburg,
314 Germany). The dried extract was resuspended in 100 µL of mix of running solvent A and
315 running solvent B (1:1).

316 For LC-MS/MS measurement 10 µL of the resuspended extract was injected into a HPLC-
317 MS-System (RSLC Ultimate 3000 Thermo Fisher coupled with Q-Trap 5500 AB Sciex).
318 Metabolites were separated on ACQUITY UPLC BEH 300 C18 (1,7 µm, Waters) with a flow
319 rate of 0.3 mL/min in a gradient of running solvent A (0.1% formic acid in water) and
320 running solvent B (0.1% formic acid in methanol): 0.5 min 100% A, 0.6-4min 0%-100%
321 B, hold 3 min, 3min 100% A. The Q-Trap was set up to positive MRM mode (Riboflavin
322 MRM: parent ion: 377, product ions: 243, 198, and 172; Internal Standard MRM: parent
323 ion: 383, product ions: 249, 202, and 175). Bar plots were generated with the GraphPad
324 PRISM v7.04 software.

325 ***DNA extraction and 16S rRNA gene analysis***

326 Pellets were resuspended in 50 µL sterile Millipore water. One part cell slurry was mixed
327 with 30 parts 10% Chelex suspended in sterile Millipore water. RNA was removed by the
328 addition of 2 µL of RNase A (Invitrogen…). For cell disruption and extraction of genomic
329 DNA (gDNA), the mixture was incubated at 56 °C for 6h. Chelex and cell debris were
330 pelleted (13.000 g, 3 min, RT). Supernatant containing the gDNA was transferred into a
331 fresh tube and stored at -20 °C (protocol adapted from Lienhard and Schäffer, 2019).

332 16S amplicon sequencing was performed at Eurofins genomics (Eurofins Genomics GmbH,
333 Ebersberg, Germany) in randomized sample order. The V3-V5 region from the 16S rRNA
334 gene were PCR-amplified using the 341F forward primer CCTACGGGNGGCWGCAG
335 (Klindworth et al., 2013) and the 981R reverse primer GGGTTGCGCTCGTTGCGGG (Sacchi
336 et al., 2002). Sequencing was performed by Illumina paired end sequencing. Raw
337 sequences were processed using the *dada2* pipeline (Callahan et al., 2016) in combination
338 with *cutadapt* (Martin, 2011) for read filtering/trimming. Reads with minimum length of
339 20 nucleotides (nt) and a quality threshold below 20 were removed. The forward and

reverse reads were concatenated due to no overlap. Taxonomy was assigned using the Silva 138 data base. Data visualization was performed using the phyloseq packacke in R version 3.5.2 (McMurdie and Holmes, 2013)

Cytokine quantification with Cytokine Bead Array and ELISA

We used the same donors for cytokine analysis as we used for MAIT cell stimulation. Again PBMCs were thawed at 37 °C for 10 min and 1 x 10^6 of live PBMCs/well were seeded into 96-well plates. The next day, we stimulated PBMCs in a final volume of 200 µL with 200 BpC BpX-exposed fecal bacteria or with 20 BpC *E. coli* and exposed the cells during stimulation to BpX. Here, we used 0.5% solvent, either DMSO for BpA and BpS or ethanol for BpF exposure. The negative control remained unstimulated; the positive control was stimulated with 20 BpC *E. coli* K12. After 24 h, we stored the supernatant at -80 °C until we measured the following cytokines XXX with cytokine bead array (Hersteller etc…) or the cyotkines IL-12 and IL-18 with ELISA.

Statistical analysis

Acknowledgements

We thank the German Federal Environmental Foundation for financial support of Jannike Lea Krause. This work has been conducted within the postgraduate course *toxicology and environmental protection* at the University of Leipzig. Martin von Bergen acknowledges partial funding by DFG Priority Program 2002 We thank Jeremy Knespel, Michaela Loschinski and Nicole Gröger for technical assistance. This work was prepared in the framework of the postgraduate studies *toxicology and environmental protection* at the University of Leipzig.

Author contribution

JLK and GH conceptualized the study. JLK wrote the manuscript's first draft, and performed the microbiological and immunological experiments. BE and URK were responsible for SCFA and untargeted metabolomics. GH, AP, and MvB provided helpful discussions and revised the manuscript.

Disclosure/Conflict of Interest

The authors have no conflict of interest to declare.

References

Almeida, S., Raposo, A., Almeida-González, M., and Carrascosa, C. (2018). Bisphenol A: Food Exposure and Impact on Human Health: Bisphenol A and human health effect…. Compr. Rev. Food Sci. Food Saf. *17*, 1503–1517.

Belkaid, Y., and Harrison, O.J. (2017). Homeostatic Immunity and the Microbiota. Immunity *46*, 562–576.

den Besten, G., van Eunen, K., Groen, A.K., Venema, K., Reijngoud, D.-J., and Bakker, B.M. (2013). The role of short-chain fatty acids in the interplay between diet, gut microbiota, and host energy metabolism. J. Lipid Res. *54*, 2325–2340.

Brestoff, J.R., and Artis, D. (2013). Commensal bacteria at the interface of host metabolism and the immune system. Nat. Immunol. *14*, 676–684.

Callahan, B.J., McMurdie, P.J., Rosen, M.J., Han, A.W., Johnson, A.J.A., and Holmes, S.P. (2016). DADA2: High-resolution sample inference from Illumina amplicon data. Nat. Methods *13*, 581–583.

Chen, D., Kannan, K., Tan, H., Zheng, Z., Feng, Y.-L., Wu, Y., and Widelka, M. (2016). Bisphenol Analogues Other Than BPA: Environmental Occurrence, Human Exposure, and Toxicity—A Review. Environ. Sci. Technol. *50*, 5438–5453.

Chiba, A., Murayama, G., and Miyake, S. (2018). Mucosal-Associated Invariant T Cells in Autoimmune Diseases. Front. Immunol. *9*, 1333.

Comstock, L.E., and Coyne, M.J. (2003). Bacteroides thetaiotaomicron: a dynamic, niche-adapted human symbiont. BioEssays *25*, 926–929.

Corbett, A.J., Eckle, S.B.G., Birkinshaw, R.W., Liu, L., Patel, O., Mahony, J., Chen, Z., Reantragoon, R., Meehan, B., Cao, H., et al. (2014). T-cell activation by transitory neo-antigens derived from distinct microbial pathways. Nature *509*, 361–365.

Eckle, S.B.G., Corbett, A.J., Keller, A.N., Chen, Z., Godfrey, D.I., Liu, L., Mak, J.Y.W., Fairlie, D.P., Rossjohn, J., and McCluskey, J. (2015). Recognition of Vitamin B Precursors and Byproducts by Mucosal Associated Invariant T Cells. J. Biol. Chem. *290*, 30204–30211.

Eladak, S., Grisin, T., Moison, D., Guerquin, M.-J., N'Tumba-Byn, T., Pozzi-Gaudin, S., Benachi, A., Livera, G., Rouiller-Fabre, V., and Habert, R. (2015). A new chapter in the bisphenol A story: bisphenol S and bisphenol F are not safe alternatives to this compound. Fertil. Steril. *103*, 11–21.

European Food Safety Authority (2015). EFSA explains the Safety of Bisphenol A: scientific opinion on bisphenol A (2015). (Parma: EFSA).

Forbes, J.D., Van Domselaar, G., and Bernstein, C.N. (2016). The Gut Microbiota in Immune-Mediated Inflammatory Diseases. Front. Microbiol. *7*.

Geens, T., Aerts, D., Berthot, C., Bourguignon, J.-P., Goeyens, L., Lecomte, P., Maghuin-Rogister, G., Pironnet, A.-M., Pussemier, L., Scippo, M.-L., et al. (2012). A review of dietary and non-dietary exposure to bisphenol-A. Food Chem. Toxicol. *50*, 3725–3740.

Gherardin, N.A., Keller, A.N., Woolley, R.E., Le Nours, J., Ritchie, D.S., Neeson, P.J., Birkinshaw, R.W., Eckle, S.B.G., Waddington, J.N., Liu, L., et al. (2016). Diversity of T Cells Restricted by the MHC Class I-Related Molecule MR1 Facilitates Differential Antigen Recognition. Immunity *44*, 32–45.

Goodrich, J.K., Davenport, E.R., Beaumont, M., Jackson, M.A., Knight, R., Ober, C., Spector, T.D., Bell, J.T., Clark, A.G., and Ley, R.E. (2016). Genetic Determinants of the Gut Microbiome in UK Twins. Cell Host Microbe *19*, 731–743.

Kjer-Nielsen, L., Patel, O., Corbett, A.J., Le Nours, J., Meehan, B., Liu, L., Bhati, M., Chen, Z., Kostenko, L., Reantragoon, R., et al. (2012). MR1 presents microbial vitamin B metabolites to MAIT cells. Nature.

Klindworth, A., Pruesse, E., Schweer, T., Peplies, J., Quast, C., Horn, M., and Glöckner, F.O. (2013). Evaluation of general 16S ribosomal RNA gene PCR primers for classical and next-generation sequencing-based diversity studies. Nucleic Acids Res. *41*, e1–e1.

Krause, J.L., Schäpe, S.S., Schattenberg, F., Müller, S., Ackermann, G., Rolle-Kampczyk, U.E., Jehmlich, N., Pierzchalski, A., von Bergen, M., and Herberth, G. (2020). The Activation of Mucosal-Associated Invariant T (MAIT) Cells Is Affected by Microbial Diversity and Riboflavin Utilization in vitro. Front. Microbiol. *11*, 755.

Lai, K.-P., Chung, Y.-T., Li, R., Wan, H.-T., and Wong, C.K.-C. (2016). Bisphenol A alters gut microbiome: Comparative metagenomics analysis. Environ. Pollut. *218*, 923–930.

Levy, M., Blacher, E., and Elinav, E. (2017). Microbiome, metabolites and host immunity. Curr. Opin. Microbiol. *35*, 8–15.

Lienhard, A., and Schäffer, S. (2019). Extracting the invisible: obtaining high quality DNA is a challenging task in small arthropods. PeerJ *7*, e6753.

Magalhaes, I., Pingris, K., Poitou, C., Bessoles, S., Venteclef, N., Kiaf, B., Beaudoin, L., Da Silva, J., Allatif, O., Rossjohn, J., et al. (2015). Mucosal-associated invariant T cell alterations in obese and type 2 diabetic patients. J. Clin. Invest. *125*, 1752–1762.

433 Martin, M. (2011). Cutadapt removes adapter sequences from high-throughput sequencing
434 reads. EMBnet.Journal *17*, 10.

435 Martinson, J.N.V., Pinkham, N.V., Peters, G.W., Cho, H., Heng, J., Rauch, M., Broadaway,
436 S.C., and Walk, S.T. (2019). Rethinking gut microbiome residency and the
437 Enterobacteriaceae in healthy human adults. ISME J. *13*, 2306–2318.

438 McMurdie, P.J., and Holmes, S. (2013). phyloseq: An R Package for Reproducible
439 Interactive Analysis and Graphics of Microbiome Census Data. PLoS ONE *8*, e61217.

440 Rendtorff, R. (1967). Stool Patterns of Healthy Adult Males.

441 Rochester, J.R. (2013). Bisphenol A and human health: A review of the literature. Reprod.
442 Toxicol. *42*, 132–155.

443 Rochester, J.R., and Bolden, A.L. (2015). Bisphenol S and F: A Systematic Review and
444 Comparison of the Hormonal Activity of Bisphenol A Substitutes. Environ. Health Perspect.
445 *123*, 643–650.

446 Sacchi, C.T., Whitney, A.M., Mayer, L.W., Morey, R., Steigerwalt, A., Boras, A., Weyant,
447 R.S., and Popovic, T. (2002). Sequencing of 16S rRNA Gene: A Rapid Tool for Identification
448 of *Bacillus anthracis*. Emerg. Infect. Dis. *8*, 1117–1123.

449 Sender, R., Fuchs, S., and Milo, R. (2016). Revised estimates for the number of human
450 and bacteria cells in the body.

451 Serriari, N.-E., Eoche, M., Lamotte, L., Lion, J., Fumery, M., Marcelo, P., Chatelain, D.,
452 Barre, A., Nguyen-Khac, E., Lantz, O., et al. (2014). Innate mucosal-associated invariant
453 T (MAIT) cells are activated in inflammatory bowel diseases: MAIT cells in IBD. Clin. Exp.
454 Immunol. *176*, 266–274.

455 Thaiss, C.A., Zmora, N., Levy, M., and Elinav, E. (2016). The microbiome and innate
456 immunity. Nature *535*, 65–74.

457 Vandenberg, L.N., Hauser, R., Marcus, M., Olea, N., and Welshons, W.V. (2007). Human
458 exposure to bisphenol A (BPA). Reprod. Toxicol. *24*, 139–177.

459 Vandenberg, L.N., Hunt, P.A., Myers, J.P., and vom Saal, F.S. (2013). Human exposures
460 to bisphenol A: mismatches between data and assumptions. Rev. Environ. Health *28*.

461 Zhou, X., Kramer, J.P., Calafat, A.M., and Ye, X. (2014). Automated on-line column-
462 switching high performance liquid chromatography isotope dilution tandem mass
463 spectrometry method for the quantification of bisphenol A, bisphenol F, bisphenol S, and
464 11 other phenols in urine. J. Chromatogr. B *944*, 152–156.

465

Publication 8: Environmentally relevant concentration of Bisphenol S shows slight effects on SIHUMIx

microorganisms MDPI

Article

Environmentally relevant concentration of Bisphenol S shows slight effects on SIHUMIx

Stephanie Serena. Schäpe[1], Jannike Lea Krause[2], Rebecca Katharina Masanetz[1], Sarah Riesbeck[1], Robert Starke[3], Ulrike Rolle-Kampczyk[1], Christian Eberlein[4], Hermann Josef Heipieper[4], Gunda Herberth[2], Martin von Bergen[1,5] , Nico Jehmlich[1*]

1 Helmholtz-Centre for Environmental Research – UFZ GmbH, Department of Molecular Systems Biology, Leipzig, Germany, stephanie.schaepe@ufz.de; ulrike.rolle-kampczyk@ufz.de; nico.jehmlich@ufz.de; martin.vonbergen@ufz.de
2 Helmholtz-Centre for Environmental Research – UFZ GmbH, Department of Environmental Immunology, Leipzig, Germany; jannike-lea.krause.ufz.de; gunda.herberth@ufz.de
3 Laboratory of Environmental Microbiology, Institute of Microbiology of the Czech Academy of Sciences, Prague, Czech Republic; robert.starke@biomed.cas.cz
4 Helmholtz-Centre for Environmental Research – UFZ GmbH, Department of Environmental Biotechnology, Leipzig, Germany, christian.eberlein@ufz.de; hermann.heipiper@ufz.de
5 Institute of Biochemistry, Faculty of Biosciences, Pharmacy and Psychology, University of Leipzig, Germany

* Correspondence: nico.jehmlich@ufz.de ; phone: +49 341 235 4767

Received: date; Accepted: date; Published: date

Abstract: Bisphenol S (BPS) is an industrial chemical used in the process of polymerization of polycarbonate plastics and epoxy resins and thus can be found in various plastic products and thermal papers. The microbiota disrupting effect of BPS on the community structure of the microbiome has already been reported, but little is known on how BPS affects bacterial activity and function. To analyze these effects, we cultivated the simplified human intestinal microbiota (SIHUMIx) in bioreactors to determine the effects of BPS exposure at a concentration of 45 µM that was previously shown to affect zebrafish gut microbiota on the community structure and function. Furthermore bisphenols have been shown to affect membrane structure. By determining biomass, growth of SIHUMIx was followed but no differences during BPS exposure were observed. To validate if the membrane composition was affected, fatty acid methyl esters (FAMEs) profiles were compared. Changes in the individual membrane fatty acid composition could not been described; however, the saturation level of the membranes slightly increased during BPS exposure. By applying targeted metabolomics to quantify short-chain fatty acids (SCFA), it was shown that the activity of SIHUMIx was unaffected. Metaproteomics revealed temporal effect on the community structure and function, showing that BPS has in contrast to a zebrafish microbiome no effect on the structure or functionality of SIHUMIx.

Keywords: In vitro model; bisphenol S; metaproteomics; short-chain fatty acids; fatty acid methyl ester; intestinal microbiota

1. Introduction

Bisphenols are an initial material in the production of polycarbonate plastics and epoxies resins, and thus can be found in a variety of everyday products e.g., plastic bottles and boxes used for liquid and food storage or the inner coating of food cans [1,2]. However, a growing number of studies indicate that bisphenols show health-threatening effects on humans [3].

The most commonly applied bisphenol A (BPA) has been classified as endocrine disruptor and has been associated with the development of diseases e.g. diabetes [4]. Due to its endocrine disrupting properties BPA has been banned from products in food packaging and consumer products used by small children and has been added to the EU candidate list for substances of very high concern (SVHC) [5]. BPA is increasingly replaced by structure analogues, including bisphenol S (BPS). However, BPS was also found to impact human health. It was reported that BPS impairs blood functions by affecting blood cells, glucose and cholesterol metabolism and inducing cardiovascular risks in rats [6]. It has also similar estrogenic activity when compared with BPA, although it showed lower acute toxicity in vivo [3]. In 2017, BPS has been added to the Chemicals of High Concern to Children (CHCC) Reporting List in Washington state [7].

Bisphenols are detected in the environment up to concentrations of 1,000 µg/L [8,9]. They enter the human body through different exposure routes and also find their way towards human gut microbiota. Studies reported the accumulation of BPA and its analogues in the human body [10] and quantified metabolites in blood and urine [11-13]. The host-microbiota-interactions in the human gut are essential for human health [14]. This interaction can be effected by environmental chemicals if they support or suppress bacterial growth or if taxonomic composition and functions are effected, both has been shown for bacterial communities in the past [15,16]. Furthermore bacterial growth can also be supported by environmental chemicals due to the provision of its energy or carbon supplying properties mostly due to hydrolytic and reductive reactions [17]. The transformation potential has been proved to mediate BPA and BPS degradation by bacteria in industrial wastewater treatment plants, water and seawater [18,19].

It was reported that bisphenols can also be toxic to bacteria by destabilizing cell membranes, thereby disturbing its integrity and effecting specifically the membrane permeabilization [20]. Recently, it was observed that bisphenols (especially BPA, BPS and BPF) are likely to accumulate at bacterial membranes due to their lipophilicity and therefore may lead to disturbances in the cell functioning and to cell destruction [21]. Importantly, bisphenols were also shown to modify microbial composition. In mice, at a concentration of 120 µg/mL BPA solved in DMSO, the alpha- and beta-diversity of the intestinal microbiota was altered by favoring the growth of *Proteobacteria* [22]. In zebrafish, a different concentration of BPA and its analogues including BPS were shown to affect zebrafish gut microbiota [23]. Catron et *al.* found that different bisphenols alter the intestinal microbiota by changing specific family abundances (e.g., *Neisseriaceae*, *Cryomorphaceae*), with BPS being the least toxic BPA analogues for host development and estrogenicity but the most potent in microbial disruption at a concentration of 45 µM (11.2 µg/mL) BPS solved in DMSO. However, little is known about how the intestinal microbiota is altered on a functional level when exposed to BPS. To our knowledge, concentrations of bisphenols in the human gut have not been measured yet, hence we used the concentration of 45 µM/mL that was previously shown to affect zebrafish gut microbiota to investigate how BPS affected microbial functions.

Recently, we established an *in vitro* bioreactor model for continuous cultivation of the extended simplified human intestinal microbiota (SIHUMIx) [24]. SIHUMIx comprises of eight species representing a majority of metabolic activities typically found in the human intestine. The cultivation *in vitro* is is highly reproducible and reaches a constant state giving a starting point for stress exposure studies [25]. In this study, we investigated how the exposure of 45 µM BPS in DMSO modulates (i) overall growth, (ii) membrane fatty acid composition, (iii) taxonomic composition and(iv) functional changes of SIHUMIx.

2. Materials and Methods

2.1 Simplified human intestinal microbiota - SIHUMIx

The extended simplified human intestinal microbiota (SIHUMIx) consists out of the following eight species: *Anaerostipes caccae* (DSMZ 14662), *Bacteroides thetaiotaomicron* (DSMZ 2079), *Bifidobacterium longum* (NCC 2705), *Blautia producta* (DSMZ 2950), *Clostridium butyricum* (DSMZ 10702), *Clostridium ramosum* (DSMZ 1402), *Escherichia coli* K-12 *(MG1655)* and *Lactobacillus plantarum*

(DSMZ 20174) [26]. The cultivation protocol, the growth conditions and the medium ingredients were used as reported [Supplementary material Table S1].

2.2 Experimental set-up

For inoculation of the bioreactor system, the single strain bacteria were thawed from a fresh glycerol stock two weeks before the experiment started and grown in Brain-Heart-Infusion (BHI) as described (Supplementary material Table S1). Bacteria from three-day old cultures were counted at a Multisizer 3 (Beckman Coulter, Brea, United States) prior to inoculation. $1 \cdot x10^9$ bacteria per strain (a total of $8x10^9$ bacteria per 250 mL) were inoculated into the bioreactors (d0). The continuous cultivation was started after 24 h.

The bioreactor run consists of two phases: (i) the adaption phase where the community established and reached a constant community state (d1-d7) and the treatment phase (d8-d14) in which the effect of 7 days BPS exposure was investigated (Figure 1).

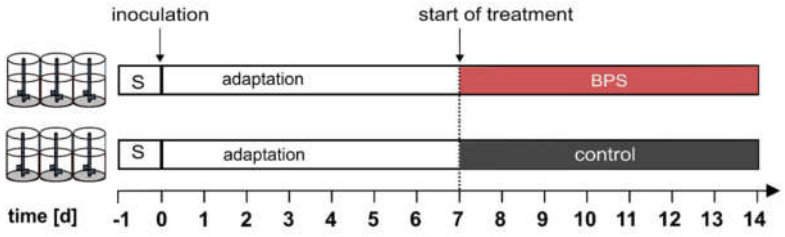

Figure 1: Experimental set-up of the bioreactor run: six bioreactors were inoculated with 1 x 10^9 cells/250 mL and run for 7 days under continuous culture conditions. On day 7, three bioreactors were exposed to BPS resulting in a constant BPS exposure of 45 µM until day 14.

A concentration of 45 µM BPS dissolved in DMSO (final concentration in the bioreactor 1.2%) was applied, since this concentration has been reported to alter the intestinal microbiota taxonomy in zebrafish [23]. It represents a concentration equal to the 4x ADI of BpA in humans. In the control bioreactors, an equal amount of DMSO was added as solvent control. During the whole experiment, samples were taken every 24 h starting the day after inoculation (d1). Community adaption was followed by targeted metabolomics of short-chain fatty acid [27,28]. Microbiota growth was evaluated with determination of absolute biomass. The community structure and function of SIHUMIx was analyzed with metaproteomics on day 5, 6, 7, 8, 12, 13 and 14. Bacteria suspensions were centrifuged at 3200 x g for 10 min at 4 °C and immediately frozen at -80 °C for subsequent sample analysis.

2.4 Microbial growth

For microbial biomass determination, 4 mL of bioreactor liquid including bacterial cells were centrifuged (5000 x g, 10 min), washed twice (Phosphate Saline Buffer; PBS), dried in a centrifugal vacuum concentrator (350 x g, 40 °C; N-Biotek, Germany) and weighed using a standard precision scale.

2.5 Metaproteomics

Protein extraction

2 mL bioreactor liquid was centrifuged (3,200 x g, 10 min, 4 °C) and the pellet was solved in 1 mL lysis buffer (8M Urea, 2M Thiourea, 1mM PMSF). Bacteria were disrupted by bead beating (FastPrep-24, MP Biomedicals, Sanra Ana, CA, USA; 5.5 ms, 1 min, 3 cycles) followed by ultra-sonication (UP50H, Hielscher, Teltow, Germany; cycle 0.5, amplitude 60%) and centrifugation (10,000 x g,

10 min) [29]. The supernatant was used for protein concentration determination using the Pierce™ 660 nm Protein Assay (Thermo Scientific, Thermo Fischer Scientific, Waltham, MA, USA). 10 µg of protein lysate was incubated with 25 mM 1,4-dithiothreitol (in 20 mM ammonium bicarbonate) for 1 h and 100 mM iodoacetamide (in 20 mM ammonium bicarbonate) for 30 min. Protein cleaning, cleavage and peptide cleaning were done with hydrophobic Sera-Mag SpeedBead Carboxylate-Modified Magnetic Particles (GE Healthcare, U.S.) as described elsewhere [30]. Proteins were digested with Trypsin (1:50), peptides were eluted with 2% dimethylsulfoxide solved in water without fragmentation. Peptides were solved in 0.1% formic acid for mass spectrometric measurement.

Nano LC MS/MS measurement

5 µg peptides were injected into nano high-performance liquid chromatograph (HPLC) (UltiMate 3000 RSLCnano, Dionex, Thermo Fisher Scientific, Waltham, MA, USA). Peptide separation was performed on a C18-reverse-phase trapping column (C18 PepMap100, 300 µm x 5 mm, particle size 5 µm, nano viper, Thermo Fischer Scientific, Waltham, MA, USA), followed by a C18-reverse-phase analytical column (Acclaim PepMap® 100, 75 µm x 25 cm, particle size 3 µm, nanoViper, Thermo Fischer Scientific). Mass spectrometric analysis of peptides was performed on a Q Exactive HF mass spectrometer (Thermo Fisher Scientific, Waltham, MA, USA) coupled with a TriVersa NanoMate (Advion, Ltd., Harlow, UK) source in LC chip coupling mode. LC gradient, ionization mode and mass spectrometry mode have been used as described before [31].

Data analysis

Raw data were processed with Proteome Discoverer (v2.2, Thermo Fischer Scientific, Waltham, MA, USA). Search settings for the Sequest HT search engine were set to trypsin (Full), max. missed cleavage: 2, precursor mass tolerance: 10 ppm, fragment mass tolerance: 0.02 Da. The protein-coding sequences of the eight SIHUMIx strains were downloaded from UniProt (http://www.uniprot.org/), combined and used as database resulting in 29,558 protein sequences. The false discovery rates (FDR) were determined with the node Percolator [32] embedded in Proteome Discoverer and we set to the FDR threshold at a peptide level of <1%. The same threshold was set for the protein FDR (<1%). Protein grouping was performed as described [25]. *GhostKOALA* was used to assign KO numbers from Kyoto Encyclopedia of Genes and Genomes (KEGG) to identified functions of identified protein sequences [33,34]. Protein report from Proteome Discoverer with assigned taxa and functional information from KEEG are provided (Supplementary Material Table S2). Only pathways with sufficient coverage (>10%) on total per sample were used for analysis. For specific pathway abundances only pathways with sufficient relative abundance (>0.1%) and pathway coverage (>3 proteins) per sample were evaluated. Visualization and statistical analysis were done with GraphPad Prism (v8.0.2) using unpaired multiple t-tests per p-value adjustment and are given for taxa and pathways (Supplementary Material Table S2). Principal component analysis was performed using the prcomp function with default setting in R and visualized with ggplot. Statistical protein analysis was performed with MSqRob [35,36]. Protein report from Proteome Discoverer was used as input matrix and pre-processing was applied by log2 transformation, linear regression normalization (Rlr) and no further filtering. Diagnostic plots are shown (Supplementary Material Figure S2). Quantification was done by setting treatment per day as fixed settings and bioreactor as random effects, Analysis type: standard, Minimum Fold Change: 0, Number of contrast 1, Contrasts: -1/4 for DMSO control day 8, 12, 13,14, respectively and 1/4 for BPS day 8, 12,13 and 14 respectively. Result table is shown (Supplementary Material Table S3). Volcano plot and boxplots of relevant proteins are provided (Supplementary Material Figure S2).

2.6 Short-chain fatty acid analysis

Metabolite extraction

For the short-chain fatty acids (SCFAs) analysis the method of Han et al. was modified [27,28]. Briefly, the samples were mixed with acetonitrile to a final concentration of 50 % acetonitrile. SCFAs were derivatized with 0.5 volumes of 200 mM 3-nitrophenylhydrazine and 0.5 volumes of 120 mM N-(3-dimethylaminopropyl)-N'-ethylcarbodiimide hydrochloride in pyridine for 30 min at 40 °C. The derivatized SCFA solutions were then diluted 1:50 in 10 % acetonitrile.

Measurement and data analysis

For identification and quantitation, 50 µL of the diluted SCFA derivatives was injected into the LC-MS/MS system. Chromatographic separation of SCFAs was performed on an Acquity UPLC BEH C18 column (1.7 µm; Waters, Eschborn, Germany) using H_2O (0.01 % formic acid, FA) and acetonitrile (0.01% FA) as the mobile phases. The column flow rate was set to 0.35 mL/min, the column temperature at 40 °C. The gradient elution was performed as follows: 2 min at 15% B, 15-50% B in 15 min, then held at 100% B for 1 min. Finally, the column was equilibrated for 3 min at 15% B. Mass spectrometric analysis of metabolites was performed QTRAP®5500 (AB Sciex Framingham, USA). For identification and quantitation, a scheduled MRM method was used, with specific transitions for every SCFA. Peak areas were determined in Analyst® Software (v1.6.2, AB Sciex) and areas for single SCFAs were exported. Normalization and statistics were performed with in-house written *R* scripts

2.7 Lipid analysis

Lipid extraction and derivatization to fatty acid methyl esters (FAME)

Extraction and derivatization of membrane lipids was carried out according to Bligh and Dyer [37]. 2 mL bioreactor liquid was taken, centrifuged (3,200 x g, 10 min, 4 °C) and the lipids were extracted with chloroform/methanol/water as described [37]. Fatty acid methyl esters (FAME) were prepared by incubation for 15 min at 80 °C in boron trifluoride/methanol, applying the method of Morrison and Smith, and FAME samples were extracted with hexane [38].

Analysis of fatty acid composition by GC-FID

Analysis of FAME in hexane was performed using a quadruple GC System (HP5890, Hewlett & Packard, Palo Alto, USA) equipped with a split/splitless injector. A CPSil 88 capillary column (Chrompack, Middelburg, The Netherlands; length, 50 m; inner diameter, 0.25 mm; 0.25 lm film) was used for the separation of the FAME. GC conditions were: injector temperature was held at 240 °C, detector temperature was held at 270 °C. The injection was splitless, carrier gas was helium at a flow of 2 mL/min. The temperature program was: 40 °C, 2 min isothermal; 8 °C/min to 220 °C; 15 min isothermal at 220 °C. The pressure program was: 27.7 psi (=186.15 kPa), 2 min isobaric; 0.82 psi/min (5.65 kPa/min) to the final pressure 45.7 psi; 15.55 min isobaric at 45.7 psi (310.26 kPa). The relative amount of FAMEs were calculated based on peak areas of the total ion chromatograms (TIC). Fatty acids were identified by GC and co-injection of authentic reference compounds obtained from Supelco (Bellefonte, USA).

Data analysis

The degree of saturation of membrane fatty acids was calculated as described [39] and is defined as the ratio between the two saturated fatty acids (16:0 and 18:0), the two unsaturated fatty acids (16:1cis, 18:1cis 18:1cis). Furthermore, two cyclopropane fatty acids (17*cyc* and 19*cyc*) and the two-branched fatty acids (15:0iso, 15:0anteiso) were detected. The degree saturation of the membrane of SIHUMIx was calculated based on the ratio of saturated to unsaturated fatty acids and cyclopropyl fatty acids (1) and based on the ratio of saturated anteiso- and iso-methyl-branched fatty acids (2)[39,40].

$$\text{sat/unsat+cyclo} = \frac{(16{:}0 + 18{:}0)}{(16{:}1\ cis + 17\ cyc + 18{:}1\ cis + 19\ cyc)}, \quad (1)$$

$$\text{anteiso/iso} = \frac{(15{:}0\ anteiso)}{(15{:}0\ iso\ )}, \quad (2)$$

3. Results

3.1 BPS does not affect total biomass or membrane fatty acids

First, biomass production of SIHUMIx was followed, to investigate growth supressing effect of BPS exposure. Bioreactors (n = 6) were inoculated with $1x10^9$ cells/250 mL per species (n = 8) and cultivated for seven days until reaching a structural and functional constant state [24]. After sampling on day 7, BPS solved in DMSO or DMSO (equal volume in the control) was spiked into the bioreactors and added to the feed medium to maintain a constant BPS concentration of 45 µM. The redox potential and pH were followed during the experiment (Supplementary Material Figure S1). The bacterial biomass increased starting from day 1 until day 7 to 11.4 ± 0.63 mg/mL in all bioreactors (Figure 2).

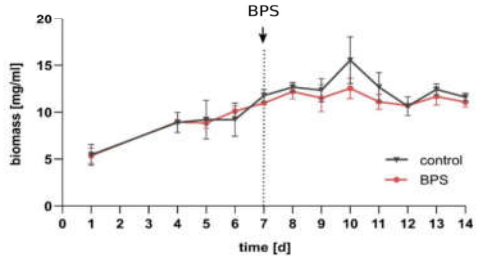

Figure 2: Bacterial growth of SIHUMIx indicated by biomass development (mean of n=3 bioreactors).

After BPS addition, the biomass was slightly lower in the BPS vessels, however, no statistical significance was observed. Except on day 10, the biomass increased and the variation among the three bioreactors vessels was larger compared to the other days. On the last sampling day, the BPS and control bioreactor vessels had similar biomass of 11.6 ± 0.42 mg/mL and 11.1 ± 0.5 mg/mL, respectively.

3.3 BPS does not affect SCFA concentrations

To investigate microbial activity, SCFA concentrations were measured. The total amount of all analysed SCFA and the three highest SCFA propionate, acetate and butyrate, are shown (Figure 3). Less abundant SCFAs are given in the supplement (Supplementary Material Figure S3).

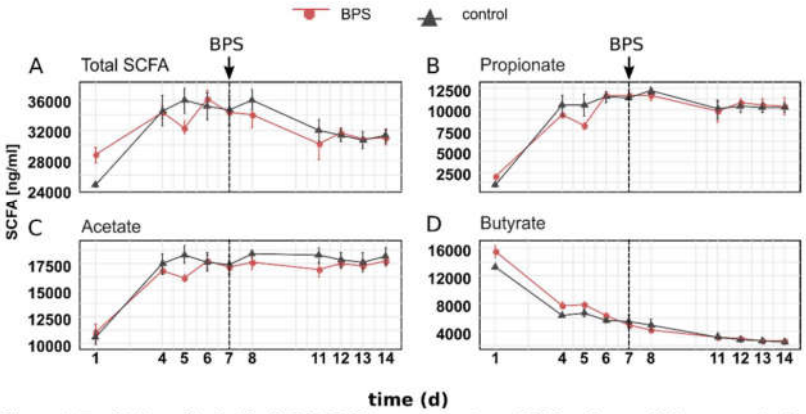

Figure 3: Total (A) and individual (B-D) SCFA concentrations of BPS and control bioreactors (n=3).

During the establishment of SIHUMIx, the SCFA concentrations were statistically similar in all six bioreactor vessels until day 7. After reaching a comparable concentration at day 7, the total SCFA further deceased after day 7 in all 6 bioreactors, before again reaching a comparable concentration of 31,264.9 ± 1,522.8 ng/mL (DMSO control) and 31,030.2 ± 1,722.1 ng/mL (BPS), respectively, at day 14. After BPS addition, no statistical significant change was observed on day 8, 11, 12, 13 or 14. Maximal concentration in BPS treated bioreactors of total SCFA (34,314 ± 27,887 ng/mL), acetate (172,467 ± 967 ng/mL), propionate (11,760 ± 1,193 ng/mL), isobutyrate (167 ± 8 ng/mL) and isovalerate (168 ± 5 ng/mL) were reached at day 7 and remained unchanged until day 14. 2-methylbutyrate and valerate reached a concentration of 47 ± 4 ng/mL (2-methylbutyrate) and 42.1 ± 10 ng/mL (valerate) at day 7 but decreased afterward towards 24 ± 17 ng/mL and 16 ± 3 ng/mL, respectively at day 14. Butyrate and caproate decreased until day 7 to 4,880 ± 642 ng/mL (butyrate) and 1 ± 0.3 ng/mL (caproate), whereas butyrate further decreased to 2,613 ± 140 ng/mL at day 14 and caproate concentrations remained unchanged. Overall, no significant difference was found between the BPS treated bioreactor vessels and the control.

3.2 BPS slightly increases membrane saturation level

A recent study of Hąc-Wydro *et al.* reported that bisphenols are likely to interfere with bacterial membranes [21].To validate changes in the lipid composition, the relative abundance of saturated (16:0, 18:0), unsaturated (16:1*cis*, 18:1*cis*), saturated branched-chain fatty acids (15:0*iso*, 15:0*anteiso*) and cyclopropane fatty acids (17:0cyc, 19:0cyc) during the last two days of the experiment were determined (Figure 4A).

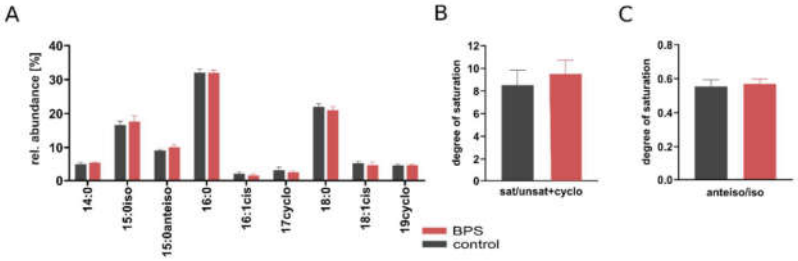

Figure 4: (A)The relative abundance of membrane fatty acids in BPS treated and control bioreactors based on the average concentrations at day 13 and 14 (n=6). Degree of saturation of the membrane of SIHUMIx based on the ratio of saturated to unsaturated and cyclopropyl fatty acids (B) and on the

ratio of anteiso- and iso-methyl-branched fatty acids (C). No statistical differences were found between BPS-treated and control samples.

In the BPS treated and the control bioreactors, the proportion of fatty acids was ranked by its proportion as followed: C16:0 >C18:0 >15:0*iso* >15:0*antiso* >C14 >C18*cis* >C19cyc >C17cyc >C16:1*cis* while no significant difference between BPS exposure SIHUMIx and the control was observed. To investigate the bacterial membrane response to environmental stress, the degree of saturation was calculated as described before (see section 2.3.3 [39]). The degree of saturation of sat/unsat+cyclo was moderately but not significantly higher in the BPS exposed SIHUMIx (3.9 ± 0.4) compared to the control (3.6 ± 0.5; Figure 4B). However, no statistical difference was observed in the degree of saturation of *anteiso/iso* branched-chain fatty acids in the BPS treated bioreactors (0.55 ± 0.03) and the control (0.57 ± 0.03; Figure 4C). The Sample size necessary to detect significant differences between the BPS-treatment and control was calculated with the following parameter: mu1= 3.9, mu2= 3.6, sigma= 0.5, α = .05, desired power = 90 (https://www.stat.ubc.ca/~rollin/stats/ssize/n2.html) and showed that 59 replicates are needed.

3.4. Metaproteomics revealed only temporal effects on the community structure and functionality

To describe communities changes during BPS exposure, individual protein abundances were analyzed. In the dataset (n = 42 samples), a total of 4,931 different proteins were quantified and fold change between BPS treated and DMSO-control bioreactors were calculated (see Volcano plot in Supplementary Material S2). 16 proteins showed significantly higher abundances within the DMSO control bioreactors (n= 12, day 8, 12, 13, 14, bioreactor A,B,C) and 30 proteins were significantly higher abundant in the BPS treated bioreactors (n = 12, day 8, 12, 13, 14 bioreactor D,E,F). An overview of significantly changed proteins is provided (Supplementary Material Table S3). However, from 46 differently abundant proteins, only 17 were functionally annotated by KEGG. Functions assigned to the proteins higher in the BPS treated bioreactors included a subunit of an Acetyl-CoA carboxylase and a phosphoglucosamine mutase from *A. caccae* (Uniprot Accession B0MI45 and B0MGA4), involved in fatty acid synthesis as well as peptidoglycan and lipopolysaccharide (LPS) synthesis, respectively. Also three transporters, two assigned to *B. thetaiotaomicron* (Uniprot Accession Q8A992 and Q8A991), one assigned to *B. producta* (Uniprot Accession AOA1C7|531) are functional associated with teichoic acid and LPS export. All were less abundant in the DMSO control (Supplementary Material Figure S2).

To assess the species distribution of SIHUMIx, the label-free quantification (LFQ) of species-specific proteins was performed [41]. The list of protein identifications per sample is provided (Supplementary Material Table S2). In all six bioreactor vessels, the relative species abundances were similar on day 7 (Supplementary Material Figure S2A). Between day 8 and day 14, the species abundances slightly changed to day 7 in both, the BPS treated and the control bioreactors, respectively. Significant changes in species abundances are given (Supplementary Material Figure S2A). Figure 5A shows the Principal Component Analysis (PCA) based on the relative protein intensity per taxa.

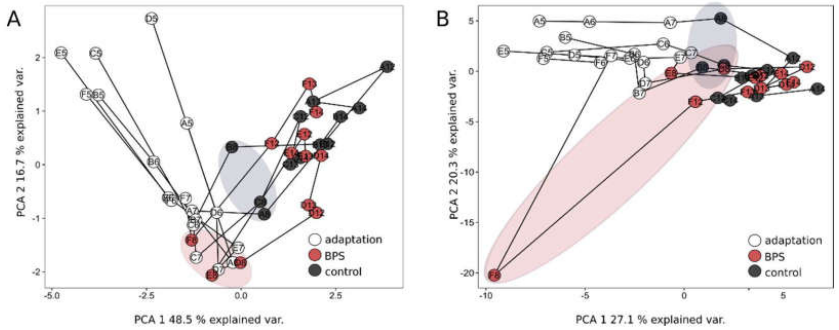

Figure 5: PCA analysis based on the relative protein abundance per species (A) and pathway (B). Lines connect different time points (day 5,6,7,8,12.13,14) per bioreactor (A,B,C,D,E,F). Ellipses mark the first day after the exposure to BPS.

During the adaptation, all bioreactors developed into the same direction until day 7. After the addition of BPS-DMSO (red ellipse) or DMSO (black ellipse), the bacterial community structure differed on day 8 between the groups as highlighted (Figure 5A). However, after 14 days both community structures developed into a similar structure again (Figure 5A). This was mainly based on the abundance changes of the low abundant (>1 %) of SIHUMIx that were more abundant (*E. ramosum*) or less abundant (*B. longum*) in the BPS treated bioreactors on day 8 (Supplementary Material Table S2). After day 8, the species reached similar abundances again, indicating no long-term effect of BPS on the community structure (Figure 5A). As also the control bioreactors differed from day 7 after the DMSO solvent control was added but reached a similar state again at day 14, this difference is most likely the result of the solvent itself on the bacterial community.

To investigate weather specific functions of SIHUMIx were affected during BPS exposure, functional categories were determined by metaproteomics. LFQ values of protein groups assigned to a KEGG pathway-level were summed up for each sample. After quality filtering (criteria see section 2.5.3), in the total dataset, 73 different pathways passed quality filtering and were selected for further data interpretation. Principal component analysis (PCA) was performed based on the relative abundance per day (Figure 5B). For biological interpretation, individual pathways were compared (Supplementary Material Table S2). We observed no significant changes in the relative abundances of assigned pathways BPS exposure compared to the DMSO control (Supplementary Material Table S2. Only one bioreactor (F) responded functionally at day 8, which was not the case for the two other biological replicates D and E.

4. Discussion

The investigation of different model organisms that were exposed to the BPA alternative BPS revealed concerning findings. Effects were observed in estrogenic activity, serum consumption and reproduction in rats, mice or zebrafish [6,9,42]. Recent findings showed a concentration-dependent disruption of the microbial community structure in zebrafish after exposure to different bisphenol analogues *in vivo* [4,23]. Catron *et al*. tested different bisphenols at concentrations from 0.2 to 45 µM. Interestingly, they found that microbial disruption was inversely related to host developmental toxicity with BPS being the bisphenol with the highest microbiota-disrupting potential [23]. Considering the fact that the median estimated daily intake of BPS ranges between 0.023 - 1.67 µg/person [43] and there is clear evidence that gut microbiota are affected by environmental chemicals, potentially affecting health[16], it is of great interest how BPS impacts the human intestinal microbiota.

In this study, we used SCFA analysis and metaproteomics to analyze the impact of BPS on the structure and function of the human intestinal model community. Together with the investigation of membrane fatty acids composition, we obtained deeper insights into how BPS can affect human intestinal bacterial cells. We showed that a 7-day exposure of SIHUMIx to 45 µM BPS had no effect on the community growth or SCFA metabolism. FAME analysis showed that the membrane saturation level was slightly increased after 7 days of BPS exposure compared to the solvent control. This is in agreement with previous findings showing that BPS changes the organization of bacterial membranes [21]. Additionally, functional analysis revealed differences between the DMSO control and the BPS treated bioreactors, regarding fatty acid, peptidoglycan and LPS synthesis and transport. We observed that SIHUMIx species abundances temporally differed after 24h of the treatment at day 8 but reached a similar state after 14 days. This temporal response was observed in all bioreactors, indicating an effect of DMSO itself, which might interfered with the function and membranes of SIHUMIx.

4.1 Overall biomass and activity of SIHUMIx comparable to DMSO control

Although most environmental chemicals, such as BPS, are do not target the gut microbiota directly, they can enter the body and might interact with bacteria [15]. As a result, they potentially affect growth or function of bacterial community members.

The biomass development was similar in the control and BPS treated bioreactors, indicating no obvious effect of BPS on the overall growth of SIHUMIx (Figure 2). For single species, it was shown that BPA exposure at high concentrations (>10 mM) resulted in a reduction of total biomass [44], whereas 5 mM showed no effect.

To describe the effect of BPS exposure on the metabolic activity of SIHUMIx, the SCFA production of SIHUMIx was analyzed. Fermentation products like SCFA play a beneficial role for the host health and changes would directly impact host metabolism [45,46]. In BPA exposed rats (200 μg/kg body weight/day), a decrease in SCFA acids was already shown [47]. So far, this is the first time that the effect of BPS on SCFA acid production of intestinal bacteria outside of a host has been described. Apparently, enzymes from carbohydrate metabolism involved in SCFA synthesis were not affected by BPA exposure. Although the concentration of the SCFA of SIHUMIx reached a comparable amount on day 7, it decreased after the treatment in the DMSO control and the BPS treated bioreactors. However, no changes were observed in the BPS treated bioreactors compared to the control (Figure 3A-D). This suggests that the solvent itself affected the fermentation capacity of SIHUMIx.

.

4.2 BPS exposure slightly increased membrane saturation

Since Hąc-Wydro *et al.* revealed that bisphenols are likely to accumulate at bacterial membranes and therefore may lead to destruction alteration in the membranes of SIHUMIx were investigated. Bacteria can alter their cell membrane fluidity by changing the protein content, the phospholipid head groups or the fatty acid composition in the lipid bilayers [20]. The bacterial lipid metabolism, including regulation, structure and biosynthetic machinery of fatty acid synthesis in bacteria, showed extremely high diversity [48]. SIHUMIx is dominated by the Gram-negative bacterial species *B. thetaiotaomicron* and *E. coli* and Gram-positive *B. producta* (Supplementary Material Figure S2A). In *B. thetaiotaomicron* the main fatty acids are branched-chain fatty acids from C13 to C17 whereas saturated C16:0 is present in a low amount [49,50]. In strains closely related to *B. producta* the dominant lipid is C16:0, followed by C18:0 C18:1 *cis* [51,52]. Together the FAME profile of *B. thetaiotaomicron* and *B. producta* correspond to the FAME profile of SIHUMIx, were saturated (C16:0 > C18:0) and branched-chain (C18:0 > C15) fatty acids were the most abundant. However, studies analyzing the membrane composition of single strains can only partly be compared to findings in communities since lipid profiles in terms of quantitative and qualitative distribution differ when bacteria grow in communities [53].

As the change in fatty acid saturation is known as a long term adaptation, fatty acid composition at the last days after the begin of the exposure were compared [54]. Bacterial membranes consist of saturated and unsaturated fatty acids. *Cis*-unsaturated fatty acids can be transformed into cyclopropyl fatty acids [55], leading to the conversion of 16:1 *cis* to 17:0 cyclopropane (17:0cyc) and 18:1 *cis* to 19:0 cyclopropane (19:0cyc). Bacterial membranes also consist of branched-chain fatty acids. Differences in the amount of *iso*-branched chained fatty and *anteiso*-branched-chain fatty acids have been described in bacteria from contaminated environments since they directly affect membrane fluidity [54]. To validate weather BPS caused changes in the membrane composition of SIHUMIx, fatty acids methyl esters (FAME) were measured (Figure 4B).

When comparing individual FAME abundances, membrane composition in terms of saturated to unsaturated and cyclopropane fatty acids have not been clearly changed between the BPS treated bioreactors and the control. In addition, the degree of saturation calculated by *anteiso*/*iso* ratio of branched fatty acids was not affected. Bacteria are known to increase their *anteiso*/*iso* ratio (see section 2.4.3.), leading to a more rigid membrane and counteracting the fluidity to resist environmental stress [40]. However, when calculating the degree of saturation of the sat/unsat+cyclo (see section 2.4.3.), the level was moderately but not significantly increased in the BPS treated bioreactors.

Generally, the degree of saturation increases with the incorporation of saturated fatty acids in the bacterial membrane, resulting in greater membrane stability able to resist the toxic effects of external stressors [56]. Mechanisms differ between Gram-negative and Gram-positive bacteria: Gram-negative bacteria adapt by the levels of cyclopropane fatty acids or by *cis*/*trans*-isomerization while Gram-positive bacteria produce branched-chain fatty acids next to changing fatty acid chain length [57]. SIHUMIx comprises of both Gram-negative and Gram–positive, since there was no clear evidence in individual FAME profile, further studies are necessary to describe if only Gram-negative or both bacteria are affected by BPS. The here described moderate effect of BPS on the membrane fluidity was in accordance to recent findings of Hąc-Wydro *et.al*: although the incorporation of BPS leaded to fluidization of bacterial membranes, BPS was the least toxic bisphenol when compared to other BPA alternatives. Bisphenols also showed a much higher affinity to the membranes of plants and fungi then to bacterial membranes [21]. If other adaptation processes involved e.g. cis/trans isomerization of unsaturated fatty acids or outer membrane vesicle secretion needs to be further verified [58].

The enzymes involved in fatty acid synthesis vary between bacterial species but have been extensively investigated in *E. coli* [48,59,60]. After the initial reaction of the fatty acid synthesis, involving an acetyl-CoA carboxylase complex (*accABCD*), malonyl-CoA is transferred by *FabD* to the Acetyl-Carrier Protein (ACP) to further be condensed with acetyl- or a branched-chained acyl-residue by F*abH* [61]. This reaction is followed by repeated cycles of reactions involving reduction (*FabG*), dehydration (*FabZ*), reduction (*FabI*, *FabL*, *FabK*) and elongation (*FabB*, *FabF*) resulting in different lengths of saturated, unsaturated and branched-chain fatty acids. These fatty acids are then transferred to glycerol-3-phosphate, which functions as the precursor in the formation of phospholipids [61]. The regulation of the synthesis rate and the product structure is influenced by various enzymes in the process [48]. If BPS exposure increases the synthesis of fatty acids to more saturated and branched-chain fatty acids or if it causes a conversion of the fatty acids already present in the membranes, it needs to be addressed in further studies.

4.3 SIHUMIx showed treatment-dependent temporal responses

DMSO is often used in biological research to solve hydrophobic compounds [62]. However, DMSO might be able to directly affect bacterial cells itself. It has been reported that it affects the structure and properties of cell membranes, even at low concentrations [63]. We assumed that the observed temporal changes were caused by the DMSO itself rather than the BPS as reported previously [64] due to no significant differences between the BPS treatment and the control. DMSO influences the packing of hydrocarbon chains of lipid as a result of the dehydration of membrane surface [63] . This means that both DMSO and BPS might cause changes in the bacterial membrane saturation, which cannot be distinguished within this experimental set up.

Metaproteomics revealed that species abundances slightly fluctuated during the exposure (days 7 to 14) in both, BPS treated and control bioreactors. When comparing the relative species abundances at day 8, it was shown that the low abundant species *E. ramosum* and *B. longum* were either less or higher abundant in the BPS treated bioreactors, but with no statistical significance (Supplementary Material Table S2). At day 14, the individual species abundances reached again a comparable cell number. This led us to the conclusion that the microbes showed a temporal response to the treatment. SIHUMIx responded to the treatment, but reaches a constant state as reported previously [25]. This may still indicate that microbes are affected, but can cope with chemicals occurring in the gut. Previous findings revealed disruption of the microbial structure during BPS-DMSO exposure [23]. Catron *et al.* reported that the growth of the family *Cytophagaceae* was affected by BPS exposure in zebrafish. However, these findings can only partly be compared since the zebrafish intestinal microbiota differ compared to the gut microbiota found in humans. As SIHUMIx does not consist of a species belonging to *Cytophagaceae*, it most likely does not include BPS growth-sensitive species.

The outer layer of the bacterial membrane functions as a barrier to protect the cells from external influences and preventing environmental chemicals from reaching the cytosol. As a typical stress response bacteria modify the outer membrane either by alteration of the membrane structure or by

accumulation of hydrophobic substances [58]. When comparing KEGG-pathways, BPS showed no specific effect on SIHUMIx on the functional level (Figure 5B). PCA analysis showed that all bioreactors differed at day 8 from day 7 but reached a similar state again at day 14. Changes in three SIHUMIx species (*A. caccae*, *B. thetaiotaomicron*, *B. producta*) could be found, when fold change of the individual protein abundances were compared. Three transporters and two proteins involved in fatty acid, peptidoglycan and LPS export and synthesis were increased in the BPS treated bioreactors, compared to the DMSO control at day 8 (Supplementary Material S3).

Both proteins upregulated in the fatty acid, peptidoglycan and LPS synthesis are assigned to *A. caccae*, which is known to appear as gram variable bacterial strain [65]. Upregulation of the biotin carboxylase subunit of the acetyl-CoA carboxylase complex, implies an increased production of membrane fatty acids. This initial step of fatty acid synthesis leads to an increase of malonyl-CoA in the cell and is known as the rate limiting step in *E.coli* [66]. Enhanced production of fatty acids could be a coping mechanism for disturbances in the lipid membrane, likely by changing the fluidity of the membrane, as shown in our finding of moderate increase in degree of saturation of sat/unsat+cyclo (see section 4.2). Furthermore, the second protein altered in abundance was a phosphoglucosamine mutase, which is catalysing the formation of glucosamine-1-phosphate from glucosamine-6-phosphate. A first step in the reaction series leading to UDP-N-acetylglucosamine, the essential precursor for peptidoglycan and LPS synthesis [67]. LPS is known to function as a rigid permeability barrier in gram negative bacteria, decelerating the diffusion of hydrophobic compounds (i.e. steroids, antibiotics) across the outer membrane [68]. Bacteria with reduced LPS are more sensitive to antibiotics and therefore more vulnerable in changing environments [69]. In *E.coli* enhanced production of LPS copes with a decreased quantity of LPS in the outer membrane [70], which implies a disturbance in LPS barrier with BPS treatment.

The upregulated ATP binding cassette (ABC) transporter from *B. producta* is the ATP binding region of a two component transport system, encoded by the *tagGH* operon and involved in the export of wall teichoic acids (WTAs) [71]. Teichoic acids can be divided into wall teichoic acids (WTAs) and lipoteichoic acids (LTAs). Both are anionic glycopolymers, either covalently attached to the peptidoglycan or the plasma membrane of gram positive bacteria [72,73]. WTAs are capable of binding cations and are relevant for cation homoeostasis, ensuring a barrier function of the bacterial cell envelope. Deficiency of WTAs leads to increased temperature sensitivity, can induce defective septum initiation, promoting the generation of round offspring of bacterial cells and influence biofilm forming capacity [74-76].

Furthermore, two ABC transporter subunits from the gram negative bacterium *B. thetaiotaomicron* were overrepresented in the BPS treated SIHUMIx community. Both are associated with ABC type-2 transporter units, one functioning as permease component for gating and the other as ATP binding domain for energy supply. ABC type 2 transporter are assigned with exporting LPS or teichoic acids from the cytosol for integration into the cell membrane or wall [77].

In our findings an increased production and export of LPS, peptidoglycan and WTAs, indicate the need of cell envelope modification during BPS treatment.

The integrity of the other parts of the membrane and the homeostasis of various overall cell envelope components are critical for growth and the viability of bacteria. It requires a balance between synthesis of peptidoglycan, phospholipids and LPS [78]. Due to changing the lipid, phospholipid and glycan metabolism, SIHUMIx might adapted the composition of the membrane to resist organic chemical toxicity. However, no functional differences were found when comparing the BPS exposed bioreactors to the DMSO control. As both BPS and DMSO have been reported to affect bacterial membranes, solvent tolerance of the model system should be taken into account in future studies to investigate bisphenols.

5. Conclusion

519 It was shown that the overall growth of SIHUMIx remained unchanged and SCFA production
520 was unaffected by the exposure to 45 μM BPS in 1.2% DMSO. Changes in individual membrane fatty
521 acid composition could not be clearly distinguished; however, the adaptation and saturation level of
522 the membranes slightly increased during BPS exposure. Metaproteomics revealed temporal
523 functional and structural response to the treatment, independent of BPS exposure. So far, this is the
524 first study investigating the function of intestinal bacteria after BPS exposure when cultivated in
525 continuous bioreactors. At the tested concentration of 45 μM BPS, we observed changes that were
526 restricted to the bacterial membrane indicating that through their adaptation no key physiological
527 function of intestinal bacteria was affected. However, due to the capability of bisphenols to
528 accumulate in the human body it is necessary to test the effects of a range of concentrations. It is still
529 of interest to evaluate the impact of other substitutes used for BPA, taking into account that the
530 structural analogy could imply similar effects. Additionally, the exposure of chemical mixtures could
531 uncover cooperative effects on the gut microbiota and contribute to a more environmentally relevant
532 picture.

533

534 **Supplementary Materials:**
535 Supplementary Material Table S1: Growth conditions and media
536 Supplementary Material Table S2: Metaproteomics
537 Supplementary Material Figure S1: PH and redox potential of CIM during the bioreactor run (quality control)
538 Supplementary Material Figure S2: MSqRob protein report with taxa and function
539 Supplementary Material Figure S3: SCFA concentrations
540 Supplementary Material Figure S4: Relative protein abundance SIHUMIx species

541 **Author Contributions: Stephanie Serena Schäpe**: Conceptualization, Investigation, Visualization, Data
542 curation, Writing - Original Draft,; **Jannike Lea Krause**: Investigation, Writing - Review & Editing; **Rebecca K.**
543 **Masanetz**: Investigation; **Sarah Riesbeck:** Writing – Review & Editing; **Robert Starke**: Visualization, Data
544 curation, Writing - Review & Editing **Ulrike Rolle-Kampczyk**: Data curation, Supervision, Writing - Review &
545 Editing; **Christian Eberlein**: Investigation; **Hermann Josef Heipieper**: Data Curation, Writing - Review &
546 Editing; **Gunda Herberth**: Supervision, Writing - Review & Editing; **Martin von Bergen**: Supervision, Writing -
547 Review & Editing; **Nico Jehmlich**: Conceptualization, Data Curation, Writing - Review & Editing.

548 **Funding: Stephanie S. Schäpe** acknowledges funding by DFG SPP 1656. **Jannike L. Krause** is thankful for
549 funding by the German Federal Environmental Foundation (DBU) and **Martin von Bergen** is grateful for the
550 partial funding by DFG Priority Program 2002.

551 **Acknowledgments:** We are thankful for technical assistance from Jeremy Knespel, Kathleen Eismann, and
552 Nicole Gröger and for culture medium supply from Martina Kolbe.

553
554

References

1. Pjanic, M. The role of polycarbonate monomer bisphenol-A in insulin resistance. *PeerJ* **2017**, *5*, e3809, doi:10.7717/peerj.3809.
2. Arnold, S.M.; Clark, K.E.; Staples, C.A.; Klecka, G.M.; Dimond, S.S.; Caspers, N.; Hentges, S.G. Relevance of drinking water as a source of human exposure to bisphenol A. *J Expo Sci Environ Epidemiol* **2013**, *23*, 137-144, doi:10.1038/jes.2012.66.
3. Rochester, J.R.; Bolden, A.L. Bisphenol S and F: A Systematic Review and Comparison of the Hormonal Activity of Bisphenol A Substitutes. *Environ Health Perspect* **2015**, *123*, 643-650, doi:10.1289/ehp.1408989.
4. Cano-Nicolau, J.; Vaillant, C.; Pellegrini, E.; Charlier, T.D.; Kah, O.; Coumailleau, P. Estrogenic Effects of Several BPA Analogs in the Developing Zebrafish Brain. *Front Neurosci* **2016**, *10*, 112, doi:10.3389/fnins.2016.00112.
5. ECHA. Inclusion of substances of very high concern in the Candidate List for eventual inclusion in Annex XIV. Europeen Chemicals Agency: Helsinki, 2018; Vol. ED/01/2018.
6. Pal, S.; Sarkar, K.; Nath, P.P.; Mondal, M.; Khatun, A.; Paul, G. Bisphenol S impairs blood functions and induces cardiovascular risks in rats. *Toxicol Rep* **2017**, *4*, 560-565, doi:10.1016/j.toxrep.2017.10.006.
7. CHCC. *Chemicals of High Concern to Children (CHCC) Reporting List* http://portal.mts-global.com/en/technical_update/CPIE-026-17.html, 2017.
8. Qiu, W.; Yang, M.; Liu, S.; Lei, P.; Hu, L.; Chen, B.; Wu, M.; Wang, K.J. Toxic Effects of Bisphenol S Showing Immunomodulation in Fish Macrophages. *Environ Sci Technol* **2018**, *52*, 831-838, doi:10.1021/acs.est.7b04226.
9. Eladak, S.; Grisin, T.; Moison, D.; Guerquin, M.J.; N'Tumba-Byn, T.; Pozzi-Gaudin, S.; Benachi, A.; Livera, G.; Rouiller-Fabre, V.; Habert, R. A new chapter in the bisphenol A story: bisphenol S and bisphenol F are not safe alternatives to this compound. *Fertil Steril* **2015**, *103*, 11-21, doi:10.1016/j.fertnstert.2014.11.005.
10. Tzatzarakis, M.N.; Vakonaki, E.; Kavvalakis, M.P.; Barmpas, M.; Kokkinakis, E.N.; Xenos, K.; Tsatsakis, A.M. Biomonitoring of bisphenol A in hair of Greek population. *Chemosphere* **2015**, *118*, 336-341, doi:10.1016/j.chemosphere.2014.10.044.
11. Liao, C.; Kannan, K. Concentrations and profiles of bisphenol A and other bisphenol analogues in foodstuffs from the United States and their implications for human exposure. *Journal of Agricultural and Food Chemistry* **2013**, *61*, 4655-4662, doi:10.1021/jf400445n.
12. Melzer, D.; Rice, N.E.; Lewis, C.; Henley, W.E.; Galloway, T.S. Association of urinary bisphenol a concentration with heart disease: evidence from NHANES 2003/06. *PLoS One* **2010**, *5*, e8673-e8673, doi:10.1371/journal.pone.0008673.
13. Yang, Y.; Guan, J.; Yin, J.; Shao, B.; Li, H. Urinary levels of bisphenol analogues in residents living near a manufacturing plant in south China. *Chemosphere* **2014**, *112*, 481-486, doi:10.1016/j.chemosphere.2014.05.004.
14. Kinross, J.M.; Darzi, A.W.; Nicholson, J.K. Gut microbiome-host interactions in health and disease. *Genome Med* **2011**, *3*, 14, doi:10.1186/gm228.
15. Koppel, N.; Maini Rekdal, V.; Balskus, E.P. Chemical transformation of xenobiotics by the human gut microbiota. *Science* **2017**, *356*, doi:10.1126/science.aag2770.
16. Claus, S.P.; Guillou, H.; Ellero-Simatos, S. The gut microbiota: a major player in the toxicity of environmental pollutants? *npj Biofilms and Microbiomes* **2016**, *2*, 16003, doi:10.1038/npjbiofilms.2016.3.

17. Spanogiannopoulos, P.; Bess, E.N.; Carmody, R.N.; Turnbaugh, P.J. The microbial pharmacists within us: a metagenomic view of xenobiotic metabolism. *Nat Rev Microbiol* **2016**, *14*, 273-287, doi:10.1038/nrmicro.2016.17.
18. Zhang, W.; Yin, K.; Chen, L. Bacteria-mediated bisphenol A degradation. *Appl Microbiol Biotechnol* **2013**, *97*, 5681-5689, doi:10.1007/s00253-013-4949-z.
19. Danzl, E.; Sei, K.; Soda, S.; Ike, M.; Fujita, M. Biodegradation of bisphenol A, bisphenol F and bisphenol S in seawater. *Int J Environ Res Public Health* **2009**, *6*, 1472-1484, doi:10.3390/ijerph6041472.
20. Heipieper, H.J.; Weber, F.J.; Sikkema, J.; Keweloh, H.; de Bont, J.A.M. Mechanisms of resistance of whole cells to toxic organic solvents. *Trends in Biotechnology* **1994**, *12*, 409-415, doi:https://doi.org/10.1016/0167-7799(94)90029-9.
21. Hąc-Wydro, K.; Połeć, K.; Broniatowski, M. The comparative analysis of the effect of environmental toxicants: Bisphenol A, S and F on model plant, fungi and bacteria membranes. The studies on multicomponent systems. *Journal of Molecular Liquids* **2019**, *289*.
22. Lai, K.P.; Chung, Y.T.; Li, R.; Wan, H.T.; Wong, C.K. Bisphenol A alters gut microbiome: Comparative metagenomics analysis. *Environ Pollut* **2016**, *218*, 923-930, doi:10.1016/j.envpol.2016.08.039.
23. Catron, T.R.; Keely, S.P.; Brinkman, N.E.; Zurlinden, T.J.; Wood, C.E.; Wright, J.R.; Phelps, D.; Wheaton, E.; Kvasnicka, A.; Gaballah, S., et al. Host Developmental Toxicity of BPA and BPA Alternatives Is Inversely Related to Microbiota Disruption in Zebrafish. *Toxicol Sci* **2019**, *167*, 468-483, doi:10.1093/toxsci/kfy261.
24. Krause, J.L.; Schaepe, S.S.; Fritz-Wallace, K.; Engelmann, B.; Rolle-Kampczyk, U.; Kleinsteuber, S.; Schattenberg, F.; Liu, Z.; Mueller, S.; Jehmlich, N., et al. Following the community development of SIHUMIx – a new intestinal in vitro model for bioreactor use. *Gut Microbes* **2019**, 10.1080/19490976.2019.1702431, doi:10.1080/19490976.2019.1702431.
25. Schäpe, S.S.; Krause, J.L.; Engelmann, B.; Fritz-Wallace, K.; Schattenberg, F.; Liu, Z.; Müller, S.; Jehmlich, N.; Rolle-Kampczyk, U.; Herberth, G., et al. The Simplified Human Intestinal Microbiota (SIHUMIx) Shows High Structural and Functional Resistance against Changing Transit Times in In Vitro Bioreactors. *Microorganisms* **2019**, *7*, 641, doi:https://doi.org/10.3390/microorganisms7120641.
26. Becker, N.; Kunath, J.; Loh, G.; Blaut, M. Human intestinal microbiota: characterization of a simplified and stable gnotobiotic rat model. *Gut Microbes* **2011**, *2*, 25-33, doi:10.4161/gmic.2.1.14651.
27. Wissenbach, D.K.; Oliphant, K.; Rolle-Kampczyk, U.; Yen, S.; Hoke, H.; Baumann, S.; Haange, S.B.; Verdu, E.F.; Allen-Vercoe, E.; von Bergen, M. Optimization of metabolomics of defined in vitro gut microbial ecosystems. *Int J Med Microbiol* **2016**, *306*, 280-289, doi:10.1016/j.ijmm.2016.03.007.
28. Han, J.; Lin, K.; Sequeira, C.; Borchers, C.H. An isotope-labeled chemical derivatization method for the quantitation of short-chain fatty acids in human feces by liquid chromatography-tandem mass spectrometry. *Anal Chim Acta* **2015**, *854*, 86-94, doi:10.1016/j.aca.2014.11.015.
29. Starke, R.; Jehmlich, N.; Alfaro, T.; Dohnalkova, A.; Capek, P.; Bell, S.L.; Hofmockel, K.S. Incomplete cell disruption of resistant microbes. *Sci Rep* **2019**, *9*, 5618, doi:10.1038/s41598-019-42188-9.
30. Hughes, C.S.; Foehr, S.; Garfield, D.A.; Furlong, E.E.; Steinmetz, L.M.; Krijgsveld, J. Ultrasensitive proteome analysis using paramagnetic bead technology. *Mol Syst Biol* **2014**, *10*, 757, doi:10.15252/msb.20145625.
31. Haange, S.B.; Jehmlich, N.; Hoffmann, M.; Weber, K.; Lehmann, J.; von Bergen, M.; Slanina, U. Disease Development Is Accompanied by Changes in Bacterial Protein Abundance and Functions in a Refined

639 Model of Dextran Sulfate Sodium (DSS)-Induced Colitis. *J Proteome Res* **2019**, *18*, 1774-1786,
640 doi:10.1021/acs.jproteome.8b00974.
641 32. Käll, L.; Canterbury, J.D.; Weston, J.; Noble, W.S.; MacCoss, M.J. Semi-supervised learning for peptide
642 identification from shotgun proteomics datasets. *Nature Methods* **2007**, *4*, 923-925,
643 doi:10.1038/nmeth1113.
644 33. Kanehisa, M.; Sato, Y.; Kawashima, M.; Furumichi, M.; Tanabe, M. KEGG as a reference resource for
645 gene and protein annotation. *Nucleic acids research* **2016**, *44*, D457-462, doi:10.1093/nar/gkv1070.
646 34. Kanehisa, M.; Sato, Y.; Morishima, K. BlastKOALA and GhostKOALA: KEGG Tools for Functional
647 Characterization of Genome and Metagenome Sequences. *Journal of Molecular Biology* **2016**, *428*, 726-
648 731, doi:10.1016/j.jmb.2015.11.006.
649 35. Goeminne, L.J.; Gevaert, K.; Clement, L. Peptide-level Robust Ridge Regression Improves Estimation,
650 Sensitivity, and Specificity in Data-dependent Quantitative Label-free Shotgun Proteomics. *Mol Cell*
651 *Proteomics* **2016**, *15*, 657-668, doi:10.1074/mcp.M115.055897.
652 36. Goeminne, L.J.E.; Gevaert, K.; Clement, L. Experimental design and data-analysis in label-free
653 quantitative LC/MS proteomics: A tutorial with MSqRob. *J Proteomics* **2018**, *171*, 23-36,
654 doi:10.1016/j.jprot.2017.04.004.
655 37. Bligh, E.G.; Dyer, W.J. A Rapid Method of Total Lipid Extraction and Purification. *Can J Biochem Phys*
656 **1959**, *37*, 911-917.
657 38. Morrison, W.R.; Smith, L.M. Preparation of Fatty Acid Methyl Esters + Dimethylacetals from Lipids
658 with Boron Fluoride-Methanol. *J Lipid Res* **1964**, *5*, 600-&.
659 39. Heipieper, H.J.; de Bont, J.A. Adaptation of Pseudomonas putida S12 to ethanol and toluene at the level
660 of fatty acid composition of membranes. *Appl Environ Microbiol* **1994**, *60*, 4440-4444.
661 40. Unell, M.; Kabelitz, N.; Jansson, J.K.; Heipieper, H.J. Adaptation of the psychrotrophArthrobacter
662 chlorophenolicusA6 to growth temperature and the presence of phenols by changes in the anteiso/iso
663 ratio of branched fatty acids. *FEMS Microbiology Letters* **2007**, *266*, 138-143, doi:10.1111/j.1574-
664 6968.2006.00502.x.
665 41. Kleiner, M.; Thorson, E.; Sharp, C.E.; Dong, X.; Liu, D.; Li, C.; Strous, M. Assessing species biomass
666 contributions in microbial communities via metaproteomics. *Nat Commun* **2017**, *8*, 1558,
667 doi:10.1038/s41467-017-01544-x.
668 42. Horan, T.S.; Pulcastro, H.; Lawson, C.; Gerona, R.; Martin, S.; Gieske, M.C.; Sartain, C.V.; Hunt, P.A.
669 Replacement Bisphenols Adversely Affect Mouse Gametogenesis with Consequences for Subsequent
670 Generations. *Curr Biol* **2018**, *28*, 2948-2954 e2943, doi:10.1016/j.cub.2018.06.070.
671 43. Liao, C.; Kannan, K. Concentrations and profiles of bisphenol A and other bisphenol analogues in
672 foodstuffs from the United States and their implications for human exposure. *J Agric Food Chem* **2013**,
673 *61*, 4655-4662, doi:10.1021/jf400445n.
674 44. Vijayalakshmi, V.; Senthilkumar, P.; Mophin-Kani, K.; Sivamani, S.; Sivarajasekar, N.; Vasantharaj, S.
675 Bio-degradation of Bisphenol A by Pseudomonas aeruginosa PAb1 isolated from effluent of thermal
676 paper industry: Kinetic modeling and process optimization. *Journal of Radiation Research and Applied*
677 *Sciences* **2019**, *11*, 56-65, doi:10.1016/j.jrras.2017.08.003.
678 45. Hamer, H.M.; Jonkers, D.; Venema, K.; Vanhoutvin, S.; Troost, F.J.; Brummer, R.J. Review article: the
679 role of butyrate on colonic function. *Aliment Pharmacol Ther* **2008**, *27*, 104-119, doi:10.1111/j.1365-
680 2036.2007.03562.x.

681 46. Nyangale, E.P.; Mottram, D.S.; Gibson, G.R. Gut microbial activity, implications for health and disease:
682 the potential role of metabolite analysis. *J Proteome Res* **2012**, *11*, 5573-5585, doi:10.1021/pr300637d.
683 47. Reddivari, L.; Veeramachaneni, D.N.R.; Walters, W.A.; Lozupone, C.; Palmer, J.; Hewage, M.K.K.;
684 Bhatnagar, R.; Amir, A.; Kennett, M.J.; Knight, R., et al. Perinatal Bisphenol A Exposure Induces Chronic
685 Inflammation in Rabbit Offspring via Modulation of Gut Bacteria and Their Metabolites. *mSystems* **2017**,
686 *2*, doi:10.1128/mSystems.00093-17.
687 48. Parsons, J.B.; Rock, C.O. Bacterial lipids: metabolism and membrane homeostasis. *Prog Lipid Res* **2013**,
688 *52*, 249-276, doi:10.1016/j.plipres.2013.02.002.
689 49. Bakir, M.A.; Kitahara, M.; Sakamoto, M.; Matsumoto, M.; Benno, Y. Bacteroides finegoldii sp. nov.,
690 isolated from human faeces. *Int J Syst Evol Microbiol* **2006**, *56*, 931-935, doi:10.1099/ijs.0.64084-0.
691 50. Sakamoto, M.; Ohkuma, M. Bacteroides reticulotermitis sp. nov., isolated from the gut of a subterranean
692 termite (Reticulitermes speratus). *Int J Syst Evol Microbiol* **2013**, *63*, 691-695, doi:10.1099/ijs.0.040931-0.
693 51. Paek, J.; Shin, Y.; Kook, J.K.; Chang, Y.H. Blautia argi sp. nov., a new anaerobic bacterium isolated from
694 dog faeces. *Int J Syst Evol Micr* **2019**, *69*, 33-38, doi:10.1099/ijsem.0.002981.
695 52. Park, S.K.; Kim, M.S.; Roh, S.W.; Bae, J.W. Blautia stercoris sp. nov., isolated from human faeces. *Int J*
696 *Syst Evol Microbiol* **2012**, *62*, 776-779, doi:10.1099/ijs.0.031625-0.
697 53. Haack, S.K.; Garchow, H.; Odelson, D.A.; Forney, L.J.; Klug, M.J. Accuracy, Reproducibility, and
698 Interpretation of Fatty-Acid Methyl-Ester Profiles of Model Bacterial Communities. *Appl Environ Microb*
699 **1994**, *60*, 2483-2493.
700 54. Murinova, S.; Dercova, K. Response mechanisms of bacterial degraders to environmental contaminants
701 on the level of cell walls and cytoplasmic membrane. *Int J Microbiol* **2014**, *2014*, 873081,
702 doi:10.1155/2014/873081.
703 55. Grogan, D.W.; Cronan, J.E. Cyclopropane ring formation in membrane lipids of bacteria. *Microbiol Mol*
704 *Biol R* **1997**, *61*, 429-&.
705 56. Heipieper, H.J.; Fischer, J. Bacterial Solvent Responses and Tolerance: Cis–Trans Isomerization. In
706 *Handbook of Hydrocarbon and Lipid Microbiology*, Timmis, K.N., Ed. Springer Berlin Heidelberg: Berlin,
707 Heidelberg, 2010; 10.1007/978-3-540-77587-4_328pp. 4203-4211.
708 57. Yoon, Y.; Lee, H.; Lee, S.; Kim, S.; Choi, K.-H. Membrane fluidity-related adaptive response
709 mechanisms of foodborne bacterial pathogens under environmental stresses. *Food Research International*
710 **2015**, *72*, 25-36, doi:https://doi.org/10.1016/j.foodres.2015.03.016.
711 58. Eberlein, C.; Baumgarten, T.; Starke, S.; Heipieper, H.J. Immediate response mechanisms of Gram-
712 negative solvent-tolerant bacteria to cope with environmental stress: cis-trans isomerization of
713 unsaturated fatty acids and outer membrane vesicle secretion. *Appl Microbiol Biotechnol* **2018**, *102*, 2583-
714 2593, doi:10.1007/s00253-018-8832-9.
715 59. Oh, H.Y.; Lee, J.O.; Kim, O.B. Increase of organic solvent tolerance of Escherichia coli by the deletion of
716 two regulator genes, fadR and marR. *Appl Microbiol Biotechnol* **2012**, *96*, 1619-1627, doi:10.1007/s00253-
717 012-4463-8.
718 60. Ramos, J.L.; Duque, E.; Gallegos, M.T.; Godoy, P.; Ramos-Gonzalez, M.I.; Rojas, A.; Teran, W.; Segura,
719 A. Mechanisms of solvent tolerance in gram-negative bacteria. *Annu Rev Microbiol* **2002**, *56*, 743-768,
720 doi:10.1146/annurev.micro.56.012302.161038.
721 61. Freiberg, C.; Brunner, N.A.; Schiffer, G.; Lampe, T.; Pohlmann, J.; Brands, M.; Raabe, M.; Habich, D.;
722 Ziegelbauer, K. Identification and characterization of the first class of potent bacterial acetyl-CoA

carboxylase inhibitors with antibacterial activity. *J Biol Chem* **2004**, *279*, 26066-26073, doi:10.1074/jbc.M402989200.

62. Dyrda, G.; Boniewska-Bernacka, E.; Man, D.; Barchiewicz, K.; Slota, R. The effect of organic solvents on selected microorganisms and model liposome membrane. *Mol Biol Rep* **2019**, *46*, 3225-3232, doi:10.1007/s11033-019-04782-y.
63. Gordeliy, V.I.; Kiselev, M.A.; Lesieur, P.; Pole, A.V.; Teixeira, J. Lipid membrane structure and interactions in dimethyl sulfoxide/water mixtures. *Biophys J* **1998**, *75*, 2343-2351, doi:10.1016/S0006-3495(98)77678-7.
64. Chang, C.Y.; Simon, E. The effect of dimethyl sulfoxide (DMSO) on cellular systems. *Proc Soc Exp Biol Med* **1968**, *128*, 60-66, doi:10.3181/00379727-128-32943.
65. Schwiertz, A.; Hold, G.L.; Duncan, S.H.; Gruhl, B.; Collins, M.D.; Lawson, P.A.; Flint, H.J.; Blaut, M. Anaerostipes caccae gen. nov., sp. nov., a new saccharolytic, acetate-utilising, butyrate-producing bacterium from human faeces. *Syst Appl Microbiol* **2002**, *25*, 46-51, doi:10.1078/0723-2020-00096.
66. Davis, M.S.; Solbiati, J.; Cronan, J.E., Jr. Overproduction of acetyl-CoA carboxylase activity increases the rate of fatty acid biosynthesis in Escherichia coli. *J Biol Chem* **2000**, *275*, 28593-28598, doi:10.1074/jbc.M004756200.
67. Mengin-Lecreulx, D.; van Heijenoort, J. Characterization of the essential gene glmM encoding phosphoglucosamine mutase in Escherichia coli. *J Biol Chem* **1996**, *271*, 32-39, doi:10.1074/jbc.271.1.32.
68. Nikaido, H. Molecular basis of bacterial outer membrane permeability revisited. *Microbiol Mol Biol Rev* **2003**, *67*, 593-656, doi:10.1128/mmbr.67.4.593-656.2003.
69. Zhang, G.; Meredith, T.C.; Kahne, D. On the essentiality of lipopolysaccharide to Gram-negative bacteria. *Curr Opin Microbiol* **2013**, *16*, 779-785, doi:10.1016/j.mib.2013.09.007.
70. Putker, F.; Bos, M.P.; Tommassen, J. Transport of lipopolysaccharide to the Gram-negative bacterial cell surface. *FEMS Microbiol Rev* **2015**, *39*, 985-1002, doi:10.1093/femsre/fuv026.
71. Lazarevic, V.; Karamata, D. The tagGH operon of Bacillus subtilis 168 encodes a two-component ABC transporter involved in the metabolism of two wall teichoic acids. *Mol Microbiol* **1995**, *16*, 345-355, doi:10.1111/j.1365-2958.1995.tb02306.x.
72. Morath, S.; von Aulock, S.; Hartung, T. Structure/function relationships of lipoteichoic acids. *J Endotoxin Res* **2005**, *11*, 348-356, doi:10.1179/096805105X67328.
73. Weidenmaier, C.; Peschel, A. Teichoic acids and related cell-wall glycopolymers in Gram-positive physiology and host interactions. *Nat Rev Microbiol* **2008**, *6*, 276-287, doi:10.1038/nrmicro1861.
74. Schirner, K.; Marles-Wright, J.; Lewis, R.J.; Errington, J. Distinct and essential morphogenic functions for wall- and lipo-teichoic acids in Bacillus subtilis. *EMBO J* **2009**, *28*, 830-842, doi:10.1038/emboj.2009.25.
75. Neuhaus, F.C.; Baddiley, J. A continuum of anionic charge: structures and functions of D-alanyl-teichoic acids in gram-positive bacteria. *Microbiol Mol Biol Rev* **2003**, *67*, 686-723, doi:10.1128/mmbr.67.4.686-723.2003.
76. Vergara-Irigaray, M.; Maira-Litran, T.; Merino, N.; Pier, G.B.; Penades, J.R.; Lasa, I. Wall teichoic acids are dispensable for anchoring the PNAG exopolysaccharide to the Staphylococcus aureus cell surface. *Microbiology* **2008**, *154*, 865-877, doi:10.1099/mic.0.2007/013292-0.
77. Paulsen, I.T.; Beness, A.M.; Saier, M.H., Jr. Computer-based analyses of the protein constituents of transport systems catalysing export of complex carbohydrates in bacteria. *Microbiology* **1997**, *143 (Pt 8)*, 2685-2699, doi:10.1099/00221287-143-8-2685.

766 78. Klein, G.; Raina, S. Regulated Assembly of LPS, Its Structural Alterations and Cellular Response to LPS
767 Defects. *International Journal of Molecular Sciences* **2019**, *20*, 356, doi:10.3390/ijms20020356.
768

769

Supplementary Material Figure S1: PH and redox potential of CIM during the bioreactor run (quality control)

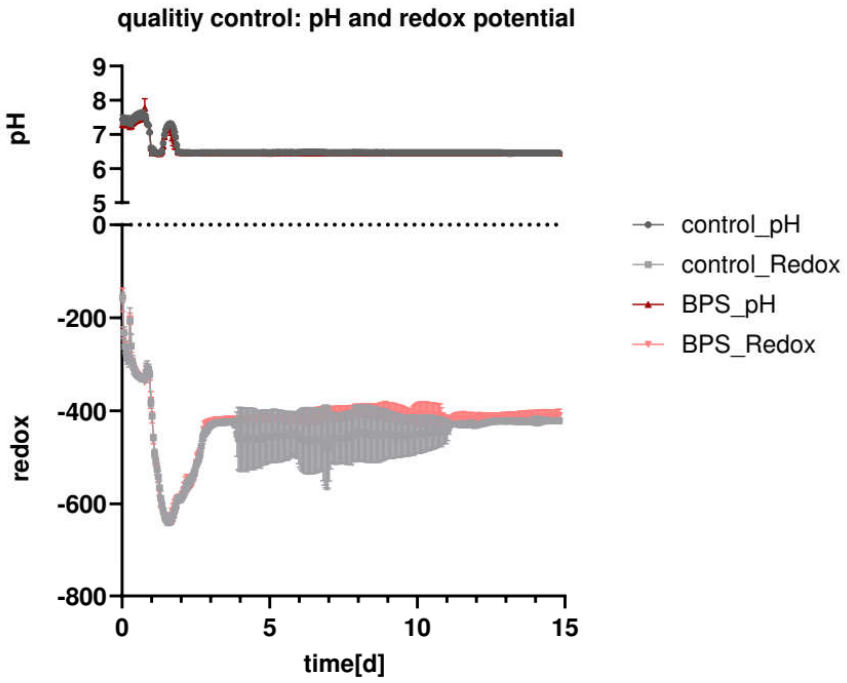

Figure S1: PH and redox potential of the Complex Intestinal Media (CIM) during the bioreactor run based in the average (with SD) of the three control and BPS treated bioreactor vessels, respectively.

Supplementary Material Figure S2: Robust statistical inference for quantitative LC-MS proteomics (MSqRob) result plots

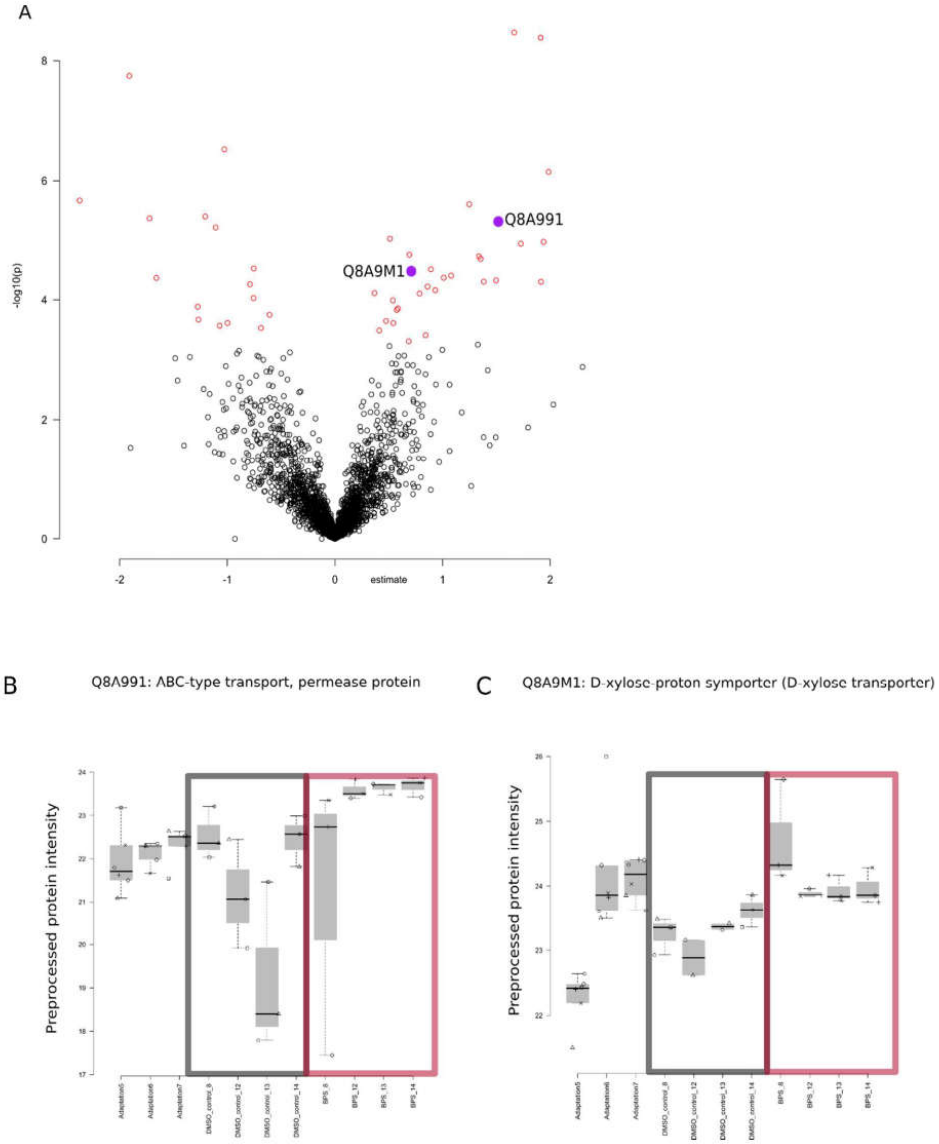

Figure S2: Volcanoplot based on protein abundances. Estimate= Log2(X/Y); Contrast compared day 8,12,13,14 of DMSO control vs BPS. Preprocessed protein intensity's of Q8A991 (B) and (C). Boxplot are based on 3 bioreactors per group; numbers of the sample names indicate time point (day 5 -14)

Supplementary Material Figure S4: SCFA concentrations over time

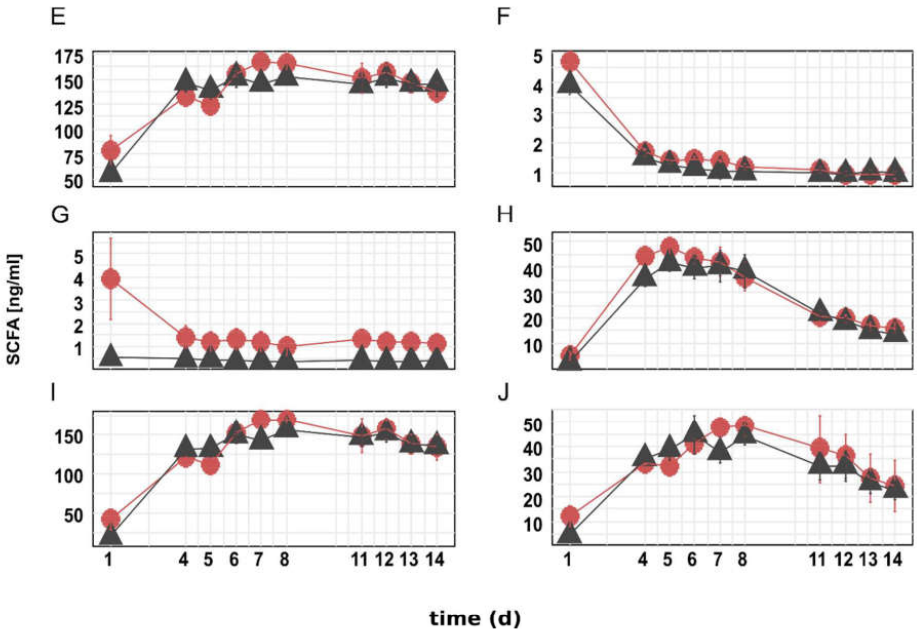

Figure S2: Individual (E-F) SCFA concentrations of BPS and control bioreactors (n=3).

Supplementary Material Figure S3: Relative species abundances

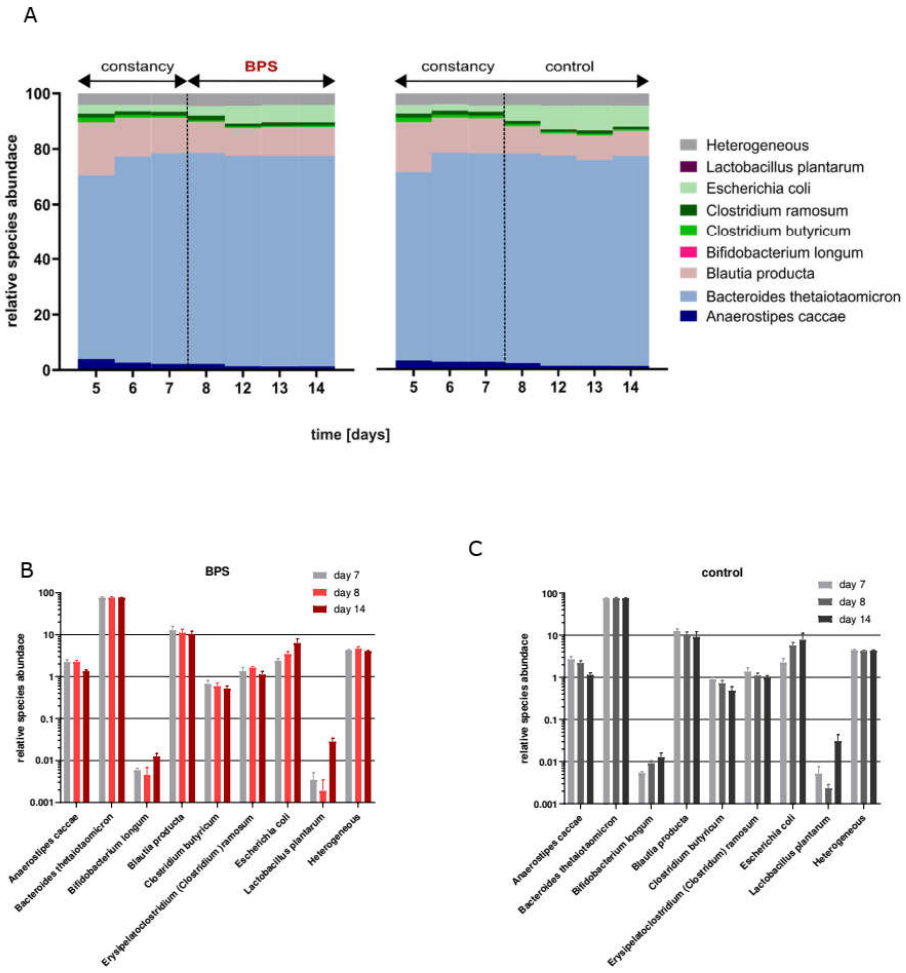

Figure S2: Relative species abundance as stacked bars (A) and individual species abundances in BPS treated (B) and control (C) bioreactors.

Supplementary Material Table S2: Growth media (Brain-Heart-Infusion; BHI), Complex intestinal medium; CIM) and growth conditions

Cultivation of SIHUMIx as single strains was performed in Brain-Heart-Infusion (BHI) medium under anaerobic conditions. All ingredients are given in Table S1.1.

Table S2.1: supplemented Brain-Heart-Infusion medium (BHI) storage at 4 C

Ingredient	Quantity [g or mL/L]	supplier
Brain-Heart-Infusion	37	Roth
L-cysteine hydrochloride	0.5	Biochemica
Resazurin	0.001	MP biomedicals
Vitamin K hemin solution	10	Becton Dickinson
Yeast extract	5	Chemsolute

BHI medium was aliquoted into Hungate tubes and closed with a butyl cap. Before autoclaving Hungates were purged with nitrogen and stored at 4 C until use. Hungates were inoculated 1:10 with freshly thawed bacterial cells and incubated at 37°C and 175 rpm.

For the experiment SIHUMIx was continuously cultivated in a Multifors 2 bioreactor system (Infors, Switzerland) with six parallel 250 mL culture bioreactors filled with complex intestinal medium (CIM). CIM was slightly modified after McDonald et al. (2013) and all ingredients are given in Table S1.2 [1].

Table S2.2: Complex intestinal medium (CIM): Medium formulation was adopted from McDonald *et al.* (2013). PH was adjusted to pH 6.7 with NaOH, storage at 4 C

Ingredient	Quantity [g/L]	supplier
Arabinogalactan (larch wood)	2	Sigma-Aldrich
Bile Acids sodium salt	0.5	Sigma-Aldrich
Calcium chloride x 2 H_2O	0.01	Merck
Casein peptone (pancreatic)	4.3	Roth
Di-Potassium hydrogen phosphate	0.04	Roth
Hemin (bovine)	0.005	Sigma-Aldrich
Inulin	1	Serva
L-cysteine hydrochloride	0.5	Biochemica
Magnesium sulfate	0.01	Roth
Menadione	0.001	Sigma-Aldrich
Mucin (porcine gastric Type II)	4	Sigma-Aldrich
Pectin, citrus peel	2	Sigma-Aldrich
Potassium di-hydrogen phosphate	0.04	Roth
Sodium chloride	0.72	Roth
Sodium hydrogen carbonate	2	Roth
Starch, wheat	5	Roth
Xylo-oligosaccharide (corn)	2	Roth
Yeast extract	2	Chemsolut

For sterile autoclaving the bioreactors were filled with VE-water as the CIM could not be autoclaved. After autoclaving the water was removed and the bioreactors were filled with 250 mL sterile CIM, respectively, by pumping. Settling of bacterial cells was prevented by constant stirring at 150 rpm. The bioreactor system was maintained under anaerobic conditions by continuously gassing the bioreactors as well as the reservoir bottles (medium and NaOH) with sterile nitrogen. To make sure the system

was sterile after the setting up the system was run under experimental conditions (37°C, 150 rpm, no medium feed) for 24 h as a sterility control. For this purpose fermentation the antifoam probe was used to constantly remove excess medium keeping the bioreactor volume at 250 mL.

1. McDonald, J.A.; Schroeter, K.; Fuentes, S.; Heikamp-Dejong, I.; Khursigara, C.M.; de Vos, W.M.; Allen-Vercoe, E. Evaluation of microbial community reproducibility, stability and composition in a human distal gut chemostat model. *J Microbiol Methods* **2013**, *95*, 167-174.

3 Discussion

In recent decades, the human intestinal microbiota prove essential for human health, but the complex interactions of the intestinal microbiota and the host are far from being fully understood (Lloyd-Price et al., 2016). The intestinal microbiota is an essential contributor to human health, which directly affects the host immune system. E.g., a reduced microbial diversity in the intestine often is associated with disease (Mosca et al., 2016). People from the Westernized world have less diverse intestinal microbiota and simultaneously show an increased incidence of chronic inflammatory diseases compared to people from low developed countries (Zuo et al., 2018a). The process of Westernization, which in this context parallels urbanization, is accompanied by the intake of a less healthy diet (Conlon and Bird, 2014) and, furthermore, an increase in medication and exposure to pollutants (Zuo et al., 2018b). Both, pharmaceuticals and environmental chemicals have only recently been recognized as a potential modulators of the intestinal microbiota (Jin et al., 2017; Li et al., 2020; Licht and Bahl, 2019). The intestinal microbiota modulate the immune system by *de novo* synthesis or modulation of metabolites. E.g., SCFAs promote the expansion of regulatory T cells as well as antibody production by B cells. Secondary bile acids exert anti-inflammatory effects on dendritic cells and macrophages (Postler and Ghosh, 2017). And, the recently discovered MAIT cells, that reside in the liver and the intestinal mucosa, recognize microbial vitamin B2 and B9 metabolites (Kjer-Nielsen et al., 2012; Treiner et al., 2003). These findings potentially link chemicals -exposure of intestinal microbiota to an altered immune response.

In the present work, the central question was whether and how environmental chemicals modulate the response of MAIT cells *via* the microbiota. In the first step, suitable model systems for the cultivation of intestinal microbiota and subsequent exposure to environmental chemicals were established. In the next step, potential microbiota-mediated effects of environmental chemicals on MAIT cells were addressed. Beforehand, a proof-of-concept regarding the linkage of microbiota-exposure and MAIT cell modulation was performed, which finally allowed the testing of chemicals with regard to microbiota-mediated MAIT cells modulation.

3.1 Using *in vitro* models to cultivate intestinal microbiota

Investigating the intestinal microbiota by using *in vitro* models poses advantages in terms of feasibility, reproducibility and costs and most importantly has relevance for the human situation (Wissenbach et al., 2016). Moreover, such models allow high throughput analysis (Li et al., 2020; Payne et al., 2012) and when assessing the effects e.g. of chemical exposure on the microbiota confounding factors such as variation in diet, age etc. can be eliminated (Licht and Bahl, 2019). Thus, *in vitro* cultivation allows the specific identification of microbiota-modulation without host bias. Though, the continuous cultivation of complex microbiota is challenging and true replication poses a major problem (Payne et al., 2012; Van den Abbeele et al., 2010).

The challenges regarding replication of complex microbiota (e.g. from feces, colon content) in *in vitro* bioreactors was clearly illustrated by the cultivation of microbiota from the pig colon (publication 6). Prior to inoculation, the starting material was homogenized thoroughly in anaerobic buffer for 5 min. To reduce the amount of particulate matter, the slurries were settled for a couple of minutes and after settling, the liquid supernatant was used to simultaneously inoculate two replication bioreactors. Nevertheless, after the first three days of continuous cultivation the microbiota within the replicate bioreactors started to develop into two taxonomically distinct communities (publication 6). Despite the apparent differences in taxonomy, the metaproteome analysis revealed a high functional similarity (**Figure 12**).

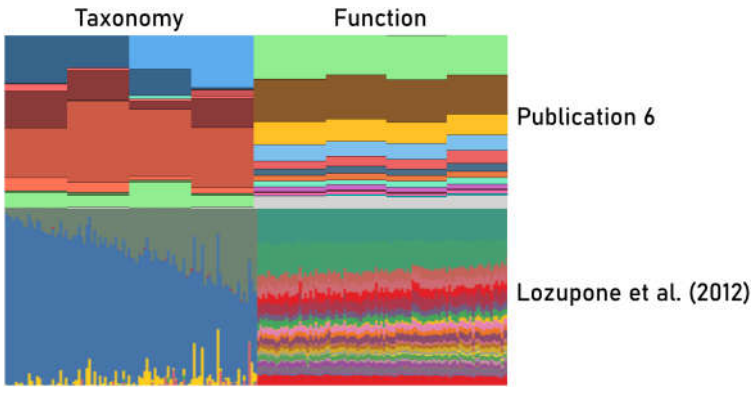

Figure 12. Comparison of taxonomic and functional analysis. The data from publication 6 "The glyphosate formulation Roundup® LB plus influences the global metabolome of pig gut microbiota *in vitro*" and Lozupone et al. (2012) show high functional redundancy despite large variations on the taxonomic level.

Lozupone et al. (2012) showed that the healthy human intestinal microbiota is very different at the taxonomic level, but has high functional redundancy, which is also reflected in the results of publication 6. The starting material from the pig colon was analyzed neither with regard to community taxonomy nor to community function. An evaluation whether the community functions can be reconstructed within the bioreactor system is hence still pending.

Similar to the observations from publication 6, a study using natural wastewater for long-term bioreactor cultivation, reported that the complex microbiota were highly dynamic in their system. Microbial taxa started to fluctuate after a few days of continuous cultivation (Liu et al., 2019). Both these experiments suggest that complex microbiota start to diverge with regard to taxonomy after the first few days of adaptation, which might be attributed to stochastic effects during community assembly (Eng and Borenstein, 2018; Oliphant et al., 2019). However, since the complex microbiota showed high similarity on the cellular level in flow cytometric analysis during the limited time of adaptation the results suggested that complex microbiota replicate in batch culture. Hence, batch cultivation is a suitable tool for chemical screening, the analysis of short-term effects (McDonald, 2017) or the determination of effect concentrations also in complex microbiota. Nevertheless, inoculation has to be performed with the same inoculum. To assess the effect of chemicals on complex microbiota a standard procedure is proposed based on the results from the present PhD project (**Figure 13**).

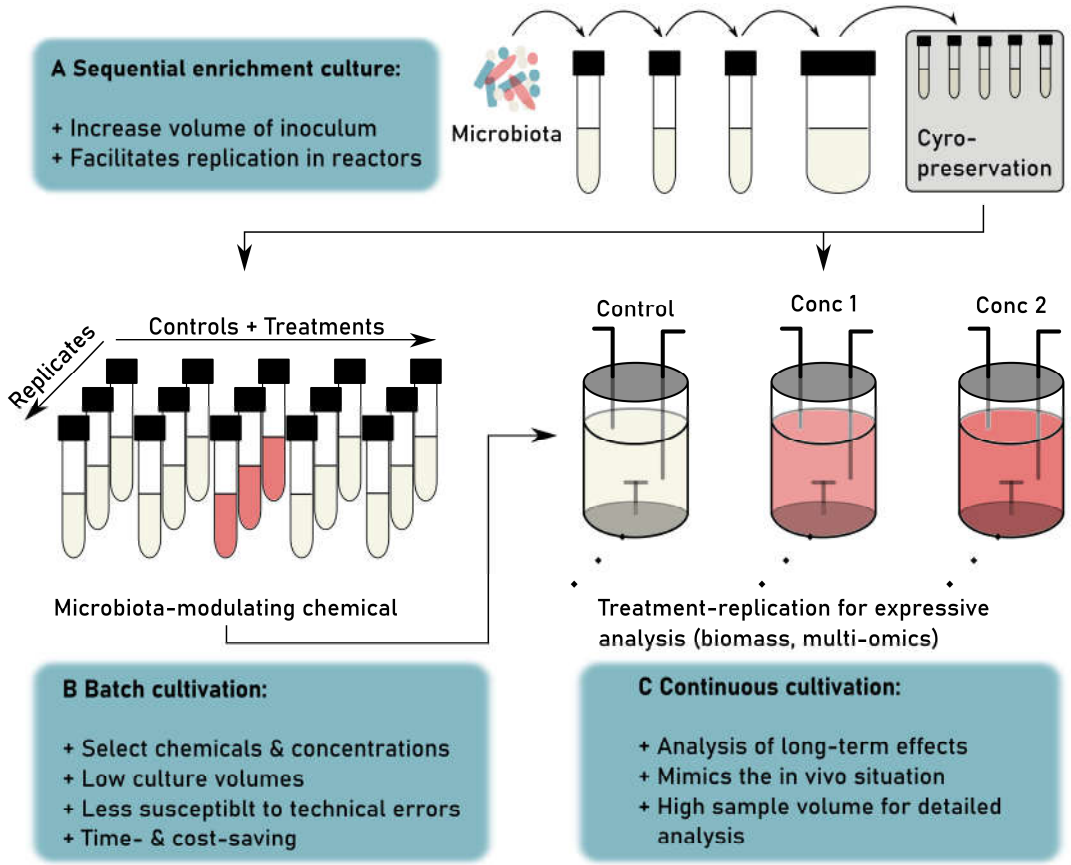

Figure 13. Proposed procedure for the analysis of microbiota-modulation by chemicals. A A sufficient amount of inoculum can be generated by a sequential enrichment culture procedure. Complex microbiota, e.g. from feces, is cultured in batch and after sequential enrichment aliquotes are cryo-preserved. This homogenous inoculum can be utilized to inoculate batch or continuous cultivation. B Batch cultivation allows the rapid and easy identification of microbiota-modulating chemicals (red) and facilitates the determination of suitable concentrations for further investigations. C Using continuous bioreactor, which more closely mimick the *in vivo* situation, the long-term effects of selected chemicals on the microbiota can be investigated.

For true replication a sufficient amount of inoculum from the same complex microbiota is needed. To increase the volume of inoculum and to facilitate replication by the elimination of particulate matter from the complex specimen a sequential enrichment culture procedure may be used (Lazuka et al., 2015). The microbiota can then be preserved in glycerol until use (**Figure 13**, A). Despite the community complexity, this procedure similarly allowed true replication both in batch and in continuous culture and hence the evaluation of microbiota-modulating properties of bisphenols (publication 7, **Figure 14**).

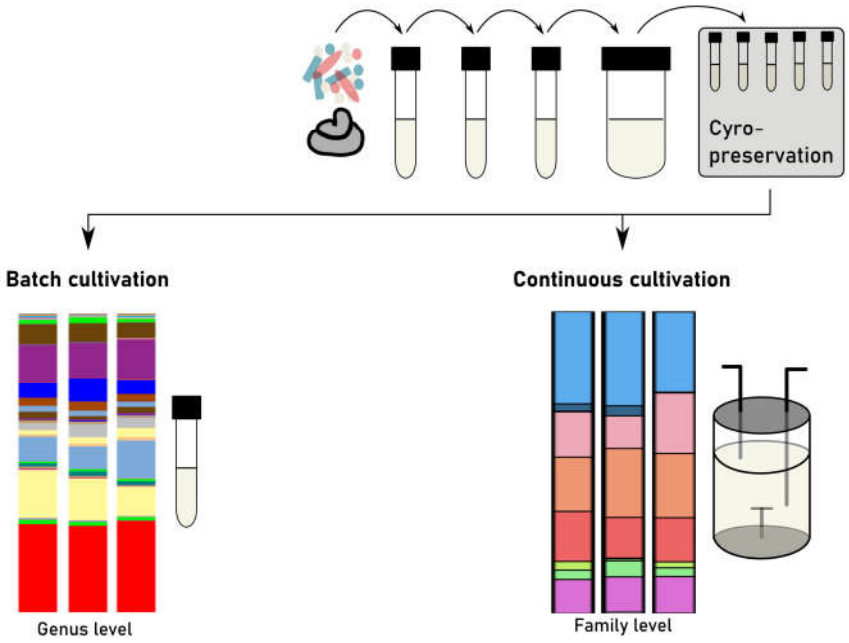

Figure 14. Sequential enrichment cultivation of complex microbiota allows true replication. The volume of human fecal material was increased and particulate matter was eliminated using a sequential enrichment procedure. The microbiota were cryo-preserved and utilized to inoculate batch and continuous cultures. Taxonomy was determined with 16S rRNA gene analysis. Batch cultivation: 24 h in in Brain-Heart Infusion (BHI). Continuous cultivation for 16 days (15x bioreactor turn-over) in complex intestinal medium (CIM). The replicate communities were highly similar on the genus and family level, respectively.

To identify microbiota-modulating environmental chemicals as well as to select suitable chemical concentrations, assays in batch culture are advisable (**Figure 13** B). Batch cultures can be setup at low culture volumes and the cultivation process is less sensitive to technical problems compared to continuous cultivation systems (Guzman-Rodriguez et al., 2018; Macfarlane and Macfarlane, 2007), as the SHIME (Molly et al., 1994), the TIM-2 (Venema, 2015) or the system used in this study. Moreover, they resemble a rapid, costly opportunity that also allow the taxonomic and functional analysis of the microbiota, as shown with the drug-screening platform RapidAIM (Li et al., 2020), but are only suitable for acute, short-term exposure. Though, to assess chemical-derived effects on intestinal microbiota, especially effects from chronic chemical exposure, continuous cultivation systems are essential (McDonald, 2017). These more closely mimic the *in vivo* situation and due to the higher culture volume facilitate sampling for several analysis methods, e.g. a comprehensive multi-omics approach (**Figure 13** C).

Another option to approach the issue of reproducibility in *in vitro* cultivation and simultaneously to gain insights in community ecology, is the use of defined model communities (Guzman-Rodriguez et al., 2018). Defined intestinal model communities consist of a defined number of species and consequently are less complex compared to the natural microbiota still serving as model for the intestinal microbiota (Elzinga et al., 2019; Guzman-Rodriguez et al., 2018). Due to the lower community complexity the depth of analysis e.g. with omics-techniques is ameliorated (Jiang et al., 2019; Lohmann et al., 2020). This may facilitate the elucidation of response mechanisms to a perturbation and the analysis of metabolic interactions. These advantages are expected to be important steps towards understanding the mode of action of microbiota-modulating chemicals. Therefore, in the present PhD project a defined human intestinal model community, SIHUMIx, was established for *in vitro* bioreactor cultivation (publication 1). The SIHUMIx community proved to be very reproducible with replicate Bray-Curtis similarities of >0.9 at the constant community state based on microbiota flow cytometry and SCFA profiling. During undisturbed cultivation, SIHUMIx simultaneously established and developed in the bioreactors toward the constant community state on the cellular, taxonomic and functional levels within five days or four bioreactor turn-overs (publication 1). The SIHUMIx community remained at the same constant state until day 16 (15x turn-over, publication 2). Despite the high reproducibility observed in publication 1, the development of SIHUMIx toward the constant state can be delayed (publication 2). The implementation of a three-turn-over buffer is advisable to ensure that all replicate communities reach the constant state before treatment initiation.

Under the influence of acid stress, we observed different community dynamics of SIHUMIx on the cellular, the taxonomic and the functional level (publication 1). Similarly, community dynamics on the functional and taxonomic community level have been shown to follow different dynamics in bioreactor systems inoculated with complex microbiota (Liu et al., 2018a). Thus, community function and taxonomy should be monitored simultaneously to fully cover the community dynamics. As determined in publication 1, a variety of fingerprinting techniques proved to be appropriate to follow the community dynamics and the choice of methods should be adapted to the objectives of the experiment.

As diet is one of the drivers that shape the intestinal microbiota (Gentile and Weir, 2018; Shapira, 2016), the medium predominantly influences community taxonomy during cultivation. The model community SIHUMIx comprises of eight bacterial strains. In rats, these eight strains were shown to inhabit the rat intestine with *B. thetaiotaomicron* and *B. producta* at the highest relative abundance (38% and 28%, respectively). The other bacterial strains, *B. longum, C. ramosum*, *A. caccae*, *E. coli*, *L. plantarum* and *C. butyricum* established lower relative abundance with 17%, 12%, 5%, 2%, 0.03% and less, respectively (Becker et al., 2011). In contrast, the SIHUMIx community in publication 1, publication 2 and publication 7 were dominated by *B. thetaiotaomicron* with >70% relative species abundance at the constant state. The bacterial strains *B. producta*, *E. coli* and *A. caccae* were present at 16%, 7% and 4.5% relative species abundance, respectively. The other bacterial strains, *B. longum, C. ramosum*, *L. plantarum* and *C. butyricum* established at very low abundances with less than 1% relative species abundance each. Though, they remained within the community until day 16 of cultivation. To closely mimic the colon environment, a complex intestinal medium (CIM) was used for the cultivation of SIHUMIx after the first preliminary tests. CIM or CIM-related culture media were designed to cultivate complex intestinal microbiota, e.g. from fecal specimen (Macfarlane et al., 1998; McDonald et al., 2013; Tanner et al., 2014). CIM contains mucin, since in the *in vivo* situation the mucus layer supplies the microbiota with mucins at the intestinal barrier (Knoop and Newberry, 2018; Maynard et al., 2012; Mowat and Agace, 2014). Within the SIHUMIx community, *B. thetaiotaomicron* is the only mucin-degrading bacterial strain (Tsai et al., 1991) and consequently, growth of *B. thetaiotaomicron* is promoted by mucin supply from the CIM. The growth advantage of *B. thetaiotaomicron* due to mucin supply has also been demonstrated in a modelling analysis of SIHUMIx applying media with and without mucin. Models are important tools to advance the behavior of microbial ecosystems upon alterations in the cultivation process (Kreft et al., 2017). Furthermore, modeling of microbiota can help to understand the interaction of microbes and the organization within a community based on metabolic interactions (Bauer et al., 2017). Bauer et al. (2017) reported dominant growth of *B. thetaiotaomicron* in the presence of mucin and dominant growth of *E. coli* in the absence of mucin. Thereby, the authors demonstrated a high impact of mucin

on the SIHUMIx community taxonomy (Bauer et al., 2017), though the obtained results differ from the result of our *in vitro* analysis and the *in vivo* analysis from Becker et al. (2011, **Figure 15**).

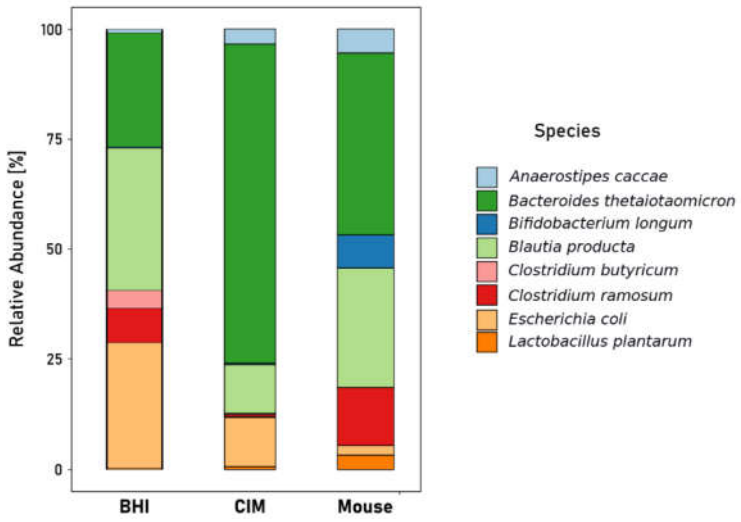

Figure 15. Taxonomy of SIHUMIx. The taxonomy of SIHUMIx differs when cultivated in Brain-Heart Infusion (BHI) medium, complex intestinal medium (CIM) or after inoculation in gnotobiotic mice.

However, it is also evident that the ground truth, i.e. the reality predicted by the modelling approach, may differ from the observations of experiments. Therefore, the results obtained by the modelling approach must be substantiated by further experimental approaches. Based on the before-mentioned observations, it was assumed that a lower mucin concentration in CIM could reduce the relative abundance of *B. thetaiotaomicron*. In parallel, the relative species abundances of the other strains might increase. This modification would allow (i) to more closely mimic the SIHUMIx composition observed *in vivo* and (ii) to obtain an *in vitro* model community that indeed comprises of eight bacterial strains at reasonable abundances. In contrast to SIHUMIx, complex microbiota potentially encompass more mucin-degrading bacterial species. Despite this, the porcine complex microbiota clearly changed on the taxonomic level during continuous cultivation. The communities adapted to the bioreactor system and thereby especially lost the genera *Lactobacillus*, *Bifidobacteria* and *Coriobacteriaceae* (publication 6).

One major drawback of the CIM are its optical properties. This liquid medium is of brown color and very opaque due to mucin dispersion. Furthermore, CIM comprises of a non-autoclavable and an

autoclavable part and currently does not include the addition of a redox-indicator to prove anaerobicity. This poses several difficulties for the utilization of CIM, especially in batch culture. 1. The preparation of sterile and anaerobic Hungates tubes, which are used for batch cultivation, is challenging particularly without access to an anaerobic chamber. However, a valid protocol could be established and optimized with the current laboratory equipment. 2. For batch cultivation the addition of a redox-indicator such as resazurin is advisable to discover oxygen contamination. The lowest percentage of resazurin to prove anaerobicity in CIM needs to be determined. 3. Growth analysis is complicated due to the mucin-derived intrinsic turbidity. Mucin hinders optical density measurement, biomass quantification as well as cell counting at particle counting instruments.

In contrast, brain-heart infusion (BHI) medium, a clear yellowish medium, facilitates batch cultivation in various ways. 1. All ingredients can be autoclaved together and oxygen contamination is clearly visible due to the redox-indicator resazurin. 2. The determination of microbial growth by optical density measurement, biomass quantification and cell counting is possible. As chemical-related growth inhibition was one evaluation criterion for microbiota-modulation, BHI medium has been utilized for sequential enrichment of human fecal microbiota and chemical exposure in batch culture (publication 7). Since diet is one of the most influencing factors on community composition *in vivo* (Gentile and Weir, 2018; Shapira, 2016), it is assumed that the taxonomy of communities grown in BHI will differ from communities grown in CIM. This has been shown for the model community SIHUMIx already (see **Figure 15**).

A recently published study evaluated the effects of four CIM medium ingredients, i.e. inorganic salts, bile salts, mucin and SCFA, on intestinal microbiota functions by metaproteomics *in vitro* (Li et al., 2018a). The authors reported that the strongest effects on microbiota functionality resulted from the addition of inorganic salts and bile salts, followed by mucin. The addition of SCFA did only have minor effects (Li et al., 2018a). Inorganic salts and bile salts dissolve completely and hence result in a clear liquid. Since these two components were shown to have the strongest effect on the functional level of complex intestinal microbiota *in vitro*, the addition of inorganic salts and bile salts to the currently used BHI medium might mimic an intestinal environment more closely. Depending on the research question, for sequential enrichment the use of CIM or adapted BHI

might be advantageous to provide a sufficient amount of feces-derived microbiota and to better preserve taxonomic and functional properties of the original community.

For testing the effects of chemicals, it is not essential to mimic the *in vivo* situation as close as possible, though the established procedure from publication 7 meets the requirements. For other purposes, however, the sequential enrichment procedure should be adapted.

3.2 Identification of microbiota-modulating properties of environmental chemicals

The majority of environmental chemicals enter the human body *via* the oral route. In the present PhD project, compounds with oral human exposure and a high annual production volume were selected. These were pesticides and components of plastic products with food contact, namely the herbicide glyphosate, the insecticide chlorpyrifos and bisphenols. To investigate the microbiota-modulating properties of glyphosate, chlorpyrifos and bisphenols, both batch and continuous cultivation procedures have been utilized.

Microbiota-modulation by bisphenols

To date, bisphenol analogues comprise 16 compounds with a shared common structure of two hydroxyphenyl functionalities. From these, bisphenol A is the best studied compound (Chen et al., 2016). Since 2018, Bisphenol A (BpA) is listed as substance of very high concern (SVHC) as adverse health effects, especially endocrine disrupting properties based on hormonal activity due to endocrine receptor binding have been attributed to BpA-exposure (Rochester, 2013). Though, the adverse health effect also include the modulation of intestinal microbiota (Catron et al., 2019a), whereby the actual mode of action remains to be elucidated. Due to the increasing restrictions on BpA, BpA-analogues such as Bisphenol F (BpF) and bisphenol S (BpS) are increasingly utilized to replace BpA, leading to a rising public exposure (Lehmler et al., 2018).

In publication 7, the microbiota-modulating properties of BpA, BpF and BpS have been compared using batch cultivation. *Bacteroides thetaiotaomicron* is a common member of the human intestinal microbiota (Comstock and Coyne, 2003) and the model organism *Escherichia coli* is the most

dominant *Enterobacteriacaea* in humans (Martinson et al., 2019). Therefore, these bacterial strains as well as fecal human microbiota were used to evaluate whether the BpA-analogues BpF and BpS are safer alternatives with respect to microbiota-modulation. The single strain level is most suitable to unravel the still unknown mode of action regarding microbiota modulation. In our study, *B. thetaiotaomicron* was most susceptible to bisphenol (BpX)-exposure. Growth was most severely inhibited by BpA-exposure, followed by BpF and then BpS. In contrast, *E. coli* was less susceptible to BpX-exposure. BpF had the biggest impact on growth followed by BpA and then BpS. The reduced microbial growth at single strain level was also reflected in the microbial viability. The effect of BpX-exposure on growth of the complex intestinal microbiota from high to low growth inhibition was by BpA, BpF and BpS. The impaired growth did not reflect on microbial viability, although this could have been expected. Microbial viability was determined using a microbial viability assay kit (Dojindo Molecular Technologies, Inc., Kumamoto, Japan), which quantifies the reduction of the tetrazolium salt WST-8 by dehydrogenases from viable cells colorimetrically. According to the manufacturer, the assay was validated with a variety of single strain bacteria, but not with complex microbial communities. This might cause the non-consistent results from BpX-exposure on growth and viability in the complex microbiota (publication 7 Figure 1).

Determination of viability of complex microbiota is not trivial, as discrimination of live/dead cells can already be complicated on the single strain level due to dormant cells or spores. Especially live/dead staining procedures, alike the staining procedure utilized with the Quantom Tx™ (Logos Biosystems, South Korea), have to be adapted and optimized to the specific microbiota and finally validated using appropriate methods (Emerson et al., 2017).

All in all the metabolome analysis reproduced the results from growth and viability analysis, attributing the strongest microbiota-modulating effects to BpA, followed by BpF and the least effects to BpS. Furthermore, the results from publication 7, which determined effects on microbial growth, viability and the global metabolome, suggest a microbiota-specific response to BpX-exposure. Metaproteomics on existing samples should be used to elucidate the reasons of these specific responses and to unravel the mode of action of each BpX by analyzing the (meta-) proteome of single strain bacteria on the one hand and the fecal community on the other hand.

Recently the effects of BpX-exposure, also using BpA, BpF and BpS, have been addressed on complex organisms, i.e. zebrafish. Catron *et al.* (2019) observed an indirect association between BpX-developmental toxicity, which was determined by behavior in locomotion assays, and microbiota-modulation. There, effects emerged at considerably lower BpX concentrations already, both on zebrafish development and on the intestinal microbiota. The authors reported a high developmental toxicity from BpF-exposure, similar to that of BpA, and no developmental toxicity of BpS. In their study the microbiota-modulating properties of BpS were rather high, similar to BpA, and those of BpF were comparably low (Catron et al., 2019b). The results recorded by Catron *et al.* (2019) contrast our results and might derive from the experimental procedures. We exposed microbiota from exponential to stationary growth phase *in vitro.* Significant effects on the microbiota were only observed at concentrations >100 µM BpX. Catron *et al.* exposed zebrafish during embryo and larvae development within the first ten days after fertilization. During this time the intestinal microbiota colonize the larvae, which is essential for proper larvae development and thus a critical time window (Galindo-Villegas et al., 2012). They observed BpX-derived alterations within the microbiota composition and functions, though the authors did not identify effects on larval behavior (Catron et al., 2019a). Thus, it is not clear whether the reported BpX-derived changes in microbiota composition and functions are associated with adverse outcomes in zebrafish. Moreover, due to the nature of *in vivo* studies, the host also responds to BpX-exposure. Similar to the human situation, it is not clear whether alterations within the intestinal microbiota are cause or consequence (Maynard et al., 2012) and whether the microbiota affects the toxic kinetics of BpX by degradation or resorption.

Based on the results of Catron *et al.* (2019), in which BpS exhibited microbiota-modulating properties in all concentrations tested, this compound was selected for further analysis (publication 8). Due to the comparable low complexity and the simultaneously increasing analysis depth, the model community SIHUMIx was assumed to be suitable to elucidate the mode of action of BpS within a microbial community setting (Lohmann et al., 2020). SIHUMIx adapts to the bioreactor system within five to seven days (publication 1 and publication 2). Therefore, it was assumed that SIHUMIx responds and adapts to a perturbation within the same timescale. Hence,

taxonomic and functional analysis were performed at day one post exposure, shortly after the perturbation was initiated, as well as at days five to seven post exposure in order to investigate immediate effects and long-term changes. The applied BpS-concentration of 45 µM resembled the highest concentration utilized by Catron *et al.* (2019) and lies between the low and intermediate concentration utilized in publication 7, at which no significant effects were observed. At day 1 after exposure, the BpS-exposed SIHUMIx had a slightly lower biomass and displayed minor changes in taxonomy, primarily within the low abundant species, although these effects were not significant. By days 5 to 7 of exposure, the effects had disappeared in terms of both biomass and taxonomy, indicating a mild reaction to the perturbation and then adaption (publication 8). These observations resemble one possibility for communities to respond to a perturbation (**Figure 16**).

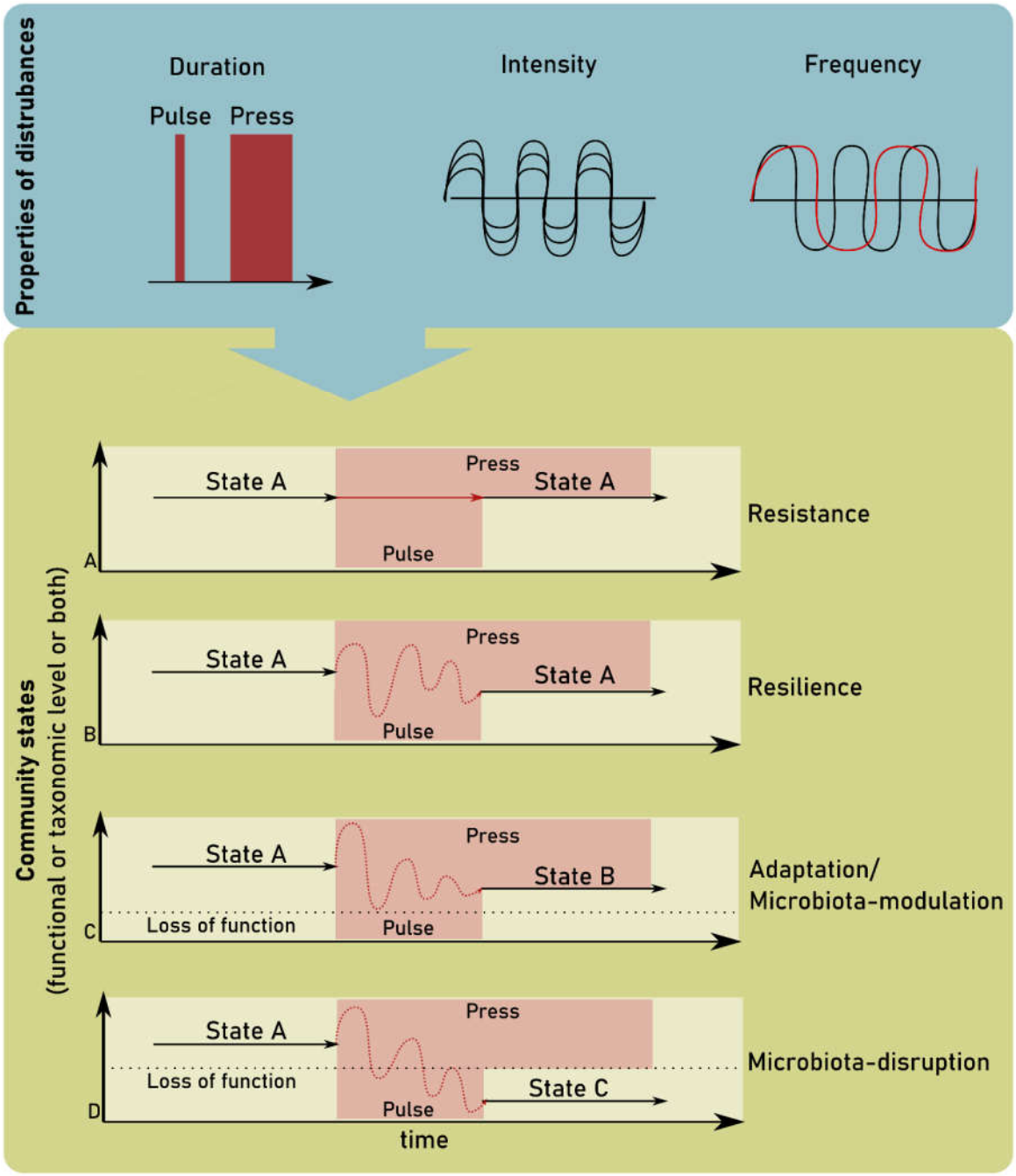

Figure 16. Perturbations and possible response scenarios on the microbiota level. In ecology, perturbations are categorized in short-term (pulse) and long-term (press) perturbations, but they also differ with regard to perturbation intensity and frequency (teal background). Depending on the perturbation several response scenarios can be discriminated based on functional and/or taxonomix analysis that define the community state (green background). A A microbial community can resist a perturbation, which means they remain unaffected. B A resilient community returns to the initial community state after the perturbation ends. Furthermore, a microbial community can adapt to another community state by C modulation of the microbiota or D the community looses its functional properties, which describes microbiota-disruption. Modified from Sommer et al., 2017.

Perturbations can differ in various ways (**Figure 16**, teal background). Depending on the duration of a perturbation, pulse and press perturbations are discriminated. Pulse perturbations are short-term events, whereas press perturbations resemble continuous or long-term events. Furthermore, perturbations exhibit difference regarding frequency and intensity (Bender et al., 1984). The discrimination of pulse and press perturbation depends on the time scales of the ecosystem (Shade et al., 2012), which for microbes is simultaneously related to the specific growth rate in batch culture and the system retention time in continuous culture. Thus, in publication 7 and publication 8, we similarly applied press perturbations. During batch cultivation, the exposure covered the whole microbial development from exponential to stationary growth phase. Similarly, in publication 8, the SIHUMIx were exposed for the time the community needs to adapt to the bioreactor system.

Upon perturbation several response scenarios are possible and should be evaluated in terms of community functional and taxonomic states (**Figure 16**, green background, Konopka et al., 2015; Shade et al., 2012). 1. The community is resistant to the perturbation and does not alter. 2. The microbiota is resilient and upon perturbation changes on the functional or taxonomic level but thereafter recovers to the initial state. 3. The community responds to the perturbation and adapts its function or taxonomy, which results in a modulated community. 4. The community is severely impaired and the community function or taxonomy is disrupted (Shade et al., 2012; Sommer et al., 2017).

Microbial stress response is initiated by changes in gene expression and enzymatic processes within one hour (Schubert et al., 2018; Shamir et al., 2016), as microbes shift their enzymatic functions toward survival promoting metabolism (Schimel et al., 2007). This is possible since the intestinal microbiota exhibit highly adaptive capacities based on their community genetic potential (Konopka et al., 2015), which might result from the permanent exposure to inconstant environmental factors, e.g., variation in diet, uptake of bacteria, fungi and viruses (Sommer et al., 2017). If the individuals within a community respond differently to the perturbation the community composition changes. However, this depends on the perturbation properties and the community stability in terms of resistance and resilience (Shade et al., 2012).

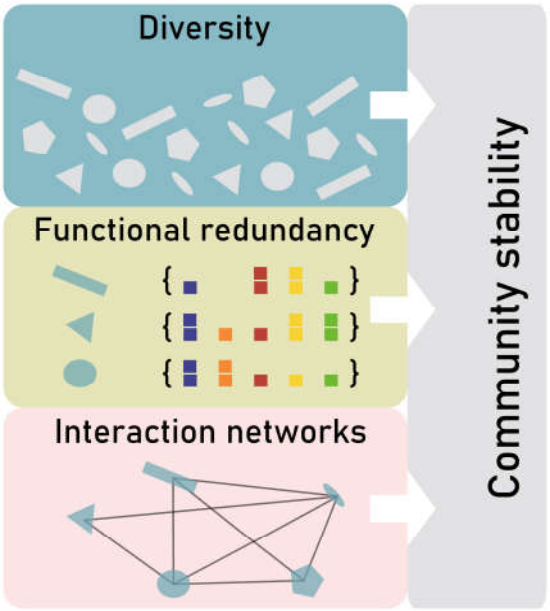

Figure 17. Community stability relies on several factors. Factors that influence community stability are community diversity, functional redundancy within the microbiota and the existence of interaction networks.

Though, functional and taxonomic alterations can affect the interactions networks within the community (Konopka et al., 2015). Community diversity positively correlates with community stability, but community stability is not solely driven by diversity (**Figure 17**). Other factors, such as the differential response of species to a perturbation, functional redundancy and diversity increase community stability, as do cross-feeding with weak interactions (McCann, 2000). SIHUMIx is a model community of eight bacterial strains with only low diversity. Consequently, this community would be expected to exhibit low stability. Our finding, however, show that SIHUMIx shows high resistance to a pulsed acid stress (publication 1), to changes in medium retention times (publication 2) and to BpS-exposure (publication 8). There are two possible reasons (i) the perturbations had too low intensity to initiate changes within the community or (ii) SIHUMIx has a high degree of stability with regard to resistance and resilience. Bauer et al. (2017) modelled a metabolic interaction network that shows potential metabolic fluxes. As all SIHUMIx strains can be cultured individually and do not rely on the cross feeding, the metabolic interactions might be considered weak. These weak interactions potentially enhance the resistance upon perturbations. The functional repertoire of SIHUMIx community should be determined by proteome and genome analysis of the individual members to determine functional redundancy and functional diversity within the community. These information potentially facilitate the understanding of the community stability during a perturbation.

The comparison of the before-mentioned *in vivo* study by Catron et al. (2019) and the *in vitro* study from the present PhD project, both applying bisphenols to intestinal microbiota, indicate that analyzing the microbiota-modulating properties of environmental chemicals *in vitro* is not

sufficient to fully assess health risks. Furthermore, the host response might amplify the chemical-derived effects. Consequently, an alleviation of microbiota-modulating effects by the host is also conceivable. However, to selectively identify the microbiota-modulating properties of environmental chemicals, the exclusion of the host is essential (Macfarlane and Macfarlane, 2007).

Microbiota-modulation by Roundup® LB plus, a glyphosate-based herbicide

The effect of glyphosate exposure on the intestinal microbiota has been addressed in several studies using *in vitro* and *in vivo* approaches, though contrasting results were reported (Mesnage et al., 2019; Nielsen et al., 2018; Riede et al., 2016; Shehata et al., 2013). From batch cultures of single strain bacteria it was reported that especially pathogenic species, like *Clostridium botulinum*, were resistant to glyphosate-exposure, whereas beneficial species, such as *Bifidobacterium adolescentis* and *Lactobacillus* spp. were susceptible to glyphosate-expsoure (Shehata et al., 2013). In contrast to this study, Riede *et al.* (2016), e.g., did not observe changes on taxonomy or metabolism *in vitro* under continuous cultivation of ruminal microbiota. Furthermore, glyphosate-exposure did not provide a growth advantage to *Clostridium botulinum* as suggested by Shehata et al. (2013) (Riede et al., 2016). Another study observed only slight taxonomic changes in the rat caecal microbiota combined with an increase in intermediate metabolites from the shikimate pathway upon exposure to 175 mg/kg body weight glyphosate (no observed adverse effect level (NOAEL) concentration, USA, Mesnage et al., 2019, non-reviewed preprint). Though, most studies focused on glyphosate-related taxonomic changes only. Therefore, in the present PhD-project, the effect of glyphosate-exposure, on the one hand, was investigated on the single strain level by exposure of *E. coli*, *B. adolescentis* and *L. reuteri* at different concentrations of glyphosate from Roundup® LB plus (publication 4) and on complex porcine microbiota (publication 6) also evaluating functional effects.

In publication 4 the effect of Roundup-exposure was determined with emphasis on immune modulation. Hence, only limited information on microbiota-modulating effects was gathered. The only microbial-related analysis was the functional analysis of riboflavin and folate metabolism, which did not show significant effects. These results contrast the observations of Shehata et al.

(2013), as both *Bifodobacterium adolescentis* and *Lactobacillus reuteri* were not affected by glyphosate-exposure (publication 4).

Unlike publication 4, publication 6 focused on the microbiota-modulating properties of glyphosate both on the taxonomic and functional level. Therefore, diverse microbiota from pig colon were short-term exposed to a three times higher concentration of Roundup (900 mg/L) during continuous cultivation compared to the highest concentration from publication 4. The colonic microbiota was not affected on the taxonomic level and only showed minor effects on the functional level. We did not observe effects on the abundance of SCFA, aromatic amino acids, but slight changes in the global metabolome after Roundup-exposure. The effects have been further specified and a tendentially increased concentration of cholic acid was measured on day 1 of exposure. The metabolic alterations did not correspond to significant changes on the proteome level (publication 6). One reason might be that the metaproteome coverage was too low to detect changes, which potentially result from the high community complexity (Lohmann et al., 2020). Another reason for these minor effects could derive from the complex intestinal medium (CIM) composition The CIM was adapted to the porcine colonic environment and contained a high concentration of peptone (Tanner et al., 2014). Peptone serves as nitrogen source and is composed of hydrolyzed peptides and amino acids. Indeed, we measured high levels of free amino acids in the pure culture medium, which were clearly reduced during cultivation. This indicates microbial uptake of amino acids, including the aromatic amino acids phenylalanine, tyrosine and tryptophan. The presence of these aromatic amino acids potentially inhibits their biosynthesis *via* the shikimate pathway (Nielsen et al., 2018) and negates the effect of glyphosate on this compound targets the EPSPS from the same biosynthetic pathway.

Based on our results Roundup exhibits mild effects at the tested concentrations, which already resembled high concentrations. To investigate the influence of glyphosate, both studies have one significant drawback. I.e., the frequently used glyphosate formulation Roundup® LB plus was applied in both studies. Roundup ® LB plus is a mixture of water (42.5%), glyphosate isopropylamine salt (41.5%), and surface-active-ingredient (16%, safety data sheet, MONSANTO

Europe). The chemical composition of those surface-active ingredients is unknown and thus the distinction of glyphosate-derived or formulation-derived effects was not possible. Based on our analyses, it cannot be excluded (i) that glyphosate interferes with enzymes other than the primary target enzyme EPSPS or (ii) that it affects processes upstream of EPSPS. And (iii) adverse effects of surface-active ingredients cannot be excluded. To determine glyphosate-derived effect, the microbiota should be exposed to the active compound, which is glyphosate isopropylamine salt. However, the purchase of glyphosate isopropylamine salt in quantities suitable for *in vitro* cultivation experiments (~50 g) prove difficult.

3.3 Modulation of MAIT cell activation

Proof of concept

The identification of environmental chemicals that directly modulate the immune system has driven the emergence of immunotoxicology as independent research field in toxicology research (Burchiel, 1999). Only recently specialized immune cells that recognize microbial metabolites, such as MAIT cells (Treiner et al., 2003) or regulatory T cells (Sakaguchi, 2000), have been discovered. These discoveries, beyond direct immunomodulatory effects, provide the potential for microbiota-mediated, indirect immunomodulation by chemicals (**Figure 18**).

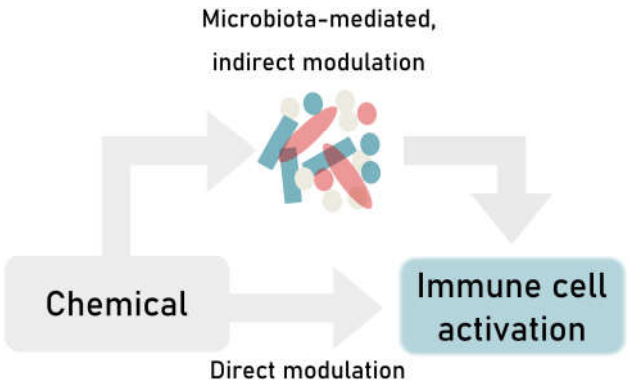

Figure 18. Discrimination of chemical effects on immune cells. Chemicals exert direct effects and potentially microbiota-mediated, indirect effects on immune cells.

MAIT cells are activated by microbial riboflavin (vitamin B2) pre-cursors and also recognize folate (vitamin B9) metabolites, which inhibit MAIT cell activation (Kjer-Nielsen et al., 2012). The indirect

modulation of these cells *via* chemical-exposed intestinal microbiota has been assumed, although the concept had to be evaluated (**Figure 19**).

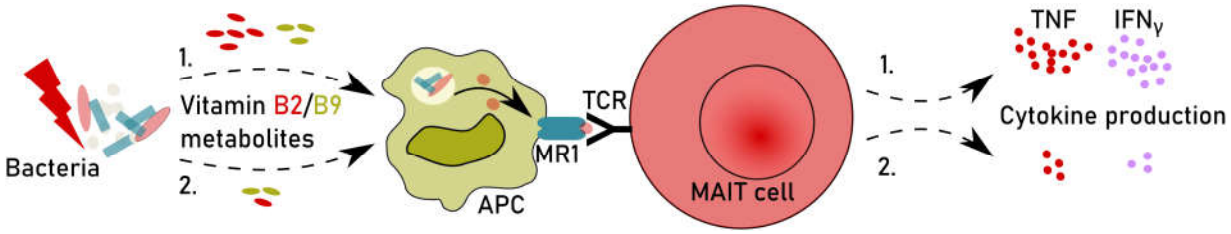

Figure 19. Concept of microbiota-mediated MAIT cell modulation by environmental chemicals. Upon exposure the quantity and quality of microbial riboflavin and folate metabolites might change, which potentially affects the activation of MAIT cells and thereby cytokine production. 1. Chemical exposure elevates the availability of riboflavin metabolites and thus increases MAIT cell activation. 2. Due to chemical exposure the amount of riboflavin metabolites decreases and simultaneously MAIT cell activation declines.

As proof-of-concept, the model community SIHUMIx was exposed to an acute acid stress (publication 1). The MAIT cell activating potential of SIHUMIx before, during and after acid stress was analyzed (publication 3). Indeed, microbial acid stress reduced the MAIT cell activating potential of SIHUMIx, although the community taxonomy was barely affected. In line with Schimel et al. (2007), we primarily observed changes on the metabolic level. The authors stated that the microbial stress response induces functional changes to promote survival, but effects on community composition were thought to occur as a long-term response to stress (Schimel et al., 2007). The reduced MAIT cell activating potential in our study was associated with an increased riboflavin uptake. Riboflavin metabolism is essential for the synthesis of flavin mononucleotide (FMN) and flavin adenine dinucleotide (FAD). Both FMN and FAD are cofactors for flavoenzymes, which catalyze manifold reactions e.g. in redox or detoxification processes (Joosten and van Berkel, 2007). E.g., the effects of heat-induced oxidative stress in *Lactocoocus lactis* were reduced by the addition of riboflavin and thereby elevated FAD biosynthesis (Chen et al., 2013). Similarly, for *E. coli,* the contribution of flavoenzymes to the oxidative stress response has been demonstrated (García-Angulo, 2017; Maurer et al., 2005). Due to the involvement of flavoenzymes in oxidative stress response, detoxification and apoptosis (Joosten and van Berkel, 2007) and based upon our results (publication 3), riboflavin might serve as microbial stress sensor linking the exposure of

microbiota to environmental chemicals to modulation of the MAIT cell response. To date, riboflavin has been quantified in the culture supernatant as proxy for the MAIT cell activating metabolites, 5-(2-oxopropylideneamino)-6-D-ribitylaminouracil (5-OP-RU) and 5-(2-oxoethylideneamino)-6-D-ribitylaminouracil (5-OE-RU), since these metabolites are instable and thus difficult to quantify.

Biotic factors that affect MAIT cell activation

In the human body MAIT cells reside at barrier sites and potentially recognize diverse microbiota there (Gibbs et al., 2017; Hinks et al., 2016; Teunissen et al., 2014; Treiner et al., 2003). In publication 3, the influence of biotic factors on MAIT cell activation have been addressed for the first time. The response of MAIT cells to microbial communities of different complexity and the contribution of individual community members on MAIT cell activation were investigated. In line with the study by Tastan et al. (2018), we observed a direct association between MAIT cell activation and riboflavin secretion on the single strain level. From our analysis using the SIHUMIx model community, we assumed a correlation between the relative species abundances in a community and the MAIT cell activating potential of the community itself. Furthermore, our data indicate that the MAIT cell activating potential of microbial communities decreases with increasing community diversity. This effect may be based upon the presence of MAIT cell activating metabolites from the riboflavin biosynthesis pathway (Kjer-Nielsen et al., 2012; Tastan et al., 2018). It was reported, that, especially in symbiotic or commensal interactions like those found in intestinal microbiota, the secretion of metabolites such as riboflavin is important for symbiosis establishment, maintenance and microbial cross-feeding (LeBlanc et al., 2013; Rodionov et al., 2019; Rowland et al., 2018). With increasing community complexity, the balance between prototrophic bacteria that supply riboflavin and possess MAIT cell activating metabolites and auxotrophic bacteria, which have to take up riboflavin, seemed to be shifted, thereby decreasing the MAIT cell activating potential. To date no other studies investigated the effects of communities, more specifically microbial diversity, on MAIT cell activation, although a variety of chronic inflammatory diseases is associated with a reduced microbial diversity (Blüher, 2019; Jangi et al., 2016; Manichanh et al., 2012; Turnbaugh et al., 2009; Zheng et al., 2018).

The modulation of the MAIT cell response by environmental chemicals

The microbiota-mediated modulatory effects of environmental chemicals on MAIT cell activation have primarily been addressed in publication 4 and publication 7, in which microbiota were acutely exposed to chemicals during batch cultivation and afterwards used for MAIT cell stimulation.

In publication 4, we investigated the microbiota-mediated effects of glyphosate and chlorpyrifos on the MAIT cell response to *Escherichia coli*, *Bifidobacterium adolescentis* and *Lactobacillus reuteri*. Already in 2013 the microbiota-modulating properties of chlorpyrifos have been identified *in vitro* (Joly et al., 2013; Joly Condette et al., 2014; Reygner et al., 2016). However, the causal connection of chemical-exposure and microbiota-mediated immunomodulation of MAIT cells is a new approach. Indeed, chlorpyrifos increased the *E. coli*-mediated MAIT cell activation and in parallel lowered the inhibiting potential of *B. adolescentis* and *L. reuteri* at the tested concentrations in our study. This is also reflected in an altered riboflavin and folate biosynthesis. However, since bacteria lack acetyl choline esterase, the target of chlorpyrifos in animals (Qiao et al., 2001), the mode of action regarding microbiota-modulation remains unknown and thus should be investigated. A recent *in vivo* study analyzed the effects of chronic chlorpyrifos-exposure on the microbiota, serum hormone levels, e.g. luteinizing hormone, follicle stimulating hormone, testosterone and ghrelin, and inflammation of rats *in vivo*. The authors observed chlorpyrifos-related effects on the intestinal microbiota, changes in hormone levels and more importantly effects on the inflammatory status of the animals. Thereby, the authors evidenced a mechanism by which chlorpyrifos-exposure might contribute to the development of inflammatory diseases (Li et al., 2019). In contrast to chlorpyrifos, glyphosate-exposure exhibited only minor microbiota-mediated effects on MAIT cells. Glyphosate decreased the potential of *L. reuteri* to inhibit MAIT cell activation by *E. coli*, despite the other bacterial strains remained unaffected. Since single strain bacteria have an individual stress response and stress tolerance due to their limited genetic repertoire (Shade et al., 2012), the microbiota-mediated immunomodulatory effect of chlorpyrifos and glyphosate on MAIT cells needs to be confirmed using complex microbiota.

In publication 7, *E. coli*, *B. thetaiotaomicron* and complex fecal microbiota were exposed to bisphenol A (BpA), bisphenol F (BpF) and bisphenol S (BpS) at three different concentrations. Thereafter, the modulation of the MAIT cell response was determined. The MAIT cell response mirrored to effects of BpA on microbial growth and viability for BpA at the single strain level. BpF reduced growth and viability in both bacterial strains, *B. thetaiotaomicron* and *E. coli*, though the down-stream MAIT cell response was different. Growth, viability and metabolic shift of *E. coli* were positively correlated with MAIT cell activation, which all decreased with increasing BpF concentration. In contrast, for *B. thetaiotaomicron* the MAIT cell response was elevated and negatively correlated with growth, viability and metabolic changes at rising BpF concentration. Surprisingly, in the complex community the effect of BpA- and BpF-exposure observed within the microbiota did not reflect on MAIT cell activation. Although BpS affected growth and metabolism of all microbiota, the BpS-related changes did not result in a modulated MAIT cell response. The different microbiota showed different susceptibility towards BpA-, BpF- and BpS-exposure. Although the BpX-related effects on the microbiota-level partly correlated with MAIT cell modulation, these effects were lost when complex microbiota were used.

These data show that the use of individual bacterial strains is suitable to estimate the ability of chemicals for microbiota-mediated MAIT cell modulation. However, bacterial single strains do not represent the intestinal microbiota. Consequently, experiment exposing complex microbiota to the same chemicals are essential to validate the ability of chemicals for microbiota-mediated MAIT cell modulation. At the same time, these data suggest that the microbial stress-response does not always affect riboflavin utilization. Though, the role of riboflavin in microbial stress response should be investigated in more detail.

The utilization of chemical-exposure in batch is assumed more fruitful to identify immediate microbiota-mediated effects by chemicals on MAIT cell activation. In the present PhD project the microbiota showed immediate effects and seemed to adapt during further continuous cultivation, although the chemicals applied to these continuous cultures indeed only show minor effects on the microbiota. In future experiments more than one concentration of chemical should be utilized for chronic exposure and then the downstream effects on MAIT cell activation should be determined

in more detail. The presented results revealed one major problem when assessing microbiota-mediated immunomodulatory properties of chemicals, i.e. peripheral blood mononuclear cells donor variability. The donor variability observed in MAIT cell stimulation assays potentially reduced or mask the modulatory effects, as MAIT cells were shown to be age- and sex-dependent (Novak et al., 2014). In future experiments, this donor-bias should be eliminated by choosing donors of similar age and sex.

The existence of direct immunomodulatory properties of chemicals have already been shown (Guo et al., 2015). To assess direct modulatory effects on MAIT cells, MAIT cells were stimulated in the presence of BpX (publication 7). The number of activated MAIT cells declined with increasing BpX concentration independent from the compound. This effect seemed to derive from an impaired viability of MAIT cells. Similarly, the viability of other lymphocyte populations has been affected. To discriminate immunomodulation from immunotoxicity analyzing viability is essential and experiments should focus on concentrations were no immunotoxicity has been observed. Regarding MAIT cell modulation, we observed a decrease in MAIT cell activation at concentrations that did not affect cell viability (publication 7).

3.4 Concluding remarks and future perspectives

In vitro cultivation procedures resemble useful tools to investigate the microbiota-modulating properties of (environmental) chemicals. In combination with up-to-date omics-techniques (metatranscriptomics, metagenomics, metaproteomics and metametabolomics), the microbial response and the dynamics upon exposure as well as the mode of action can be uncovered both on the taxonomic and functional level (Gao et al., 2017, 2013b; Wilmes et al., 2015).

In the present PhD project, some aspects regarding microbiota cultivation have been identified, which should be addressed in future experiments. SIHUMIx was proven suitable to investigate the effects of chemical exposure *in vitro* (publication 1, publication 2 and publication 8). However, at the constant community state SIHUMIx comprises of only four dominant members with *Bacteroides thetaiotaomicron* making >70% relative species abundance. It is assumed that the dominance of *Bacteroides thetaiotaomicron* results from the high concentration of mucin in the complex

intestinal medium (CIM). To achieve a more *in vivo*-like composition of SIHUMIx *in vitro* the mucin concentration should be lowered. Moreover, SIHUMIx showed a high resistance toward the perturbations that were applied, i.e. acid stress (publication 1), changes in medium retention times (publication 2) and the exposure to BpS (publication 8). The mechanisms that promote the resistance of SIHUMIx should be evaluated. Therefore, proteome and genome analysis of the individual bacterial strains should be performed to elucidate the functional repertoire of all SIHUMIx members. This will help to evaluate the functional redundancy and functional diversity within the community, which might be the basis for the observed high resistance.

Based on the present PhD project, an effect concentration (EC) should be determined beforehand in future experiments using batch cultures. Since complex microbiota have a broader range of genetically encoded response mechanisms compare to individual bacterial strains (Shade et al., 2012) and are more relevant for the *in vivo* situation, the use of complex microbiota for this purpose seems to be advisable. By exposing these microbiota to a broad range of chemical concentrations, a dose-response curve might be generated e.g. regarding growth reduction. This allows the identification of the half maximal effective concentration EC50, which represents a medium concentration. From these analyses also a low concentration, resembled by the EC25, and a high concentration, equal to the EC75, can be obtained and used for further investigations. However, metaproteome analysis can be applied to identify the mode of action in terms of functional microbiota-modulation since the identification of a potential mode of action demands functional analysis. Due to the limitation of metaproteomics and metagenomics to sufficiently resolve effects in complex communities (Jiang et al., 2019; Lohmann et al., 2020), experiments that aim at clarifying the mode of action should evaluate effects on different levels of complexity. These may be (i) the single strain level using batch cultures, (ii) a defined model community, such as SIHUMIx (or any other defined community) and (iii) complex communities in *in vitro* bioreactors.

Moreover, in the context of microbiota-modulation, suitable analyses to assess microbial viability need to be established to discriminate microbiota-modulation from microbiota-disruption, since the results from publication 7 show that a reduction in growth did not correlate with microbial viability within the complex microbiota. Microbiota-modulation should be differentiated from

microbiota-disruption, with microbiota-disruption being based on a reduced viability due to toxic effects.

Regarding the analysis of complex intestinal microbiota, the sequential enrichment procedure applied in publication 7 may be refined, especially for purposes other than chemical testing. It should be determined how much similarity between cultivated complex microbiota and the corresponding starting material (inoculum) is retained during enrichment on the functional and taxonomic level. This is important for the development of *in vitro* models of diseased microbiota or the microbiota of children, since these microbiota are more susceptible to perturbations (Sommer et al., 2017). For this purpose, it seems exceedingly important to prove whether the functional phenotype can be retained *in vitro*. In addition, it seems advisable to investigate the loss of function and/or loss of species that results from the use of BHI medium compared to the use of CIM. To apply CIM for sequential enrichment, a redox-indicator should be added to the autoclavable part of the medium. It should be determined whether this medium can be prepared with the present equipment avoiding oxygen contamination. If the before-mentioned approach is proven impossible the supplementation of BHI by inorganic salt and bile salt should be considered. Furthermore, to limit the loss of taxonomic and functional properties the number of enrichments steps should be as low as possible to still facilitate the reproducible cultivation of the microbiota in continuous culture. Since the reproducible cultivation of complex microbiota has been established within the present PhD project (**Figure 14**), the utilization of these reproducible complex microbiota for chemical exposure should be considered in the future.

Based on the results from publication 1, riboflavin was assumed to be involved in the microbial stress response. In contrast, the results obtained in publication 7, did not show an effect of bisphenol exposure on MAIT cells although microbial growth and metabolism were clearly affected. To determine microbiota-mediated modulation of MAIT cells the role of riboflavin during microbial stress response should be evaluated in future experiments. In the present PhD project blood peripheral mononuclear cells, containing MAIT cells, have been used to assess these effects. MAIT cell frequency and phenotype were shown to depend on age and sex (Novak et al., 2014). Thus,

in future experiments, a potential donor-bias should be eliminated by choosing donors of similar age and sex.

The present PhD project solely focused on the modulation of MAIT cells, but several immune cells can be modulated by microbial metabolites, such as B cells, regulatory T cells, macrophages or dendritic cells. Future approaches should involve these other cell types into analysis concerning microbiota-mediated effects of chemicals. In this study, the experimental groundwork was established to investigate the effects of chemicals, especially on microbial communities, *in vitro*. Moreover, a framework was created to investigate microbiota-mediated effects on MAIT cells.

Nevertheless, *in vitro* studies only cover the microbiota-modulating properties of chemicals, due to host exclusion. To validate the relevance and to completely assess the chemicals risk regarding microbiota-modulation or microbiota-mediated immune modulation, the results need to be reproduced *in vivo* together aiming at causality, i.e. disease phenotype.

4 References

Almeida, A., Mitchell, A.L., Boland, M., Forster, S.C., Gloor, G.B., Tarkowska, A., Lawley, T.D., and Finn, R.D. (2019). A new genomic blueprint of the human gut microbiota. Nature *568*, 499–504.

Almeida, S., Raposo, A., Almeida-González, M., and Carrascosa, C. (2018). Bisphenol A: Food Exposure and Impact on Human Health: Bisphenol A and human health effect…. Comprehensive Reviews in Food Science and Food Safety *17*, 1503–1517.

Amrhein, N., Schab, J., and Steinrücken, H.C. (1980). The mode of action of the herbicide glyphosate. Naturwissenschaften *67*, 356–357.

Auchtung, J.M., Robinson, C.D., and Britton, R.A. (2015). Cultivation of stable, reproducible microbial communities from different fecal donors using minibioreactor arrays (MBRAs). Microbiome *3*.

Bäckhed, F., Ley, R.E., Sonnenburg, J.L., Peterson, D.A., and Gordon, J.I. (2005). Host-bacterial mutualism in the human intestine. Science *307*, 1915–1920.

Bäckhed, F., Roswall, J., Peng, Y., Feng, Q., Jia, H., Kovatcheva-Datchary, P., Li, Y., Xia, Y., Xie, H., Zhong, H., et al. (2015). Dynamics and Stabilization of the Human Gut Microbiome during the First Year of Life. Cell Host & Microbe *17*, 690–703.

Bauer, E., Zimmermann, J., Baldini, F., Thiele, I., and Kaleta, C. (2017). BacArena: Individual-based metabolic modeling of heterogeneous microbes in complex communities. PLOS Computational Biology *13*, e1005544.

Becker, N., Kunath, J., Loh, G., and Blaut, M. (2011). Human intestinal microbiota: Characterization of a simplified and stable gnotobiotic rat model. Gut Microbes *2*, 25–33.

Belkaid, Y., and Hand, T.W. (2014). Role of the Microbiota in Immunity and Inflammation. Cell *157*, 121–141.

Benbrook, C.M. (2016). Trends in glyphosate herbicide use in the United States and globally. Environmental Sciences Europe *28*.

Bender, E.A., Case, T.J., and Gilpin, M.E. (1984). Perturbation Experiments in Community Ecology: Theory and Practice. Ecology *65*, 1–13.

Berkson, J.D., and Prlic, M. (2017). The MAIT conundrum – how human MAIT cells distinguish bacterial colonization from infection in mucosal barrier tissues. Immunology Letters *192*, 7–11.

den Besten, G., Lange, K., Havinga, R., van Dijk, T.H., Gerding, A., van Eunen, K., Müller, M., Groen, A.K., Hooiveld, G.J., Bakker, B.M., et al. (2013a). Gut-derived short-chain fatty acids are vividly

assimilated into host carbohydrates and lipids. American Journal of Physiology-Gastrointestinal and Liver Physiology *305*, G900–G910.

den Besten, G., van Eunen, K., Groen, A.K., Venema, K., Reijngoud, D.-J., and Bakker, B.M. (2013b). The role of short-chain fatty acids in the interplay between diet, gut microbiota, and host energy metabolism. J. Lipid Res. *54*, 2325–2340.

Blacher, E., Levy, M., Tatirovsky, E., and Elinav, E. (2017). Microbiome-Modulated Metabolites at the Interface of Host Immunity. The Journal of Immunology *198*, 572–580.

Blaser, M.J. (2017). The theory of disappearing microbiota and the epidemics of chronic diseases. Nat Rev Immunol *17*, 461–463.

Blüher, M. (2019). Obesity: global epidemiology and pathogenesis. Nat Rev Endocrinol *15*, 288–298.

Bokulich, N.A., Chung, J., Battaglia, T., Henderson, N., Jay, M., Li, H., D. Lieber, A., Wu, F., Perez-Perez, G.I., Chen, Y., et al. (2016). Antibiotics, birth mode, and diet shape microbiome maturation during early life. Sci. Transl. Med. *8*, 343ra82-343ra82.

Brandtzaeg, P., and Pabst, R. (2004). Let's go mucosal: communication on slippery ground. Trends in Immunology *25*, 570–577.

Brandtzaeg, P., Kiyono, H., Pabst, R., and Russell, M.W. (2008). Terminology: nomenclature of mucosa-associated lymphoid tissue. Mucosal Immunol *1*, 31–37.

Burchiel, S.W. (1999). The Effects of Environmental and Other Chemicals on the Human Immune System: The Emergence of Immunotoxicology. Clinical Immunology *90*, 285–286.

Catron, T.R., Swank, A., Wehmas, L.C., Phelps, D., Keely, S.P., Brinkman, N.E., McCord, J., Singh, R., Sobus, J., Wood, C.E., et al. (2019a). Microbiota alter metabolism and mediate neurodevelopmental toxicity of 17β-estradiol. Sci Rep *9*, 7064.

Catron, T.R., Keely, S.P., Brinkman, N.E., Zurlinden, T.J., Wood, C.E., Wright, J.R., Phelps, D., Wheaton, E., Kvasnicka, A., Gaballah, S., et al. (2019b). Host Developmental Toxicity of BPA and BPA Alternatives Is Inversely Related to Microbiota Disruption in Zebrafish. Toxicological Sciences *167*, 468–483.

Chanda, S. (1996). Neurochemical and neurobehavioral effects of repeated gestational exposure to chlorpyrifos in maternal and developing rats. Pharmacology Biochemistry and Behavior *53*, 771–776.

Chen, D., Kannan, K., Tan, H., Zheng, Z., Feng, Y.-L., Wu, Y., and Widelka, M. (2016). Bisphenol Analogues Other Than BPA: Environmental Occurrence, Human Exposure, and Toxicity—A Review. Environ. Sci. Technol. *50*, 5438–5453.

Chen, J., Shen, J., Solem, C., and Jensen, P.R. (2013). Oxidative Stress at High Temperatures in Lactococcus lactis Due to an Insufficient Supply of Riboflavin. Appl. Environ. Microbiol. *79*, 6140–6147.

Chen, M.L., Takeda, K., and Sundrud, M.S. (2019). Emerging roles of bile acids in mucosal immunity and inflammation. Mucosal Immunol *12*, 851–861.

Cheng, J., Ringel-Kulka, T., Heikamp-de Jong, I., Ringel, Y., Carroll, I., de Vos, W.M., Salojärvi, J., and Satokari, R. (2016). Discordant temporal development of bacterial phyla and the emergence of core in the fecal microbiota of young children. ISME J *10*, 1002–1014.

Chow, J., Tang, H., and Mazmanian, S.K. (2011). Pathobionts of the gastrointestinal microbiota and inflammatory disease. Current Opinion in Immunology *23*, 473–480.

Chu, D.M., Ma, J., Prince, A.L., Antony, K.M., Seferovic, M.D., and Aagaard, K.M. (2017). Maturation of the infant microbiome community structure and function across multiple body sites and in relation to mode of delivery. Nat Med *23*, 314–326.

Claus, S.P., Guillou, H., and Ellero-Simatos, S. (2016). The gut microbiota: a major player in the toxicity of environmental pollutants? Npj Biofilms Microbiomes *2*, 16003.

Colebrook, L. (1936). THE MODE OF ACTION OF p-AMINOBENZENESULPHONAMIDE AND PRONTOSIL IN HqMOLYTIC STREPTOCOCCAL INFECTIONS. The Lancet *228*, 1323–1326.

Collins, S.L., and Patterson, A.D. (2020). The gut microbiome: an orchestrator of xenobiotic metabolism. Acta Pharmaceutica Sinica B *10*, 19–32.

Combes, R.D., Gaunt, I., and Balls, M. (2004). A Scientific and Animal Welfare Assessment of the OECD Health Effects Test Guidelines for the Safety Testing of Chemicals under the European Union REACH System. Alternatives to Laboratory Animals *32*, 163–208.

Comstock, L.E., and Coyne, M.J. (2003). Bacteroides thetaiotaomicron: a dynamic, niche-adapted human symbiont. Bioessays *25*, 926–929.

Conlon, M., and Bird, A. (2014). The Impact of Diet and Lifestyle on Gut Microbiota and Human Health. Nutrients *7*, 17–44.

Corbett, A.J., Eckle, S.B.G., Birkinshaw, R.W., Liu, L., Patel, O., Mahony, J., Chen, Z., Reantragoon, R., Meehan, B., Cao, H., et al. (2014). T-cell activation by transitory neo-antigens derived from distinct microbial pathways. Nature *509*, 361–365.

Cordain, L., Eaton, S.B., Sebastian, A., Mann, N., Lindeberg, S., Watkins, B.A., O'Keefe, J.H., and Brand-Miller, J. (2005). Origins and evolution of the Western diet: health implications for the 21st century. The American Journal of Clinical Nutrition *81*, 341–354.

Corrêa-Oliveira, R., Fachi, J.L., Vieira, A., Sato, F.T., and Vinolo, M.A.R. (2016). Regulation of immune cell function by short-chain fatty acids. Clinical & Translational Immunology *5*, e73.

Costello, E.K., Lauber, C.L., Hamady, M., Fierer, N., Gordon, J.I., and Knight, R. (2009). Bacterial Community Variation in Human Body Habitats Across Space and Time. Science *326*, 1694–1697.

Cummings, J.H., Pomare, E.W., Branch, W.J., Naylor, C.P.E., and Macfarlane, G.T. (1987). Short chain fatty acids in human large intestine, portal, hepatic and venous blood. Gut *28*, 1221–1227.

David, L.A., Maurice, C.F., Carmody, R.N., Gootenberg, D.B., Button, J.E., Wolfe, B.E., Ling, A.V., Devlin, A.S., Varma, Y., Fischbach, M.A., et al. (2014). Diet rapidly and reproducibly alters the human gut microbiome. Nature *505*, 559–563.

de Aguiar Vallim, T.Q., Tarling, E.J., and Edwards, P.A. (2013). Pleiotropic Roles of Bile Acids in Metabolism. Cell Metabolism *17*, 657–669.

Deschasaux, M., Bouter, K.E., Prodan, A., Levin, E., Groen, A.K., Herrema, H., Tremaroli, V., Bakker, G.J., Attaye, I., Pinto-Sietsma, S.-J., et al. (2018). Depicting the composition of gut microbiota in a population with varied ethnic origins but shared geography. Nat Med *24*, 1526–1531.

Dethlefsen, L., and Relman, D.A. (2011). Incomplete recovery and individualized responses of the human distal gut microbiota to repeated antibiotic perturbation. Proceedings of the National Academy of Sciences *108*, 4554–4561.

Dominguez-Bello, M.G., Costello, E.K., Contreras, M., Magris, M., Hidalgo, G., Fierer, N., and Knight, R. (2010). Delivery mode shapes the acquisition and structure of the initial microbiota across multiple body habitats in newborns. Proceedings of the National Academy of Sciences *107*, 11971–11975.

Dranoff, G. (2004). Cytokines in cancer pathogenesis and cancer therapy. Nat Rev Cancer *4*, 11–22.

Dusseaux, M., Martin, E., Serriari, N., Peguillet, I., Premel, V., Louis, D., Milder, M., Le Bourhis, L., Soudais, C., Treiner, E., et al. (2011). Human MAIT cells are xenobiotic-resistant, tissue-targeted, CD161hi IL-17-secreting T cells. Blood *117*, 1250–1259.

Eckburg, P.B. (2005). Diversity of the Human Intestinal Microbial Flora. Science *308*, 1635–1638.

Eckle, S.B.G., Corbett, A.J., Keller, A.N., Chen, Z., Godfrey, D.I., Liu, L., Mak, J.Y.W., Fairlie, D.P., Rossjohn, J., and McCluskey, J. (2015). Recognition of Vitamin B Precursors and Byproducts by Mucosal Associated Invariant T Cells. Journal of Biological Chemistry *290*, 30204–30211.

EFSA (2008). Opinion of the Scientific Panel on Contaminants in the Food chain on Perfluorooctane sulfonate (PFOS), perfluorooctanoic acid (PFOA) and their salts. The EFSA Journal 1–131.

Elzinga, J., van der Oost, J., de Vos, W.M., and Smidt, H. (2019). The Use of Defined Microbial Communities To Model Host-Microbe Interactions in the Human Gut. Microbiol Mol Biol Rev *83*, e00054-18, /mmbr/83/2/MMBR.00054-18.atom.

Emerson, J.B., Adams, R.I., Román, C.M.B., Brooks, B., Coil, D.A., Dahlhausen, K., Ganz, H.H., Hartmann, E.M., Hsu, T., Justice, N.B., et al. (2017). Schrödinger's microbes: Tools for distinguishing the living from the dead in microbial ecosystems. Microbiome *5*, 86.

Eng, A., and Borenstein, E. (2018). Taxa-function robustness in microbial communities. Microbiome *6*, 45.

European Chemicals Agency (2017). Registration.

European Food Safety Authority (2015). EFSA explains the Safety of Bisphenol A: scientific opinion on bisphenol A (2015). (Parma: EFSA).

European Food Safety Authority (2017). The 2015 European Union report on pesticide residues in food. EFSA Journal *15*.

Faith, J.J., Guruge, J.L., Charbonneau, M., Subramanian, S., Seedorf, H., Goodman, A.L., Clemente, J.C., Knight, R., Heath, A.C., Leibel, R.L., et al. (2013). The Long-Term Stability of the Human Gut Microbiota. Science *341*, 1237439.

Fan, P., Bian, B., Teng, L., Nelson, C.D., Driver, J., Elzo, M.A., and Jeong, K.C. (2020). Host genetic effects upon the early gut microbiota in a bovine model with graduated spectrum of genetic variation. ISME J *14*, 302–317.

Filippi, M., Bar-Or, A., Piehl, F., Preziosa, P., Solari, A., Vukusic, S., and Rocca, M.A. (2018). Multiple sclerosis. Nat Rev Dis Primers *4*, 43.

Flajnik, M., and Dupasquier, L. (2004). Evolution of innate and adaptive immunity: can we draw a line? Trends in Immunology *25*, 640–644.

Flint, H.J., Scott, K.P., Duncan, S.H., Louis, P., and Forano, E. (2012). Microbial degradation of complex carbohydrates in the gut. Gut Microbes *3*, 289–306.

Fritz, J.V., Desai, M.S., Shah, P., Schneider, J.G., and Wilmes, P. (2013). From meta-omics to causality: experimental models for human microbiome research. Microbiome *1*, 14.

Funke, T., Yang, Y., Han, H., Healy-Fried, M., Olesen, S., Becker, A., and Schönbrunn, E. (2009). Structural Basis of Glyphosate Resistance Resulting from the Double Mutation Thr ^{97} → Ile and Pro ^{101} → Ser in 5-Enolpyruvylshikimate-3-phosphate Synthase from *Escherichia coli*. J. Biol. Chem. *284*, 9854–9860.

Galindo-Villegas, J., Garcia-Moreno, D., de Oliveira, S., Meseguer, J., and Mulero, V. (2012). Regulation of immunity and disease resistance by commensal microbes and chromatin modifications during zebrafish development. Proceedings of the National Academy of Sciences *109*, E2605–E2614.

Gao, B., Chi, L., Mahbub, R., Bian, X., Tu, P., Ru, H., and Lu, K. (2017). Multi-Omics Reveals that Lead Exposure Disturbs Gut Microbiome Development, Key Metabolites, and Metabolic Pathways. Chem. Res. Toxicol. *30*, 996–1005.

García-Angulo, V.A. (2017). Overlapping riboflavin supply pathways in bacteria. Critical Reviews in Microbiology *43*, 196–209.

Gentile, C.L., and Weir, T.L. (2018). The gut microbiota at the intersection of diet and human health. Science *362*, 776–780.

Ghazarian, L., Caillat-Zucman, S., and Houdouin, V. (2017). Mucosal-Associated Invariant T Cell Interactions with Commensal and Pathogenic Bacteria: Potential Role in Antimicrobial Immunity in the Child. Front. Immunol. *8*, 1837.

Gherardin, N.A., Keller, A.N., Woolley, R.E., Le Nours, J., Ritchie, D.S., Neeson, P.J., Birkinshaw, R.W., Eckle, S.B.G., Waddington, J.N., Liu, L., et al. (2016). Diversity of T Cells Restricted by the MHC Class I-Related Molecule MR1 Facilitates Differential Antigen Recognition. Immunity *44*, 32–45.

Gibbs, A., Leeansyah, E., Introini, A., Paquin-Proulx, D., Hasselrot, K., Andersson, E., Broliden, K., Sandberg, J.K., and Tjernlund, A. (2017). MAIT cells reside in the female genital mucosa and are biased towards IL-17 and IL-22 production in response to bacterial stimulation. Mucosal Immunology *10*, 35–45.

Gill, N., and Finlay, B.B. (2011). The gut microbiota: challenging immunology. Nat Rev Immunol *11*, 636–637.

Gillezeau, C., van Gerwen, M., Shaffer, R.M., Rana, I., Zhang, L., Sheppard, L., and Taioli, E. (2019). The evidence of human exposure to glyphosate: a review. Environ Health *18*, 2.

Godfrey, D.I., Koay, H.-F., McCluskey, J., and Gherardin, N.A. (2019). The biology and functional importance of MAIT cells. Nat Immunol *20*, 1110–1128.

Gold, M.C., Cerri, S., Smyk-Pearson, S., Cansler, M.E., Vogt, T.M., Delepine, J., Winata, E., Swarbrick, G.M., Chua, W.-J., Yu, Y.Y.L., et al. (2010). Human Mucosal Associated Invariant T Cells Detect Bacterially Infected Cells. PLoS Biol *8*, e1000407.

Goodrich, J.K., Waters, J.L., Poole, A.C., Sutter, J.L., Koren, O., Blekhman, R., Beaumont, M., Van Treuren, W., Knight, R., Bell, J.T., et al. (2014). Human Genetics Shape the Gut Microbiome. Cell *159*, 789–799.

Grimm, V., Schmidt, E., and Wissel, C. (1992). On the application of stability concepts in ecology. Ecological Modelling 143–161.

Guo, A., He, D., Xu, H.-B., Geng, C.-A., and Zhao, J. (2015). Promotion of regulatory T cell induction by immunomodulatory herbal medicine licorice and its two constituents. Sci Rep *5*, 14046.

Gutiérrez-Preciado, A., Torres, A.G., Merino, E., Bonomi, H.R., Goldbaum, F.A., and García-Angulo, V.A. (2015). Extensive Identification of Bacterial Riboflavin Transporters and Their Distribution across Bacterial Species. PLOS ONE *10*, e0126124.

Guzman-Rodriguez, M., McDonald, J.A.K., Hyde, R., Allen-Vercoe, E., Claud, E.C., Sheth, P.M., and Petrof, E.O. (2018). Using bioreactors to study the effects of drugs on the human microbiota. Methods *149*, 31–41.

Hague, A., Butt, A.J., and Paraskeva, C. (1996). The role of butyrate in human colonic epithelial cells: an energy source or inducer of differentiation and apoptosis? Proc. Nutr. Soc. *55*, 937–943.

Hand, T.W., Vujkovic-Cvijin, I., Ridaura, V.K., and Belkaid, Y. (2016). Linking the Microbiota, Chronic Disease, and the Immune System. Trends in Endocrinology & Metabolism *27*, 831–843.

Hanke, I., Wittmer, I., Bischofberger, S., Stamm, C., and Singer, H. (2010). Relevance of urban glyphosate use for surface water quality. Chemosphere *81*, 422–429.

Harishankar, M.K., Sasikala, C., and Ramya, M. (2013). Efficiency of the intestinal bacteria in the degradation of the toxic pesticide, chlorpyrifos. 3 Biotech *3*, 137–142.

Hartung, T., and Rovida, C. (2009). Chemical regulators have overreached. Nature *460*, 1080–1081.

Hashimoto, K., Hirai, M., and Kurosawa, Y. (1995). A gene outside the human MHC related to classical HLA class I genes. Science *269*, 693–695.

Hill, M.J. (1997). Intestinal flora and endogenous vitamin synthesis. European Journal of Cancer Prevention 43–45.

Hinks, T.S.C., Wallington, J.C., Williams, A.P., Djukanović, R., Staples, K.J., and Wilkinson, T.M.A. (2016). Steroid-induced Deficiency of Mucosal-associated Invariant T Cells in the Chronic Obstructive Pulmonary Disease Lung. Implications for Nontypeable *Haemophilus influenzae* Infection. American Journal of Respiratory and Critical Care Medicine *194*, 1208–1218.

Hooper, L.V., Littman, D.R., and Macpherson, A.J. (2012). Interactions Between the Microbiota and the Immune System. Science *336*, 1268–1273.

Huang, S., Gilfillan, S., Cella, M., Miley, M.J., Lantz, O., Lybarger, L., Fremont, D.H., and Hansen, T.H. (2005). Evidence for MR1 Antigen Presentation to Mucosal-associated Invariant T Cells. J. Biol. Chem. *280*, 21183–21193.

Hugenholtz, P., and Tyson, G.W. (2008). Metagenomics. Nature *455*, 481–483.

Huttenhower, C., Gevers, D., Knight, R., Abubucker, S., Badger, J.H., Chinwalla, A.T., Creasy, H.H., Earl, A.M., FitzGerald, M.G., Fulton, R.S., et al. (2012). Structure, function and diversity of the healthy human microbiome. Nature *486*, 207–214.

Janeway, C.A. (1989). Approaching the Asymptote? Evolution and Revolution in Immunology. Cold Spring Harbor Symposia on Quantitative Biology *54*, 1–13.

Jangi, S., Gandhi, R., Cox, L.M., Li, N., von Glehn, F., Yan, R., Patel, B., Mazzola, M.A., Liu, S., Glanz, B.L., et al. (2016). Alterations of the human gut microbiome in multiple sclerosis. Nat Commun *7*, 12015.

Jia, W., Xie, G., and Jia, W. (2018). Bile acid–microbiota crosstalk in gastrointestinal inflammation and carcinogenesis. Nat Rev Gastroenterol Hepatol *15*, 111–128.

Jiang, D., Armour, C.R., Hu, C., Mei, M., Tian, C., Sharpton, T.J., and Jiang, Y. (2019). Microbiome Multi-Omics Network Analysis: Statistical Considerations, Limitations, and Opportunities. Front. Genet. *10*, 995.

Jin, Y., Wu, S., Zeng, Z., and Fu, Z. (2017). Effects of environmental pollutants on gut microbiota. Environmental Pollution *222*, 1–9.

John, E.M., and Shaike, J.M. (2015). Chlorpyrifos: pollution and remediation. Environ Chem Lett *13*, 269–291.

Joly, C., Gay-Quéheillard, J., Léké, A., Chardon, K., Delanaud, S., Bach, V., and Khorsi-Cauet, H. (2013). Impact of chronic exposure to low doses of chlorpyrifos on the intestinal microbiota in the Simulator of the Human Intestinal Microbial Ecosystem (SHIME®) and in the rat. Environmental Science and Pollution Research *20*, 2726–2734.

Joly Condette, C., Khorsi-Cauet, H., Morlière, P., Zabijak, L., Reygner, J., Bach, V., and Gay-Quéheillard, J. (2014). Increased Gut Permeability and Bacterial Translocation after Chronic Chlorpyrifos Exposure in Rats. PLoS ONE *9*, e102217.

Joosten, V., and van Berkel, W.J. (2007). Flavoenzymes. Current Opinion in Chemical Biology *11*, 195–202.

Kaoutari, A.E., Armougom, F., Gordon, J.I., Raoult, D., and Henrissat, B. (2013). The abundance and variety of carbohydrate-active enzymes in the human gut microbiota. Nat Rev Microbiol *11*, 497–504.

Kaplan, G.G. (2015). The global burden of IBD: from 2015 to 2025. Nat Rev Gastroenterol Hepatol *12*, 720–727.

Karl, J.P., Hatch, A.M., Arcidiacono, S.M., Pearce, S.C., Pantoja-Feliciano, I.G., Doherty, L.A., and Soares, J.W. (2018). Effects of Psychological, Environmental and Physical Stressors on the Gut Microbiota. Front. Microbiol. *9*, 2013.

Karrer, C., Roiss, T., von Goetz, N., Gramec Skledar, D., Peterlin Mašič, L., and Hungerbühler, K. (2018). Physiologically Based Pharmacokinetic (PBPK) Modeling of the Bisphenols BPA, BPS, BPF, and BPAF with New Experimental Metabolic Parameters: Comparing the Pharmacokinetic Behavior of BPA with Its Substitutes. Environ Health Perspect *126*, 077002.

Kawachi, I., Maldonado, J., Strader, C., and Gilfillan, S. (2006). MR1-Restricted Vα19 *i* Mucosal-Associated Invariant T Cells Are Innate T Cells in the Gut Lamina Propria That Provide a Rapid and Diverse Cytokine Response. J Immunol *176*, 1618–1627.

Kendall, A.I. (1909). SOME OBSERVATIONS ON THE STUDY OF THE INTESTINAL BACTERIA. J. Biol. Chem 499–507.

Kjer-Nielsen, L., Patel, O., Corbett, A.J., Le Nours, J., Meehan, B., Liu, L., Bhati, M., Chen, Z., Kostenko, L., Reantragoon, R., et al. (2012). MR1 presents microbial vitamin B metabolites to MAIT cells. Nature.

Kjer-Nielsen, L., Corbett, A.J., Chen, Z., Liu, L., Mak, J.Y., Godfrey, D.I., Rossjohn, J., Fairlie, D.P., McCluskey, J., and Eckle, S.B. (2018). An overview on the identification of MAIT cell antigens. Immunol Cell Biol *96*, 573–587.

Kleiner, M. (2019). Metaproteomics: Much More than Measuring Gene Expression in Microbial Communities. MSystems *4*, e00115-19, /msystems/4/3/msys.00115-19.atom.

Knoop, K.A., and Newberry, R.D. (2018). Goblet cells: multifaceted players in immunity at mucosal surfaces. Mucosal Immunol *11*, 1551–1557.

Koch, C., Günther, S., Desta, A.F., Hübschmann, T., and Müller, S. (2013). Cytometric fingerprinting for analyzing microbial intracommunity structure variation and identifying subcommunity function. Nature Protocols *8*, 190–202.

Konopka, A., Lindemann, S., and Fredrickson, J. (2015). Dynamics in microbial communities: unraveling mechanisms to identify principles. ISME J *9*, 1488–1495.

Koppel, N., Maini Rekdal, V., and Balskus, E.P. (2017). Chemical transformation of xenobiotics by the human gut microbiota. Science *356*, eaag2770.

Koropatnick, T.A. (2004). Microbial Factor-Mediated Development in a Host-Bacterial Mutualism. Science *306*, 1186–1188.

Kostic, A.D., Gevers, D., Siljander, H., Vatanen, T., Hyötyläinen, T., Hämäläinen, A.-M., Peet, A., Tillmann, V., Pöhö, P., Mattila, I., et al. (2015). The Dynamics of the Human Infant Gut Microbiome in Development and in Progression toward Type 1 Diabetes. Cell Host & Microbe *17*, 260–273.

Kreft, J.-U., Plugge, C.M., Prats, C., Leveau, J.H.J., Zhang, W., and Hellweger, F.L. (2017). From Genes to Ecosystems in Microbiology: Modeling Approaches and the Importance of Individuality. Front. Microbiol. *8*, 2299.

Kurioka, A., Ussher, J.E., Cosgrove, C., Clough, C., Fergusson, J.R., Smith, K., Kang, Y.-H., Walker, L.J., Hansen, T.H., Willberg, C.B., et al. (2015). MAIT cells are licensed through granzyme exchange to kill bacterially sensitized targets. Mucosal Immunology *8*, 429–440.

Kurioka, A., Walker, L.J., Klenerman, P., and Willberg, C.B. (2016). MAIT cells: new guardians of the liver. Clinical & Translational Immunology *5*, e98.

Kurokawa, K., Itoh, T., Kuwahara, T., Oshima, K., Toh, H., Toyoda, A., Takami, H., Morita, H., Sharma, V.K., Srivastava, T.P., et al. (2007). Comparative Metagenomics Revealed Commonly Enriched Gene Sets in Human Gut Microbiomes. DNA Research *14*, 169–181.

L. Millard, A., Mertes, P.M., Ittelet, D., Villard, F., Jeannesson, P., and Bernard, J. (2002). Butyrate affects differentiation, maturation and function of human monocyte-derived dendritic cells and macrophages. Clin Exp Immunol *130*, 245–255.

Lagier, J.-C., Khelaifia, S., Alou, M.T., Ndongo, S., Dione, N., Hugon, P., Caputo, A., Cadoret, F., Traore, S.I., Seck, E.H., et al. (2016). Culture of previously uncultured members of the human gut microbiota by culturomics. Nat Microbiol *1*, 16203.

Lai, K.-P., Chung, Y.-T., Li, R., Wan, H.-T., and Wong, C.K.-C. (2016). Bisphenol A alters gut microbiome: Comparative metagenomics analysis. Environmental Pollution *218*, 923–930.

Lanier, L.L., and Sun, J.C. (2009). Do the terms innate and adaptive immunity create conceptual barriers? Nat Rev Immunol *9*, 302–303.

Lazuka, A., Auer, L., Bozonnet, S., Morgavi, D.P., O'Donohue, M., and Hernandez-Raquet, G. (2015). Efficient anaerobic transformation of raw wheat straw by a robust cow rumen-derived microbial consortium. Bioresource Technology *196*, 241–249.

Le Bourhis, L., Martin, E., Péguillet, I., Guihot, A., Froux, N., Coré, M., Lévy, E., Dusseaux, M., Meyssonnier, V., Premel, V., et al. (2010). Antimicrobial activity of mucosal-associated invariant T cells. Nature Immunology *11*, 701–708.

LeBlanc, J.G., Milani, C., de Giori, G.S., Sesma, F., van Sinderen, D., and Ventura, M. (2013). Bacteria as vitamin suppliers to their host: a gut microbiota perspective. Current Opinion in Biotechnology *24*, 160–168.

LeBlanc, J.G., Chain, F., Martín, R., Bermúdez-Humarán, L.G., Courau, S., and Langella, P. (2017). Beneficial effects on host energy metabolism of short-chain fatty acids and vitamins produced by commensal and probiotic bacteria. Microbial Cell Factories *16*.

Lehmler, H.-J., Liu, B., Gadogbe, M., and Bao, W. (2018). Exposure to Bisphenol A, Bisphenol F, and Bisphenol S in U.S. Adults and Children: The National Health and Nutrition Examination Survey 2013–2014. ACS Omega *3*, 6523–6532.

Levy, M., Kolodziejczyk, A.A., Thaiss, C.A., and Elinav, E. (2017a). Dysbiosis and the immune system. Nat Rev Immunol *17*, 219–232.

Levy, M., Blacher, E., and Elinav, E. (2017b). Microbiome, metabolites and host immunity. Current Opinion in Microbiology *35*, 8–15.

Ley, R.E., Peterson, D.A., and Gordon, J.I. (2006). Ecological and Evolutionary Forces Shaping Microbial Diversity in the Human Intestine. Cell *124*, 837–848.

Ley, R.E., Hamady, M., Lozupone, C., Turnbaugh, P.J., Ramey, R.R., Bircher, J.S., Schlegel, M.L., Tucker, T.A., Schrenzel, M.D., Knight, R., et al. (2008). Evolution of Mammals and Their Gut Microbes. Science *320*, 1647–1651.

Li, J.-W., Fang, B., Pang, G.-F., Zhang, M., and Ren, F.-Z. (2019). Age- and diet-specific effects of chronic exposure to chlorpyrifos on hormones, inflammation and gut microbiota in rats. Pesticide Biochemistry and Physiology *159*, 68–79.

Li, L., Zhang, X., Ning, Z., Mayne, J., Moore, J.I., Butcher, J., Chiang, C.-K., Mack, D., Stintzi, A., and Figeys, D. (2018a). Evaluating in Vitro Culture Medium of Gut Microbiome with Orthogonal Experimental Design and a Metaproteomics Approach. J. Proteome Res. *17*, 154–163.

Li, L., Ning, Z., Zhang, X., Mayne, J., Cheng, K., Stintzi, A., and Figeys, D. (2020). RapidAIM: a culture- and metaproteomics-based Rapid Assay of Individual Microbiome responses to drugs. Microbiome *8*, 33.

Li, Z., Quan, G., Jiang, X., Yang, Y., Ding, X., Zhang, D., Wang, X., Hardwidge, P.R., Ren, W., and Zhu, G. (2018b). Effects of Metabolites Derived From Gut Microbiota and Hosts on Pathogens. Front. Cell. Infect. Microbiol. *8*, 314.

Licht, T.R., and Bahl, M.I. (2019). Impact of the gut microbiota on chemical risk assessment. Current Opinion in Toxicology *15*, 109–113.

Liu, L., Firrman, J., Tanes, C., Bittinger, K., Thomas-Gahring, A., Wu, G.D., Van den Abbeele, P., and Tomasula, P.M. (2018a). Establishing a mucosal gut microbial community in vitro using an artificial simulator. PLOS ONE *13*, e0197692.

Liu, Z., Cichocki, N., Bonk, F., Günther, S., Schattenberg, F., Harms, H., Centler, F., and Müller, S. (2018b). Ecological Stability Properties of Microbial Communities Assessed by Flow Cytometry. MSphere *3*.

Liu, Z., Cichocki, N., Hübschmann, T., Süring, C., Ofiţeru, I.D., Sloan, W.T., Grimm, V., and Müller, S. (2019). Neutral mechanisms and niche differentiation in steady-state insular microbial communities revealed by single cell analysis: Non-equilibria systems. Environmental Microbiology *21*, 164–181.

Lloyd-Price, J., Abu-Ali, G., and Huttenhower, C. (2016). The healthy human microbiome. Genome Med *8*, 51.

Lohmann, P., Schäpe, S.S., Haange, S.-B., Oliphant, K., Allen-Vercoe, E., Jehmlich, N., and Von Bergen, M. (2020). Function is what counts: how microbial community complexity affects species, proteome and pathway coverage in metaproteomics. Expert Review of Proteomics *17*, 163–173.

Louis, P., Scott, K.P., Duncan, S.H., and Flint, H.J. (2007). Understanding the effects of diet on bacterial metabolism in the large intestine. Journal of Applied Microbiology *102*, 1197–1208.

Lozupone, C.A., Stombaugh, J.I., Gordon, J.I., Jansson, J.K., and Knight, R. (2012). Diversity, stability and resilience of the human gut microbiota. Nature *489*, 220–230.

Macfarlane, G.T., and Macfarlane, S. (2007). Models for intestinal fermentation: association between food components, delivery systems, bioavailability and functional interactions in the gut. Current Opinion in Biotechnology *18*, 156–162.

Macfarlane, G.T., Macfarlane, S., and Gibson, G.R. (1998). Validation of a Three-Stage Compound Continuous Culture System for Investigating the Effect of Retention Time on the Ecology and Metabolism of Bacteria in the Human Colon. Microbial Ecology 180–187.

Macpherson, A.J., and McCoy, K.D. (2015). Standardised animal models of host microbial mutualism. Mucosal Immunol *8*, 476–486.

Macpherson, A.J., Slack, E., Geuking, M.B., and McCoy, K.D. (2009). The mucosal firewalls against commensal intestinal microbes. Semin Immunopathol *31*, 145–149.

Magnusdottir, S., Ravcheev, D., de Cr?cy-Lagard, V., and Thiele, I. (2015). Systematic genome assessment of B-vitamin biosynthesis suggests co-operation among gut microbes. Frontiers in Genetics *6*.

Mailing, L.J., Allen, J.M., Buford, T.W., Fields, C.J., and Woods, J.A. (2019). Exercise and the Gut Microbiome: A Review of the Evidence, Potential Mechanisms, and Implications for Human Health. Exercise and Sport Sciences Reviews *47*, 75–85.

Manges, A.R., Steiner, T.S., and Wright, A.J. (2016). Fecal microbiota transplantation for the intestinal decolonization of extensively antimicrobial-resistant opportunistic pathogens: a review. Infectious Diseases *48*, 587–592.

Manichanh, C., Borruel, N., Casellas, F., and Guarner, F. (2012). The gut microbiota in IBD. Nat Rev Gastroenterol Hepatol *9*, 599–608.

Martinson, J.N.V., Pinkham, N.V., Peters, G.W., Cho, H., Heng, J., Rauch, M., Broadaway, S.C., and Walk, S.T. (2019). Rethinking gut microbiome residency and the Enterobacteriaceae in healthy human adults. ISME J *13*, 2306–2318.

Maurer, L.M., Yohannes, E., Bondurant, S.S., Radmacher, M., and Slonczewski, J.L. (2005). pH Regulates Genes for Flagellar Motility, Catabolism, and Oxidative Stress in Escherichia coli K-12. Journal of Bacteriology *187*, 304–319.

Maurice, C.F., Haiser, H.J., and Turnbaugh, P.J. (2013). Xenobiotics Shape the Physiology and Gene Expression of the Active Human Gut Microbiome. Cell *152*, 39–50.

Maynard, C.L., Elson, C.O., Hatton, R.D., and Weaver, C.T. (2012). Reciprocal interactions of the intestinal microbiota and immune system. Nature *489*, 231–241.

McCann, K.S. (2000). The diversity–stability debate. Nature *405*, 228–233.

McDonald, J.A.K. (2017). In vitro models of the human microbiota and microbiome. Emerging Topics in Life Sciences *1*, 373–384.

McDonald, J.A.K., Schroeter, K., Fuentes, S., Heikamp-deJong, I., Khursigara, C.M., de Vos, W.M., and Allen-Vercoe, E. (2013). Evaluation of microbial community reproducibility, stability and composition in a human distal gut chemostat model. Journal of Microbiological Methods *95*, 167–174.

McFall-Ngai, M. (2007). Care for the community. Nature *445*, 153–153.

McNeil, B., and Harvey, L.M. (2008). Practical fermentation technology (Chichester, England ; Hoboken, NJ: Wiley).

Medzhitov, R., and Janeway, C.A. (1997). Innate Immunity: The Virtues of a Nonclonal System of Recognition. Cell *91*, 295–298.

Mesnage, R., Teixeira, M., Mandrioli, D., Falcioni, L., Ducarmon, Q.R., Zwittink, R.D., Amiel, C., Panoff, J.-M., Belpoggi, F., and Antoniou, M.N. (2019). Shotgun metagenomics and metabolomics reveal glyphosate alters the gut microbiome of Sprague-Dawley rats by inhibiting the shikimate pathway (Pharmacology and Toxicology).

MetaHIT Consortium, Qin, J., Li, R., Raes, J., Arumugam, M., Burgdorf, K.S., Manichanh, C., Nielsen, T., Pons, N., Levenez, F., et al. (2010). A human gut microbial gene catalogue established by metagenomic sequencing. Nature *464*, 59–65.

Milo, R., and Kahana, E. (2010). Multiple sclerosis: Geoepidemiology, genetics and the environment. Autoimmunity Reviews *9*, A387–A394.

Molly, K., Woestyne, M.V., Smet, I.D., and Verstraete, W. (1994). Validation of the Simulator of the Human Intestinal Microbial Ecosystem (SHIME) Reactor Using Microorganism-associated Activities. Microbial Ecology in Health and Disease *7*, 191–200.

Mora, J.R., Iwata, M., and von Andrian, U.H. (2008). Vitamin effects on the immune system: vitamins A and D take centre stage. Nat Rev Immunol *8*, 685–698.

Moreira, A.P.B., Texeira, T.F.S., Ferreira, A.B., do Carmo Gouveia Peluzio, M., and de Cássia Gonçalves Alfenas, R. (2012). Influence of a high-fat diet on gut microbiota, intestinal permeability and metabolic endotoxaemia. Br J Nutr *108*, 801–809.

Mosca, A., Leclerc, M., and Hugot, J.P. (2016). Gut Microbiota Diversity and Human Diseases: Should We Reintroduce Key Predators in Our Ecosystem? Frontiers in Microbiology *7*.

Mowat, A.M., and Agace, W.W. (2014). Regional specialization within the intestinal immune system. Nature Reviews Immunology *14*, 667–685.

Mu, Q., Kirby, J., Reilly, C.M., and Luo, X.M. (2017). Leaky Gut As a Danger Signal for Autoimmune Diseases. Front. Immunol. *8*, 598.

Mukherjee, S., and Hooper, L.V. (2015). Antimicrobial Defense of the Intestine. Immunity *42*, 28–39.

Myers, J.P., Antoniou, M.N., Blumberg, B., Carroll, L., Colborn, T., Everett, L.G., Hansen, M., Landrigan, P.J., Lanphear, B.P., Mesnage, R., et al. (2016). Concerns over use of glyphosate-based herbicides and risks associated with exposures: a consensus statement. Environmental Health *15*.

Napier, R.J., Adams, E.J., Gold, M.C., and Lewinsohn, D.M. (2015). The Role of Mucosal Associated Invariant T Cells in Antimicrobial Immunity. Frontiers in Immunology *6*.

Nielsen, L.N., Roager, H.M., Casas, M.E., Frandsen, H.L., Gosewinkel, U., Bester, K., Licht, T.R., Hendriksen, N.B., and Bahl, M.I. (2018). Glyphosate has limited short-term effects on commensal bacterial community composition in the gut environment due to sufficient aromatic amino acid levels. Environmental Pollution *233*, 364–376.

Novak, J., Dobrovolny, J., Novakova, L., and Kozak, T. (2014). The Decrease in Number and Change in Phenotype of Mucosal-Associated Invariant T cells in the Elderly and Differences in Men and Women of Reproductive Age. Scand J Immunol *80*, 271–275.

Oates, L., and Cohen, M. (2011). Assessing Diet as a Modifiable Risk Factor for Pesticide Exposure. International Journal of Environmental Research and Public Health *8*, 1792–1804.

O'Keefe, S.J.D., Li, J.V., Lahti, L., Ou, J., Carbonero, F., Mohammed, K., Posma, J.M., Kinross, J., Wahl, E., Ruder, E., et al. (2015). Fat, fibre and cancer risk in African Americans and rural Africans. Nat Commun *6*, 6342.

Oliphant, K., and Allen-Vercoe, E. (2019). Macronutrient metabolism by the human gut microbiome: major fermentation by-products and their impact on host health. Microbiome *7*, 91.

Oliphant, K., Parreira, V.R., Cochrane, K., and Allen-Vercoe, E. (2019). Drivers of human gut microbial community assembly: coadaptation, determinism and stochasticity. ISME J *13*, 3080–3092.

Org, E., Parks, B.W., Joo, J.W.J., Emert, B., Schwartzman, W., Kang, E.Y., Mehrabian, M., Pan, C., Knight, R., Gunsalus, R., et al. (2015). Genetic and environmental control of host-gut microbiota interactions. Genome Res. *25*, 1558–1569.

Pabst, O., and Slack, E. (2020). IgA and the intestinal microbiota: the importance of being specific. Mucosal Immunol *13*, 12–21.

Pancer, Z., and Cooper, M.D. (2006). THE EVOLUTION OF ADAPTIVE IMMUNITY. Annu. Rev. Immunol. *24*, 497–518.

Payne, A.N., Zihler, A., Chassard, C., and Lacroix, C. (2012). Advances and perspectives in in vitro human gut fermentation modeling. Trends in Biotechnology *30*, 17–25.

Perez-Lopez, A., Behnsen, J., Nuccio, S.-P., and Raffatellu, M. (2016). Mucosal immunity to pathogenic intestinal bacteria. Nat Rev Immunol *16*, 135–148.

Popkin, B.M., Adair, L.S., and Ng, S.W. (2012). Global nutrition transition and the pandemic of obesity in developing countries. Nutrition Reviews *70*, 3–21.

Possemiers, S., VerthÃ©, K., Uyttendaele, S., and Verstraete, W. (2004). PCR-DGGE-based quantification of stability of the microbial community in a simulator of the human intestinal microbial ecosystem. FEMS Microbiology Ecology *49*, 495–507.

Postler, T.S., and Ghosh, S. (2017). Understanding the Holobiont: How Microbial Metabolites Affect Human Health and Shape the Immune System. Cell Metabolism *26*, 110–130.

Qiao, D., Seidler, F.J., and Slotkin, T.A. (2001). Developmental neurotoxicity of chlorpyrifos modeled in vitro: comparative effects of metabolites and other cholinesterase inhibitors on DNA synthesis in PC12 and C6 cells. Environmental Health Perspectives *109*, 909–913.

Rajilić-Stojanović, M., Heilig, H.G.H.J., Tims, S., Zoetendal, E.G., and de Vos, W.M. (2013). Long-term monitoring of the human intestinal microbiota composition: Long-term monitoring of the human intestinal microbiota. Environ Microbiol *15*, 1146–1159.

Reichardt, N., Duncan, S.H., Young, P., Belenguer, A., McWilliam Leitch, C., Scott, K.P., Flint, H.J., and Louis, P. (2014). Phylogenetic distribution of three pathways for propionate production within the human gut microbiota. ISME J *8*, 1323–1335.

Relman, D.A. (2012). The human microbiome: ecosystem resilience and health. Nutrition Reviews *70*, S2–S9.

Reygner, J., Joly Condette, C., Bruneau, A., Delanaud, S., Rhazi, L., Depeint, F., Abdennebi-Najar, L., Bach, V., Mayeur, C., and Khorsi-Cauet, H. (2016). Changes in Composition and Function of Human Intestinal Microbiota Exposed to Chlorpyrifos in Oil as Assessed by the SHIME® Model. International Journal of Environmental Research and Public Health *13*, 1088.

Reyman, M., van Houten, M.A., van Baarle, D., Bosch, A.A.T.M., Man, W.H., Chu, M.L.J.N., Arp, K., Watson, R.L., Sanders, E.A.M., Fuentes, S., et al. (2019). Impact of delivery mode-associated gut microbiota dynamics on health in the first year of life. Nat Commun *10*, 4997.

Ridlon, J.M., Kang, D.-J., and Hylemon, P.B. (2006). Bile salt biotransformations by human intestinal bacteria. J. Lipid Res. *47*, 241–259.

Riede, S., Toboldt, A., Breves, G., Metzner, M., Köhler, B., Bräunig, J., Schafft, H., Lahrssen-Wiederholt, M., and Niemann, L. (2016). Investigations on the possible impact of a glyphosate-containing herbicide on ruminal metabolism and bacteria *in vitro* by means of the 'Rumen Simulation Technique.' J Appl Microbiol *121*, 644–656.

Riegert, P., Wanner, V., and Bahram, S. (1998). Genomics, isoforms, expression, and phylogeny of the MHC class I-related MR1 gene. J. Immunol. *161*, 4066–4077.

Ríos-Covián, D., Ruas-Madiedo, P., Margolles, A., Gueimonde, M., de los Reyes-Gavilán, C.G., and Salazar, N. (2016). Intestinal Short Chain Fatty Acids and their Link with Diet and Human Health. Frontiers in Microbiology *7*.

Rios-Covian, D., Salazar, N., Gueimonde, M., and de los Reyes-Gavilan, C.G. (2017). Shaping the Metabolism of Intestinal Bacteroides Population through Diet to Improve Human Health. Front. Microbiol. *8*.

Rochester, J.R. (2013). Bisphenol A and human health: A review of the literature. Reproductive Toxicology *42*, 132–155.

Rochester, J.R., and Bolden, A.L. (2015). Bisphenol S and F: A Systematic Review and Comparison of the Hormonal Activity of Bisphenol A Substitutes. Environmental Health Perspectives *123*, 643–650.

Rodionov, D.A., Arzamasov, A.A., Khoroshkin, M.S., Iablokov, S.N., Leyn, S.A., Peterson, S.N., Novichkov, P.S., and Osterman, A.L. (2019). Micronutrient Requirements and Sharing Capabilities of the Human Gut Microbiome. Frontiers in Microbiology *10*, 1316.

Rodrigues, H.G., Takeo Sato, F., Curi, R., and Vinolo, M.A.R. (2016). Fatty acids as modulators of neutrophil recruitment, function and survival. European Journal of Pharmacology *785*, 50–58.

Rothschild, D., Weissbrod, O., Barkan, E., Kurilshikov, A., Korem, T., Zeevi, D., Costea, P.I., Godneva, A., Kalka, I.N., Bar, N., et al. (2018). Environment dominates over host genetics in shaping human gut microbiota. Nature *555*, 210–215.

Rowland, I., Gibson, G., Heinken, A., Scott, K., Swann, J., Thiele, I., and Tuohy, K. (2018). Gut microbiota functions: metabolism of nutrients and other food components. European Journal of Nutrition *57*, 1–24.

Roy, C.C., Kien, C.L., Bouthillier, L., and Levy, E. (2006). Short-Chain Fatty Acids: Ready for Prime Time? Nutr Clin Pract *21*, 351–366.

Sakaguchi, S. (2000). Regulatory T Cells. Cell *101*, 455–458.

Savin, Z., Kivity, S., Yonath, H., and Yehuda, S. (2018). Smoking and the intestinal microbiome. Arch Microbiol *200*, 677–684.

Schaedler, R.W., Dubos, R., and Costello, R. (1965). ASSOCIATION OF GERMFREE MICE WITH BACTERIA ISOLATED FROM NORMAL MICE. The Journal of Experimental Medicine *122*, 77–82.

Schimel, J., Balser, T.C., and Wallenstein, M. (2007). MICROBIAL STRESS-RESPONSE PHYSIOLOGY AND ITS IMPLICATIONS FOR ECOSYSTEM FUNCTION. Ecology *88*, 1386–1394.

Schubert, K., Olde Damink, S.W.M., von Bergen, M., and Schaap, F.G. (2017). Interactions between bile salts, gut microbiota, and hepatic innate immunity. Immunol Rev *279*, 23–35.

Schubert, M., Klinger, B., Klünemann, M., Sieber, A., Uhlitz, F., Sauer, S., Garnett, M.J., Blüthgen, N., and Saez-Rodriguez, J. (2018). Perturbation-response genes reveal signaling footprints in cancer gene expression. Nat Commun *9*, 20.

Sender, R., Fuchs, S., and Milo, R. (2016). Revised estimates for the number of human and bacteria cells in the body.

Shade, A., Peter, H., Allison, S.D., Baho, D.L., Berga, M., Bürgmann, H., Huber, D.H., Langenheder, S., Lennon, J.T., Martiny, J.B.H., et al. (2012). Fundamentals of Microbial Community Resistance and Resilience. Front. Microbio. *3*.

Shafquat, A., Joice, R., Simmons, S.L., and Huttenhower, C. (2014). Functional and phylogenetic assembly of microbial communities in the human microbiome. Trends in Microbiology *22*, 261–266.

Shakya, M., Lo, C.-C., and Chain, P.S.G. (2019). Advances and Challenges in Metatranscriptomic Analysis. Front. Genet. *10*, 904.

Shamir, M., Bar-On, Y., Phillips, R., and Milo, R. (2016). SnapShot: Timescales in Cell Biology. Cell *164*, 1302-1302.e1.

Shapira, M. (2016). Gut Microbiotas and Host Evolution: Scaling Up Symbiosis. Trends in Ecology & Evolution *31*, 539–549.

Sharon, G., Sampson, T.R., Geschwind, D.H., and Mazmanian, S.K. (2016). The Central Nervous System and the Gut Microbiome. Cell *167*, 915–932.

Shehata, A.A., Schrödl, W., Aldin, Alaa.A., Hafez, H.M., and Krüger, M. (2013). The Effect of Glyphosate on Potential Pathogens and Beneficial Members of Poultry Microbiota In Vitro. Curr Microbiol *66*, 350–358.

Silva, V., Montanarella, L., Jones, A., Fernández-Ugalde, O., Mol, H.G.J., Ritsema, C.J., and Geissen, V. (2017). Distribution of glyphosate and aminomethylphosphonic acid (AMPA) in agricultural topsoils of the European Union. Science of The Total Environment.

Silva, V., Mol, H.G.J., Zomer, P., Tienstra, M., Ritsema, C.J., and Geissen, V. (2019). Pesticide residues in European agricultural soils – A hidden reality unfolded. Science of The Total Environment *653*, 1532–1545.

Singh, J., Metrani, R., Shivanagoudra, S.R., Jayaprakasha, G.K., and Patil, B.S. (2019). Review on Bile Acids: Effects of the Gut Microbiome, Interactions with Dietary Fiber, and Alterations in the Bioaccessibility of Bioactive Compounds. J. Agric. Food Chem. *67*, 9124–9138.

Sommer, F., Anderson, J.M., Bharti, R., Raes, J., and Rosenstiel, P. (2017). The resilience of the intestinal microbiota influences health and disease. Nat Rev Microbiol *15*, 630–638.

Sonnenburg, E.D., and Sonnenburg, J.L. (2014). Starving our Microbial Self: The Deleterious Consequences of a Diet Deficient in Microbiota-Accessible Carbohydrates. Cell Metabolism *20*, 779–786.

Sonnenburg, E.D., Smits, S.A., Tikhonov, M., Higginbottom, S.K., Wingreen, N.S., and Sonnenburg, J.L. (2016). Diet-induced extinctions in the gut microbiota compound over generations. Nature *529*, 212–215.

Spanogiannopoulos, P., Bess, E.N., Carmody, R.N., and Turnbaugh, P.J. (2016). The microbial pharmacists within us: a metagenomic view of xenobiotic metabolism. Nat Rev Microbiol *14*, 273–287.

Suckale, J., Sim, R.B., and Dodds, A.W. (2005). Evolution of innate immune systems. Biochem. Mol. Biol. Educ. *33*, 177–183.

Suez, J., Korem, T., Zeevi, D., Zilberman-Schapira, G., Thaiss, C.A., Maza, O., Israeli, D., Zmora, N., Gilad, S., Weinberger, A., et al. (2014). Artificial sweeteners induce glucose intolerance by altering the gut microbiota. Nature *514*, 181–186.

Takeuchi, O., and Akira, S. (2010). Pattern Recognition Receptors and Inflammation. Cell *140*, 805–820.

Tang, J. (2011). Microbial Metabolomics. CG *12*, 391–403.

Tanner, S.A., Zihler Berner, A., Rigozzi, E., Grattepanche, F., Chassard, C., and Lacroix, C. (2014). In Vitro Continuous Fermentation Model (PolyFermS) of the Swine Proximal Colon for Simultaneous Testing on the Same Gut Microbiota. PLoS ONE *9*, e94123.

Tasnim, N., Abulizi, N., Pither, J., Hart, M.M., and Gibson, D.L. (2017). Linking the Gut Microbial Ecosystem with the Environment: Does Gut Health Depend on Where We Live? Front. Microbiol. *8*, 1935.

Tastan, C., Karhan, E., Zhou, W., Fleming, E., Voigt, A.Y., Yao, X., Wang, L., Horne, M., Placek, L., Kozhaya, L., et al. (2018). Tuning of human MAIT cell activation by commensal bacteria species and MR1-dependent T-cell presentation. Mucosal Immunol *11*, 1591–1605.

Teunissen, M.B.M., Yeremenko, N.G., Baeten, D.L.P., Chielie, S., Spuls, P.I., de Rie, M.A., Lantz, O., and Res, P.C.M. (2014). The IL-17A-Producing CD8 + T-Cell Population in Psoriatic Lesional Skin Comprises Mucosa-Associated Invariant T Cells and Conventional T Cells. Journal of Investigative Dermatology *134*, 2898–2907.

Tilloy, F., Treiner, E., Park, S.-H., Garcia, C., Lemonnier, F., de la Salle, H., Bendelac, A., Bonneville, M., and Lantz, O. (1999). An Invariant T Cell Receptor α Chain Defines a Novel TAP-independent Major Histocompatibility Complex Class Ib–restricted α/β T Cell Subpopulation in Mammals. The Journal of Experimental Medicine *189*, 1907–1921.

Toubal, A., Nel, I., Lotersztajn, S., and Lehuen, A. (2019). Mucosal-associated invariant T cells and disease. Nat Rev Immunol *19*, 643–657.

Treiner, E., Duban, L., Bahram, S., Radosavljevic, M., Wanner, V., Tilloy, F., Affaticati, P., Gilfillan, S., and Lantz, O. (2003). Selection of evolutionarily conserved mucosal-associated invariant T cells by MR1. Nature *422*, 164–169.

Treiner, E., Duban, L., Moura, I.C., Hansen, T., Gilfillan, S., and Lantz, O. (2005). Mucosal-associated invariant T (MAIT) cells: an evolutionarily conserved T cell subset. Microbes and Infection *7*, 552–559.

Tsai, H.H., Hart, C.A., and Rhodes, J.M. (1991). Production of mucin degrading sulphatase and glycosidases by Bacteroides thetaiotaomicron. Lett Appl Microbiol *13*, 97–101.

Turnbaugh, P.J., Ley, R.E., Hamady, M., Fraser-Liggett, C.M., Knight, R., and Gordon, J.I. (2007). The Human Microbiome Project. Nature *449*, 804–810.

Turnbaugh, P.J., Hamady, M., Yatsunenko, T., Cantarel, B.L., Duncan, A., Ley, R.E., Sogin, M.L., Jones, W.J., Roe, B.A., Affourtit, J.P., et al. (2009). A core gut microbiome in obese and lean twins. Nature *457*, 480–484.

Van den Abbeele, P., Grootaert, C., Marzorati, M., Possemiers, S., Verstraete, W., Gerard, P., Rabot, S., Bruneau, A., El Aidy, S., Derrien, M., et al. (2010). Microbial Community Development in a Dynamic Gut Model Is Reproducible, Colon Region Specific, and Selective for Bacteroidetes and Clostridium Cluster IX. Applied and Environmental Microbiology *76*, 5237–5246.

Van der Waaij, D., Berghuis-de Vries, J.M., and Lekkerkerk-van der Wees, J.E.C. (1971). Colonization resistance of the digestive tract in conventional and antibiotic-treated mice. J. Hyg. *69*, 405–411.

Van Kaer, L., Postoak, J.L., Wang, C., Yang, G., and Wu, L. (2019). Innate, innate-like and adaptive lymphocytes in the pathogenesis of MS and EAE. Cell Mol Immunol *16*, 531–539.

Vandenberg, L.N., Hauser, R., Marcus, M., Olea, N., and Welshons, W.V. (2007). Human exposure to bisphenol A (BPA). Reproductive Toxicology *24*, 139–177.

Vandenberg, L.N., Hunt, P.A., Myers, J.P., and vom Saal, F.S. (2013). Human exposures to bisphenol A: mismatches between data and assumptions. Reviews on Environmental Health *28*.

Venema, K. (2015). The TNO In Vitro Model of the Colon (TIM-2). In The Impact of Food Bioactives on Health, K. Verhoeckx, P. Cotter, I. López-Expósito, C. Kleiveland, T. Lea, A. Mackie, T. Requena, D. Swiatecka, and H. Wichers, eds. (Cham: Springer International Publishing), pp. 293–304.

de Vos, W.M., and de Vos, E.A. (2012). Role of the intestinal microbiome in health and disease: from correlation to causation. Nutrition Reviews *70*, S45–S56.

Vrancken, G., Gregory, A.C., Huys, G.R.B., Faust, K., and Raes, J. (2019). Synthetic ecology of the human gut microbiota. Nat Rev Microbiol *17*, 754–763.

Walter, J., and Ley, R. (2011). The Human Gut Microbiome: Ecology and Recent Evolutionary Changes. Annu. Rev. Microbiol. *65*, 411–429.

Wang, X., Zhang, A., Miao, J., Sun, H., Yan, G., Wu, F., and Wang, X. (2018). Gut microbiota as important modulator of metabolism in health and disease. RSC Adv. *8*, 42380–42389.

Wilgenburg, B. van, STOP-HCV consortium, Scherwitzl, I., Hutchinson, E.C., Leng, T., Kurioka, A., Kulicke, C., de Lara, C., Cole, S., Vasanawathana, S., et al. (2016). MAIT cells are activated during human viral infections. Nature Communications *7*, 11653.

Wilmes, P., Heintz-Buschart, A., and Bond, P.L. (2015). A decade of metaproteomics: Where we stand and what the future holds: PROTEOMICS. Proteomics *15*, 3409–3417.

Wilson, M.P., and Schwarzman, M.R. (2009). Toward a New U.S. Chemicals Policy: Rebuilding the Foundation to Advance New Science, Green Chemistry, and Environmental Health. Environmental Health Perspectives *117*, 1202–1209.

Wissenbach, D.K., Oliphant, K., Rolle-Kampczyk, U., Yen, S., Höke, H., Baumann, S., Haange, S.B., Verdu, E.F., Allen-Vercoe, E., and von Bergen, M. (2016). Optimization of metabolomics of defined in vitro gut microbial ecosystems. International Journal of Medical Microbiology *306*, 280–289.

Zheng, X., Xie, G., Zhao, A., Zhao, L., Yao, C., Chiu, N.H.L., Zhou, Z., Bao, Y., Jia, W., Nicholson, J.K., et al. (2011). The Footprints of Gut Microbial–Mammalian Co-Metabolism. J. Proteome Res. *10*, 5512–5522.

Zheng, Y., Ley, S.H., and Hu, F.B. (2018). Global aetiology and epidemiology of type 2 diabetes mellitus and its complications. Nat Rev Endocrinol *14*, 88–98.

Zhong, H., Penders, J., Shi, Z., Ren, H., Cai, K., Fang, C., Ding, Q., Thijs, C., Blaak, E.E., Stehouwer, C.D.A., et al. (2019). Impact of early events and lifestyle on the gut microbiota and metabolic phenotypes in young school-age children. Microbiome *7*, 2.

Zhou, D., Zhang, H., Bai, Z., Zhang, A., Bai, F., Luo, X., Hou, Y., Ding, X., Sun, B., Sun, X., et al. (2016). Exposure to soil, house dust and decaying plants increases gut microbial diversity and decreases serum immunoglobulin E levels in BALB/c mice: Impact of living environment sanitation on gut flora. Environ Microbiol *18*, 1326–1337.

Zhou, X., Kramer, J.P., Calafat, A.M., and Ye, X. (2014). Automated on-line column-switching high performance liquid chromatography isotope dilution tandem mass spectrometry method for the quantification of bisphenol A, bisphenol F, bisphenol S, and 11 other phenols in urine. Journal of Chromatography B *944*, 152–156.

Zuo, T., Kamm, M.A., Colombel, J.-F., and Ng, S.C. (2018a). Urbanization and the gut microbiota in health and inflammatory bowel disease. Nat Rev Gastroenterol Hepatol *15*, 440–452.

Zuo, T., Kamm, M.A., Colombel, J.-F., and Ng, S.C. (2018b). Urbanization and the gut microbiota in health and inflammatory bowel disease. Nat Rev Gastroenterol Hepatol *15*, 440–452.

(2005). Immunobiology: the immune system in health and disease (New York: Garland Science).

(2013a). Pediatric Inflammatory Bowel Disease (New York, NY: Springer New York).

(2013b). Omics: applications in biomedical, agricultural, and environmental sciences (Boca Raton: CRC Press/Taylor & Francis).

AUTHOR CONTRIBUTIONS OF LISTED ARTICLES

Nachweis über Anteile der Co-Autoren, Jannike Lea Krause

Author contribution statement

Titel: Following the community development of SIHUMIx – a new intestinal in vitro model for bioreactor use

Journal: Gut Microbes

Autoren: Jannike Lea Krause, Stephanie Serena Schäpe, Katarina Fritz-Wallac, Beatrice Engelmann, Ulrike Rolle-Kampczyk, Sabine Kleinsteuber, Florian Schattenberg, Zishu Liu, Susann Mueller, Nico Jehmlich, Martin von Bergen, Gunda Herberth

---

Jannike L. Krause (First Author):	Bioreactor run, Flow cytometry sample preparation & data analysis, t-RFLP sample preparation, measurement & data analysis, Data interpretation, Manuscript writing
Stephanie S. Schäpe (First Author):	Bioreactor run, MS sample preparation, MS measurement, Metaproteomic data analysis, Data interpretation, Manuscript writing
Katarina Fritz-Wallacw:	Metabolomic data analysis
Beatrice Engelmann:	Metabolomic data analysis
Ulrike Rolle-Kampczyk:	Supervision, Manuscript revision
Sabine Kleinsteuber:	t-RFLP data analysis, Manuscript revision
Florian Schattenberg:	FC measurement
Zishu Liu:	FC data analysis
Susann Müller:	Supervision, Manuscript revision
Nico Jehmlich:	Supervision, Manuscript revision
Martin von Bergen (Senior Author):	Conceptualization, Manuscript revision
Gunda Herberth (Senior Author):	Conceptualization, Manuscript revision

22.07.20 Jannike Krause
(Datum, Jannike L. Krause)

09.07.20 Stephanie Schäpe
(Datum, Stephanie S. Schäpe)

22.07.2020
(Datum, Dr. Gunda Herberth)

(Datum, Prof. Martin von Bergen)

Nachweis über Anteile der Co-Autoren, Jannike Lea Krause

Author contribution statement

Titel: Following the community development of SIHUMIx – a new intestinal in vitro model for bioreactor use

Journal: Gut Microbes

Autoren: Jannike Lea Krause, Stephanie Serena Schäpe, Katarina Fritz-Wallac, Beatrice Engelmann, Ulrike Rolle-Kampczyk, Sabine Kleinsteuber, Florian Schattenberg, Zishu Liu, Susann Mueller, Nico Jehmlich, Martin von Bergen, Gunda Herberth

Jannike L. Krause (First Author):	Bioreactor run, Flow cytometry sample preparation & data analysis, t-RFLP sample preparation, measurement & data analysis, Data interpretation, Manuscript writing
Stephanie S. Schäpe (First Author):	Bioreactor run, MS sample preparation, MS measurement, Metaproteomic data analysis, Data interpretation, Manuscript writing
Katarina Fritz-Wallacw:	Metabolomic data analysis
Beatrice Engelmann:	Metabolomic data analysis
Ulrike Rolle-Kampczyk:	Supervision, Manuscript revision
Sabine Kleinsteuber:	t-RFLP data analysis, Manuscript revision
Florian Schattenberg:	FC measurement
Zishu Liu:	FC data analysis
Susann Müller:	Supervision, Manuscript revision
Nico Jehmlich:	Supervision, Manuscript revision
Martin von Bergen (Senior Author):	Conceptualization, Manuscript revision
Gunda Herberth (Senior Author):	Conceptualization, Manuscript revision

22.07.20 Jannike Krause
(Datum, Jannike L. Krause)

09.07.20 Stephanie Schäpe
(Datum, Stephanie S. Schäpe)

21.07.2020
(Datum, Dr. Gunda Herberth)

(Datum, Prof. Martin von Bergen)

Nachweis über Anteile der Co-Autoren, Jannike Lea Krause

Author contribution statement

Title:	The simplified human intestinal microbiota (SIHUMIx) shows high structural and functional resistance against changing transit times in in vitro bioreactors
Journal:	Microorganisms
Autoren:	Stephanie Serena Schäpe, Jannike Lea Krause, Beatrice Engelmann, Katarina Fritz-Wallac, , Florian Schattenberg, Zishu Liu, Susann Müller, Nico Jehmlich, Ulrike Rolle-Kampczyk, Gunda Herberth, Martin von Bergen

Jannike L. Krause (First Author):	Bioreactor run, Flow cytometry (FC) sample preparation & data analysis, Biomass determination, Data interpretation, Manuscript writing
Stephanie S. Schäpe (First Author):	Bioreactor run, Mass Spectrometry (MS) sample preparation & measurement & data analysis, Data interpretation, Manuscript writing
Katarina Fritz-Wallace:	Metabolomics data analysis
Beatrice Engelmann:	Metabolomics data analysis
Ulrike Rolle-Kampczyk:	Supervision, Manuscript revision
Florian Schattenberg:	FC measurement, Manuscript revision
Zishu Liu:	FC data analysis, Manuscript revision
Susann Müller:	Supervision, Manuscript revision
Nico Jehmlich:	Supervision, Manuscript revision
Gunda Herberth (Senior Autor):	Conceptualization, Manuscript revision
Martin von Bergen (Senior Autorin):	Conceptualization, Manuscript revision

21.07.20 ---------- (Datum, Jannike L. Krause)

09.07.20 ---------- (Datum, Stephanie S. Schäpe)

17.07.2020 ---------- (Datum, Dr. Gunda Herberth)

---------- (Datum, Prof. Martin von Bergen)

Nachweis über Anteile der Co-Autoren, Jannike Lea Krause

Author contribution statement

Titel: The activation of mucosal-associated invariant T (MAIT) cells is affected by microbial diversity and riboflavin utilization in vitro

Journal: Frontiers in Microbiology

Autoren: Jannike Lea Krause, Stephanie Serena Schäpe, Florian Schattenberg, Susann Mueller, Grit Ackermann, Ulrike Elisabeth Rolle-Kampczyk, Nico Jehmlich, Arkadiusz Pierzchalski, Martin von Bergen, Gunda Herberth.

Jannike L. Krause (First Author):	Conceptualization, Cultivation of microbiota, immunologic experiments, Bioreactor run, Flow cytometry sample preparation & data analysis, t-RFLP sample preparation, measurement & data analysis, Data interpretation, Manuscript writing
Stephanie S. Schäpe:	Metaproteomics sample preparation & data analysis
Beatrice Engelmann:	Metabolomic data analysis
Ulrike Rolle-Kampczyk:	Riboflavin analysis, Manuscript revision
Sabine Kleinsteuber:	t-RFLP data analysis, Manuscript revision
Florian Schattenberg:	Flow cytometric (FC) measurement
Zishu Liu:	FC data analysis
Susann Müller:	FC data analysis, Manuscript revision
Nico Jehmlich:	Metaproteomics data analysis
Grit Ackermann:	Folate analysis
Arkadiusz Pierzchalski:	Discussion on data analysis Immunology, Manuscript revision
Martin von Bergen:	Manuscript revision
Gunda Herberth (Senior Author):	Conceptualization, Folate analysis, Manuscript revision

15.07.20 Jannike

(Datum, Jannike L. Krause)

20.07.2020

(Datum, Dr. Gunda Herberth)

Nachweis über Anteile der Co-Autoren, Jannike Lea Krause

Author contribution statement

Title: Mucosal-associated invariant T-Cell (MAIT) activation is altered by chlorpyrifos- and glyphosate-treated commensal gut bacteria

Journal: Journal of Immunotoxicology

Autoren: Anne Mendler, Florian Geier, Sven-Bastiaan Haange, Arkadiusz Pierzchalski, Jannike Lea Krause, Ivonne Nijenhuis, Jean Froment, Nico Jehmlich, Urs Berger, Grit Ackermann, Ulrike Rolle-Kampczyk, Martin von Bergen & Gunda Herberth

Anne Mendler (First Author):	Microbiology work, MAIT cell stimulation, Data analysis & interpretation, Manuscript writing
Florian Geier:	Microbiology work, MAIT cell stimulation, Data analysis
Sven-Bastiaan Hannge:	Metaproteomics data analysis
Arkadiusz Pierzchalski:	Panel development immunology
Jannike Lea Krause:	Manuscript revision, support of review process
Ivonne Nijenhuis:	Microbiology work, Manuscript revision
Jean Froment:	Metabolomics analysis, Manuscript revision
Nico Jehmlich:	Supervision, Manuscript revision
Urs Berger:	Folate analysis, Manuscript revision
Grit Ackermann:	Folate analysis
Ulrike Rolle-Kampczyk:	Metabolomics, Supervision, Manuscript revision
Martin von Bergen:	Manuscript revision
Gunda Herberth (Senior Autor):	Conceptualization, Manuscript revision

Fr. Mendler für uns nicht erreichbar

(Datum, Anne Mendler)

20.07.2020

20.07.2020

(Datum, Dr. Gunda Herberth)

Nachweis über Anteile der Co-Autoren, Jannike Lea Krause

Author contribution statement

Title:	Quantification of glyphosate and AMPA from microbiome reactor fluids
Journal:	Rapid Communications in Mass Spectrometry
Autoren:	Katarina Fritz-Wallace#, Beatrice Engelmann#, Jannike Lea Krause, Stephanie Serena Schäpe, Judith Pöppe, Gunda Herberth, Uwe Rösler, Nico Jehmlich, Martin von Bergen, Ulrike Rolle-Kampczyk.

Katarina Fritz-Wallace (First Author):	Method establishment, Manuscript writing
Beatrice Engelmann (First Author):	Method establishment, Manuscript writing
Jannike Lea Krause:	Bioreactor cultivation, Manuscript revision
Stephanie Serena Schäpe:	Bioreactor cultivation
Judith Pöppe:	Animal housing
Gunda Herberth:	Supervision, Manuscript revision
Uwe Rösler:	Supervision
Nico Jehmlich:	Supervision, Manuscript revision
Martin von Bergen:	Conceptualization, Manuscript revision
Ulrike Rolle-Kampczyk (Senior Autorin):	Conceptualization, Manuscript revision

K. Fritz-Wallace
(Datum, Dr. Katarina Fritz-Wallace)

Beatrice Engelmann
(Datum, Dr. Beatrice Engelmann)

U. Rolle-Kampczyk
(Datum, Dr. Ulrike Rolle-Kampczyk)

Nachweis über Anteile der Co-Autoren, Jannike Lea Krause

Author contribution statement

Titel: The glyphosate formulation Roundup® LB plus influences the global metabolome of pig gut microbiota in vitro

Journal: Science of the total Environment

Autoren: Jannike Lea Krause, Sven-Bastiaan Haange, Stephanie Serena Schäpe, Beatrice Engelmann, Ulrike Rolle-Kampczyk, Katarina Fritz-Wallace, Zhipeng Wang, Nico Jehmlich, Dominique Türkowsky, Kristin Schubert, Judith Pöppe, Katrin Bote, Uwe Rösler, Gunda Herberth, Martin von Bergen.

Jannike L. Krause (First Author):	Conceptualization, Bioreactor cultivation, Flow cytometry, Data analysis and visualization Manuscript writing
Sven-Bastiaan Haange (First Author):	16S rRNA gene profiling, Data analysis and visualization, Manuscript writing
Stephanie S. Schäpe:	Bioreactor cultivation, Metaproteomics sample preparation & data analysis
Beatrice Engelmann:	Metabolomic data analysis, Manuscript revision
Ulrike Rolle-Kampczyk:	Metabolomic data analysis, Supervision. Manuscript revision
Katarina Fritz-Wallace:	Metabolomic data analysis, Manuscript revision
Zhipeng Wang:	Metabolomic data analysis, Manuscript revision
Nico Jehmlich:	Metaproteomics data analysis
Dominique Türkowsky:	Manuscript revision
Kristin Schubert:	Supervision
Judith Pöppe:	Animal housing, Microbiota extraction
Katrin Bote:	Animal housing, Microbiota extraction
Uwe Rösler:	Funding Aquisition
Gunda Herberth:	Supervision, Manuscript revision
Martin von Bergen (Senior Author):	Conceptualization, Funding Acquisition, Manuscript revision

15.07.20 ---------- (Datum, Jannike L. Krause)

15.7.20 ---------- (Datum, Dr. Sven-Bastiaan Haange)

15.07.20 ---------- (Datum, Prof. Martin von Bergen)

Nachweis über Anteile der Co-Autoren, Jannike Lea Krause

Author contribution statement

Title:	Bisphenol A, bisphenol F and bisphenol S directly modulate MAIT cell activation
Journal:	Environmental Pollution
Autoren:	Jannike Lea Krause, Beatrice Engelmann, Ulisses Nunes da Rocha, Ulrike Rolle-Kampczyk, Arkadiusz Pierzchalski, Martin von Bergen, Gunda Herberth

Jannike Lea Krause (First Author):	Conceptualization, Microbiology work, MAIT cell stimulation, Data analysis & interpretation, Manuscript writing
Beatrice Engelmann:	Metabolomics, Manuscript revision
Arkadiusz Pierzchalski:	Panel development immunology, Manuscript revision
Ulisses Nunes da Rocha:	16S analysis, Manuscript revision
Martin von Bergen:	Manuscript revision
Gunda Herberth (Senior Autor):	Conceptualization, Manuscript revision

24.07.20 _____ 24.07.2020 _____

(Datum, Jannike Lea Krause) (Datum, Dr. Gunda Herberth)

Nachweis über Anteile der Co-Autoren, Jannike Lea Krause

Author contribution statement

Titel: Environmentally relevant concentration of Bisphenol S shows only slight effects on SIHUMIx

Journal: Microorganisms

Autoren: Stephanie Serena Schäpe, Jannike Lea Krause, Rebecca Katharina Masanetz, Robert Starke, Sarah Riesbeck, Ulrike Rolle-Kampczyk, Christian Eberlein, Hermann Josef Heipieper, Gunda Herberth, Martin von Bergen, Nico Jehmlich

Stephanie S. Schäpe (First Author):	Metaproteomics measurement & data analysis, Data interpretation, Manuscript writing
Jannike Lea Krause:	Bioreactor run, Manuscript revision
Rebecca Katharina Masanetz:	Bioreactor run, Metaproteomics sample preparation
Robert Starke:	Metaproteomics data analysis, Manuscript revision
Sarah Riesbeck:	Manuscript writing
Ulrike Rolle-Kampczyk:	Metabolomics, Supervision, Manuscript revision
Christian Eberlein:	FAME analysis
Hermann Josef Heipieper:	FAME analysis, Manuscript revision
Gunda Herberth:	Supervision, Manuscript revision
Martin von Bergen:	Supervision, Manuscript revision
Nico Jehmlich (Senior Author):	Concenptualization, Manuscript revision

09.07.20 Stephanie Schäpe

(Datum, Stephanie S. Schäpe)

(Datum, Dr. Nico Jehmlich)

ACKNOWLEDGEMENTS

First of all I thank the German Federal Environmental Foundation for financial support and the great seminars during the scholarship period.

I would like to express my gratitude to Dr. Gunda Herberth for her motivation, help and guidance during the application for the PhD scholarship at the German Federal Environmental Foundation, which made this work possible. I am also very grateful for her constant support and the great creative freedom I had during my PhD. Likewise, I am very grateful to Prof. Dr. Martin von Bergen for the opportunity to delve into the manifold possibilities of bacterial cultivation, in particular the rather technical and complex problem-solving oriented work with the bioreactors. Thank you for your support, both scientific and administrative, during my PhD!

I very much thank Jeremy Knespel for the time we worked together, complementing each other very well in the lab and in the office. I would like to express my thanks to Dr. Beatrice Engelmann, who carefully proofread my work and made the time of my PhD much more pleasant, both inside and outside the UFZ. A special thanks to Stephanie Schäpe and Florian Schattenberg for the vivid and funny time together in the lab doing *Spökes*, the coffee and chats in between and afterwards. I thank Dr. Arkadiusz Pierzchalski and Michaela Loschinski for advice regarding flow cytometry and immunologic work and Dr. Matthias Bernt for his patience and advice during 16S analysis. I am grateful to Martina Kolbe who made my lab life a little easier by support with medium preparation for the bioreactors.

I am also grateful for the encouragement and friendliness I was offered by my fellow PhD students and co-workers in the departments Environmental Immunology and Molecular Systems Biology, especially Dr. Nico Jehmlich, Dr. Sven-Bastiaan Haange, Dr. Ulrike Rolle-Kampzyck, who significantly contributed to the success of this project.

And finally, I want to thank my small, supercool family, Tobias and Ella, my parents and friends for their support through all the ups and downs of my PhD project.

DECLARATION OF AUTHORSHIP

I herewith declare that

- I have written this thesis autonomously incorporating my own ideas and judgments; I have made use of no other resources than stated and direct or indirect quotations from other work have been marked accordingly; full reference of their source has been provided in the proper way.

- all persons are listed that provided me with support for the selection and evaluation of the material for my thesis; nature and scope of my own contribution and the share of the co-authors is listed in Documentation of Co-authors contributions.

- no other persons have provided support and thereby contributed to the thesis; in particular, no PhD consultants were used, and no third party has received direct or indirect financial benefits in goods and services for work that stands in relation to the work presented in the thesis.

- this thesis has not been submitted in an equal or similar form for examination for the degree of doctorate or any other degree at another academic institution, and has not been published.

- no further unsuccessful doctoral examination process has taken place.

_____	_____	_____
Place	Date	Signature
Ort	Datum	Unterschrift

CURRICULUM VITAE

MSc Jannike Lea Krause

Schwarzackerstraße 2, 04299 Leipzig, Germany

Email: Jannike.L.Krause@gmx.de

Telefone+49 171 7957315

Academic education

01/2017 – to date	**Helmholtz Centre for Environmental Research (UFZ) GmbH Leipzig and Leipzig University, Germany** **Departments: Environmental Immunology and Molecular Systems Biology** Supervisors: Dr. Gunda Herberth, Prof. Dr. Martin von Bergen PhD project: Analyzing the microbiota-mediated effects of environmental chemicals on MAIT cells
10/2015 – to date	**Postgraduate studies *toxicology and environment protection*** **Leipzig University, Germany** Preliminary thesis: 'BpA, BpF and BpS barely affect the intestinal microbiota and thereby mucosal-associated invariant T cells, but trigger direct immune toxic effects on MAIT cells *in vitro'*
10/2012 – 06/2015	**Master of Science - Molecular Life Sciences** **University of Hamburg, Germany**
09/2014 – 06/2015	**Bernhard Nocht Institute for Tropical Medicine**

Department: Molecular Biology and Immunology

Supervisor: PD Dr. Th. Jacobs

Master thesis: 'Analysis concerning the influence of programmed death ligand-1 (PD-L1) in $CD8^+$ T cell stimulation'

10/2009 – 09/2012 **Bachelor of Science - Molecular Life Sciences**

University of Hamburg, Germany

05/2012 – 08/2012 **University of Hamburg, Germany**

Department: Molecular Biology of Plants

Supervisor: Dr. J. Kluth

Bachelor thesis: 'Analyzing the interaction of the mitochondrial proteins AtZR3 and mtHSP70 from *Arabidopsis thaliana* (L.) HEYHN.'

Research experience

08/2010 – 08/2011 **University of Hamburg, Germany**

Department: Structural Biology

Supervisor: Prof. Dr. Dr. Chr. Betzel

Project: 'Purification and Crystallization of the Superoxiddismutase from *Onchocerca volvulus'*

08/2011 – 10/2011 **Leibniz Institute Borstel, Germany**

Department: Biophysics

Supervisor: Prof. Dr. J. Andrä

Project: 'Visualization of the impact of antimicrobial peptides (AMP) on various cancer cell lines (live cell imaging) and permeabilisation

of large unilammelar vesicles by AMP (Fluorescence spectrometry)'

05/2013 – 08/2013 **UKE Hamburg, Germany**

Department: Molecular Biology

Supervisor: Dr. S. Pohl

Project: 'Dependence of the proteolytic activation of the GlcNAc-1-Phosphotransferase by Site-1-Protease on N-Glycosylation'

08/2013 – 09/2013 **Institute for Bee Research Hohen Neuendorf, Germany**

Department: Bee Pathology/Molecular Microbiology

Supervisor: PD Dr. E. Genersch

Project: 'in vivo Functional Analysis of the Secondary Metabolites Sevadicin, Paenilamycin and the Siderophor entF by *Paenibacillus larvae'*

Scholarships

01/2017 – to date German Federal Environmental Foundation (DBU) PhD scholarship

Vocational education

08/2004 – 08/2006 **Bernd-Blindow-Schulen-GmbH, Leipzig, Germany**

Technical assistance for chemical & biological laboratories

09/2006 – 06/2007 **Bildungsinstitut Pscherer gGmbH, Lengenfeld, Germany**

Skilled employee for biotechnological work

Work experience

02/2008 – 04/2009	**mibe GmbH Pharmaceutica, Brehna, Germany**
	Laboratory assistant – quality control laboratory/microbiology
	GLP/GMP-work, sterile control (S3-laboratory)
01/2012 – 03/2015	**Nordische Ölwerke Walther Carroux GmbH & Co. KG, Hamburg**
	Laboratory assistant – quality control laboratory/chemistry
	Fatty acid analysis by gas chromatography, wet chemical analyses

Computer applications

GraphPad Prism	R
FlowJo	Inkscape (vector graphics)
Latex	Endnote/Zotero
ImageJ/FIJI	QTI-Plot & Origin
EVE (bioreactor software)	

Languages

English (Certificate in Advanced English)

French (basics)

Spanish (basics)

Supervision

2 years education of a biological laboratory assistant (practical examination: 1.0)

Scientific skills

Certificate on handling laboratory animals (mouse/rat)

Good Scientific Practice

GLP experiences

Cell biological methods

- Murine T cell isolation from spleen, isolation and differentiation of murine DC from bone marrow
- Human T cell isolation from blood (Buffy Coat)
- Cell culture (HepG2, Hepa1-6, HEK-293)
- Multicolor flow cytometry (Accuri, FACS Canto II)
- Confocal and fluorescence microscopy
- ELISA
- Transfection and generation of stable know down cell lines using CRISPR/Cas9 and TALEN
- Proliferation assays
- Cell purification with magnetic cell separation (MACS)

Molecular biological and biochemical methods

- Isolation of RNA, DNA and protein
- SDS-PAGE and agarose gel electrophoresis
- Southern and western blot
- RT-PCR and PCR
- T-RFLP
- Gene cloning
- Protein over-expression, purification and crystallization

Microbiological methods

- Aerobic and anaerobic cultivation of bacteria (Hungate technique)
- Cultivation of bacteria in continuous bioreactors
- Determination of minimal inhibitory concentrations, growth inhibition tests
- Plasmid transfection
- Yeast-two-hybrid system
- Species identification using API (biomérieux) and 16S rRNA gene analysis
- Preparation of complex culture media and isolation of single bacterial species from communities
- Microbial flow cytometry

SCIENTIFIC CONTRIBUTIONS

Publications - Published/Accepted

2020 JL Krause, SS Schaepe, F Schattenberg, S Mueller, U Rolle-Kampczyk, N Jehmlich, A Pierzchalski, M von Bergen, G Herberth (2020): The activation of mucosal-associated invariant T (MAIT) cells is affected by microbial diversity and riboflavin utilization *in vitro*. *Frontiers in Microbiology* (2020), DOI: 10.3389/fmicb.2020.00755

Jannike Lea Krause#, Sven-Bastiaan Haange#, Stephanie Serena Schäpe, Beatrice Engelmann, Ulrike Rolle-Kampczyk, Katarina Fritz-Wallace, Zhipeng Wang, Nico Jehmlich, Dominique Türkowsky, Kristin Schubert, Judith Pöppe, Katrin Bote, Uwe Rösler, Gunda Herberth, Martin von Bergen (2020): The glyphosate formulation Roundup® LB plus influences the global metabolome of pig gut microbiota in vitro. *Science of the total environment*. (# equal contribution). DOI: https://doi.org/10.1016/j.scitotenv.2020.140932

Krause JL*, Schaepe SS*, Fritz-Wallace K, Engelmann B, Rolle-Kampczyk U, Kleinsteuber S, Schattenberg F, Liu Z, Mueller S, Jehmlich N, von Bergen M#, Herberth G# (2020): Following the community development of SIHUMIx – a new intestinal in vitro model for bioreactor use. *Gut Microbes.* (*#equal contribution). DOI: 10.1080/19490976.2019.1702431.

Anne Mendler, Florian Geier, Sven-Bastiaan Haange, Arkadiusz Pierzchalski, Jannike Lea Krause, Ivonne Nijenhuis, Jean Froment, Nico Jehmlich, Urs Berger, Grit Ackermann, Ulrike Rolle-Kampczyk, Martin von Bergen & Gunda Herberth (2020): Mucosal-associated invariant T-Cell (MAIT) activation is altered by chlorpyrifos- and glyphosate-treated commensal gut bacteria. *Journal of Immuntoxicology*. DOI: 10.1080/1547691X.2019.1706672

2019 Schaepe SS*, Krause JL*, Fritz-Wallace K, Engelmann B, Rolle-Kampczyk U, Kleinsteuber S, Schattenberg F, Liu Z, Mueller S, Jehmlich N, Herberth G#, von Bergen M# (2019): The simplified human intestinal microbiota (SIHUMIx) shows high structural and functional resistance against changing transit times in in vitro bioreactors. *Microorganisms*. (* # equal contribution). DOI: 10.3390/microorganisms7120641.

Katarina Fritz-Wallace*, Beatrice Engelmann*, Jannike L. Krause, Stephanie S. Schäpe, Judith Pöppe, Gunda Herberth, Uwe Rösler, Nico Jehmlich, Martin v. Bergen, Ulrike Rolle-Kampczyk (2019): Quantification of glyphosate and AMPA from microbiome reactor fluids.

Rapid Communications in Mass Spectrometry. (* equal contribution). DOI: https://doi.org/10.1002/rcm.8668

2013 Gross S, Wilms D, Krause J, Brezesinski G, Andrä J. (2013): Design of NK-2-derived peptides with improved activity against equine sarcoid cells. *Journal of Peptide Science*. DOI: 10.1002/psc.2540.

Banković J*, Andrä J*, Todorović N, Ana P-R, Đorđe M, Krause J, Ruždijić S, Tanić N, Pešić (2013): The elimination of P-glycoprotein over-expressing cancer cells by antimicrobial cationic peptide NK-2: the unique way of multi-drug resistance modulation. *Experimental Cell Research*. (*equal contribution). DOI: 10.1016/j.yexcr.2012.12.017.

Publications - Under review/In preparation

Stephanie Serena Schaepe, Jannike Lea Krause, Rebecca Katharina Masanetz, Sarah Riesbeck, Beatrice Engelmann, Ulrike Roplle-Kampczyk, Christian Eberlein, Herman Heipieper, Gunda Herberth, Martin von Bergen, Nico Jehmlich: The simplified intestinal human microbiota (SIHUMIx) adapts membrane composition to resist Bisphenol-S exposure. In preparation. Planned submission to *Microorganisms.*

JL Krause, U Rolle-Kampczyk, B Engelmann, A Pierzchalski, M von Bergen, G Herberth: Bisphenol A, F and S directly modulate MAIT cell activation. In preparation. Planned submission to *Environmental Pollution.*

Conference contribution

10/2019 **Exploring human host-microbiome interactions in health and disease (Cambridge)**
Poster title: Community diversity affects the MAIT cell response to intestinal microbiota *in vitro*
Poster title: Changes in pH can modify the ability of a simplified human intestinal microbiota to stimulate MAIT cells

09/2019 **German Society for Cytometry (DGfZ) Annual Meeting (Berlin)**
Talk title: Community diversity affects the MAIT cell response to intestinal microbiota *in vitro*

09/2019 **II Joint Meeting of the German Society for Immunology (DGfI) and the Italian Society of Immunology, Clinical Immunology and Allergology (SIICA) (Munich)**
Talk title: Changes in pH can modify the ability of a simplified human intestinal microbiota (SIHUMIx) to stimulate Mucosal-associated invariant T (MAIT) cells *in vitro*

08/2019 **HIGRADE conference (Leipzig)**
Poster title: Changes in pH can modify the ability of a simplified human intestinal microbiota to stimulate MAIT cells

07/2019 **Pestizide in der Umwelt – Defizite erkennen, Handlungsoptionen entwickeln (Osnabrück)**

12/2018 **3rd International Metaproteome Symposium (Leipzig)**
Poster title: Following bacterial community dynamics – a comparison of different fingerprinting methods

10/2018 **Targeting Microbiota (Porto)**
Poster title: Following bacterial community dynamics – a comparison of different fingerprinting methods

Workshops

11/2019 **Scientific writing**

10/2019 **Slide writing**

06/2019 **Proposal writing**

03/2019 **15th Spring School on Immunology**
Poster title: Changes in pH can modify the ability of bacteria to stimulate MAIT cells

12/2018 **Academic presenting**

07/2018 **Summer school on microbiome in health and disease**

10/2017 **Good Scientific Practice**